CYTOTOXIC INVESTIGATION OF CRUDE EXTRACTS AND ISOLATED COMPOUNDS FROM *Ruta angustifolia* Pers. LEAVES AND EFFECTS OF CHALEPIN ON THE EXPRESSION OF SELECTED CANCER-RELATED PROTEINS IN HUMAN LUNG CARCINOMA CELLS A549

JAIME STELLA A/P MOSES RICHARDSON

FACULTY OF SCIENCE
UNIVERSITY OF MALAYA
KUALA LUMPUR

2018

CYTOTOXIC INVESTIGATION OF CRUDE EXTRACTS AND ISOLATED COMPOUNDS FROM *Ruta angustifolia* Pers. LEAVES AND EFFECTS OF CHALEPIN ON THE EXPRESSION OF SELECTED CANCER-RELATED PROTEINS IN HUMAN LUNG CARCINOMA CELLS A549

JAIME STELLA A/P MOSES RICHARDSON

THESIS SUBMITTED IN FULFILMENT OF THE REQUIREMENTS FOR THE DEGREE OF DOCTOR OF PHILOSOPHY

INSTITUTE OF BIOLOGICAL SCIENCES
FACULTY OF SCIENCE
UNIVERSITY OF MALAYA
KUALA LUMPUR

2018

UNIVERSITY OF MALAYA

ORIGINAL LITERARY WORK DECLARATION

Name of Candidate: Jaime Stella A/P Moses Richardson

Registration/Matric No: SHC130057

Name of Degree: Doctor of Philosophy

Title of Thesis ("this Work"):

CYTOTOXIC INVESTIGATION OF CRUDE EXTRACTS AND ISOLATED COMPOUNDS FROM *Ruta angustifolia* Pers. LEAVES AND EFFECTS OF CHALEPIN ON THE EXPRESSION OF SELECTED CANCER-RELATED PROTEINS IN HUMAN LUNG CARCINOMA CELLS A549

Field of Study: Biochemistry

I do solemnly and sincerely declare that:

(1) I am the sole author/writer of this Work;
(2) This Work is original;
(3) Any use of any work in which copyright exists was done by way of fair dealing and for permitted purposes and any excerpt or extract from, or reference to or reproduction of any copyright work has been disclosed expressly and sufficiently and the title of the Work and its authorship have been acknowledged in this Work;
(4) I do not have any actual knowledge nor do I ought reasonably to know that the making of this work constitutes an infringement of any copyright work;
(5) I hereby assign all and every rights in the copyright to this Work to the University of Malaya ("UM"), who henceforth shall be owner of the copyright in this Work and that any reproduction or use in any form or by any means whatsoever is prohibited without the written consent of UM having been first had and obtained;
(6) I am fully aware that if in the course of making this Work I have infringed any copyright whether intentionally or otherwise, I may be subject to legal action or any other action as may be determined by UM.

Candidate's Signature Date:

Subscribed and solemnly declared before,

Witness's Signature Date:

Name:

Designation:

CYTOTOXIC INVESTIGATION OF CRUDE EXTRACTS AND ISOLATED COMPOUNDS FROM *Ruta angustifolia* Pers. LEAVES AND EFFECTS OF CHALEPIN ON THE EXPRESSION OF SELECTED CANCER-RELATED PROTEINS IN HUMAN LUNG CARCINOMA CELLS A549

ABSTRACT

Plants have been a major source of inspiration in developing novel drug compounds for the treatment of various diseases that afflict human beings worldwide. *Ruta angustifolia* Pers. known locally as garuda, has been traditionally used for various medicinal purposes. One of the common ethnopharmacological uses includes usage in treatment of cancer by the local chinese community in Malaysia and Singapore. The methanol and fractionated extracts of *R. angustifolia* were tested with sulforhodamide (SRB) cytotoxicity assay against HCT-116, A549, Ca Ski and MRC5 cell lines. The chloroform extract (without chlorophyll) exhibited the highest cytotoxicity with IC_{50} value of 8.8 ± 0.32 μg/mL. The chemical investigation of the plant has resulted in isolation of 12 compounds. Among the compounds, chalepin (dihydrofuranocoumarin) exhibited the best cytotoxicity against A549 cell line with an IC_{50} value of 8.69 ± 2.43 μg/mL (27.64 μM) and was futher tested for induction of apoptosis in A549 cells. The morphological changes in the cell were observed via phase contrast microscopy and Hoechst/PI fluorescent staining. Phosphatidylserine externalisation and DNA fragmentation was perceived. Mitochondrial mediated apoptosis exhibits attenuation of mitochondrial membrane potential and increase in ROS production also activation of caspase 9 and 3. Western blot analysis also showed upregulation of p53, Bax and Bak while the anti-apoptotic proteins Bcl-2, survivin, XIAP, Bcl-X_L, cFLIP decreased in a time-dependent manner in A549 cells treated with chalepin. PARP was found to decrease. These findings indicated that chalepin-induced cell death involving the

intrinsic mitochondrial pathway. Death receptors (DR4 & DR5) were upregulated and caspase 8 showed activation in a dose and time dependant manner showed the initiation of extrinsic pathway. Activated caspase 8 induced cleavage of BID to tBID, which would initiate a mitochondrial dependent or independent apoptosis. The cell cycle analysis showed that cell cycle was arrested at the S phase. Inhibition of cyclins (cyclin D1 and E) and cyclin dependant kinases (CDK2, CDK4), upregulation of inhibitors of CDKs (p21 and p27) and the hypophosphorylation of Rb protein corresponds to a cell cycle arrest at the S phase. Chalepin also suppressed the NF-kB pathway by inhibition of phosphorylation of IkBa, inhibition of phosphorylation of p65 and obstructed the translocation of p65 to nucleus. The phosphorylation of EGFR receptor was inhibited by chalepin and thus further downregulated the downstream MAPK-ERK pathway and Akt/mTOR pathway. Upregulation of SAPK/JNK and p38 protein was observed. Chalepin also exhibited suppression in inhibitors of apoptosis (MCL-1, CIAP-1, and CIAP-2), STAT-3, COX-2 and c-myc. Metastatic proteins such as ICAM-1 and VEGF was suppressed by chalepin suggesting that it has anti-metastatic property. An anti-metastatic investigation on methanol and chloroform extracts conducted showed that both the extracts possessed excellent anti-invasion and anti-migration property, prevent cell attachment, inhibit cell motility via wound closure assay, prevent cell adhesion by inhibiting the cell adhesion molecules and inhibit proliferation. Proteolytic enzyme (MMP 2) showed suppresion through gelatin zymography studies. Chalepin however showed to possess moderate anti-metastatic property in these assays. Our findings suggest the potential of this compound to be further developed as an excellent chemotherapeutic agent.

Keywords: *Ruta angustifolia* Pers., apoptosis, chalepin, NF-kB, metastatic proteins

PENYIASATAN SITOTOKSIK TERHADAP EKSTRAK MENTAH DAN KOMPAUN YANG DIPISAHKAN DARI DAUN *Ruta angustifolia* Pers. DAN KESAN CHALEPIN TERHADAP EKSPRESI PROTEIN YANG BERKAITAN DENGAN KANSER PADA SEL KARSINOMA PEPARU MANUSIA A549

ABSTRAK

Tumbuhan telah menjadi sumber inspirasi utama dalam penemuan ubat baru untuk merawat pelbagai penyakit yang menimpa manusia. *Ruta angustifolia* Pers. yang lebih dikenali sebagai garuda telah digunakan secara tradisional untuk merawat pelbagai penyakit. Salah satu kegunaan etnofarmakologi tumbuhan ini adalah dalam rawatan kanser oleh golongan berbangsa cina di Malaysia dan Singapura. Ekstrak metanol dan ekstrak hasil pemeringkatan daripada *R.angustifolia* telah diuji dengan esei sitotoksik sulforhodamide (SRB) terhadap sel kanser HCT-116, A549, Ca Ski dan MRC5. Ekstrak kloroform (tanpa klorofil) menunjukkan aktiviti sitotoksik yang tertinggi dengan nilai IC_{50} 8.8 ± 0.32 μg/ml. Penyiasatan kimia telah menghasilkan 12 kompaun. Daripada kompaun ini, chalepin yang merupakan suatu dihydrofuranocoumarin telah menunjukkan sitotoksisiti yang terbaik dengan nilai IC_{50} 8.69 ± 2.43 μg/ml (27.64 μM) dan ianya telah dipilih untuk diselidik dengan lebih lanjut bagi aspek induksi apoptosis dalam sel A549. Pertukaran dalam morfologi pada sel telah diteliti dengan mikroskop 'phase contrast' dan pewarnaan pendaflour Hoechst/PI. Pengeluaran phosphatidylserine dan fragmentasi DNA juga dilihat. Apoptosis yang diperantarakan oleh mitokondria memaparkan pengurangan potensi pada membran mitokondria dan juga meningkatkan produksi ROS. Ia juga meningkatkan aktiviti 'caspase' 9 dan 3. Analisis berdasarkan 'western blot' menunjukan peningkatan regulasi dalam protein p53, Bax dan Bak. Manakala bagi protein yang bersifat anti-apoptotik seperti Bcl-2, survivin, XIAP, Bcl-X_L ,cFLIP menunjukkan penurunan bergantung pada masa dalam sel A549 yang diberi rawatan chalepin. Tahap PARP juga menunjukkan penurunan. Penemuan-penemuan ini

menunjukkan bahawa chalepin menginduksikan kematian sel yang melibatkan apoptosis intrinsik melibatkan mitokondria. Reseptor kematian (DR4 & DR5) menunjukkan peningkatan dalam ekspresi dan juga aktiviti caspase 8 meningkat berdasarkan dos dan masa. Pengaktifan caspase 8 mengaruhkan pembelahan BID kepada tBID yang akan memulakan apoptosis sama ada diperantarakan oleh mitokondria ataupun tanpa perantaraan mitokondria. Analisis kitaran sel menunjukkan bahawa kitaran sel telah direncatkan pada fasa S. Perencatan 'cyclin' (cyclin D1 dan E) dan kinase yang bergantung kepada 'cyclin' (CDK2 dan CDK4), peningkatan regulasi dalam tahap perencat kinase yang bergantung kepada cyclin (p21 dan p27) dan juga penurunan tahap pemfosforilan pada protein Rb adalah selaras dengan ciri perencatan fasa S. Chalepin juga menindas NF-kB dengan merencatkan pemfosforilan IkBa dan p65 dan juga menghindari translokasi p65 ke nukleus. Pemfosforilan reseptor EGFR juga dihentikan oleh chalepin dan ini merencatkan laluan MAPK-ERK dan AKT/mTOR. Peningkatan pada protein SAPK/JNK dan p38 juga diperhatikan. Chalepin juga didapati mengurangkan tahap perencat apoptosis seperti MCL-1, CIAP-1, CIAP-2, STAT3, COX-2 dan c-myc. Protein yang terlibat dalam metastasis seperti ICAM-1 dan VEGF juga didapati menurun dan ini mencadangkan bahawa chalepin mempunyai ciri-ciri anti metastatik. Penyelidikan anti-metastasis mengunakan ekstrak metanol dan kloroform menunjukkan bahawa ianya mempunyai sifat anti-migrasi dan 'anti-invasion', merencatkan penempelan sel, esei penutupan luka dan merencatkan molekul yang terlibat dalam perlekatan sel. Kajian zimografi gelatin menunjukkan enzim proteolitik MMP2 juga dihalang. Walaubagaimanapun, esei-esei tersebut menunjukan chalepin mempunyai ciri anti metastatik yang sederhana. Penemuan kami mencadangkan bahawa kompaun ini dapat dieksploitasikan untuk dijadikan sebagai suatu agen kemoterapeutik.

Kata Kunci: *Ruta angustifolia* Pers., apoptosis, chalepin, NF-kB, protein metastatik

ACKNOWLEDGEMENTS

First of all, I would like to thank and praise the Lord Jesus Almighty for making it possible in every way for me to complete my PhD programme successfully. Without His grace, guidance, wisdom and mercy, I would have never been able to make it through this far. I would like to extend my deepest appreciation and gratitude to my wonderful supervisors, Professor Datin Dr. Sri Nurestri Abdul Malek and Associate Professor Dr. Norhaniza Aminudin for their invaluable guidances and for always leading me in the right way throughout this project. I would also like to express my sincere thanks to the Institute of Biological Sciences, Faculty of Science and the staffs for the support and help. I am grateful and thankful to my lab mates from Functional Molecules HIR Lab (ISB) for making the whole experience a fun and knowledgeable one. I would like to express my sincere thanks to Dr. Gautam Sethi and Pharmacology Team in NUS for helping and accomodating me to conduct my research in their lab. I also thank Mr. Slamet Wahyono from Tawangmangu, Jogjakarta, Indonesia for helping in the verification of plant. My deepest appreciation also to the Ministry of Higher Education for granting the scholarship of MyPhD under the MyBrain15 Scheme that kept me financially sound. IPPP played an equally important role in enabling me to conduct my project without any difficulty by granting me PPP grant (PG200/2014B). I also appreciate the encouragements from my brothers (Winston, Patrick, Joe and Jack) and their family. Finally, I would like to dedicate this thesis to my dad, Mr. Moses Richardson who has always inspired me to learn and achieve more in life. He has always been present to give sound advices and encouragements when the journey was rough and to rejoice together in good times and also to pray for success in every step. It is true that they say behind every successful woman, there is a truly amazing father who believed in his daughter. To my late mom (Madam. S. Rani Kanagabai) whom I always love, I know you would be smiling in heaven that I have finally completed this journey.

TABLE OF CONTENTS

LIST OF FIGURES

LIST OF TABLES

LIST OF SYMBOLS AND ABBREVIATIONS

Abbreviations	Description
α	alpha
5-BrdUTP	5-Bromo-2′-deoxyuridine 5′-triphosphate
°C	Degree celcius
δ	Delta (represents chemical shift in NMR data)
γ	gamma
%	percentage
^{1}H NMR	Proton NMR
A549	Non-small cell human lung carcinoma
ACN	Acetonitrile
AIF	Apoptosis-inducing factor
Akt	Protein kinase B
ALS	Automatic Liquid Sampler
ANOVA	Analysis of variance
Apaf-1	Apoptotic proteases activating factor 1 protein
APS	Ammonium persulphate
ATCC	American type culture collection
ATP	Adenosine triphosphate
Bak	BCL-2 homologous antagonist/killer
Bax	BCL2-associated X protein
BCL-2	B-cell CLL/lymphoma 2
Bcl-xL	B-cell lymphoma extra-large
BH3	Bcl-2 homology 3
BID	BH3-interacting domain death agonist

BIR	Baculovirus inhibitor of apoptosis protein repeat
bp	Base-pair
BrdUTP	Bromodeoxyuridine triphosphate
BSA	Bovine serum albumin
CAM	Cell adhesion molecules
CaSki	Human cervical cancer cells
Caspases	Cysteinyl aspartate-specific proteases
CD95	Cluster of differentiation 95 receptor
Cdk	Cyclin dependent kinase
cFLIP	Cellular FLICE-like inhibitory protein
cIAP	Cellular inhibitor of apoptosis protein
CO_2	Carbon dioxide
COX-2	Cyclooxygenase-2 protein
CST	Cell Signalling Technologies
d (in NMR data)	Doublet peak
DAD	Diode array detector
dATP	Deoxyadenosine triphosphate
DCFH-DA	2'7'-dichlorofluorescein diacetate
dd (in NMR data)	Doublet doublet peak
ddd (in NMR data)	Doublet doublet doublet peak
Diablo	Direct IAP-binding protein with low pI
DISC	Death inducing signalling complex
DISC	Death-inducing signaling complex
DMBA	7,12-Dimethylbenz[a]anthracene
DMEM	Dulbecco's minimum essential media
DMSO	Dimethyl sulfoxide

DNA	Deoxyribonucleic acid
DR	Death receptor
DR4	Death receptor 4
DR5	Death receptor 5
DTT	Dithiothreitol
dUTP	deoxyuridine triphosphate
E1a	adenovirus early region 1A
ECL	Enhanced chemiluminescence
ECM	Extracellular matrix
EDTA	Ethylenediaminetetraacetic acid
EGFR	Epidermal growth factor receptor
EIMS	Electron ionization mass spectrometry
ELISA	Enzyme-linked immunosorbent assay
EMEM	Eagle's minimal essential medium
ER	Endoplasmic reticulum
ERK	Extracellular-signal regulated kinases
etc	*et cetera*
EtOAc	Ethyl acetate
EtOAc	Ethyl acetate
eV	electron Volt (unit)
FADD	Fas-associated protein with death domain
Fas	Apoptosis-stimulating fragment receptor
FasL	Fas Ligand
FBS	Feotal bovine serum
FBS	Feotal bovine serum
FC-AS	Fraction collector – Auto sampler

FITC	Fluorescein isothiocyanate
FL1	First fluorescence channel
g	gram
G1	Gap 1
G2	Gap 2
GCMS	Gas chromatography mass spectrometry
GLUT4	Isotype 4 of the glucose transporter protein
HCT-116	Human colon cancer cells
HCV	Hepatitis C virus
HEPES	4-(2-hydroxyethyl)-1-piperazineethanesulfonic acid
HIR	High impact research
HPLC	High performance liquid chromatography
HRP	Horseradish peroxidase
HRP	Horseradish peroxidase
Hz	Hertz
IAA	Iodoacetamide
IAPs	Inhibitor of apoptosis proteins
IC_{50}	Inhibitory concentration at half maximal
ICAM-1	Intercellular adhesion molecule 1
IKK	IκB kinase
IKK-α	Inhibitor of nuclear factor kappa-B kinase subunit alpha
IKK-β	Inhibitor of nuclear factor kappa-B kinase subunit beta
IKK-γ	Inhibitor of nuclear factor kappa-B kinase subunit gamma
IL6	Interleukin 6
IκBα	nuclear factor of kappa light polypeptide gene enhancer in B-cells inhibitor, alpha
J (NMR)	Joule

Jak	Janus kinase protein
JC-1	5,5’,6,6’-tetrachloro-1,1’,3,3’tetraethylbehzimidazolyl carbocyanine iodide
JNK	Jun amino-terminal kinases
kDa	Kilo Dalton
LL	Lower left
LR	Lower right
m	metre
M	Mitotic
m/z	mass-to-charge ratio
MAPK	Mitogen-activated protein kinase
Mcl-1	Myeloid cell leukemia 1 protein
MEK	Mitogen extracellular signal-regulated kinase
MEM	Minimum essential media
MeOH	Methanol
mHz	Mega Hertz
mm	milimetre
MMP	Mitochondrial membrane potential
MPT	Mitochondrial permeability transition
MRC 5	Normal human lung fibroblast
mRNA	messenger ribonucleic acid
MS	Mass spectrometry
mTOR	Mechanistic target of rapamycin
MTT	3-(4,5-dimethylthiazol-2-yl)-2,5-diphenyltetrazolium bromide
MW	Molecular weight
Myc	Myelocytomatosis oncogene cellular homolog protein

n.d.	no date
NaCl	Natrium chloride
$NaVO_4$	Sodium orthovanadate
NCR	National Cancer Registry
NEMO	NF-Kappa B essential modulator
NF-κB	Nuclear factor kappa-light chain- enhancer of activated B cells
NIST	National Institute of Standards and Technology
NMR	Nuclear magnetic resonance
NSCLC	Non-small cell lung carcinoma
pAkt	Phosphorylated protein kinase B
PARP	Poly ADP (Adenosine Diphosphate)-Ribose Polymerase
PBS	Phosphate buffered saline
pEGFR	Phosphorylated epidermal growth factor receptor
PFA	Paraformaldehyde
PGE1	Prostaglandin E2
pH	Potential hydrogen
PI	Propidium iodide
PI3K	Phosphatidylinositol-3-kinase
PMSF	Phenylmethyl-sulfonyl fluoride
ppm	Parts per million
pRB	Phosphorylated retinoblastoma
pRb	Phosphorylated retinoblastoma
PS	Phosphatidylserine
PTEN	Phosphatase and tensin homolog
Puma	p53-upregulated modulator of apoptosis
PUMA	p53 upregulated modulator of apoptosis

R. angustifolia	*Ruta angustifolia* Pers.
Ras	Rat sarcoma oncogene
Rb	Retinoblastoma
Rf	Retention factor
RIPA	Radioimmunoprecipitation assay
ROS	Reactive Oxygen Species
rpm	Revolutions per minute
RPMI	Roswell Park Memorial Institute
s (NMR)	singlet
S phase	Synthesis phase
SAPK	Stress-activated protein kinases
SCLC	Small cell lung carcinoma
SD	Standard deviation
SE	Standard error
SDS-PAGE	Sodium dodecyl sulfate polyacrylamide gel electrophoresis
Smac	Second mitochondria-derived activator of caspase
spp.	Plural of species
SPSS	Statistical package for the social sciences
SRB	Sulforhodamide
STAT3	Signal tranducer and activation of transcription 3
tBID	truncated BH3-interacting domain death agonist
TCA	Trichloroacetic acid
TCC	Thermostatted column compartment
TdT	Terminal deoxynucleotidyl transferase enzyme
TEMED	tetramethylethylenediamine
TLC	Thin layer chromatography

TNF	Tumor necrosis factor
TP53	Tumor protein p53
TRADD	Tumor necrosis factor receptor type-1 associated death domain
TRAIL	TNF-related apoptosis-inducing ligand
TUNEL	Terminal deoxynucleotidyl transferase dUTP nick end labeling
UL	Upper left
UR	Upper right
US	United States
USA	United States of America
UV	Ultraviolet
UVA	ultraviolet A
v/v	Volume over volume
VEGF	Vascular endothelial growth factor
XIAP	X-linked inhibitor of apoptosis protein

LIST OF APPENDICES

CHAPTER 1: INTRODUCTION

1.1 Introduction

Natural products have been the most successful source of drugs ever and the most important natural sources have been plants (Tulp et al., 2004). Plants, vegetables and herbs used as food and in the folk and traditional medicine have been accepted currently as one of the main source of cancer chemoprevention drug discovery and development (Nascimento et al., 2006). Herbal plants and plant-derived medicines have been used as a source of potential anticancer agents in traditional cultures worldwide and have become increasingly popular in modern society (Tang et al., 2010).

Cancer is a disease in which disorder occurs in the normal processes of cell division, which are controlled by the genetic material (DNA) of the cell. There are few factors that have been implicated as the cause of cancer and this includes viruses, chemical carcinogens, chromosomal rearrangement, tumor suppressor genes, or spontaneous transformation. The transformation of a normal cell into a cancerous cell is believed to proceed through many stages over a number of years or even decades. The stages of carcinogenesis involve initiation, promotion, and progression (Reddy et al., 2003).

In the last decade, cancer research has contributed towards our understanding on cancer biology and cancer genetics. One of the most important finding is the realization that apoptosis and genes that control it has great effect on the malignant phenotype (Lowe et al., 2000). Defective apoptosis shows a major causative factor in the development and progression of cancer (Kasibhatla et al., 2003). A characteristic of cancer is that its resistance towards apoptosis that contributes to the non-effectiveness of cytotoxic drug to kill cancer cells (Ho et al., 2013). Apoptosis or more commonly known as programmed cell death, functions in tissue development and homeostasis

which is shown by a series of morphological and biochemical changes. These changes include nuclear condensation, DNA fragmentation, membrane blebbing, phosphatidylserine externalization and loss of mitochondrial membrane potential (Lowe et al., 2000). An important role in apoptosis is played by mitochondria. A loss in the mitochondrial potential would result in translocation of proapoptotic Bax to the mitochondria and release of cytochrome c into the cytosol which would initiate the caspase cascading. The majority of chemotherapeutic agents including radiation employs the apoptotic pathway to initiate cancer cell death. Resistance to standard chemotherapeutic methods also seems to be due to changes in the apoptotic pathway of cancer cells. Recent research on apoptosis has provided the basis for therapies that manipulates and uses apoptosis to treat cancer (Russo et al., 2013). An intense research effort is discovering the mechanisms of apoptosis that in next decade, this information may produce new strategies to manipulate apoptosis for therapeutic benefits (Lowe et al., 2000). Apoptosis provides a conceptual framework to link genetics with cancer therapy (Lowe et al., 2000).

Many reports have shown that phytochemicals from natural products induces apoptosis in cancer cell lines. Many have already been used in cancer chemoprevention and also cancer treatment. Based on that, extensive research have been made to identify new bioactive compounds from natural products through isolating apoptosis inducing agents from natural products and determining the apoptosis mechanisms (Pezzuto, 1997).

Ruta species is the most commonly used genus in Italian and Mediterranean medicine, economic botany and folk life (Pollio et al., 2008). *Ruta* species are sources of diverse classes of natural products such as flavonoids, alkaloids, essential oils, coumarins, phenols, saponins lignans, and triterpenes, with biological activities

including antifungal, antioxidant, phytotoxic, abortive, depressant, antidotal and anti-inflammatory (Amar et al., 2012). *Ruta angustifolia* Pers. belongs to the botanical family of Rutaceae. The native geographic distribution of *R.angustifolia* occurs in Mediterranean region. It is used for medicinal and culinary purposes since ancient times. It has been introduced in the Near East and India in Southeast Asia. The plant normally grows in mountainous areas i.e. about 1000 meters above sea level. Besides that, it is also cultivated as a pot plant in Malaysia and occasionally in Vietnam and Java for medicinal purposes (Wahyuni et al., 2014). The plant's decoction is commonly used to cure cramps, flatulence and fever (ROCHEM, 2012). On a recent research the cytotoxic effect of rutamarin isolated from the leaves of *R. angustifolia* on human colon carcinoma and it's cell death mechanism was described (Suhaimi et al., 2017).

Sulphorhodamine B or the SRB assay is one of the commonly prefered method to determine cytotoxicity of a test sample. This assay relies on the uptake of the negatively charged pink aminoxanthine dye, SRB by basic amino acids which are present in the cells. The greater the number of viable cells, there would be more amount of dye taken up to give greater absorbance value. SRB is sensitive, reproducible, simple, stable and gives better linearity (Houghton et al., 2007).

Apoptosis is a tightly controlled programmed cell death which has distinct biochemical and genetic pathways. It has important role in development and homeostasis of normal tissues. It contributes in elimination of unnecessary and unwanted cells to maintain a healthy balance between cell death and cell survival (Hassan et al., 2014). A defect in apoptosis would often lead to development and progression of cancer. The capability of tumor cells to evade apoptosis can play an important role in their resistance to conventional therapeutic regimens (Kasibhatla et al., 2003). Defects in apoptosis is an important factor in progression of cancer apart

from role that is played by the protooncogenes in activating cancer cell proliferation. Many deregulated oncoproteins that drive cell division also triggers apoptosis (e.g. Myc, E1a and Cyclin-D1). Non-cancerous cells has DNA repair mechanisms that could trigger cell suicide as defense mechanism in eliminating cells which are genetically unstable (Hassan et al., 2014).

Cells undergoing apoptosis are characterised by cell shrinkage, blebbing of plasma membrane, and maintenance of organelle integrity, chromatin condensation and fragmentation of DNA, followed by programmed removal of dead cells by phagocytes. It is like a "suicide" program but does not cause any damage to the surrounding tissues. Apoptosis has been subclassified into two types of death pathways, namely, the extrinsic pathway and the mitochondria-mediated pathway (Indran et al., 2011). All pathways of apoptosis converge upon the activation of caspases, which are a family of cysteine proteases that orchestrate the efficient and noninflammatory demolition of cells. Two main pathways leading to caspase activation have been well characterized i.e. the extrinsic route initiated by cell surface receptors leading directly to caspase 8 activation and the intrinsic path that is regulated by the mitochondria (Suen et al., 2008).

Apoptotic characteristics could be determined by various experiments as proposed. One of the biochemical hallmarks of the apoptosis is the nuclear DNA fragmentation and this could be determined by TUNEL (terminal deoxynucleotidyl transferase dUTP nick end labeling) assay. This technique allows detection of apoptotic cells by labelling the free end of apoptotic DNA with a marker which can be measured by flow cytometer. Hoechst 33342/PI double staining was used to identify the morphological changes in apoptotic nuclei. Morphological changes associated with apoptotic cell death include nuclear shrinkage, chromosome condensation, and appearance of apoptotic bodies. Reactive oxygen species (ROS) are widely generated in biological systems. Due

to this, humans have evolved antioxidant defence systems that limit their production. Intracellular production of active oxygen species such as •OH, O_2^- and H_2O_2 is associated with the arrest of cell proliferation. Similarly, generation of oxidative stress in response to various external stimuli has been implicated in the activation of transcription factors and to the triggering of apoptosis (Matés et al., 2000). It was described that ROS and the mitochondria play a major role in apoptosis induction under both physiologic and pathologic conditions (Simon et al., 2000). The amount of ROS in treated cells were determined by using the 2′,7′-Dichlorofluorescin diacetate (DCFH-DA) dye. Mitochondrial dysfunction such as loss of mitochondrial membrane potential is an early apoptotic event that happens following induction of apoptosis. JC-1 assay is performed to check the change of mitochondrial membrane potential. JC-1 is a dye which is widely used to detect mitochondrial depolarization which occurs in the early stages of apoptosis. In healthy cells, the mitochondrion has a high mitochondrial membrane potential and JC-1 would form J-aggregates and emit red fluorescence. During apoptosis, the mitochondrial membrane potential decreases and the JC-1 remain in monomeric form and emit green fluorescence. The ratio of red to green fluorescence can measure high to low mitochondrial membrane potential and the images can be captured using a fluorescence microscope. Other than that, Annexin V/PI staining was done to confirm the early and late stages of apoptosis. Annexin V is a phosphatidylserine (PS) binding protein while PI is a DNA-binding dye and this dual staining analyses the externalization of phosphatidylserine (PS) from the inner to the outer leaflet of membranes during the early phase of apoptosis. Hence, Annexin V/PI could be used as a marker to identify apoptosis. Caspases have found to be important mediators of apoptosis induced by various apoptotic stimuli. Caspases are aspartate-directed cysteine proteases that play an important role in the initiation and execution of apoptosis, necrosis and inflammation. Caspases activate other downstream caspases that

leads to execution stage of apoptosis. In apoptosis study, cell lysates are analyzed for the activation for caspase 3, caspase 8 and caspase 9 after treatment with *R. angustifolia* samples. As for the cell cycle arrest analysis, it is done to assess the distribution of cells in different phases of cell cycle. It determines at which phase the cell cycle progression is inhibited. If cell cycle is arrested, simultaneously cell proliferation would be halted and this could lead to apoptosis.

Protein expression studies gives an insight on the effect of a certain test material on the expression of proteins in a cell. This enables us to understand on the effect of the compound on the molecular pathways. Proteomic characteristics seems to be a more realistic platform for identification of cancer-related alterations in molecular and signalling pathways. This could hugely contribute towards understanding the carcinogenic developments (Martinkova et al., 2009). Western blot analysis was done to determine the expression of cancer related proteins on human cancer cell line treated with the active constituent which was isolated from *R. angustifolia.* Western blotting is a well known technique which has been used for more than 30 years to detect protein target in a complex sample. Over the past three decades, the sensitivity, reproducibility, and flexibility of the corresponding indicator systems have grown significantly (Taylor et al., 2014). The changes and effect in the expression in cancer related proteins when treated with the active constituents is studied.

Metastasis is the main cause of death in cancer patients, the molecular and cellular processes underlying metastasis continue to be a major focus of cancer research (Pouliot et al., 2000). It includes four main steps which is detachment of cancer cells from primary loci, entry of the cancer cells into circulation which is also known as intravasation, exit from the circulation which is also known as extravasation and finally the survival and growth in a distant organ. Metastasis is generally a slow process and

often revealed only after years of latency (Mohanty et al., 2010). Metastasis initiating from a solid tumor undergoes complex multistep process. Proliferating neoplastic cells would first breach the basement membrane and migrate away from the primary tumor environment to invade the surrounding stroma and enter the vasculature. After entering circulation, tumor would arrest in capillary beds and extravasate into secondary sites and colonize a distant organ. The survivability depend on the ability of the tumor cells to colonize, proliferate and promote vascularization in order to give rise to secondary tumor. Each of the step offers potential therapeutic intervention (Pouliot et al., 2000). The ability of the selected extracts and active constituent from *R. angustifolia* to inhibit the metastatic process was researched upon. Various *in vitro* assays to measure the ability of the test samples to inhibit the cell attachment, migration, invasion, adherance and to suppress certain proteins involved in metastasis were studied.

Hence, the hypothesis that *R. angustifolia* may possess chemotherapeutic property in the prevention and treatment of cancer was derived and in the present study, *R. angustifolia* was investigated for its cytotoxicity, apoptosis inducing activities, chemical constituents based on bioassay-guided fractionation, effects on the protein expression of a selected cell line and its anti-metastatic property. The biochemical steps linking the cytotoxic active chemical constituents of *R. angustifolia* to the apoptotic process in human cancer cells and also its anti-metastatic property were investigated. The findings obtained from the study will certainly provide some scientific validation on the use of *R. angustifolia* in the treatment of cancer.

1.2 Research Objectives

This study embarks on the following objectives:

i. To evaluate the *in vitro* cytotoxic activity of *R. angustifolia* extracts on selected human cancer cell lines using SRB assay and the active extract is determined.
ii. To isolate and identify the chemical constituents from the active extracts of *R. angustifolia* using chromatography techniques.
iii. To assess the *in vitro* cytotoxic activities of the identified chemical constituents on selected human cancer cell lines using SRB assay.
iv. To investigate the induction of apoptosis by the active compounds using relevant assays.
v. To investigate apoptotic related proteins and determine the effect of the active compound towards expression of protein on cancer related pathways.
vi. To determine the effect of the selected extracts of *R. angustifolia* and the active compound on their ability to inhibit metastasis of the selected cancer cell line.

By achieving the research objectives, this research would be able to provide comprehension and knowledge on the potential of the plant and its active constituent as a chemotherapeutic agent and the cancer related molecular pathways that it modulates.

CHAPTER 2: LITERATURE REVIEW

2.1 Natural Products

Natural products have been the most successful source of drugs ever and the most important natural sources have been plants (Tulp et al., 2004). Plants, vegetables and herbs used as food and in the folk and traditional medicine have been accepted currently as one of the main source of cancer chemoprevention drug discovery and development (Nascimento et al., 2006). Herbal plants and plant-derived medicines have been used as a source of potential anticancer agents in traditional cultures worldwide and have become increasingly popular in modern society (Tang et al., 2010). Natural products have served as the primary source of starting material in pharmaceutical discovery over the past century. Initially, crude formulations have been used however with the advancement of technology, drug formulation are purified and is more targetted. The chemical compounds which were identified from natural products are normally novel and complex in their structure which enables them to be more potent in their interactions and could act specifically on the target and this could enhance the survivability and also the competitiveness of an organism (Mishra et al., 2011). Analysis of small molecules natural products which has been developed into drugs generally show that they would follow the Lipinski's Rule of Five (Harvey, 2008). Is a rule to evaluate if a chemical compound with certain pharmacological or biological activity has properties that would make it likely to be orally active drug in humans. The rule was formulated by Christopher A Lipinski in 1997 based on observation that all drugs are relatively small and lipohilic molecules. The rule describes that ,

1. Not more than 5 hydrogen bond donors which is nitrogen or oxygen atoms with one or more hydrogen atoms .

2. Not more than 10 hydrogen bond acceptors (nitrogen or oxygen atoms)

3. A molecular mass less than 500 daltons

4. An octanol water partition coefficient log P not greater than 5

It is to be noted that all numbers are multiple of five which is origin of the rule's name (McChesney et al., 2007). Natural products are on average, more readily absorbed than synthetic drugs (Harvey, 2008).

Although there are many advantages in exploiting natural products in drug discovery, there are some disadvantages in which leads to the use of it in large pharmaceutical companies. The difficulties in access and supply, complexities of natural product chemistry and slowness of working with natural products and intellectual property rights concerns are some of the disadvantages. Naturally occuring compounds which are isolated may have poor stability, solubility, bioavailability and not abiding the Lipinski's Rule of Five.

According to Lam (2007), natural products discovery has several drawbacks as compared to synthetic chemical drug discovery. These drawbacks includes the factor in which natural products are obtained in small quantities and present in a mixture of extract which requires effort for further purification. To build a high quality natural product library would require skill set that is generally not available in industries. Natural products are also found to be structurally more complex and thus modification of natural products using organic chemistry is often challenging and not preferred by combinatorial chemists.

However, all these problems are being overcomed by the use of technology. This includes using new approaches in fractionation techniques to isolate and purify natural products (e.g. counter-current chromatography) and in analytical techniques to determine the chemical structures, screening of natural product mixtures is now more

compatible with the expected timescale of high-throughput screening. Isolated and structurally characterised natural products are often extremely time consuming and also expensive to create hence there is ideas to screen mixtures of compounds obtained from plant extracts and microbial broths. Natural products are used as an inspiration in creating more synthetic highly diverse chemical libraries. This approach is called as biology-orientated synthesis. High throughput screening is now vastly available however the cost that incurs in screening large collection of compounds could be enormous. This brings us to a more sensible approach of using virtual screening which is also known as *in silico* screening approach which could filter down the number of compounds that are potential to be tested in the wet lab. These alternative approaches are being explored in effort to increase the speed and efficiency with which natural products can be applied to drug discovery (Harvey, 2008).

2.1.1 Natural Products in Cancer

Natural products are the most important anti-cancer agents. About 75% of anti-tumor compounds that are used in medicine are either natural products or related to them (Demain et al., 2011) A detailed report published in 2016 reported that only 17% of the total numbers of small-molecule anticancer drugs available in the year 1981-2010 were purely synthetic. The remaining 83% were either natural products or were inspired by natural products (Newman et al., 2016). Natural products constitute a large portion of pharmaceutical component at the current time. More than 60% of the current anticancer drugs that are currently in clinical use were attained in one way or another from natural products from plants, microorganisms and marine organisms (Rayan et al., 2017). These includes Taxol, vinblastine and camptothecin that are some of the prominent chemotherapy drugs (Cragg et al., 2016). Polysaccharides, saponins, alkaloids, flavonoids, terpenoids and others have been found as natural bioactive compounds with

potent anticancer activity. The anti cancer property of the majority of the natural products are through regulation of immune function, induction of apoptosis or autophagy and cell proliferation inhibition (Rayan et al., 2017). Prevention, surgery, radiotherapy are the common treatment for early stage cancer. In treatment of metastatic and advance stage cancer, chemotherapy is one of the main treatment options. Many of the advances in chemotherapy are due to the discovery of biologically active natural products (Cragg et al., 2016). Side effects and toxicity is the major disadvantages of conventional chemotherapy and radiotherapy in the treatment of cancer. Many synthetic anti-cancer drugs have caused harms such as suppression of immune system to the patients (Rayan et al., 2017). The rate of morbidity and mortality of cancer has given huge economic burden and this calls for effective strategies to preferably prevent the disease. Discovery of vaccines to prevent the occurance of cervical cancer and liver cancer offers promise. Vaccines to completely eradicate cancer has yet to be discovered however certain natural products which could inhibit the formation of cancer cells such as a separate class of aromatase inhibitors known as raloxifene in preventation of breast cancer. Finasteride has shown assurance in prevention of prostate cancer (Cragg et al., 2016). Chemoprevention through phytochemicals is acquiring interest as it is inexpensive, readily available, and is an accessible approach in cancer control and management. Various studies have already shown that high dietary consumption of vegetables and fruits could reduce the risk of cancer (Rajesh et al., 2015).

2.1.2 Common Drugs Derived from Natural Products for Cancer

Drugs in the early days came from plants, however the modern drug discovery has developed into synthesis of synthetic compounds and monoclonal antibodies. According to natural product experts, the best drugs leads are found in natural products (Brower, 2008). Presently there are a few compounds derived from plant products that are being

used in the treatment of cancer. Commercially, there are 4 classes of plant derived anti-cancer agents. These include vinca alkaloids such as vincristine and vinblastine, epipodophyllotoxins such as teniposide and etoposide, camptothecin derivatives such as camptotecin and irinotecan and taxanes such as paclitaxel and docetaxel (Desai et al., 2008). Besides terrestrial plants, various other natural products also have provided starting materials in the development of cancer chemotherapeutic agents. Bleomycin, doxorubicin and staurosporin were derived from microbes. Epothilone B was derived from slime molds. Halichondrin B and dolastatins were derived from marine environment (Cragg et al., 2016).

Taxol or originally derived compound paclitaxel, which is a diterpene alkaloid, has been a excellent anti-tumor molecule. It was originally isolated from the bark of Pacific yew tree (*Taxus brevifolia*) (Demain et al., 2011). It exerts its activity by inhibiting tubulin formation during cell cycle (Brower, 2008). The limitation with taxol is that it takes six trees of 100 yeas of age to treat a cancer patient. Currently, it is being produced by plant cell culture or through semisynthesis of taxoid (Demain et al., 2011).

Camptothecin was first isolated from the bark of *Camptotheca acuminata,* which is also commonly known as Happy tree. It is a naturally occuring pentacyclic quinoline alkaloid which possesses high cytotoxicity towards cancer cells. It acts through inhibiting the DNA topoisomerase I, however, it suffers from several limitations such as poor solubility and inactivity at physiological conditions that prevents full clinical utilization. To overcome these issues, various derivatives of campthotecin were created and only 2 compounds were approved for clinical use i.e. irinotecan and topotecan. Irinotecan has been used primarily for the treatment of metastatic colorectal cancer. Topotecan is used in the treatment of cervical cancer, ovarian cancer and non-small cell lung carcinoma (Venditto et al., 2010).

Vinca monoterpene indole alkaloids such as vincristine and vinblastine were isolated from Madagascar periwinkle plant (*Catharanthus roseus*) (Demain et al., 2011). It is a popular ornamental plant, planted at homes across the world. These compounds act as inhibitors of microtubule formation during cell cycle that inhibits the development of mitotic spindle (Brower, 2008) and in tumor cells they inhibit DNA repair and RNA synthesis mechanisms which results in inhibition of DNA-dependent RNA polymerase (Keglevich et al., 2012). Vincristine has been used for treatment of childhood acute lymphoblastic leukaemia and non-Hodgkin lymphomas. It exhibits an outcome of increasing the chance of surviving from 10% to 95%. Vinblastine acts via inhibition of cell division and is used as a combination with other chemotherapeutic drugs against lymphomas, lung, breast, bladder, testicular, and ovarian cancers (Caputi, 2018). Madagascar periwinkle also produces a class of anti cancer agents which is known as serpentines (Demain et al., 2011).

Clinically effective etoposide and tenoside was derived from podophyllotoxin, which is a toxin that is found in American Mayapple/American Mandrake (*Podophyllum peltatum*), which is a perennial herb. The plant is commonly found in eastern US and the Himalayas (Brower, 2008). It is used in the treatment of various types of cancer especially in small cell lung cancer and testicular cancer. It acts by targetting DNA topoisomerase II which is an important enzyme for cancer cells to divide, this in which causes DNA breaks. It also acts by affecting metabolism of cell (Montecucco et al., 2015).

Besides plant source, various anti-cancer drugs have also been derived from marine organisms. One of the examples is dolastatins. It was isolated from extracts of the marine sea hare *Dolabella auricularia,* which is a shell-less mollusk. It acts through the inhibition of mitosis. Dolastatin 10 and 15 are small peptides that showed interaction and inhibition in tubulin assembly. Both these compounds are excellent cell growth

inhibitors (Aherne et al., 1996). Dolastatins have been reported to show cytotoxicity with low doses against breast cancer, lung cancer, leukemia and lymphomas (Sato et al., 2007).

Apart from plants and marine organisms, microorganisms contribute a repertoire of cytotoxic compounds in the treatment of cancer. Antibiotics, which have anti-tumor effects, are among the most important chemotherapeutic agents. These include members of the actinomycin, ansamycin, anthracycline, bleomycin, epothilone, and staurosporin classes (Cragg et al., 2016). Bleomycin, which is a glycopeptide, originally isolated from the fungus *Streptomyces verticillus*. It is used in the treatment of curable diseases such as germinative tumors and Hodgkin's lymphoma. Bleomycin exerts its activity by forming free radicals, which caused DNA strand breaks and then cause cell death to cancer cells. This compound also causes oxidative degradation to cellular RNAses (Reinert et al., 2013).

Rapamycin, which is, produced via fermentation of a strain of *Streptomyces hygroscopicus* was isolated from soil samples in Rapa Nui (Easter Island). Rapamycin was found to inhibit the mTOR (mammalian target of rapamycin) with high specificity. The mTOR pathway regulates cell growth, proliferation, metabolism and survival. Abnormalities in this pathway have been observed in most of cancers and thus this pathway has been studied extensively for targetted therapy (Mukhopadhyay et al., 2016).

Besides these popular compounds, there are also many other derivatives from natural products such as yondelis isolated from sea squirt has the ability to interfere with cell division and blocks transcription of cell. Combretastatins that are isolated from South African bush willow has the capacity to disrupt tumor vasculature (Brower, 2008). Nature promises vast source of potential chemotherapeutic compounds due to its

biodiversity and chemical diversity that are found in millions of species of plants, animals, marine organisms and microorganisms.

2.2 Rutaceae Family

The Rutaceae family, also named as Rutaceae, belongs to the order of Sapindales with about 150 genera and over 1600 species. They are hugely distributed throughout the tropical and temperate regions of the globe, being more abundant in tropical America, South Africa and Australia (Orlanda et al., 2015). The Rutaceae family is also commonly known as rue or citrus family. This family consists of herbs, shrubs, small trees that is able to grow in all parts of the world. The plants from this family is known for its medicinal property in treating snake bites, stomatitis, rheumatism, bronchitis and many other diseases. This plant family is a source of furanocoumarines, furochinoline alkaloids, phenolic-structured compounds, terpenes and others. Some of the main compounds isolated from this family are skimmianine, kokusaginine and dictamnine (Adamska-Szewczyk et al., 2016). The plants in this family usually has strong foetid smell which is due to the presence of pellucid gland (Benazir et al., 2011). The genus which has economical importance in this family is Citrus. The genus Citrus includes oranges, lemon, grapefruit and lime. It is distributed worldwide but optimally grow in tropical and subtropical climatical conditions. It normally has compound or alternate leaves (Akalin et al., 2003).

2.3 The Ruta Genus

Ruta which is commonly known as rue is a genus consisting of strongly scented evergreen shrubs that could grow up to 20-60 cm tall in the Rutaceae family. There are probably about 40 species in this genus with *R. graveolens* being the most prominent. Among other members of this genus includes *R. chalepensis*, *R. angustifolia* and *R. montana,* which are commonly studied and researched upon. It is native to the

Mediterranean region and present in traditional medicine of this region since Antiquity. The three most diffused species *R. chalepensis* L., *R. graveolens* L., and *R. montana* (L.) L., are morphologically poorly differentiated and were probably interchangeably used during Antiquity (Pollio et al., 2008).

Traditionally, *Ruta* species were used in medical preparations by Hippocratic physicians especially as an abortifacient and emmenagogue. The leaves, roots and seeds were administered for internal use after been soaked in wine or mixed with honey or its derivatives (Pollio et al., 2008). *Ruta* species is the most commonly used genus in Italian and Mediterranean medicine, economic botany and folk life (Pollio et al., 2008). *Ruta* species is a source of diverse classes of natural products such as flavonoids, alkaloids, essential oils, coumarins, phenols, saponins lignans, and triterpenes, with biological activities including antifungal, antioxidant, phytotoxic, abortive, depressant, antidotal and anti-inflammatory (Amar et al., 2012). Rue is also commonly used as an insect repellant. The juice of the plant may be applied to the skin to repel spiders, wasps, flies and mosquitoes. It is also traditionally used in home gardens to prevent pests from entering (Miguel, 2003).

2.3.1 *Ruta graveolens*, the common rue

It is one of the oldest garden plants that was planted for medicinal use. It was introduced in England by the Romans as it was commonly used in the ancient times to ward of insects and fleas. It was one of the ingredient in the famous 'Vinegar of Four Thieves' which was used to prevent plague during the Medieval times. This plant was also believed to be a magical herb which was used to ward of evil influences. It is also commonly known as 'Herb of Grace" as its leaves tied together was used to sprinkle holy water in Catholic churches. Rue was also believed to improve eyesight and creativity and the leaves were regularly eaten by Michelangelo and Leornado Da Vinci.

Other than that, the legend of rue lives on in playing cards where the symbol representing clubs was said to be inspired by the leaf of a rue (Annie's Remedy, n.d.).

Ruta graveolens is a medicinal and culinary plant that commonly grows in Mediterranean region of southern Europe and northern Africa (Fadlalla et al., 2011). It is a medicinal plant which is traditionally used for various ailments such as emmenagogue, ecbolic, antihelminthic and antispasmodic, menstrual disorders, skin inflammation, cramps, headache since ancient times (Orlanda et al., 2015). Pharmacological trials showed *R. graveolens* has antihelmintic, abortive, antiparasitic, anti-inflammatory, anti-diarrheic, anti-rheumatic, anti-febrile, antiulcer, vermicide repellent, anti-diabetics, anti-rheumatism and antimicrobial properties (Orlanda et al., 2015). The plant was also found to exhibit anti-fungal, antibacterial and hypotensive properties however it was reported to be toxic at higher concentrations (Preethi et al., 2006).

The plant has been found to contain quinolone alkaloids, flavonoids particularly rutin and quercetin, glycosides and furanocoumarins such as psoralens and methoxy psoralens. Phyto-constituents alcohol, aliphatic ketones and acids were isolated from its volatile oil. The volatile oil from *R. graveolens* are used as flavoring agent and also for therapeutic uses (Tarique et al., 2016). The plant has also been commonly used to season some food items such as soup, cheese, butter, coffee, and tea (Fadlalla et al., 2011). It has been approved by Food and Drug Administration (FDA) as a flavouring agent.

Phototoxicity is a condition where skin inflammatory reaction occurs as a result of exposure to a chemical in combination with light radiation exposure. *Ruta graveolens*, commonly known as rue, has been reported in numerous publications as a substance causing phototoxicity reactions (Zayas-Pinedo et al., 2014). This is mainly due to

furanocoumarin compounds that is present in the plant. *R. graveolens* has several furanocoumarins which could contribute to this effect, namely bergapten, psoralen, xanthoxanthin, xanthotoxin, isopimpenilline, and rutamarin and methoxalen (Stansbury, 2011). Furanocoumarins are excited upon exposure to ultraviolet radiation type A through phototoxic mechanism. The photoxic mechanism results in formation of ROS that causes epidermal, dermal and endothelial cell damage. Application of a high concentration of rue infusion and subsequent sun exposure causes the sudden onset of symptoms, since furocoumarins are fat soluble and penetrate more readily (Arias-Santiago et al., 2009). Previous reseach has shown that furanochromes (linear furanocoumarins) could form photoadducts with DNA of microbes and this could lead to treatment of dematoses such as psoriasis and vitiligo (Stansbury, 2011). Since its development in 1974, oral methoxsalen photochemotherapy, which is, psoralen and ultraviolet-A light (PUVA), has been widely used to treat patients with psoriasis (Stern et al., 1998). Patients with psoriasis ingested psoralens for their photosensitizing effects and spent some time each day under UV light to induce a slight sunburn. The sunburn would clear psoriatic lesions and induce the regenerative and immunomodulatory processes of the skin. Ultraviolet A is classified to be less harmful to the skin than other frequencies of the UV spectrum, such as UV-B. PUVA therapy has also been noted to be effective for treating vitiligo. It is a condition where patches of the skin lose their pigment due to an underlying fungal infection or autoimmune condition affecting melanocytes within the dermis (Stansbury, 2011).

Figure 2.1: A diagram showing morphology of common rue (Image excerpted from *Ruta graveolens*, n.d.)

2.3.2 *Ruta angustifolia*, the Egyptian rue

Ruta angustifolia belongs to the botanical family of Rutaceae. *R. angustifolia* is locally known as 'garuda' or 'sadal' in Malaysia, 'Inggu', 'godong minggu' or 'aruda' in Indonesia, rue or herb of grace in English, 'luru' in Vietnam, 'aruvatham pachai' in tamil and sudabu in Hindi. The native geographic distribution of *R.angustifolia* occurs in Mediterranean region. It is used for medicinal and culinary purposes since ancient times. Many cultures use the leaves of the plant as a flavouring agent in their cuisine. Since the plant has a bitter taste, the right amount used in as flavouring is said to give the cuisine a unique taste (Venkateshwaran, 2016). It has been introduced in the Near East and India in Southeast Asia. The plant normally grows in mountainous areas i.e. about 1000 meters above sea level. Besides that, it is also cultivated as a pot plant in

Malaysia and occasionally in Vietnam and Java for medicinal purposes (*Ruta angustifolia* Pers, n.d.). Interestingly, planting the plant at home was found to repel the presence of dogs and cats as the leaves of the plant has a foetid smell (Venkateshwaran, 2016). The leaves also have strong insectidal property (Venkateshwaran, 2016) and are commonly tied on newborn's hands to keep insects away (personal communication). It contains coumarin, alkaloid and flavonoid compounds. Angustifolin and four aromatic derivatives, moskachan A, B, C and D, have been identified as constituents of *R. angustifolia* (Wahyuni et al., 2014). The plant's decoction was commonly used to cure cramps, flatulence and fever (ROCHEM, 2012).

It is a perennial herb and woody at the base and it grows up to 0.3 to 1.5 m. It has compound leaves, length 8-20 mm. width 2-6 mm, and its light green in color. The leaves are arranged spirally, ovate to oblong-obovate in outline. It measures 4-15 cm x 2-9 cm and obovate-lanceolate to narrow oblong which were about 8-14 mm x 1.5-3.5 mm. They are conspicuously pale bluish-green, crenate, translucent-punctate-glandular and strong smelling while the flower are shortly petiolate. The flowering period is normally between April to July. The plant reproduces through seeds and also grows through stem cuttings (ROCHEM, 2012). The plant has yellow flowers and gives a very strong foetid smell. The flower petals are yellow, finged with long conspicuous upstanding tooth like hairs. Fruits are globular with 4-5 sharp pointed lobes.

Traditionally, the plant is commonly used as an abortifacient, antihelmintic, emmenagogue and ophthalmic. It is use traditionally to stimulate menstruation by boiling the dried herb (28 g) with 3 cups of water till it reduces to 1 glass and then drinking it 3 times a day (Inggu, n.d.). A decoction of this plant has been traditionally used in treatment of paralysis, coughs, stomach aches and jaundice. In Indonesia, *R. angustifolia* has been known as traditional medicine for liver disease and jaundice.

Decoction of the plant is prepared by slow boiling the plant materials (leaves and stem) in water to dissolve the chemical materials. It is boiled until the water reduces to ½ and the resulting liquid which is referred as decoction is sieved and taken orally by the patient. In case the patient encounters difficulty in ingesting the decoction, a small amount of sugar is added to the decoction (Herbal Medicine, n.d.). Its leaves have also been commonly used to treat ear ache. The leaves are separated and is gently crushed with fingers, heated and placed inside the ear. *Ruta angustifolia* was also commonly used to treat toothache where the leaves of the plant is taken and rinsed with boiled water and crushed with finger and placed in the affected area and covered with cotton (Herbal Medicine, n.d.). The leaves from the plant can also be casually chewed to cure headaches (Annie's remedy, n.d.). Besides that, the juice from the leaves of *Ruta angustifolia* can also be used in treating dandruff with addition of rice and turmeric pounded together with water to form a paste to be applied to the affected area. Due to the reason where the plant produces a hot stingy feeling, excessive usage could cause inflamed skin and burning sensation. Its essential oil also has been traditionally applied on body parts to reduce pain. However the oil is hazardous if it is ingested and should never be taken orally. A preliminary study showed promising results on extracts of *R. angustifolia* as possessing cytotoxicity activity and could be further researched on (Suhaimi et al., 2017). Scientific research is yet to be conducted on the plant in this area of research and thus it would be a promising area of research to embark on.

(a)

(b)

(c)

(d)

(e)

Figure 2.2: Pictures of *Ruta angustifolia* Pers. (a) image showing the arial view of the plant (b) image showing the flowers of the plant (c) image showing the arial view of the leaves of the plant (d) image showing the lateral view of the plant (e) Image showing the flower buds and the seeds of the plant. Images are personal collection of Ms. Jaime Stella Moses Richardson

2.3.3 Previous Studies on *Ruta graveolens*

Ruta which is a homeopathic mixture from *Ruta graveolens* was found to kill brain cancer cells and induce the growth of normal peripheral blood lymphocytes. A study with fifteen patients diagnosed with intracranial tumors were treated with a combination of Ruta 6 and $Ca_3(PO_4)_2$. Within this group, 6 of the 7 glioma patients showed complete regression of tumors. *In vivo* and *in vitro* results showed induction of survival-signaling pathways in normal lymphocytes and induction of death-signaling pathways in brain cancer cells. Unlike the conventional chemotherapy which causes the death of normal cells apart from cancer cells, the combination of Ruta 6 and $Ca_3(PO_4)_2$ selectively kills glioma brain cancer cells and induces cell division in blood-forming cells in order to protect normal lymphocyte. It was found that it could be an excellent agent in treating human brain cancer (Pathak et al., 2003).

On another study, *Ruta graveolens* methanol extract was tested on colon (HCT-116), breast (MCF7) and prostate (PC3 and DU-145) cancer cells. The IC_{50} value of methanol extract of *R. graveolens* treated against various cancer cells for 24 hours was determined via the MTS assay. The methanol extract exhibited an IC_{50} value of 75 μg/ml against PC3 cells, 150 μg/ml on MCF7 cells, 200 μg/ml on HCT-116 cells and 300 μg/ml against DU-145 cells. PC3 was the most sensitive cells against the methanol extract. Colony formation in HCT-116, RKO and DU-145 cells were completely inhibited upon treatment with the methanol extract at a dose of 60 μg/ml. Further research showed that the cell cycle of the HCT-116, DU-145 and MCF7 cells were arrested at late S and G2/M phase and disruption in mitosis was also observed. The methanol extract was also found to activate the p53 tumor supressor factor and induces DNA damage response pathway in HCT-116 cells. AKT pathway was supressed upon treatment of the extract on DU-145 cells. The extract was also found to induce activation of caspase 3 in HCT-116 cells (Fadlalla et al., 2011).

In another study, the water extract of *R. graveolens* was found to show potent antitumoral activity in human gliomablastoma cells (U87MG, C6 and U138) and in undifferentiated cells from mouse embryonic brain. The treatment of A1 cells (mes c-myc cells) with 1 mg/ml *R. graveolens* extract was able to inhibit cell proliferation in proliferating A1 cells after 24h, and to induce cell death after 48 (viability decreases of about 120% as compared to vehicle treated conditions) and 72h (viability decreases of about 200% as compared to vehicle treated conditions). It was however, harmless to non-proliferating cells. It was found to be a potential tool in brain cancer theraphy (Gentile et al., 2015). Volatile oil from *R. graveolens* was found to exhibit antibacterial property on Gram-positive and Gram-negative bacteria. The antibacterial activity against Gram-positive and Gram-negative bacteria had inhibition zones of 8.30–25.60 mm to MIC values of 0.75–1.40 μg mL^{-1}, the most susceptible bacterium was *Bacillus cereus* and *Staphylococcus aureus* (Orlanda et al., 2015). An *in vivo* and *in vitro* study to evaluate the potential of ethanolic extract of *R. graveolens* revealed that the extract caused cell death of A375 (skin melanoma cells) through caspase-3 induced apoptosis and also Beclin-1 associated autophagy. Upon exposure to (44.80±0.81) μg/mL of the exthanolic extract of *R. graveolens* for 48 h, the cell viability was reduced to about 50%. Administration of this test sample to 7,12-dimethylbenz(a)anthracene (DMBA)-induced skin cancer in Swiss albino mice showed no acute or chronic toxicity, however showed significant reduction in the skin tumor. Anti-lipid peroxidative and antioxidant effects was also demonstrated by this test sample during induction of skin tumor by DMBA (Ghosh et al., 2015). Hydro-alcoholic extract of *R. graveolens* showed antiulcerogenic activity as it showed protective effect on gastric ulcers in rats where the protective effect of hydro-alcoholic extract of *R. graveolens* was tested against indomethacin and pylorus ligation-induced gastric ulcer. It was found that percent protection in the group treated with the highest concentration of the hydro-alcoholic

extract of *R. graveolens* (400 mg) was found to be 63.32 compared to indomethacin (Tarique et al., 2016). In another research, *R. graveolens* exhibited anti-inflammatory effect on murine machrophage cells (Raghav et al., 2006). Arborinine which was isolated from *R. graveolens* has showed good cytotoxicity against MCF7, HeLa and A431 cell lines. It showed an IC_{50} value of 1.8 μM against HeLa cervical cancer cells, 11.7 μM against MCF7 breast cancer cells and 13.0 μM against A431 skin cancer cells (Réthy et al., 2007).

2.3.4 Previous studies on *Ruta angustifolia*

There are several earlier studies that has been reported on *R. angustifolia*. In 1984, Del Castillo et al, has isolated angustifolin, a coumarin, from this plant and in 1986, a new shikimate metabolite was found from the aerial parts of *R. angustifolia*. These compounds were identified as moskachan A, B, C and D. Based on this study, it was discovered that moskachan compounds were found only in *Ruta angustifolia* Pers. and this could be an important chemotaxonomic marker to differentiate this species from *Ruta graveolens* (Del Castillo et al., 1986). In another study, chalepin and pseudane IX have been isolated from *R. angustifolia* and were found to stop the replication of hepatitis C virus. Strong anti-HCV activities were shown by chalepin and pseudane IX with IC_{50} values of 1.7 ± 0.5 and 1.4 ± 0.2 μg/ml, respectively (Wahyuni et al., 2014). The cytotoxic effect of rutamarin isolated from the leaves of *R. angustifolia* on human colon carcinoma and it's cell death mechanism was described by Suhaimi et al. (2017). Results by Suhaimi et al. (2017) described that the IC_{50} value for rutamarin treated on human colon carcinoma HT29 and HCT116 are 2.3 ± 0.1 and 2.8 ± 0.1 μg/ml, respectively at 72 hours incubation time. Rutamarin also did not show any toxicity towards the normal human colon fibroblast cells (CCD-18Co) with an IC_{50} value of >100.0 at the same incubation time. On the other hand, rutin which was also isolated

from *R. angustifolia* showed to be able to kill brain cancer cells. Ruta 6 combined with $Ca_3(PO_4)_2$ caused glioma brain cancer cells' death selectively and protects normal lymphocytes by inducing cell division in blood-forming cells (Pathak et al., 2003).

2.4 Chalepin

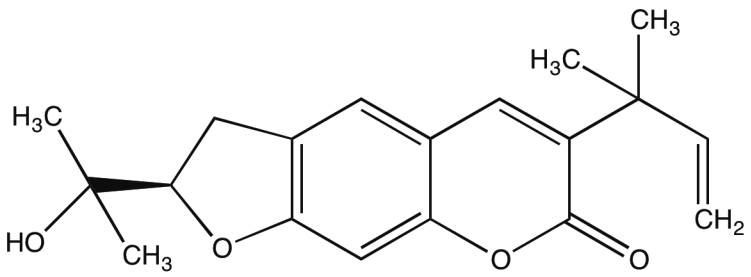

Figure 2.3: The molecular structure of chalepin

Chalepin is a compound with a molecular weight of 314.381 g/mol. It has a molecular formula of $C_{19}H_{22}O_4$ and it is a dihydrofuranocoumarin. It has a furan ring attached to coumarin. It is completely soluble in DMSO solution. It has a morphology of yellowish solid.

2.4.1 Previous research on the biological activity of chalepin

It was showed that chalepin isolated from *R. angustifolia* has the capability to inhibit the replication of hepatitis C virus with an IC_{50} value of 1.7 ± 0.5 μg/ml. It was also reported by Wahyuni et al. (2014) that chalepin showed good cytotoxicity against Huh7.5 hepatoma cells with an IC_{50} value of 14.0 ± 2.4 μg/ml. Chalepin was also found to possess anticoagulant property and causes necrosis to hepatic cells (Emerole et al., 1981). Besides that, on another report chalepin was found to cause mitochondrial respiration inhibition in rat liver mitochondria (Olorunsogo et al., 1983). Chalepin was

also found to exhibit trypanocidal activity on *Trypanosoma cruzi* with IC_{50} value of 64 μM (Pavão et al., 2002).

2.5 Cancer

Cancer has been given various definitions. It is a set of diseases characterized by unregulated cell growth leading to invasion of surrounding tissues and spread (metastasis) to other parts of the body (King, 2000).

Cancer is a leading cause of mortality worldwide and the failure of conventional chemotherapy to effect major reductions in the mortality indicates that new approaches are critically needed. The new science of chemoprevention has appeared as an attractive alternative to control malignancy. This is a pharmacological approach of intervention in order to arrest or reverse the process of carcinogenesis. In experimental chemoprevention studies, attempts are made to identify agents which could exhibit any or a combination of the following characteristics: (i) prevent the initiation of tumors, (ii) delay, or arrest the development of overt tumors, (iii) extend the cancer latency period, (iv) reduction in cancer mortality, metastasis, and (v) in some cases the prevention of recurrence of secondary tumors. At present, a major focus of research in chemoprevention of cancer includes the identification, characterization, and development of a new and safe cancer chemopreventive agent (Govinda et al., 2003). Large scale research on understanding the biological process where the normal cells transform to cancerous cells has been initiated in biomedical sciences for many years. However, total eradication of the disease or long term management strategies for metastatic cancer are as challenging today as it was 40 years ago when US president Richard Nixon declared a war on cancer. The biological process by which normal cells are transformed into malignant cancer cells has been the subject of a large research

effort in the biomedical sciences for many decades. Despite this research effort, cures or long-term management strategies for metastatic cancer are as challenging today as they were 40 years ago (Seyfried et al., 2010).

2.5.1 Hallmarks of cancer

Hanahan and Weinberg (2011), proposed that eight types of essential alterations in the cell physiology could be the generator of malignant cell growth. These eight alterations were described as the hallmarks of cancer. The hallmarks of cancer are :

1) self-sufficiency in growth signals,

2) insensitivity to growth inhibitory (antigrowth) signals,

3) evasion of programmed cell death (apoptosis),

4) limitless replicative potential,

5) sustained vascularity (angiogenesis), and

6) tissue invasion and metastasis

7) evasion of immune destruction

8) reprogramming of energy metabolism

These physiological characteristics are developed during tumor formation. It represents the success in breaking the anticancer mechanism that is programmed in cell and tissues. Most of the cancers and tumors share these eight capabilities. The complexity in defense mechanism against cancer cells is the reason why it is relatively rare for a cancer formation in average human lifetime (Hanahan et al., 2000).

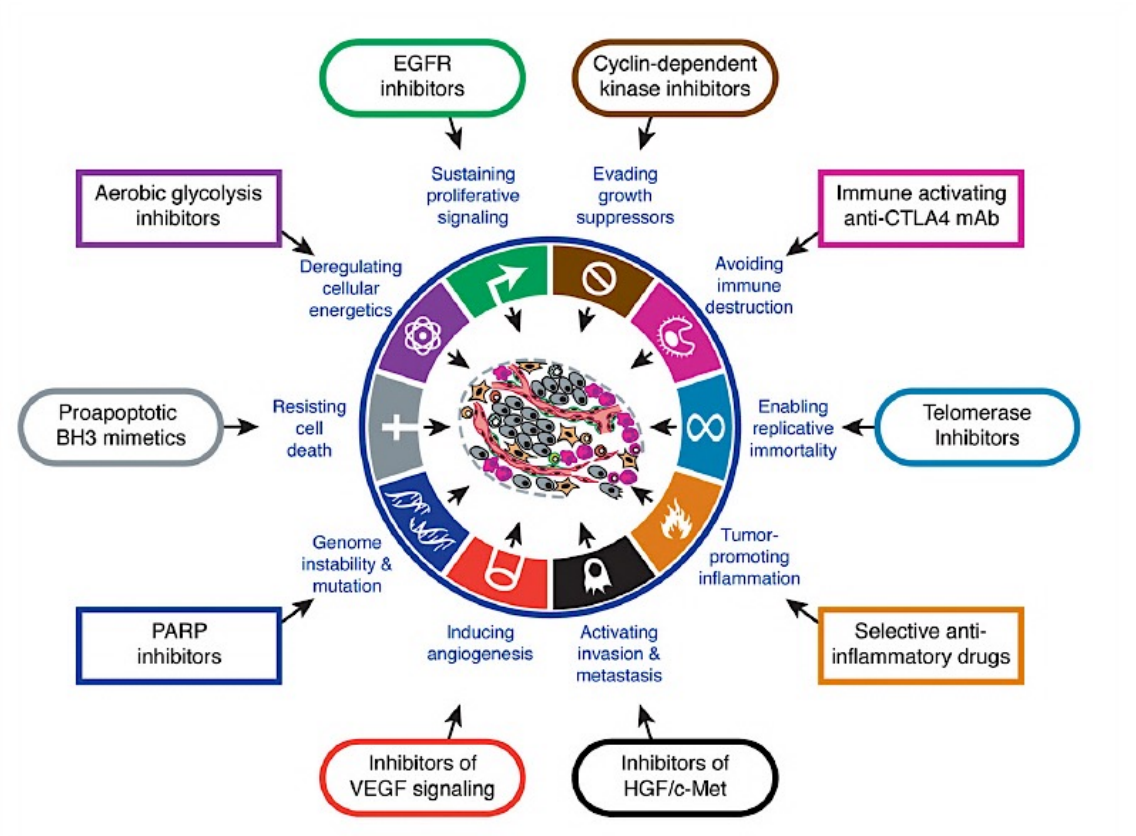

Figure 2.4: Therapeutic targetting hallmarks of cancer. Excerpted from Hanahan and Weinberg (2011).

The first hallmark that was described is the sustainability of proliferative signalling. Cancer cells may send signals to stimulate normal cells to supply cancer cells with various growth factors. Receptor signaling could also be chaotic by elevating the levels of receptor proteins displayed at the cancer cell surface. It was also found that continuous proliferative signalling is caused by somatic mutations in certain human tumors that predict constitutive activation of signaling circuits usually triggered by activated growth factor receptors. Defects in the negative feedback loop that controls and stops various types of signalling leads to uncontrolled proliferation.

The second hallmark described is the evading of growth suppressors. Although cancer cell induces various stimuli to excessively proliferate, it also must bypass various tumor suppressing stimulus that is present in order to survive. Two most prominent

tumor suppressors are RB (retinoblastoma associated) and TP53 proteins which regulates cell proliferation. Cell to cell contact suppresses further proliferation upon formation of dense population. This is known as “contact inhibition” which is important mechanism in maintaining tissue homeostasis. This mechanism is disrupted in tumorigenesis. The mechanism of this property is currently been researched on.

The third hallmark is the resistance of cell death. Programmed cell death or commonly known as apoptosis acts as a defence line in the cancer development. Several apoptosis inducing signals are triggered in response to tumorigenesis. Some of the common apoptosis inducing signals are elevated level of oncogene signalling and DNA damage which is caused by hyperproliferation. However, research showed that apoptosis is decreased in tumors which leads to malignancy and resistance to theraphy. Cellular condititions which starts apoptosis remain to be fully understood. However, several abnormalities plays an important role in the development of tumor. Most notable factor would be the DNA damage sensor which acts through TP53 tumor suppressor. DNA breaks and chromosomal abnormalities would cause TP53 to induce apoptosis. Other than this factor, insufficient survival signals such as inadequate levels of interleukin-3 in lymphocytes could cause apoptosis through BH3-only protein known as Bim. Tumor cells are able to resist apoptosis via several strategies such as through loss of the TP53 tumor suppressor function, by increasing the expression of the antiapoptotic regulators such as (Bcl-2, Bcl-xL) or of survival signals (Igf1/2), by downregulating proapoptotic factors (Bax, Bim, Puma), or by short-circuiting the extrinsic ligand-induced death pathway (Hanahan et al., 2011).

The forth hallmark of cancer was described as limitless replicative potential. Normal cells usually pass through a limited number of successive cell growth and division cycle. The limitation in the proliferation is often due to senescence, irreversible entrance

into nonproliferative but viable state and crisis which involves cell death. On unusual situations, cells would emerge from a population in crisis and show unlimited replicative potential. This is known as immortalisation where cells can proliferate without achieving senescence or crisis. The telomeres which protects the ends of chromosomes are centrally involved in the capacity to proliferate unlimitably. The telomeres which consists of multiple tandem hexanucleotide repeats would shorten progressively in non-immortalized cells propagated in culture. Eventually the ability to protect the ends of chromosomal DNAs from end to end fusion is lost and thus affecting the cell viability and the cell would enter cell death in subsequent generations. In human cancer cells, telomerase which is a specialised DNA polymerase which adds telomere repeat segments to ends of telomeric DNA is expressed at functionally significant levels. This would enable the cells to resist induction of senescence and cell death. Hence, the immortalized cells was found to have the ability to maintain telomeric DNA lengths sufficient in order to avoid triggering of senescence or apoptosis. This is most commonly achieved by upregulating the expression of telomerase (Hanahan et al., 2011).

The fifth hallmark of cancer as described by Hanahan and Weinberg is the induction of angiogenesis. Just as normal tissues, tumors need nutrients and oxygen and also the ability to excrete metabolic wastes and carbon dioxide in order to thrive and survive. The neovasculature which is generated by the process of angiogenesis addresses these needs. In an adult human, as part of the physiological processes such as wound healing and female reproductive cycling, angiogenesis is turned on transiently. During tumor progression, angiogenesis is almost always activated, causing vasculature to produce new vessels that would sustain neoplastic growths. Angiogenesis is induced during the early stage of the development of invasive cancer both in animal models and humans (Hanahan et al., 2011).

The next hallmark of cancer is tissue invasion and metastasis. Earlier findings showed that carcinomas originating from the epithelial tissues progressed to local invasion and distant metastasis. The cancer cells developed changes in their shape and attachment to other cells as well as to the extracellular matrix (ECM). It was found that increased expression of E-cadherin could inhibit invasion and metastasis, and decreased expression of this protein could promote the phenomena. Expression of genes encoding cell to cell and cell to ECM adhesion molecules appeared to be altered in highly invasive carcinomas. Adhesion molecules such as N-cadherin appeared to be upregulated. Invasion and metastasis is a sequence of events which is termed as invasion-metastasis cascade. This includes processes such as local invasion, intravasation of cancer cells into nearby blood and lymphatic vessels, movement of cancer cells through this vessels, and extravasation to a secondary site, formation of small nodules of cancer cells (micrometastasis) and finally the growth of micrometastasis lesions into macroscopic tumors (colonization) (Hanahan et al., 2011).

The seventh hallmark, which is also known as an emerging hallmark, is evasion of immune destruction. This describes the role of immune system in resisting or abolishing formation and progression cancer. Immune system plays a role in guarding cells and eliminating majority of incipient cancer cells. Based on this hypothesis, solid tumors that appears are cells that manage to evade immunological defense line. The striking increase in occurance of certain cancers in immunocompromised individuals further streghtens this hypothesis. However, these are usually virus-induced cancers where the elimination of these virus infected cells would help in attenuating the cancer. In some recent researches, immune system was found to act as a significant barrier for tumor formation and progression in non-virus induced cancers (Hanahan et al., 2011).

The final hallmark, also classified as an emerging hallmark is the reprogramming of energy metabolism. Chronic and often uncontrolled cell proliferation represents manipulation of energy metabolisms to fuel cell growth and division. In aerobic conditions, normal cells would process glucose to pyruvate through glycolysis in cytosol and then to carbon dioxide in mitochondria. Whereas in anaerobic condition, small amount of pyruvate is sent to mitochondria and glycolysis is favoured. A defective energy metabolism was observed by Otto Warburg in cancer cells. Although in surplus of oxygen, cancer cells could reprogram glucose metabolism and energy production to glycolysis, leading to a state that has been named as "aerobic glycolysis". Due to this situation, cancer cells has to compensate to the relatively lower ATP production. This is done by upregulation of glucose transporters such as GLUT1 to increase the intake of glucose into the cytoplasm. This has been observed in many types of human tumor. Glycolytic fueling has also been shown to be associated with activated oncogenes and mutant tumor suppressors. On another hypothesis, it was proposed that glycolysis could allow the diversion of glycolytic intermediates into various biosynthethic pathways. This includes those that generates nucleosides and amino acids that would facilitate assembly of new cells (Hanahan et al., 2011)

All these hallmarks and emerging hallmarks gives us outline on understanding the mechanism of cancer better and in manipulating these factors for therapeutic purposes.

2.5.2 Lung cancer

There are mainly three types of lung cancer. This includes the non-small cell lung carcinoma (NSCLC), small cell lung carcinoma (SCLC) and lung carcinoid tumor. NSCLC is the most common type of lung cancer. It contributes to approximately about 85% of the total lung cancer incidences. Squamous carcinoma and adenocarcinoma are some of the subtypes of this group. SCLC contributes to about 10-15 % occurances. This type of cancer spreads quickly. The lung carcinoid tumor is the least common type of lung cancer as it only has about 5% incidences. This type of cancer proliferates slowly and rarely spreads (Lung cancer, n.d.).

Lungs are 2-sponge like organs in our chest. The right lung has 3 sections that are referred as lobes while the left lung has two lobes. The left lung is smaller as the heart takes up a larger space in that side. When we breathe in air, air enters through our nose or mouth and passes through the trachea that would divide into two tubes like structures called as bronchus. Bronchus is divided into smaller branches known as bronchioles, which are in the lungs, and the bronchioles are divided into tiny air sacs known as alveoli in the lung. Air that reaches the alveoli undergoes absorption of oxygen and the carbon dioxide is removed from the blood and emission of carbon dioxide occurs. The lung functions in taking in oxygen and getting rid of carbon dioxide. Lung cancer usually starts in the cells lining the bronchus and part of the lung such as bronchioles and alveoli (American Cancer Society, 16 May 2016). Some of the symptoms of lung cancer includes chronic coughing, difficulty in breathing, shortness of breath, cough which expels copper colored or blood infused sputum, weight loss, feeling lethargic and ache and pain when breathing or coughing. Overall, the chance that a man will develop lung cancer in his lifetime is about 1 in 14; for a woman, the risk is about 1 in 17. These numbers include both smokers and non- smokers. Doctors employ various techniques to diagnose lung cancer. Among the techniques are chest x-ray, computated tomography

(CT) scan, magnetic resonance imaging (MRI) scan, positron emission tomography (PET) scan, bone scan, sputum cytology, thoracentesis, needle biopsy, brochoscopy, endobronchial ultrasound, throcoscopy, immunohistochemical tests, molecular tests and blood tests. Surgery remains the most successful option but 70% of patients with lung cancer would be in advanced stage and has metastatic disease by the time of diagnosis.

Chemotheraphy is useful for patients with lung cancer that has metastasize. A combination of chemotheraphy and radiation theraphy is useful for patient with stage 3 lung cancer. In some patients, EGFR is mutated and overexpressed, in this case a targetted theraphy which involves EGFR tyrosine kinase inhibitor is effective (Molina et al., 2008). For smokers the risk is much higher, while for non-smokers the risk is lower (American Cancer Society).

2.5.3 Lung cancer statistics in Malaysia

Lung cancer contributes to the largest number of fatality in cancer related deaths worldwide with a statistic of 30-40% occuring in developing nations. There were more than 1.8 million lung cancer diagnoses worldwide which resulted in 1.6 million deaths in the year 2012. The incidence of lung cancer and the fatality resulting it is expected to increase over the next decade due to increased rate of smoking (Kan et al., 2016). It is estimated that by 2030, 70% of tobacco-related deaths will occur in developing and low-income countries (Liam et al., 2015).

There are mainly two types of lung cancer i.e. the small cell lung cancer and the non-small cell lung cancer. According to the National Cancer Institute, US, tobacco smoking is the most common cause of lung cancer. In Malaysia, lung cancer is reported as the most common killer among malignancies with an estimated annual incidence of 30,000

(Lim, 2002). It is noteworthy that, the current treatment for lung cancer does not cure the disease.

According to the report by World Health Organization on 2014, lung cancer contributes to 19.1 deaths per 100,000 population in Malaysia or 4088 deaths per year i.e. 3.22% of all deaths. It is the second most common cause of death due to cancer in the country after breast cancer. In male population, lung cancer is the most common cause of fatality caused by cancer. In female population, it is the second most common death after breast cancer. In 2014, 3320 males were diagnosed with lung cancer and 1163 females were diagnosed of the same. These information on the epidemiology of lung cancer was retrieved from National Cancer Registry (NCR) (Kan et al., 2016). Overall, the mean age at which lung cancer is diagnosed in Malaysia is 60.1 years with peak age of distribution in the 7th decade (Sachithanandan et al., 2012).

It was found that in Malaysia, the Chinese community is the most afflicted by this disease with up to two fold in number if compared to non-chinese. The main reason for this factor is due to smoking volume and also genetic predisposition. Among this, 88% are classified as non-small cell lung cancer (NSCLC) with limited cases in small cell lung cancer (SCLC) category. Cigarette smoking is the major risk factor with 92% of malaysian male lung cancer patients showing significant smoking history. In Malaysia, smoking is prevalent among male population with almost 50% of the adult males being smokers. Among Asian never smoking women, indoor coal burning, cooking fumes, and infections such as tuberculosis and human papilloma virus are the main cause of cancer (Zhou et al., 2011). The treatment cost of smoking induced lung cancer reaches up to approximately 440 million ringgit annually in Malaysia (Sachithanandan et al., 2012).

The mortality rate of lung cancer is high as compared to other types of cancer is because lung cancer is often diagnosed at a later stage which disables the effective curative treatments. In US, 5 years survival ranges from 52%-24% however in Malaysia the percentage is only about 4%. However, it was also found that Asian counterparts show positive response to treatment as compared to caucasians. This is because of relatively high prevalance of epidermal growth factor receptor (EGFR) mutations in the Asians which enables favourable response towards EGFR tyrosine kinase inhibitors (Liam et al., 2015).

2.5.4 Carcinogens

The majority of human cancers result from exposure to environmental carcinogens; these include both natural and manmade chemicals, radiation, and viruses. Carcinogens may be divided into several classes: (1) Genotoxic carcinogens, if they react with nucleic acids. These can be directly acting or primary carcinogens, if they are of such reactivity so as to directly affect cellular constituents. (2) Alternatively, they may be procarcinogens that require metabolic activation to induce carcinogenesis. (3) Epigenetic carcinogens are those that are not genotoxic. Molecular diversity of the cancer-initiating compounds ranges from metals to complex organic chemicals, and there is large variation in potency. The variation in structure and potency suggests that more than one mechanism is involved in carcinogenesis. It is also clear that apart from exposure to carcinogens other factors such as the genetic predisposition have been documented. Thus, patients with the genetic xeroderma pigmentosum are more susceptible to skin cancer. Furthermore, incidence of bladder cancer is significantly higher in those individuals who have the slow acetylator phenotype, especially if they are exposed to aromatic amines. Carcinogens in the diet that trigger the initial stage include moulds and aflatoxins (for example, in peanuts and maize), nitrosamines (in

smoked meats and other cured products), rancid fats and cooking oils, alcohol, and additives and preservatives. A combination of foods may have a cumulative effect, and when incorrect diet is added to a polluted environment, smoking, UV radiation, free radicals, lack of exercise, and stress, the stage is set for DNA damage and cancer progression. On the protective side, we know that a diet rich in fruit, vegetables, and fibre is associated with a reduced risk of cancer at most sites (Reddy et al., 2003).

Table 2.1: Types of carcinogens

Type	Example
1. Genotoxic carcinogen Primary, direct-acting alkylating agents	Dimethylsulfate, ethylene imine, b-propiolactonel
2. Procarcinogens Polycyclic aromatic hydrocarbons Nitrosamines Hydrazine Inorganic	Benzo[a]pyrene Dimethylnitrosamine 1,2-Dimethylhydrazine Cadmium, plutonium
3. Epigenetic carcinogens Promoters Solid state Cocarcinogens Immunosuppressants Hormones	Phorbol esters, saccharin, bile acids Solid state Asbestos, plastic Estrogens Purine analogues Catechol
4. Unclassified Peroxisome proliferators	Chofilbrate, phthalate esters

2.5.5 Carcinogenesis

Carcinogenesis is the malignant transformation of a cell or group of cells (Cayuela, 1994). The transformation of a normal cell into a cancerous cell is believed to proceed through many stages over a number of years or even decades. The stages of

carcinogenesis include initiation, promotion, and progression. The first stage involves a reaction between the cancer-producing substance (carcinogen) and the DNA of tissue cells. There may be a genetic susceptibility. This stage may remain dormant, and the subject may only be at risk for developing cancer at a later stage. The second stage occurs very slowly over a period ranging from several months to years. During this stage, a change in diet and lifestyle can have a beneficial effect so that the person may not develop cancer during his or her lifetime. The third and final stage involves progression and spread of the cancer, at which point diet may have less of an impact. One of the most important mechanisms contributing to cancer is considered to be oxidative damage to the DNA. If a cell containing damaged DNA divides before the DNA can be repaired, the result is likely to be a permanent genetic alteration constituting a first step in carcinogenesis. Body cells that divide rapidly are more susceptible to carcinogenesis because there is less opportunity for DNA repair before cell division. Mutagenic changes in the components of signaling pathways lead to cellular transformation (cancer).

2.5.6 Multistage Carcinogenesis

The development of fully malignant tumor involves complex interactions between several factors, both exogenous (environmental) and endogenous (genetic, hormonal, immunological, etc). Carcinogenesis can proceed through few stages includes initiation, promotion (appearance of benign tumor) and progression (conversion of benign to malignant tumor).

The transition between stages can be enhanced or inhibited by different types of agent. These aspects show that formation of malignant tumor involves various factors, various cellular genes and various types of changes in gene structure and function.

Agents that initiate the carcinogenic process often do so by damaging cellular DNA. The genetic alterations brought about by the initiating agent require cell proliferation, triggered by the promoting agent, to transform a single potential cancer cell into a multicellular tumor. But, additional cellular changes are required over and above simply expanding a pool of initiated cells. The promoting agent on its own can generate proliferative changes but not cancers.

Promotion occurs by different pathways in different cells, but two common features are altered cell proliferation and the formation of new blood vessels. Tumors will grow to about 1 mm diameter in the absence of new capillaries (angiogenesis) but further expansion requires the production of angiogenic growth factors by the cancer cells. Progression reflects multiple changes in growth regulatory mechanisms. These include altered sensitivity to adjacent cells, local growth factor production, changes in receptors that initiate signal transduction and alterations to the downstream transduction pathways. The culmination of these events in autonomous cell growth is an ability to grow outside their normal environment and to metastasize to other parts of the body. (Roger, 2000).

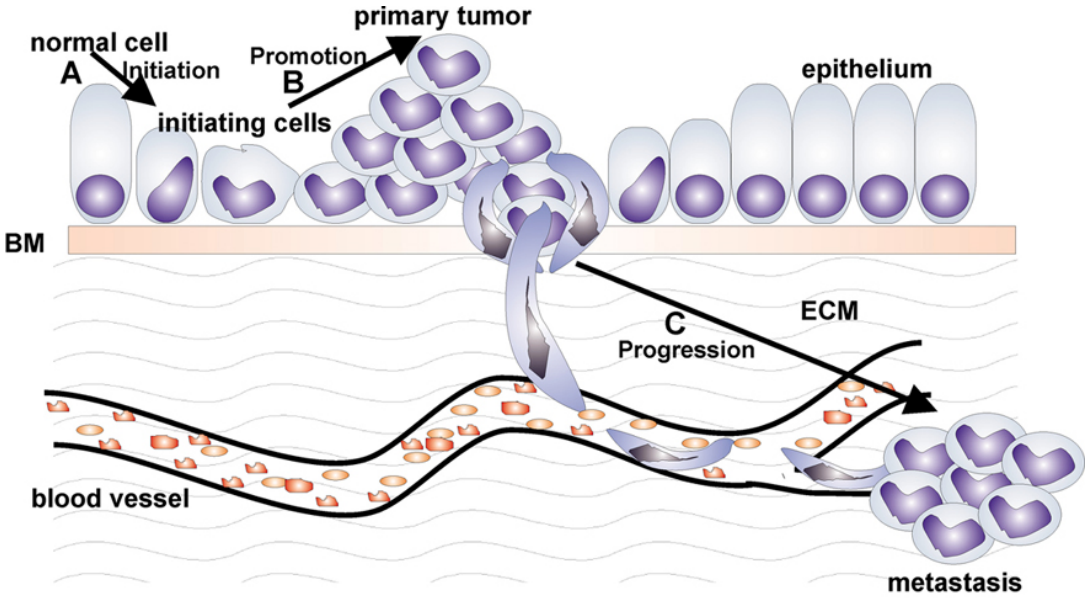

Figure 2.5: Steps of multistage carcinogenesis. (A) activation of phase I and inactivation of phase II metabolizing enzymes, enhanced free radical generation; (B) oncogenes, overexpression of growth factors, cell cycle alterations; (C) MMPs, Cytokines; TNF alpha; COX2; adhesion molecules, angiogenic factors. Image excerpted from Bachmeier et al. (2009).

2.5.7 Cancer Chemoprevention

Cancer chemoprevention is the inhibition of development of invasive cancer by using pharmacological or natural agents that would prevent the metabolic activation of procarcinogens (Hong & Sporn, 1997; Sreekanth et al., 2007). The mechanism of action of the antiproliferative effects are as follows:

a) Alterations in the cell differentiation pattern are induced. This plays an important role in metastatic progression and invasiveness of tumors.

b) Induction of apoptosis or pre neoplastic cell expansion block.

c) Metabolic activation of carcinogens is stopped by scavenging ROS. (Sreekanth et al., 2007)

d) Inhibit carcinogen uptake, formation or activation of carcinogen

e) Inhibit oncogene activity

f) Restore immune response

g) Restore tumor suppressor function (Kelloff, 2000)

Understanding the mechanisms of cancer helps us to devise better strategies to block two or more key pathways in the cancer process, and thus limit or reverse many types of cancer (Steele & Kelloff, 2005).

2.6 Apoptosis

The term apoptosis was first used in the year 1972 to explain a morphologically different form of cell death. However, its importance was underestimated for many years. Apoptosis was derived from a Greek word that means 'falling off', as leaves fall from tree. The mechanism of apoptosis in mammalian cells was deduced from the apoptosis that occurs during the development of the nematode *Caenorhabditis elegans* (Horvitz, 1999). Since then, apoptosis has been accepted as an important mode of cell death which involves genetically determined elimination of cells (Elmore, 2007). In current time, apoptosis has been found to involve in many biological processes including embryogenesis to ageing, from normal tissue homeostasis to many human diseases and it has become one of the prominent and most researched on topic (Renehan et al., 2001).

Apoptotic cell death has several important functions. The primary function would be its role in the intrauterine development. It helps to sculpture organ shape and carve out the interdigital webs of the fingers and toes (Renehan et al., 2001). Apoptosis also plays an important role in homeostasis. It is a constant process that happens in our human body. For example, in a healthy human adult, billions of cells die in the bone

marrow and intestine every hour. Cell death helps in regulating cell numbers (Raff et al., 2002).

Cells undergoing apoptosis are characterised by rounding-up of the cell, retraction of pseudopodes, reduction of cellular volume (pyknosis), chromatin condensation, nuclear fragmentation (karyorrhexis), little or no structural modifications of cytoplasmic organelles, plasma membrane blebbing (but maintenance of its integrity until the final stages of the process) and finally the engulfment by resident phagocytes (*in vivo*) (Kroemer et al., 2009). This process could be likened to a 'suicide' event. However, no damage is caused to the surrounding tissues. Apoptosis can be divided into two types of sub-pathways i.e. the extrinsic apoptotic pathway which is also known as the death receptor pathway and the intrinsic apoptotic pathway which is also known as the mitochondrial-mediated apoptotic pathway (Indran et al., 2011). The extrinsic pathway however merges with the intrinsic pathway upon activation of caspases 8. Caspases are proteases which belongs to the family of cysteines that participates in the non-inflammatory demolition of cells. The extrinsic pathway, which is activated through cell surface receptors, leads to the caspase 8 activation that is the intiator caspase of the death receptor mediated apoptotic pathway which would subsequently activate the downstream caspase 9 and 3. On the other hand, the intrinsic pathway, which is mediated by the mitochondria in the cell, leads to the activation of caspase 9. Caspase 9 is the initiator caspase for intrinsic apoptotic pathway. These two pathways converge to the next level of activation of the executioner caspase 3 which functions to initiate the DNA fragmentation and execution of the cell (Suen et al., 2008). There are several initiators of apoptosis which includes anticancer drugs, gamma and ultraviolet rays, deprivation of survival factors such as interleukin-1, and various other cytokines that activates "death receptors" such as Fas and tumor necrosis factor (TNF) receptors (Renehan et al., 2001).

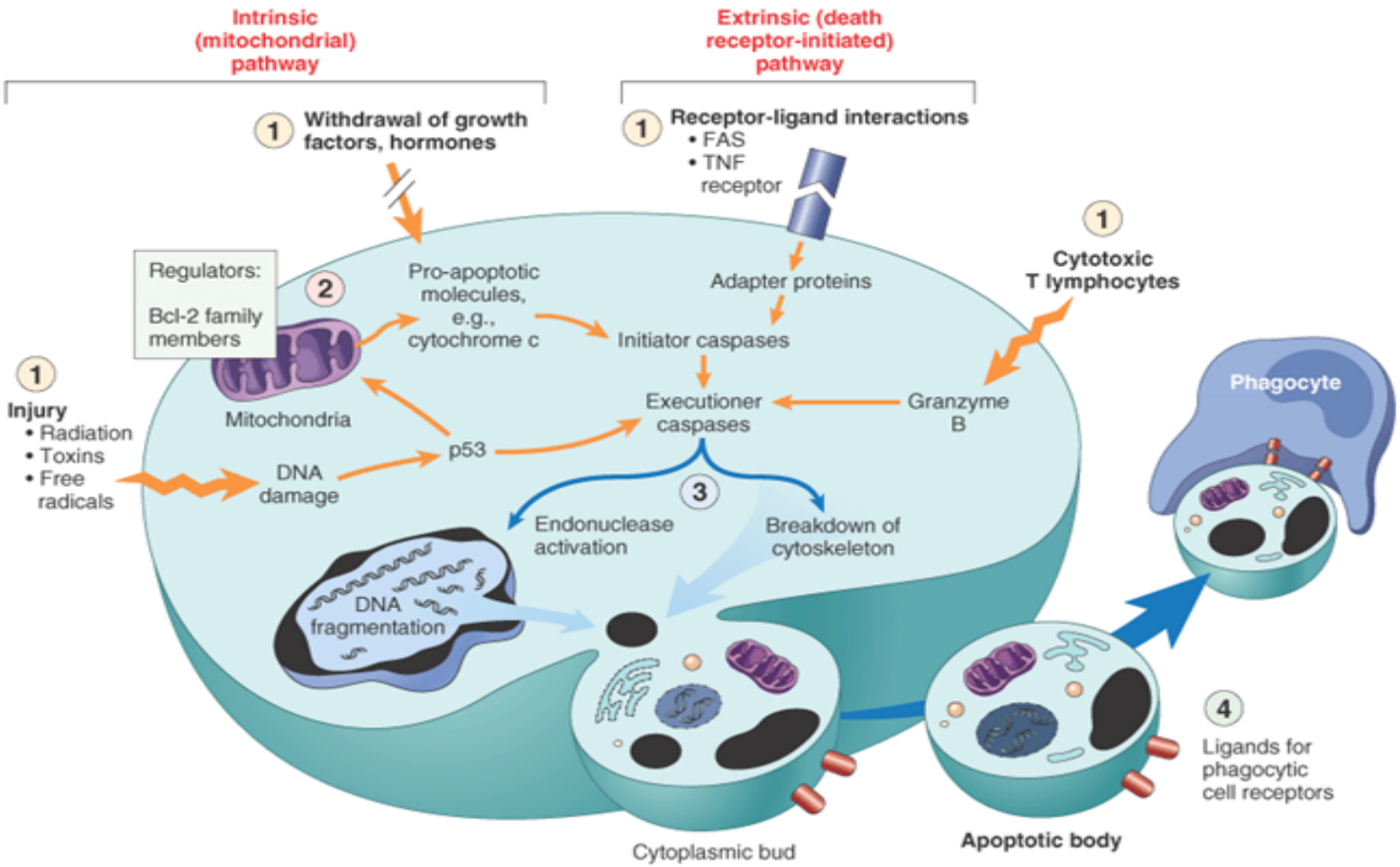

Figure 2.6: Overview of the apoptotic cell death. Image excerpted from: Programmed cell death, n.d.

2.6.1 Characteristics of apoptosis

There are several features that appear in a cell that undergoes apoptosis. One of the main hallmark in the nucleus are the chromatin condensation and nuclear fragmentation. In the initial stages, the condensation occurs along the nuclear membrane and forms a crescent or ringlike structure and at later stages, it breaks up inside the cell with cell membrane still intact. This process is described as karyorrhexis. The condensation and fragmentation is visible with light microscope or electron microscope. Chromatin condensation is significantly visible in fluorescence microscope with stains such as Hoechst. DNA fragmentation can be detected using the incorporation of labeled dUTP by the enzyme terminal deoxynucleotide transferase nick end labeling (TUNEL) method (Ziegler et al., 2004).

During early stage of apoptosis, cells lose contact with neighbouring cells. Cells would shrink and the membrane would bleb forming apoptotic bodies, which would eventually degrade. With cell shrinkage, the cells are smaller in size, the cytoplasm is dense and the organelles are more tightly packed (Elmore, 2007). Apoptosis does not initiate inflammatory response. This is because an intact membrane contains the cellular constituents and the apoptotic bodies are subsequently engulfed. Shrinkage of cells, blebbing, and formation of apoptotic bodies could be observed via light or electron microscope. Separation of cell fragments into apoptotic bodies occurs in a process known as “budding.” Apoptotic bodies consist of cytoplasm with tightly packed organelles with or without a nuclear fragment (Elmore, 2007). One of the initial characteristics of apoptosis is the externalization of phosphatidylserine (PS). This provides the “eat-me” signal for phagocytosing cells. An *in vitro* marker known as Annexin V could detect the externalisation of serine. Annexin is a calcium ion binding protein which has high affinity towards PS. Annexin V could be conjugated to

fluorochromes such as fluorescein isothiocyanate (FITC) to give fluorescence signals which could be detected using fluorescent microscope or quantified using the flow cytometer (Ziegler et al., 2004).

Mitochondria play a central role in apoptosis. Changes in cellular stress responses and bioenergetic state play a significant role in the starting of apoptosis. Mitochondrial membrane permeabilization has a central role in this process. Proapoptotic members of Bcl-2 family are upregulated during apoptosis and anti-apoptotic members are inhibited during the initiation of mitochondrial permeabilization. When mitochondrial membrane is permeabilized, several proteins such as cytochrome c, apoptosis inducing factor (AIF), Smac/DIABLO are released. A complex called apoptosome would be formed between cytochrome c and Apaf-1 that causes the binding and activation of caspase-9. Smac/DIABLO functions to activate caspase by binding to a family of proteins called the inhibitors of apoptosis proteins (Ziegler et al., 2004).

Macrophages, parenchymal cells or neoplastic cells would phagocytose the apoptotic cells. It would be then degraded within phagolysosomes. Macrophages that engulf and digest apoptotic cells are known as tangible body macrophages and are commonly found within reactive germinal centers or lymphoid follicles or within the thymic cortex. There is no inflammatory reaction in the apoptotic process or at the process of clearing the apoptotic cells. This is due to three main reasons such as below:

1. Apoptotic cells do not release their cellular constituents into the surrounding interstitial tissues.
2. It is quickly phagocytosed and hence the secondary necrosis is prevented.
3. The engulfment of cells does not produce anti-inflammatory cytokines (Elmore, 2007).

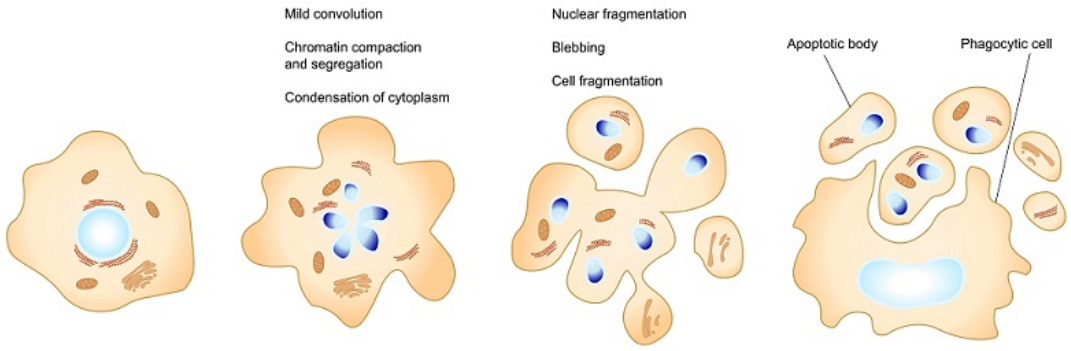

Figure 2.7: Characteristics of apoptosis. Image excerpted from: Cell senescence and apoptosis, n.d.

2.6.2 Intrinsic apoptotic pathway (mitochondrial mediated apoptotic pathway)

This pathway involves initiation of various intracellular signals which are non-receptor mediated and acts directly on targets within the cell which are mitochondrial initiated. Various stimulus initiate and blocks this pathway. Absence of certain growth factors, hormones and cytokines could lead to failure in supression of this pathway thus triggering apoptosis. On the other hand, presence of radiations, toxins, hypoxia, hyperthermia, viral infections and free radicals could induce apoptotic signals. These stimuli causes changes in the inner mitochondrial membrane that leads to opening of the mitochondrial permeability transition (MPT) pore, loss of the mitochondrial membrane potential and release of the pro-apoptotic proteins from intermembrane space into the cytosol (Elmore, 2007). The mitochondrial pathway is regulated by Bcl-2 family members. These stimuli would activate BH3 family members (initiators) which would inhibit the pro-survival Bcl-2 like proteins (guardians), thus causing the activation of pro-apoptotic effectors such as Bax and Bak. This would disrupt the mitochondrial outer membrane and cytochrome c and SMAC (second mitochondria-derived activator of caspases) would be released from the mitochondria. Cytochrome c would promote activation of caspase 9 which is the initiator caspase on the scaffold protein APAF1 (apoptotic protease activating factor 1), in the presence of ATP or dATP to form a

complex which is known as apoptosome. This complex recruits and activates procaspase 9. Activated caspase 9 can, in turn, activate other effector caspases (caspase-3, -7) that are in charge of the cell death (Desagher et al., 2000). Apoptosome formation and effector caspase activation that causes initiation of apoptotic events such as chromatin condensation, phosphotidyl serine externalisation and cellular blebbing. (Ghatage et al., 2012). On the other hand SMAC would block the caspase inhibitor XIAP (X-linked inhibitor of apoptosis protein) (Czabotar et al., 2014).

The Bcl-2 family of proteins controls the mitochondrial membrane permeability and is divided into pro-apoptotic and anti-apoptotic. Anti-apoptotic proteins includes Bcl-2, Bcl-x, Bcl-XL, Bcl-XS, Bcl-2, BAG and the pro-apoptotic proteins include Bcl-10, Bax, Bak, Bid, Bad, Blk, and Bik. These proteins determine if the cell undergoes apoptosis by regulating the release of cytochrome c from mitochondria via alteration in the mitochondrial membrane permeability (Elmore, 2007).

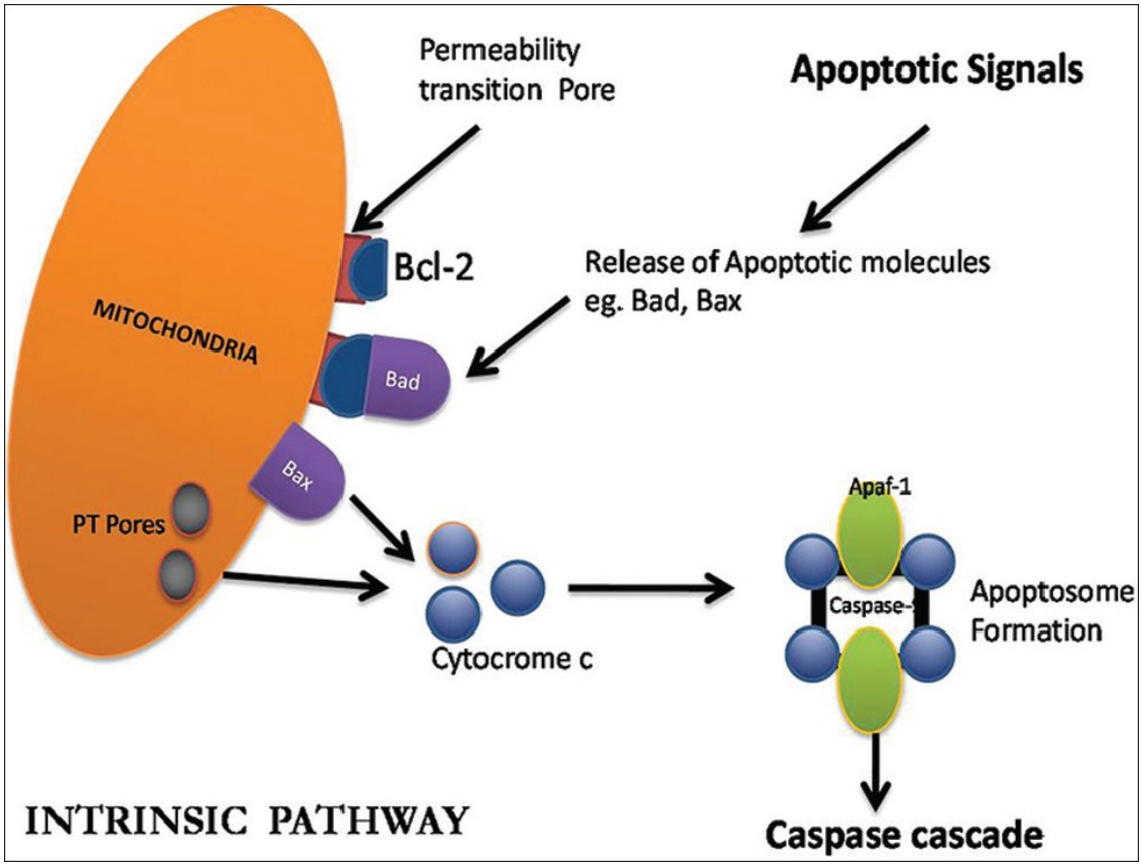

Figure 2.8: Graphical representation of intrinsic apoptotic pathway. Image excerpted from Ghatage et al. (2012).

2.6.3 Extrinsic apoptotic pathway (death receptor mediated apoptotic pathway)

The death receptor pathway is an extracellular signalling pathway (Chen et al., 2016). In this pathway, ligands which is the signalling molecule released by other cells would bind to the transmembrane death receptors such as DR4, DR5, DR3 to induce apoptosis. One of the prominent example would be the immune system's natural killer cells which possess the Fas ligand (FasL) on their surface. FasL would bind to Fas receptors which is a death receptor. This would trigger aggregation of multiple receptors on the surface of the target cells. The aggregation of receptors would then recruit an adaptor protein which is known as Fas-associated death domain protein (FADD) on the cytoplasmic side of the transmembrane receptor. FADD would then recruits caspase 8 which is an initiator caspase for this pathway to form death-inducing signalling complex

(DISC). This would activate caspase 8 and then activation of caspase 3 which is the effector caspase, occurs. Activated caspase 8 also could initiate the proteins of Bcl-2 family leading to damaged mitochondrial membrane and leaked pro-apoptotic proteins. The intrinsic apoptotic pathway is further triggered by the caspase cascade effect (Chen et al., 2016). This is commenced by cleavage of the protein BID to truncated Bid (tBID). tBID acts as a signal in the mitochondria to induce the release of cytochrome c and initiate the intrinsic apoptotic pathway. Bid is the molecular linker bridging death receptor pathway to mitochondrial pathway (Cui et al., 2016).

Caspase 8 exists in the cell as an inactive proenzyme (55kDa). It is transformed into the active form upon its recruitment to the cytoplasmic domain of the death receptors. The activation of the proenzyme is initiated by protein aggregation. Caspase 8 would either directly activates caspase 3 or indirectly activates the mitochondrial pathway via tBID. The executioner caspase which is caspase 3 in the activated form would induce PARP cleavage which results in morphological features such as DNA fragmentation (Rogalska et al., 2014).

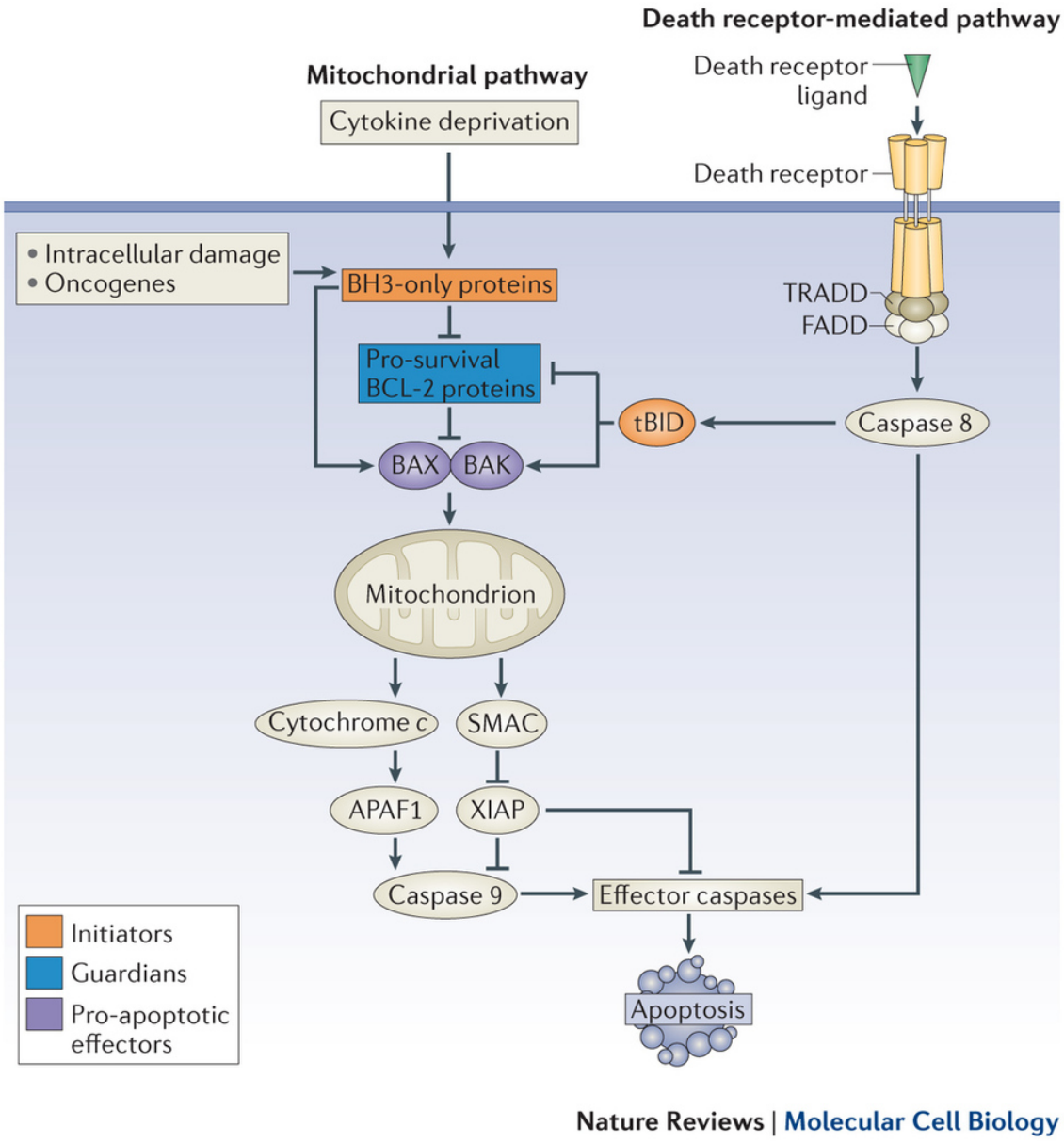

Figure 2.9: The death receptor mediated apoptotic pathway and the link between it and the mitochondrial-mediated apoptotic pathway. Image excerpted from Czabotar et al. (2014).

2.6.4 Altered apoptosis and disease

During the course of ageing, apoptotic responses to DNA damage may become less tightly controlled and exaggerated which leads to degenerative diseases. On the other hand, less sensitivity towards apoptotic responses may lead to cancer.

2.6.5 Apoptosis and cancer

Cancer is genetic changes in normal cells where it is transformed into malignant cells and one of the mode of transformation is by evading the cell death. The concept of manipulating apoptosis to eliminate malignant cells, hyperplasia and tumor progression has been developed as early as 1970s (Wong, 2011).

One of the most remarkable advances in cancer biology is the discovery of the concept that apoptosis and genes that control it have important effect in cancer. Oncogenic mutations were found to disrupt apoptosis which leads to tumor initiation, progression and metastasis. Mutations suppresses apoptosis during tumor development in carcinogenesis stage and also reduces cancer treatment sensitivity. Most of the cytotoxic anticancer agents work in the mechanism of apoptosis induction (Lowe et al., 2000). There are various ways in which cancer cells evade apoptosis among which is through disruption of the balance between pro-apoptotic an anti-apoptotic proteins, reducing the function of caspases and impairment of the death receptor signalling (Wong, 2011).

Bcl-family of proteins plays their role mainly in the intrinsic apoptotic pathway at the mitochondrial level. This family of proteins contains both the pro-apoptotic proteins and the anti-apoptotic proteins. When the balance between anti-apoptotic and pro-apoptotic members of Bcl-2 family is disrupted, there would be a deregulation in the apoptosis. Cancer could be due to overexpression of one or more anti-apoptotic proteins or underexpression of one or more pro-apoptotic proteins or a mixture of both these factors (Wong, 2011).

The well-known p53 protein or also known as tumor protein 53 is one of the best-studied tumor suppressor protein, which is encoded by the tumor suppressor gene TP53. The oncogenic property was found to be due to mutations that occur in this gene. More

than 50% of cancers were found to be due to defects in the p53 tumor suppressor gene. This gene does not only regulate cancer by inducing apoptosis but it also involves in various other functions such as cell cycle regulation, development, differentiation, DNA recombination, cellular senescence and chromosomal segregation. It is also known as the guardian of the genome (Lowe et al., 2000).

Another common cause of cancer is due to deregulation in the expression of IAPs (inhibitor of apoptosis). IAPs are a group of structurally and functionally similar proteins which regulate apoptosis, cytokinesis and signal transduction. IAPs are endogenous inhibitors of caspases where they could inhibit caspase activity via binding their conserved BIR domains to the active sites of caspases or by promoting degradation of active caspases or by restraining caspases away from their substrates. In most of the cancers, IAPs was found to be abnormally overexpressed (Wong, 2011).

Besides that, reduced activity of caspases also promotes the development of cancer. Caspases that form a central role in apoptosis can be divided into initiator caspases (caspase-2, -8, -9, and -10) and effector caspases (caspase-3, -6, and -7). Initiator caspase functions to initiate the apoptotic pathway however the effector caspases is responsible in the actual cleavage of cellular components of apoptosis. Impairment in the function of caspases may lead to decrease in apoptosis and carcinogenesis. Another common reason for cancer is the disruption in the death receptor signalling. Death receptors and ligands play an important role in the extrinsic apoptotic pathway. Death receptors have death domains which when triggered by death signal would activate signalling cascade. Abnormalities in death signaling pathways have led to evasion of extrinsic apoptotic pathway. These abnormalities includes downregulation of the receptor, reduced level in the death signals and impairment of receptor function (Wong, 2011).

2.7 Necrosis

Necrosis on the other hand, is commonly described as a nonspecific form of cell death (Kasibhatla & Tseng, 2003). Necrosis starts inflammatory response of surrounding cells through the leakage of intracellular contents (Tang et al., 2010). 'Necrotic cell death' or 'necrosis' is morphologically described by an increase in cell volume which is also known as oncosis, swelling of organelles, plasma membrane rupture and subsequent loss of intracellular contents (Kroemer et al., 2009). In necrotic cell death, plasma membrane integrity is lost and this leads to the leakage of cytoplasmic contents into the extra-cellular environment causing an inflammatory reaction (Tang et al., 2010).

Necrotic cell death has long been considered an accidental and uncontrolled mode of cell death. Cell death via necrosis occurs generally due to physico-chemical stress, which includes hypoxia, ischemia, hypoglycemia, extreme change in temperature and lack in nutrient (Vanlangenakker et al., 2008). The serine/threonine kinase receptor-interacting protein 1 (RIP1) plays an important function in initiation of necrosis induced by ligand-receptor interactions (Vanlangenakker et al., 2008). Tumor necrosis factor (TNF) induces apoptosis in the absence of RIP1/RIP3. When there is sufficient RIP3 expression, the gateways via glycogen and glutamate or glutamine is readily opened upon TNF stimulation. RIP3 and RIP1 are cleaved by caspases. Increased ROS production from the mitochondrial respiration chain that is resulted from enhanced metabolism is responsible for the function of RIP3/RIP1 in mediating necrosis (Zhang et al., 2010). The common factors in necrotic cell death irrespective of the stimuli are calcium and ROS. During necrosis, increased calcium level would lead to mitochondrial calcium overload, activation of proteases and phospholipases and also bioenergetic effects while ROS causes damage to lipids, proteins and DNA. This would lead to membrane destabilisation, mitochondrial dysfunction and ion balance deregulation.

Necrotic cells would finally release immunomodulatory factors which, leads to recognition and engulfment of phagocytes and then immunological response (Vanlangenakker et al., 2008).

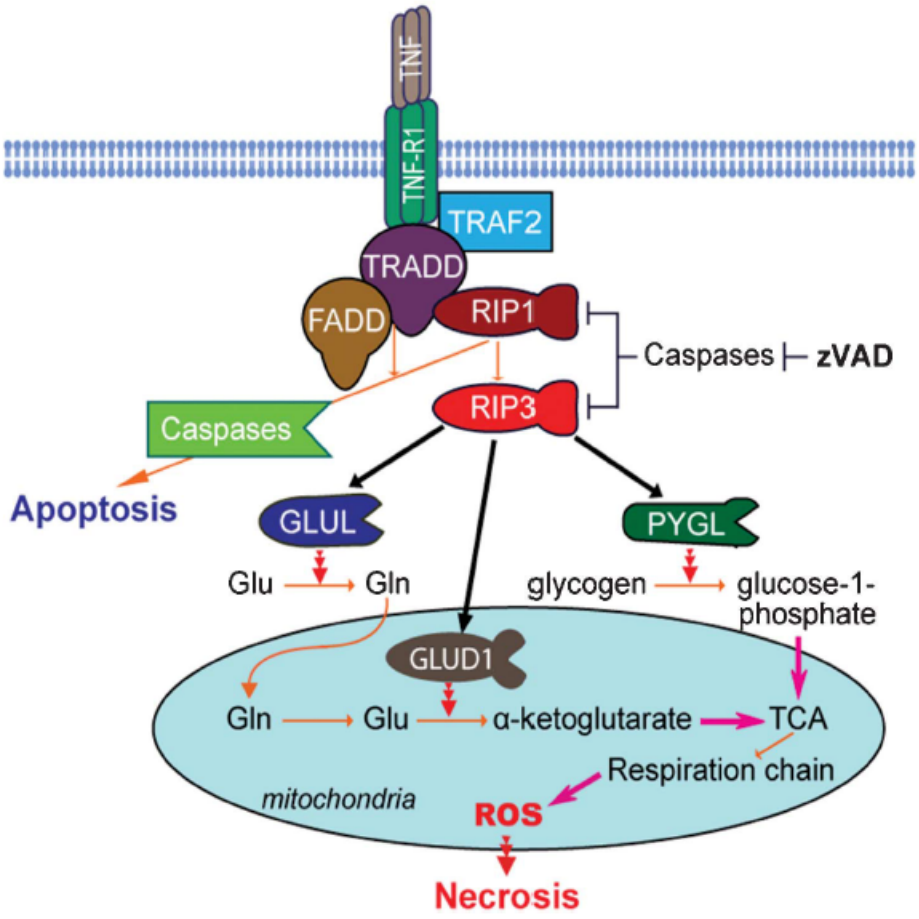

Figure 2.10: RIP kinase mediated necrosis pathway. Image excerpted from Zhang et al. (2010).

2.8 Autophagy

Autophagy is a strictly regulated lysosomal pathway that degrades organelles and cytoplasmic materials (Eskelinen et al., 2009). Autophagy is defined as an intracellular degradation system that delivers cytoplasmic constituents to the lysosome. This process plays an important role in variety of physiological and pathophysiological roles. Autophagy takes place in a few steps such as sequestration, transport to lysosomes, degradation and usage of the degradation products (Mizushima, 2007). This pathway is

activated during stress conditions such as viral infections, unfolded protein response and amino acid starvation (Eskelinen et al., 2009). There are three types of autophagy which are macro-autophagy, micro-autophagy and chaperone-mediated autophagy (Glick et al., 2010). Macroautophagy is a process in which a part of cytoplasm that is intended for degradation would be first wrapped inside a specialized organelle, which is known as autophagosome. It would then fuse with lysosomal vesicles and the engulfed cytoplasm would then be degraded. Microautophagy is a process where the lysosomal membrane itself sequesters a portion of cytoplasm by a process similar to pinching off of phagosomes or pinosomes from the plasma membrane. Finally in the chaperone-mediated autophagy, proteins which has specific sequence signal would be transported from cytoplasm through the lysosomal membrane to the lysosomal lumen (Eskelinen et al., 2009).

Autophagy has various functions such as balancing sources of energy at important events in development and in response to nutrient stress. It also plays role in removing misfolded or aggregated proteins, clearing damaged organelles such as mitochondria, endoplasmic reticulum and peroxisomes. It also functions to eliminate intracellular pathogens. In addition to this, autophagy also promotes cellular senescence and cell surface antigen presentation. It also protects against genome instability and inhibits necrosis. This role is significant in preventing diseases such as cancer, neurodegeneration, diabetes, infections and autoimmune diseases (Glick et al., 2010).

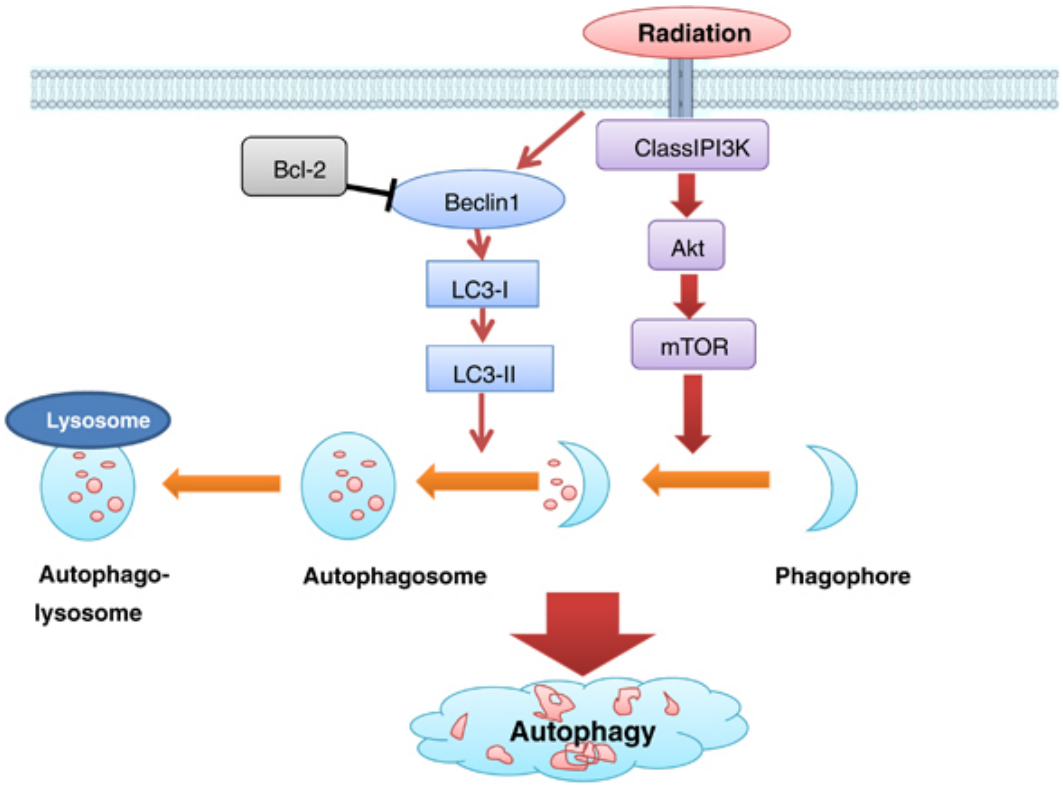

Figure 2.11: Diagram showing the induction of autophagy pathway by radiation. Excerpted from Chang et al. (2014).

2.9 Cell Cycle

Cell cycle or also known as cell-division cycle is a sequence of events that happens in a cell that consequences into division and duplication of its DNA to result in two daughter cells (Williams et al., 2012). Eukaryote cells passes through a series of stages collectively known as cell cycle. Cell cycle is divided into few phases. It has two gap phases, which are G1 and G2, S phase, which is the synthesis phase, and finally the M phase that is the mitotic phase. G1 and G2 phases separate the S and M phases. G1 phase follows on from mitosis and is a time when the cell is sensitive to positive and negative signals from the growth signaling networks. G2 phase is the gap after the S phase where the cell prepares to enter into mitosis (Williams et al., 2012). The G1 phase is a synthetic growth phase for RNA and proteins, which would be utilised for DNA synthesis in the S phase and cell growth prior to division. In the G2 phase however, DNA damage or error that has occured in the S phase would be rectified before the M

phase (Rabinovitch, n.d.). G0 phase represents a phase where cells are reversibly withdrawn from the cell division cycle in response to high cell density or mitogen deprivation. During this phase, the cells may also irreversibly withdrawn from the cell cycle into senescence stage (Williams et al., 2012).

In the G1 phase, certain metabolic changes occur which prepares the cell for division, when the cell is ready for division, it would move to the S phase. In the S phase, the DNA is replicated and each chromosome would be duplicated into two sister chromatids. The next phase is the G2 phase where cytoplasmic materials are assembled for mitosis and cytokinesis. Finally the cell goes through the M phase, which is the mitosis phase where the parent cell divides into two daughter cells.

The transitions in the cell cycle is regulated by various protein kinase complexes which consists of cyclins and cyclin-dependent kinase (cdk) molecules (Shackelford et al., 1999). Cyclin D-CDK4, cyclin D-CDK6 and cyclin E-CDK2 drive G1 progression through the restriction point, which commits the cell to complete the cycle. S phase is initiated by cyclin A-CDK2, and cyclin B-CDK1 regulates progression through G2 and entry into mitosis (Williams et al., 2012).

The process of replication of DNA and division of cell is a tightly controlled mechanism. At least two types of cell cycle control mechanisms are described. These are cascades of protein phosphorylations that relay a cell from one stage to the next and also a set of checkpoints that monitor completion of critical events and delay progression to the next stage if necessary. Kinase family regulates protein phosphorylation where the kinase activation requires association with a second subunit that is transiently expressed at certain period in the cell cycle. These second subunit is known as cyclin which associates with its cyclin dependent kinases to form an active complex which would generate the cell cycle progression to the next phase.

Phosphorylation and dephosphorylation would ensure the optimal function of the cyclin-cdk complex (Collins et al., 1997). Checkpoint controls sense errors or flaws in important cell cycle events such as DNA replication and chromosome segregation. Incomplete replications or damaged DNA would delay cell progression until these mistakes are rectified. Checkpoint control plays a more supervisory role in the cell cycle (Collins et al., 1997). Effector proteins include the CDK inhibitors (CDKIs), which can reversibly stop cell cycle progression. For example, G1 arrest can be induced through the action of the Ink4 family [INK4A (p16), INK4B (p15), INK4C (p18) and INK4D (p19)] of CDKIs, which inhibit CDK4 and CDK6, or, alternatively, via the Cip/Kip family of inhibitors (p21, p27, p57), which suppress CDK2 activity (Williams et al., 2012).

The duration of these phases varies between types of cells. Normally a cell is in G1 phase for 12 hours, S phase for about 6 hours, G2 phase for 4 hours and mitosis takes about 0.5 hours (Rabinovitch, n.d.).

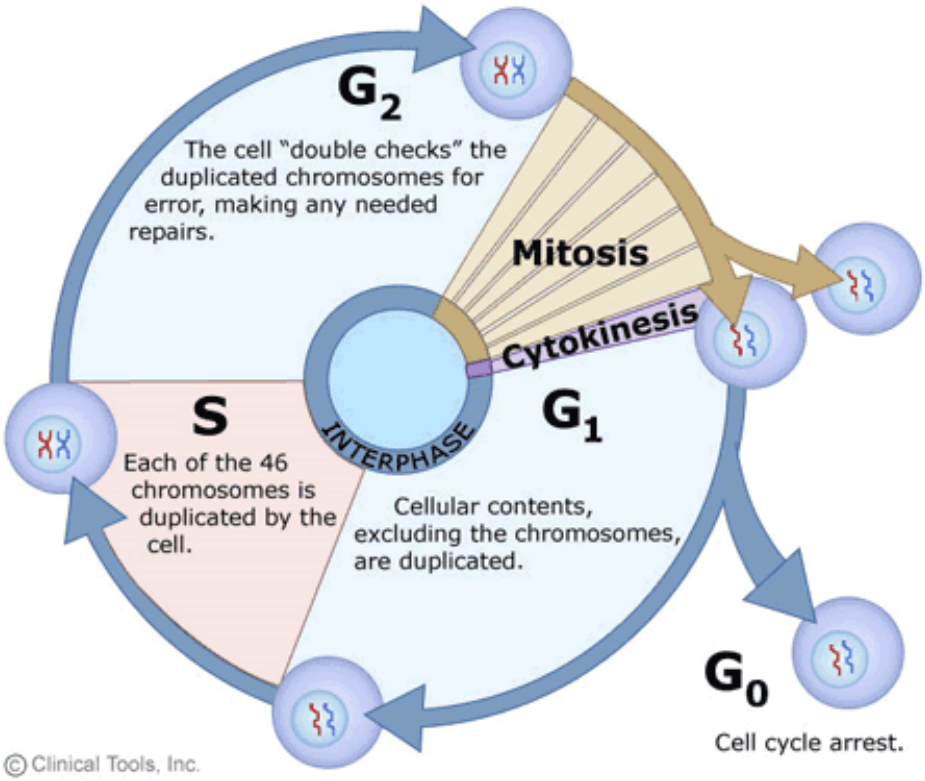

Figure 2.12: The cell cycle. Image excerpted from The cell cycle, n.d.

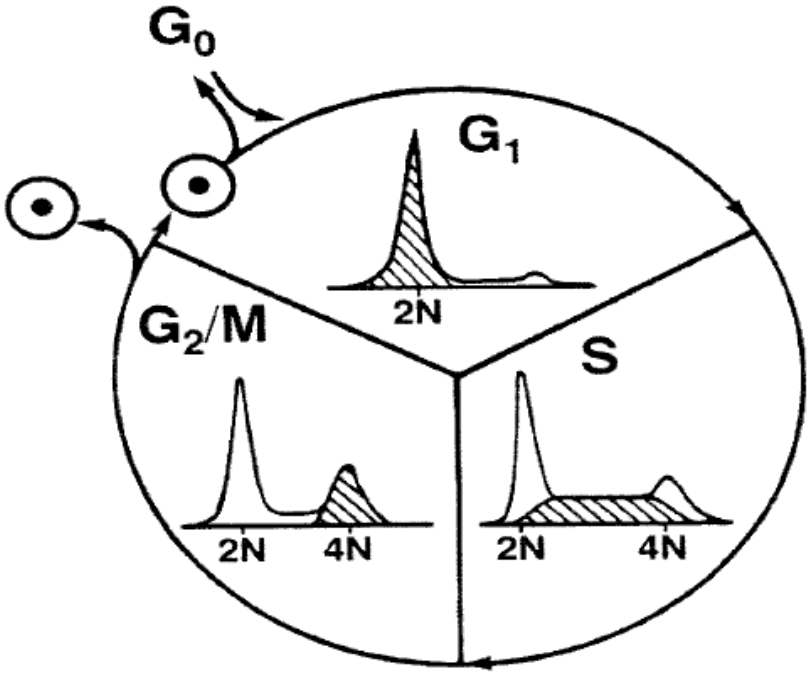

Figure 2.13: The cell cycle components at various phase based on flow cytometry analysis. Image excerpted from Rabinovitch , n.d.

2.9.1 Cell cycle and cancer

One of the hallmarks of cancer is the uncontrolled proliferation of cells. Tumor cells normally acquires damage to genes that directly regulate cell cycles (Sherr, 1996). The correlation between the cell cycle and cancer is quite an obvious one. Cell cycle is machinery, which controls cell proliferation, and cancer is a disease of inappropriate cell proliferation (Collins et al., 1997). The oncogene products are proteins that are involved in the cell cycle regulation by stimulating cellular growth and division. Oncogenes, which drive the cell cycle forward in abnormal situations, would exhibit increased activity and contribute to tumor growth. Instead of stopping within a G phase as it should, a tumor would continue to progress through subsequent phases of the cell cycle and thus leading to uncontrolled cell proliferation. Oncogenes can also rescue cells from programmed cell death. Mutations that occur may cause the oncogene activation, which results in certain proteins to be in permanently active phase where in normal situations they would fluctuate between active and inactive state. Another genetic alteration would be the chromosomal translocation where the pieces of broken chromosomes reattach haphazardly leading to either the formation of a fusion protein leading to altered regulation of protein expression. Yet another scenario is where the proto-oncogenes occur in multiple copies leading to amplified expressions which leads to increased expression of its transcriptional targets that would drive the cell cycle forward (Chow, 2010). On the other hand, tumor suppressors, which inhibit cell cycle progression, maintain cell cycle checkpoints, and induce apoptosis, are aberrant in the event of cancer. Mutated tumor suppressors leads to uncontrollable cell division, proliferation and cell cycle without a stop signal (Chow, 2010).

Table 2.2: Cell cycle targeted cancer chemotherapeutics

Agent	Class	Target	Phase affected
5-Fluorouracil	Antimetabolite	Thymidylate synthase	S
Gemcitabine	Antimetabolite	Nucleoside analogue and ribonucleotide reductase	S
Methotrexate	Antimetabolite	Dihydrofolate reductase	S
Irinotecan	Camptothecin	Topoisomerase I	S
Cisplatin	Alkylating agent	DNA interstand crosslinks	S/G_2
Docetaxel	Taxane	Tubulin	M
Paclitaxel	Taxane	Tubulin	M
Vincristine	Vinca alkaloids	Tubulin	M

Table excerpted from Williams et al. (2012)

Many of the current imminent therapeutic agents are cell cycle directed. An important component or phase in the cell cycle is the DNA replication initiation pathway which has emerged as an attractive diagnostic and therapeutic target over the last decade (Williams et al., 2012).

2.10 NF-κB Pathway

NF-κB or nuclear factor kappa-light-chain-enhancer of activated B cells was found 30 years ago. It is a transcription factor that is involved in various biological activities such as immune response, inflammation, cell growth and survival and development, particularly in immune system (Zhang et al., 2017). It is important in human and abnormality in this pathway often leads to various diseases such as atherosclerosis, inflammatory bowel diseases, cancer, rheumatoid arthritis and others (Park et al., 2016). It consists of a group of five transcription factors that could form distinct complexes. It could bind to DNA sequences to initiate transcription in regulating cellular processes (Xia et al., 2014). This pathway could be activated due to various stimuli. The stimulis includes UV rays, ionizing radiations, reactive oxygen species (ROS), DNA damage, stress, growth factors, cytokines and others. Nuclear factor-κB (NF-κB) consists of a family of five related transcription factors which includes NF-κB1/p105, NF-κB2/p100, RelA/p65, RelB and c-Rel that works as hetero- and homodimers. It could form up to 15

NF-κB complexes. Through a pathway knowan as the “canonical pathway”, causes the activated of the inhibitor of κB (IκB) kinase (IKK) complex. Activated IKK complex results in phosphorylation and degradation of IκB (inhibitor). This would cause the activation of the NF-κB pathway. Thus, the free NF-κB dimers (p50 and p65) translocates to nucleas from cytoplasm to bind to DNA to initiate transcription that would synthesize proteins that could respond to the stimuli received earlier (Xia et al., 2014). The tremendous ability of NF-κB to manipulate cell’s biology is due to the hundreds of target genes that it could activate and suppress (Zhang et al., 2017).

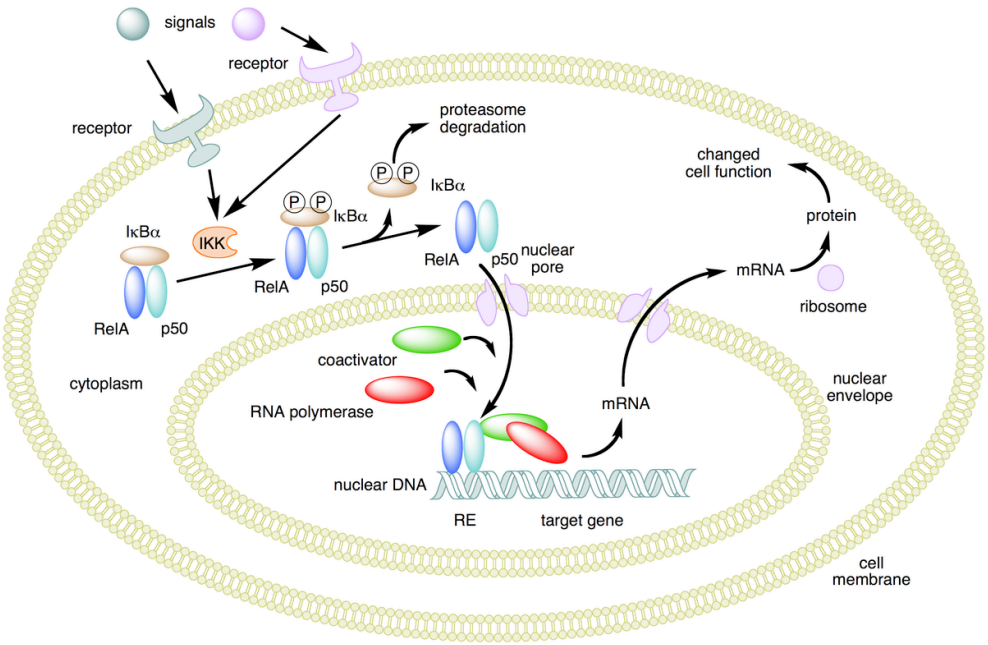

Figure 2.14: The mechanism of NF-κB pathway (Image excerpted from : NF-κB, 2007)

2.10.1 NF-κB Pathway and Cancer

NF-κB has been identified as a crucial contributor in the cancer initiation and progression steps. NF-κB has particularly been described to have a double-edged role in cancer. This is because activation of NF-κB occurs in events of immune defense which

acts to eliminate abnormal cells such as cancer cells. NF-κB also was discovered to be constitutively activated in many types of cancer and it exerts pro-tumorigenic functions (Hoesel et al., 2013). Active NF-κB upregulates the expression of genes that causes cell proliferation and evades apoptotic events. Cancer-related chromosomal translocations, mutations, deletions could disrupt genes that code NF-κB related proteins and thus cause constitutive activation of NF-κB transcription factors which could result in cancer-cell proliferation, preventing apoptosis, and angiogesis and metastasis of cancer cells (Park et al., 2016). In certain conditions, NF-κB remodels metabolism and manipulate immune system to support tumor growth. NF-κB suppression in myeloid cells or tumor cells often leads to tumor regression. This makes NF-κB pathway a promising chemotherapeutic target for targetted therapy (Xia et al., 2014).

NF-κB assists crosstalk between inflammation and cancer. In cancer cells with high activity of NF-κB, the accumulation of pro-inflammatory cytokines at the tumor site contributes to the pro-tumorigenic microenvironment. A chronic inflammatory microenvironment could lead to immunosuppression where the the cancer cells could evade immunosurveillance and also to genomic instability and mutations which could start tumor. NF-κB induces the expression of anti-apoptotic genes i.e. FLIP, c-IAP1/2, XIAP and members of Bcl2 family. NF-κB also activates VEGF and MMPs which helps to stimulate angiogenesis. Activation of metastasis by initiation of epithelial mesenchymal transition (EMT) was found to be regulated by NF-κB in breast cancers. NF-κB pathway also is responsible in regulation of various cell adhesion molecules and ligands such as integrins, selectins that facilitate the extravasation and colonization of cancer cells to secondary sites. NF-κB induces metastasis processes. Besides these factors, Various oncogenic mutations such as mutations in EGFR, Ras, PI3K and p53 causes NF-κB activation in tumor cells. NF-κB was also discovered to be able to

reprogramme metabolisms of cancer cell to promote its survival. Various NF-κB inhibitors have emerged however the effectiveness has not reached to a desired level. One of the main concern about NF-κB inhibitors is that they may impose undesired effect upon prolonged administration as NF-κB controls a pleiotropic cellular functions especially in immune system i.e. innate and adaptive immune responses. Prolonged immunosupression would bring adverse effects (Xia et al., 2014).

2.11 EGFR Pathway

Epithelial growth factor receptor (EGFR) is a 170-kDa transmembrane tyrosine kinase receptor, which is classified to ErbB family of cell membrane receptors. It is also also known as ErbB1/HER1. There are several other receptors in this family. Other members in the EGFR family include ErbB2/HER2/Neu, ErbB3/HER3, and ErbB4/HER4. The ErbB gene family that encodes this protein in human includes EGFR/ERBB1/HER1, NEU/ERBB2/HER2, ERBB3/HER3, and ERBB4/HER4 (Wee et al., 2017). Under normal conditions, this receptor functions to to regulate epithelial tissue development and homeostasis (Sigismund et al., 2018). These receptors are held in the cytoplasmic membrane and have an extracellular ligand-binding region, a hydrophobic transmembrane region and an intracytoplasmic tyrosine kinase-containing domain (Scaltriti et al., 2006).

EGFR signalling commences when a ligand binds to the ligand-binding region in the receptor. Ligand binding initiates dimerizaton of receptor with formation of homodimers and heterodimers that causes the activation of tyrosine kinase. The tyrosine kinase located in the cell is then autophosphorylated thus activating further downstream signalling pathways such as mitogen-activated protein kinase (MAPK) pathway and the phosphatidylinositol 3-kinase- (PI3K-) protein kinase B (AKT) pathway. Activation of these pathways would then activate various transcription factors

which then causes cellular responses such as proliferation, migration, differentiation, and apoptosis (Krasinskas, 2011).

Activation of EGFR pathway is a tightly regulated process. Multiple ligands are shared and lateral signalling between members of the ErbB family takes place. Positive and negative feedback mechanism controls the activation of transcription factors, depending on the cell type. When this strict regulation goes haywire, it results in malignancy and tumor progression. This occurs through increase in cell proliferation, prolonged survival of cell, angiogenesis, anti-apoptosis, invasion and metastasis (Krasinskas, 2011).

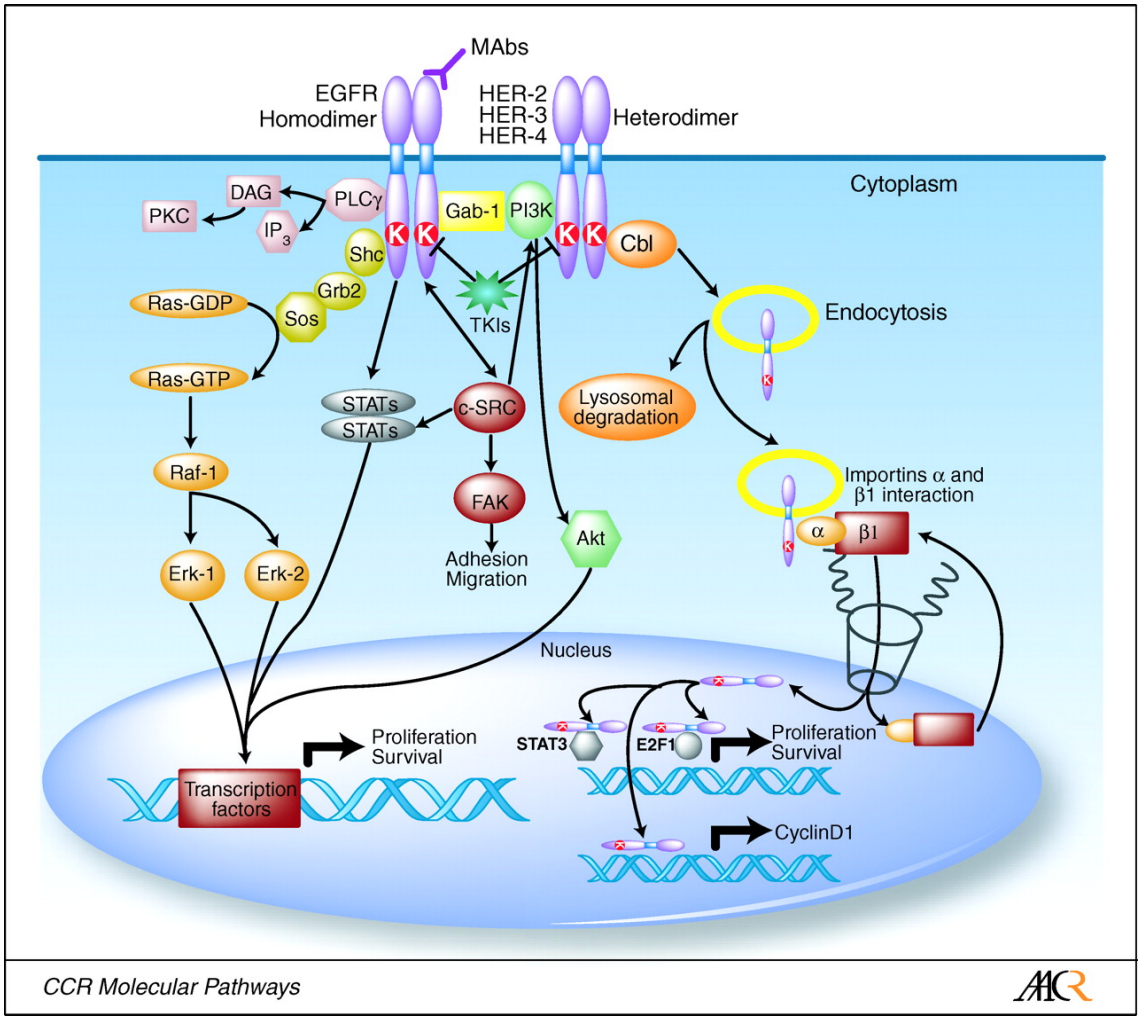

Figure 2.15: Overview of the EGFR signalling pathway and inhibitors. Image excerpted from Scaltriti et al. (2006).

2.11.1 EGFR Pathway and Cancer

EGFR is a tyrosine kinase receptor that is often expressed in epithelial tumors (Scaltriti et al., 2006). The EGFR receptor is commonly upregulated and deemed as driver of tumorigenesis in non-small cell lung cancer, head and neck cancer, breast cancer, pancreatic cancer, glioblastomas and metastatic colorectal cancer. Numerous mechanisms assist in the upregulation of EGFR activity. These include mutations and truncated extracellular domain. Aberrations in EGFR upregulate downstream pro-oncogenic signalling pathways (Wee et al., 2017). Besides amplications due to point mutations at genomic locus, overproduction of ligands due to autocrine or paracrine mechanisms has also been described as a reason for the upregulation of this pathway (Sigismund et al., 2018). Downstream signalling pathways such as RAS-RAF-MEK-ERK MAPK and AKT-PI3K-mTOR are activated in the event of cancer. These activations often result in various biological outputs that assist cancer cell proliferation (Wee et al., 2017). Besides that, EGFR has been progressively described as a biomarker of resistance in tumors. Amplifications and secondary mutations develop under drug pressure that leads to resistance and this has been utilized in pathological investigations of tumor. EGFR has turn out to be a principal target for therapeutic intervention (Sigismund et al., 2018).

More than 60% of non-small cell lung carcinomas (NSCLCs) show upregulated expression of EGFR and it has emerged as an essential therapeutic target for this type of tumors. EGFR kinase domain inhibitors have been developed and respond effectively, clinically. Tyrosine kinase inhibitors (TKIs) are effective for patients with mutations in tyrosine kinase domain of EGFR gene. Recent studies have suggested that it is best that patients with advance NSCLC with EGFR mutations, start treatment with TKI instead of the conventional chemotheraphy (da Cunha Santos et al., 2011).

2.12 Metastasis

Metastasis is a process which has several stages. It involves spreading of malignant cells from primary tumor to distant organs. In 1892, Jean Claude Recamier was the first to document metastasis — "métastase", hematogenous spread of disease (Ganapathy et al., 2015). It is a process of colonization of a cancer from the primary site to secondary site in a series of processes. These steps include separation from the primary tumor, invasion through the surrounding tissues and basement membrane, entry and survival in the circulation, lymphatics or peritoneal space and arrest in the secondary target organ. Cancer cell colonization in the secondary site includes steps such as extravasation in the surrounding tissue, survival in the foreign microenvironment, proliferation, and induction of angiogenesis. These steps occur in a constant environment of evasion of apoptosis and immunological responses (Hunter et al., 2008).

Cancer usually triggered from a primary site however, the subsequent metastasis events that cause the mortality of the patient. Metastatic tumor cells exhibit characteristics which differ from the primary tumor. It might have acquired additional genetic or epigenetic changes under exposure to chemotherapy and radiotherapy treatments, it is resistant, invasive and it resides in a microenvironment which is different from the origin. Treating a metatastatic cancer is particularly challenging (Ganapathy et al., 2015). Primary tumors could respond well to surgery and adjuvant treatment however secondary tumors often are incurable due to its systemic nature and the resistance of disseminated tumor cells to existing therapeutic agents. More than 90% of mortality due to cancer is caused by metastases and not the primary tumor. Effective treatment of cancer lies on capacity to stop metastasis of cancer cells (Valastyan et al., 2011).

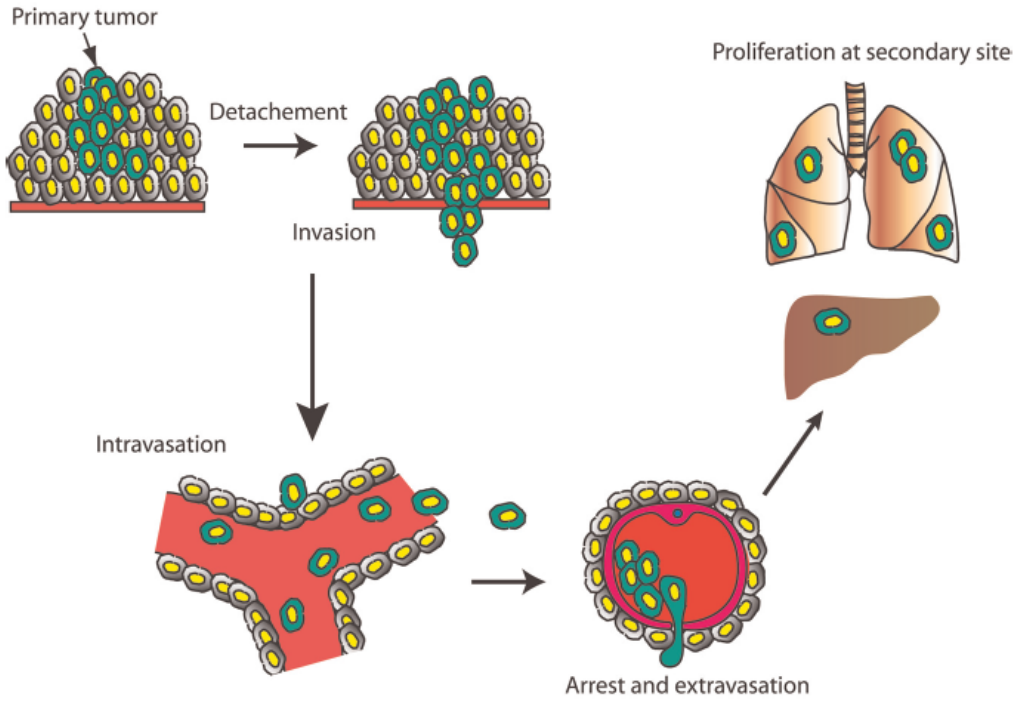

Figure 2.16: The metastatic process. Image excerpted from Hunter et al. (2008).

2.12.1 Stephen Paget's Soil and Seed Theory on the Mechanism of Metastasis

In 1889, Stephen Paget described an organ-specific pattern of metastasis (van Zijl et al., 2011). Stephen Paget's seed and soil theory of metastases, is an interesting theory where it states that a suitable microenvironment in the distal organ which is refered to as the soil promotes the growth of the disseminated tumor cells which is refered to as the seeds. This basis of research is widely accepted to summarize the mechanism of metastasis (Ganapathy et al., 2015). Example on the theory is such as metastasis of breast carcinoma are commonly at the bone, the lung and the brain whilst colorectal and pancreatic cancer shows preferential sites of distal colonization in the liver and the lung (van Zijl et al., 2011).

2.12.2 The Metastatic Cascade

The “metastatic cascade” is an observation, which was first reported in 1975. This involves significant steps such as the local invasion, intravasation into adjacent blood and lymphatic vessels, transit through circulation and evasion of host immune systems, extravasation into the parenchyma of distant organs, and colonization and formation of micro-metastases, followed by proliferation and progression to macro-metastases (Ganapathy et al., 2015).

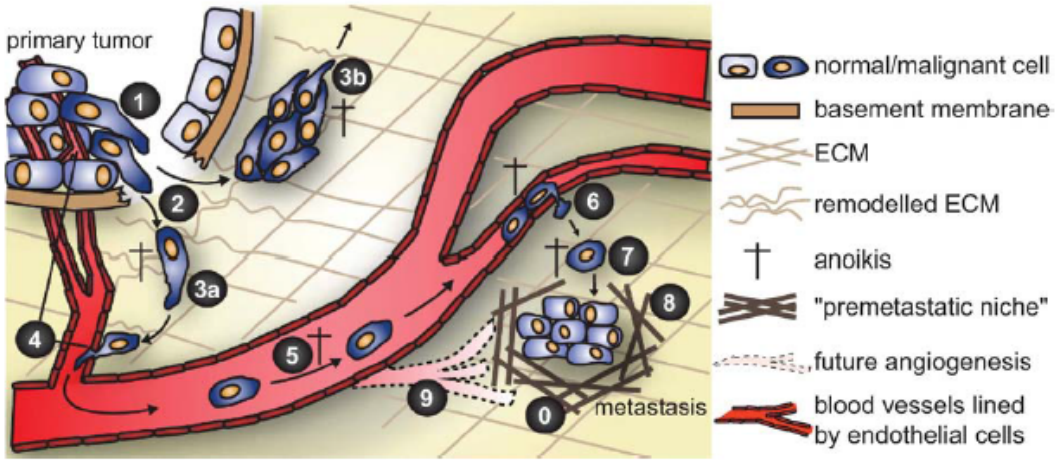

Figure 2.17: Metastatic cascade. Image excerpted from Geiger et al. (2009).

The metastatic cascase could be described as follows:

At the step (0), a “premetastatic niche” is formed before metastasis is significant. This step is induced by a distant tumor and is assisted by bone-marrow derived cells. At the step (1), cells at the primary tumor site undergoes Epithelial-Mesenchymal Transition (EMT) in order to achieve its invasive property. At the (2) step, degradation of basement membranes and remodelling of Extracellular Matrix (ECM) occurs. This step is facilitated by proteinases which promotes tumor cell invasion. Next, tumor cells invade to the surrounding tissues as single cells (3a) or in aggregate (3b). The

movement of tumor cells into vessels nearby is described as intravasation (4). In step (5), the tumor cells are transported through the vasculature and then it is arrested in a capillary bed. After this, they move out of the capillary (6) and this step is known as extravasation. Extravasated cells can remain dormant at the secondary sites for years (7). Some cells grows to secondary tumor and this steps requires ECM remodelling and angiogenesis (8). Step no (9) shows anoikis which is detachment-induced apoptosis. Anoikis could hinder the progresssion of metastasis (Geiger et al., 2009).

2.13 Rationale for The Bioassays Used in This Research

Various assays were done throughout this research. The research was started with the study of cytotoxicity of the crude extracts of the plant and also the isolated compounds. SRB assay was done and this assay is a quick, easy and stable assay. The results obtained are reproducible. This assay was done to measure the cytotoxic potency of the extracts and the isolated compounds. Going further, apoptosis assays were conducted on the selected isolated compound i.e. chalepin. Apoptotic analysis is divided into morphological and biochemical analysis. The morphological analysis includes phase contrast microscopy study and Hoesct 33324/PI staining studies. In phase contrast microscopy, we can view the changes in the morphology of the cell upon treatment with the compound chalepin, whereas in Hoesct 33342/PI staining, it was conducted to determine the different phase of apoptosis the cells are into at various timepoints and concentrations. The biochemical analysis, on the other hand, consists of Annexin V-FITC/PI apoptosis detection assay, measurement of the intracellular ROS, mitochondrial membrane potential determination, TUNEL assay and caspase 3,8,9 activation assay. The Annexin V-FITC assay was done to quantitatively determine the population of cells at different phases of apoptosis (early apoptosis or late apoptosis), necrosis or viable upon treatment with chalepin. Our focus is that upon treatment with

chalepin, the compound should be able to induce apoptosis and this could be determined via this study. Prior to initiation of apoptosis, certain drugs/compounds could induce and increase in the intracellular ROS and this would start the apoptosis in the cell. The measurement of intracellular ROS was done to determine if chalepin was able to cause any fluctuations in the intracellular ROS level of the A549 cell to initiate apoptosis. One of the most important event that happens during apoptosis is the loss of the mitochondrial membrane potential. Loss of the mitochondrial membrane potential is an indication that the cell is undergoing apoptosis. The mitochondrial membrane potential changes was studied via the above mentioned bioassay. During apotosis, there are various changes that happens in the cell which includes DNA fragmentation which would lead to cell death. The DNA fragmentation is studied via TUNEL assay which gives us an insight on the percentage of DNA fragmentation in the cell upon treatment with chalepin. Caspase activation is an imminent event in the process of apoptosis. Activation of caspase often is an indication of the initiation of apoptosis. Caspase 3 activation assay gives us an insight on the ability of chalepin to activate this caspase which acts as an executioner caspase to cause DNA fragmentation. Caspase 9 activation assay was done to determine if chalepin was able to initiate the initiator caspase in the intrinsic apoptotic pathway. Activation of caspase 8 assay was done to determine the ability of caspase to induce the extrinsic apoptotic pathway. In order for cells to propagate, it has to undergo the cell cycle which would start mitosis of the cell to produce a daughter cell. Faulty cell cycle would often cause the cell cycle switch to be always turned on and this leads to cancer. A promising chemotherapeutic drug would be able to inhibit cell cycle at its various phases to stop the cells from multiplying. The cell cycle analysis was done to determine the ability of chalepin to inhibit cell cycle in A549 cells. All of the above mentioned assay gives us a rough idea on the ability of the compound chalepin to induce apoptosis and the mechanism of action. The next level of

study is to determine how chalepin would alter the expression of proteins in certain cancer related pathways. This was studied via western blotting analysis which makes up a major part of this research. The tryphan blue dye exclusion assay was done to determine the best timepoint of study for western blotting analysis as for this study, the expression of proteins should be studied prior to the commencement of cell death i.e. the cells should be viable when harvesting the protein. In the western blot analysis, the ability of chalepin to act as a targetted therapeutic drug was studied based on selected cancer related pathways i.e. intrinsic apoptotic pathway, extrinsic apoptotic pathway, EGFR pathway, NF- κB pathway, and cell cycle related proteins. The next phase of study is the metastatic study. In this study, we determine the ability of methanol extract, chloroform extract and chalepin to inhibit metastasis. Metastasis proceed in a few steps. The bioassays chosen was done to determine the different criteria of the cell during metastasis, that the test samples could inhibit. Motility is an important feature in live cell. In order for a cell to spread, it must be able to move from its initial dwelling to its secondary site. The ability of the test samples to inhibit the motility of the cell was studied via wound closure assay, which determines the migration ability of whole cell mass and Transwell anti-migration assay, which measures the ability of cells to respond and move to chemoattactants. Next, the cell must be invasive i.e. able to pass through membrane barriers. Once tumor cells acquire the ability to penetrate the surrounding tissues, the process of invasion is started. Theses motile cells pass through the basement membrane and extracellular matrix, (intravasation) – vascular circulation. This property is studied via Transwell anti-invasion assay. Next in the process of metastasis, the cell has to be able to adhere at a secondary site in order for it to colonize. In order to colonize a secondary site it has to interact with adhesion molecules which would assist in the colonization. The ability of the test samples to inhibit the various adhesion molecules were studied using the extracellular matrix (ECM) protein array cell adhesion

molecules assay. Following this, the ability of the treated cell to attach to a secondary site was studied via the cell attachment assay. In order for the cancer cells to pass through various membrane barriers, the enzyme matrix metalloproteinase (MMPs) assists in the degradation of the matrix in order for cells to pass through easily for metastasis. The gelatin zymography was studied to determine the ability of the test samples to inhibit one of the important MMPs i.e. MMP2 which plays a vital role in metastasis via inhibiting type IV collagen to promote invasion and metastasis of tumor cells. Western blot analysis was also conducted to give a brief idea on how chalepin acts on selected metastasis related proteins.

CHAPTER 3: MATERIALS AND METHODOLOGY

3.1 Materials

3.1.1 Solvents

Acetone, chloroform, ethanol (95%), absolute ethanol, ethyl acetate, hexane, methanol were purchased from Merck (HPLC grade) and acetonitrile was purchased from JT Baker (HPLC grade).

3.1.2 Cell lines

The cell lines namely CaSki (human caucasoid cervical carcinoma cells), HCT116 (human colorectal carcinoma cell, A549 (human lung carcinoma cell) and MRC-5 (human normal fibroblast cell) were purchased from American Type Culture Collection (ATCC).

3.1.3 Growth medium

The growth medium namely EMEM (Eagle's Minimum Essential Medium), DMEM (Dulbecco's Modified Eagle's Medium), and RPMI (Roswell Park Memorial Institute) 1640 were purchased from Sigma.

3.1.4 Drugs, chemicals and reagents

The chemicals and reagents that were used in the study are as follows:

Urea (Sigma), penicillin/streptomycin (Sigma), bovine serum albumin (BSA) (Nacalai), amphotericin B (Nacalai), foetal bovine serum (FBS) (Nacalai), glacial acetic acid (Sigma), glycerol (Merck), methylbis acrylamide (Merck), acrylamide (Merck),

dithiotheriol (DTT) (Sigma), dimethyl sulphoxide (DMSO) (Sigma), phosphate saline buffer (PBS) (Sigma), thiourea (Sigma), sodium pyruvate (Sigma), trypan blue (Biorad), ammonium persulphate (APS) (Merck), hydrochloric acid (Sigma), paraformaldehyde (PFA) (Sigma), Hoechst 33342 (Sigma), HEPES (Sigma), ethylene diamine tetrachloroacetic acid (EDTA.4Na_4H_2O) (Sigma), sodium azide (Sigma), RNase A (Sigma), propidium iodide (PI) (Sigma), N,N'-Methylethylenediamine (TEMED) (Biorad) , sodium dodecyl sulphate (SDS) (Sigma), suphorodamide (SRB) dye (Sigma), trichloroacetic acid (Merck), Tris buffer (Sigma), thin layer chromatography (TLC) plates of silica gel 60 F254,of 20.25 mm thickness (Merck), DCFH-DA (Sigma), bromophenol blue (Sigma), glycine (Sigma), Laemnli buffer (Biorad), Accutase (Sigma), coomasie brilliant blue R-250 (Sigma), gelatin (Sigma), Triton X-100 (Sigma), sodium carbonate (Sigma), deuterated chloroform ($CDCl_3$) (Merck), glycine (Sigma), β-mercaptoethanol (Sigma), blocking buffer (Nacalai), transfer buffer (Merck), secondary antibody (host rabbit and host mouse) (Santa Cruz), 3-(4,5-Dimethylthiazol-2-yl)-2,5-Diphenyltetrazolium Bromide (MTT) (Sigma), activated charcoal (Merck), crystal violet dye (Sigma), cisplatin (Sigma), doxorubicin (Sigma) and anhydrous sodium sulphate (Sigma).

3.1.5 Kits

Annexin V Apoptosis Detection Kit (BD Biosciences, USA)

APO-BrDU TUNEL Assay Kit (Invitrogen)

CaspILLUME Fluorescein Active Caspase-3 Staining Kit (GeneTex)

CaspILLUME Fluorescein Active Caspase-8 Staining Kit (GeneTex)

CaspILLUME Fluorescein Active Caspase-9 Staining Kit (GeneTex)

JC1 - Mitochondrial Membrane Potential Assay Kit (Abcam)

BD™ MitoScreen (JC-1) (BD Biosciences)

QuickStart™ Bradford Protein Assay (Biorad)

WesternBright ECL HRP substrate (Advansta)

Nuclear Extract Kit (Active Motif)

Mitochondria/Cytosol Fractionation Kit (BioVision)

Merck ECM 508 QCM^{TM} 24-well cell migration assay kit

Merck ECM 554 QCM^{TM} 24-well cell invasion assay kit

Merck ECM 540 QCM^{TM} 96-well cell adhesion assay kit

3.1.6 Antibodies

The antibodies that were used in this study are as follows:

β-actin, Bcl-2, Bax, Bak, Lamin B1, GAPDH, p65, p-p65, PARP, p53, survivin, XIAP, BCL-XL, cFLIP, cytochrome c, procaspase 9, procaspase 3, cleaved caspase 3, cyclin E, cyclin D1, cdk2, cdk4, p21, p27, pRb, cIAP-1, cIAP-2, MCL-1, COX-2, c-myc, pIKβα, Ikβα, pSTAT3, STAT3, DR4, DR5, Bid, ICAM-1, VEGF, pEGFR, EGFR, Jak1, ERK, pERK, pAkt, Akt, p-c-raf, c-raf, p-mTOR, mTOR, MEK, pMEK, ras, p-SAPK/JNK, SAPK/JNK, p-p38-alpha and p38. All the antibodies were purchased from Cell Signalling Technologies (CST) and Santa Cruz.

3.1.7 Equipments

High performance liquid chromatography (HPLC) (Agilent), Gas chromatography-mass spectrometry (GC-MS) (Agilent), rotary evaporator (Buchii), Nuclear magnetic resonance (NMR) (Bruker), Agilent Semi Prep XDB-C18 column, 9.4 x 250 mm with internal diameter of 5 μm with guard column 300 SB-C3, glass slides, fluorescence microscope (Leica), phase contrast microscope (Leica), light microscope (Leica), flow cytometer (Accuri), Gel-Doc (Bio Rad), Gel electrophoresis setup (Bio Rad), spectrophotometer (BioTek), fluorescence reader (BioTek), autoclave machine, liquid

nitrogen storage, microplate reader (BioTek), CO_2 incubator (Thermofisher), Centrifuge (Lab companion), microcentrifuge (Thermo), Cell counter (Bio Rad), pH meter (Sigma), Biosafety cabinet (Esco), GC-MS vials, separating funnel, incubator, oven.

3.1.8 Softwares

Modfit, Leica Suites, Microsoft Excel, Zen 10, ImageJ, ImageLab, Accuri C6 software, Agilent ChemStation

3.2 Methodology

3.2.1 Preparation of Crude Plant Extracts

3.2.1.1 Source of plant material

The whole plant of *Ruta angustifolia* Pers. was obtained from a plant nursery near Sungai Buloh, Selangor, Malaysia. The plant was identified by Slamet Wahyono from the Research Station of Medicinal Plant and Traditional Medicine Research and Development Centre, Tawangmangu, Central Java, Indonesia. A voucher specimen numbered KLU48128 was deposited at the Herbarium of the Institute of Biological Sciences, Faculty of Science, University of Malaya.

Figure 3.1: Voucher specimen of *R.angustifolia* that was deposited in Herbarium UM

3.2.1.2 Preparation of plant extracts

i) Preparation of the methanol extracts and its fractionated extracts

The leaves of the plant were separated, washed and dried in an oven at a constant temperature of 50 ^{o}C for 3 days. The dried leaves were then ground using a commercial blender to a fine powder. The finely ground samples (175.0g) were weighed into a conical flask. Methanol was added into the conical flasks. Methanol was added into the conical flask and the sample was soaked for 3 days. The volume of methanol used was just enough to cover all the samples. At the end of the 3rd day, the methanolic solution was decanted. Anhydrous sodium sulphate was added to the filtrate to absorb any excess water. The methanol containing extract was then filtered using Whatman filter paper. Next, the filtrate was evaporated by using a rotary evaporator under reduced pressure, to give a greenish methanolic extract (55.0 g, 31.43 %). The remaining

sediment of the powdered leaves was re-soaked with fresh methanol solvent and the above-mentioned process is repeated. This is repeated for 2 times and this totals up the whole procedure of extractions to a total 9 days. The crude methanolic extract was then fractionated with hexane to give fractionated hexane soluble extract. This was done by pouring in hexane solvent into the methanol extract in the round-bottomed flask and shaking the round-bottomed flask with hexane vigorously for few minutes. The hexane solvent was then decanted and anhydrous sodium sulphate was added to the filtrate to absorb any excess water. The hexane solvent containing extract was then filtered using Whatman filter paper. The hexane solvent containing hexane soluble compounds was then evaporated under reduced pressure to get the hexane extract (2.96 g, 5.33 %). The residue, which is the hexane insoluble residue, was then partitioned between between chloroform-water (100 mL: 100 mL). This was done by mixing the hexane insoluble residue with 100 mL of chloroform solvent and 100 mL of water and shaken vigorously in the round bottomed flask. Chloroform and water in 1:1 ratio to give fractionated chloroform and water extract. This is done by liquid-liquid extraction using separating funnel. The mixture was shaken gently and left for a few minutes to allow the layers of chloroform and water to settle. The cap of the separating funnel was removed occasionally to release excessive gas. Water layer formed at the bottom of the funnel whereas chloroform layer at the top. Water layer will be eluted first into a conical flask followed by chloroform layer in another flask. The water layer was repeatedly extracted with chloroform until the chloroform layer becomes colorless. Anhydrous sodium sulphate was added to the filtrate to absorb any excess water in the chloroform layer. The chloroform solvent containing extract was then filtered using Whatman filter paper. The chloroform layer was evaporated under reduced pressure by using rotary evaporator until a green colored extract (11.85 g, 21.35%) was obtained. The aqueous layer was further partitioned to ethyl acetate and water in 1:1 ratio to give fractionated ethyl

acetate extract and water extract. This is done by liquid-liquid extraction again using a separating funnel. The mixture was shaken gently and left for a few minutes to allow the layers of ethyl acetate and water to settle. The cap of the separating funnel was removed occasionally to release excessive gas. Water layer formed at the bottom of the funnel whereas ethyl acetate layer at the top. Water layer will be eluted first into a conical flask followed by ethyl acetate layer in another flask. The water layer was repeatedly extracted with ethyl acetate until the ethyl acetate layer becomes colorless. Anhydrous sodium sulphate was added to the filtrate of ethyl acetate layer to absorb any excess water. The ethyl acetate solvent containing extract was then filtered using Whatman filter paper. The ethyl acetate layer was evaporated under reduced pressure by using rotary evaporator until a yellowish ethyl acetate extract (0.87g, 1.57%) was obtained. The water extract (30.08 g, 54.20%) could be freeze dried or evaporated with a rotary evaporator in small batches with temperature ranging 45-50ºC. Evaporation using rotary evaporator needs a rotary evaporator with strong vacuum pump. Since this process takes longer period of evaporation time, samples are advised to be prepared in small batches to avoid long time of evaporation that might affect the components present in the fraction. All the extracts were weighed and kept in glass vials and stored in refrigerator at a temperature 4ºC prior to be used for various testing. It is noteworthy that this extraction method is known as cold extraction where the compounds in the crude methanol extract are separated using polarity factor. Hexane extract would consist of non-polar compounds whereas chloroform extract would consist of semi polar compounds. Ethyl acetate extract would consist of polar compounds and water extract would consist of very polar components.

The crude MeOH and fractionated extracts (hexane, EtOAc and chloroform) were dissolved in dimethyl sulfoxide (DMSO) with the exception of the H_2O extract which

was dissolved in distilled water to form stock solutions 20 mg/mL before testing. The final concentration of DMSO in test wells was not more than 0.5% (v/v).

ii) Preparation of the chloroform extract without chlorophyll

Activated charcoal (1 teaspoon) was added to the chloroform extract (1.0 g) in 50 ml methanol and the mixture was then mixed well. The mixture was immediately filtered with a filter paper (no. 1) and evaporated under reduced pressure to obtain the chloroform extract without chlorophyll.

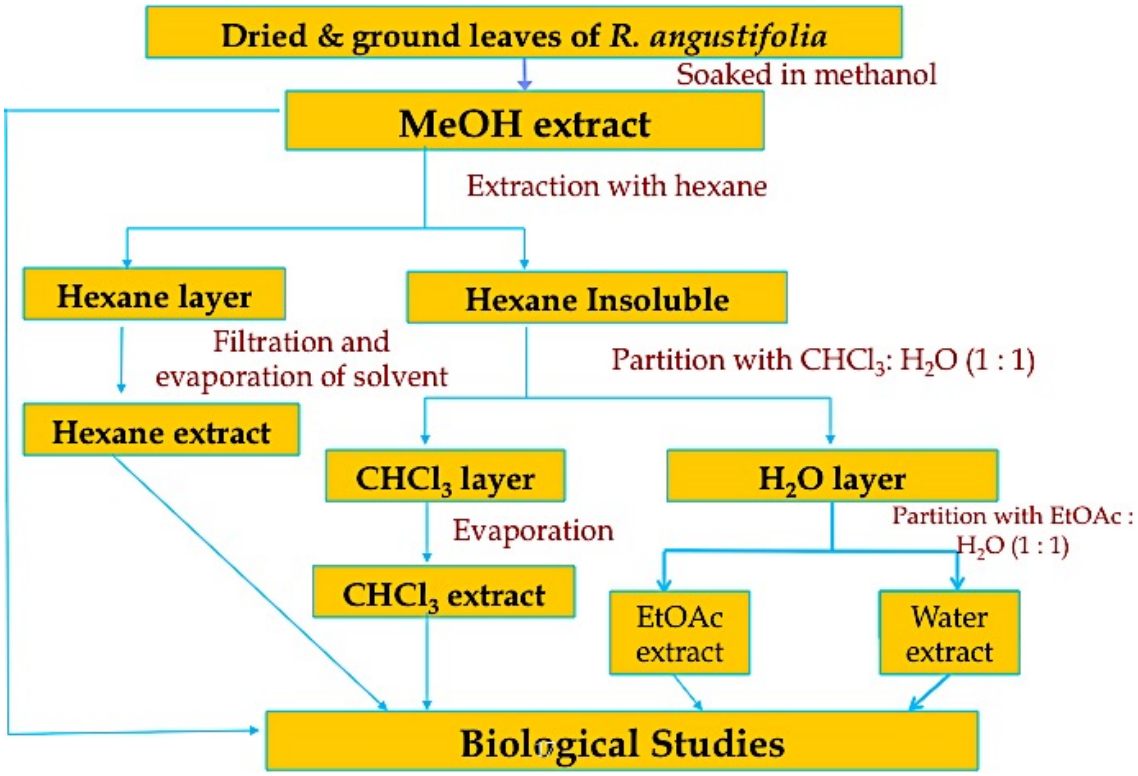

Figure 3.2: Overview of the extraction method

3.2.2 Chemical Isolation and Identification of Pure Compounds

3.2.2.1 Isolation of compounds in the chloroform extract (treated with charcoal) using High Performance Liquid Chromatography (HPLC)

The chloroform extract of *R. angustifolia* was filtered with activated charcoal to remove most of the chlorophyll and the filtrate was evaporated to dry under reduced pressure using a rotary evaporator. The extract was then prepared to a concentration of 5 mg/ml with methanol and filtered through a membrane filter (0.45 μm, Sartorius). The chloroform extract of *R. angustifolia* (treated with charcoal) was repeatedly subjected to HPLC separation. The sample (5.0 μL) was injected onto the column and peaks were detected by monitoring the UV absorbance at 200 nm.

Analytical HPLC analysis was initially performed on an Agilent 1260 infinity HPLC system consisting of a quaternary pump equipped with a 1260 autosampler (ALS), a 1290 thermostat, a 1260 thermostatted column compartment (TCC), a 1260 diode array detector (DAD VL+), a 1260 fraction collector (FC-AS) and Agilent OpenLAB CDS Chemstation for LC software. The analytical analysis was carried out using a binary eluent of chromatographic grade acetonitrile (ACN) and ultrapure water under the following gradient conditions: 0 to 20 minutes isocratic 30% ACN; 20 to 25 minutes linear gradient from 30 to 60% ACN; 25 to 35 minutes linear gradient from 60 to 100% ACN; 35 to 40 minutes isocratic 100% ACN at a flow rate of 1.0 ml/min. The column used was a ZORBAX Eclipse XDB-C18 (4.6 × 250 mm, 5 μm) and the temperature was set at 30 °C. Subsequently the sample was subjected to a semi-preparative HPLC procedure. The sample was prepared at 50 mg/ml in methanol and then 100 μl of the sample was injected into the Agilent Semi Prep XDB-C18 column (9.4 × 250 mm, 5 μm) at a flow rate of 4.18 ml/min. The solvent system used in semi-prep HPLC was exactly the same as analytical HPLC. The only change in semi prep was the increased flow rate. Selected peaks in the resulting chromatogram were repeatedly collected using

a fraction collector. Similar fractions from each round of separation were combined and the mobile phases were evaporated using a rotary evaporator at 40 °C, and the fractions were weighed.

From the analytical HPLC analysis, twenty peaks were observed, and the eluents of the peaks were collected during the semi-prep HPLC run. The fractions were then pooled to give twenty fractions (1-20) based on similarity of spots on TLC. Fractions that showed single spot on TLC were subjected to analytical HPLC analysis for determination of purity. If only one peak was observed in the total ion chromatogram of HPLC, then it is categorized as pure.

Table 3.1: Mobile Phase Solvent System for Analytical and Semi-Preparative HPLC

Time (min)	Solvent (Mobile Phase)
0-20	30 % acetonitrile: 70% ultrapure water
20-25	30-60 % acetonitrile: 70-40% ultrapure water
25-35	60-100% acetonitrile: 40-0% ultrapure water
35-40	100% acetonitrile
40-45	100-30% acetonitrile: 0-70% ultrapure water

3.2.3. Identification of the Isolated Compounds

3.2.3.1 NMR Analysis (Structure Elucidation)

Compounds isolated from HPLC were collected and subjected to Nuclear magnetic resonance (NMR) spectroscopy to deduce the structure and determine the identitiy of the compound. The analysis was conducted at High Impact Research (HIR) Centre,

University of Malaya, Malaysia. The compounds were dissolved in deuterated chloroform ($CDCl_3$) solvent, inserted into NMR tubes and then subjected to proton (^1H), Carbon-13(^{13}C) analysis. The spectra data obtained were compared with previous report by Suhaimi et al. (2017). The NMR spectra were recorded on a Bruker, NMR Avance III 600 MHz spectrometer. The internal reference standard used was tetramethylsilane (TMS).

3.2.3.2 GC-MS Analysis

Identification of compounds using gas chromatography-mass spectrometry (GCMS) was done using the Agilent Technologies 6980N gas chromatography equipped with a 5979 mass selective detector (70 eV direct inlet). The column used was HP-5MS (5% phenylmethyl siloxane) capillary column (30.0 mm x 0.25 mm, 25 μm film thickness) with helium as carrier gas at flow rate of 1mL min^{-1}. The column temperature was programmed initially at 100 ^oC, then increased to 300 ^oC, at 5 ^oC per minute after which the temperature was kept isothermally for 10 minutes. The injector port temperature was set to 230 ^oC and detector to 250 ^oC. The injection volume of sample is 10.0 μL. The total ion chromatogram obtained was autointegrated by ChemStation software and the compounds were identified by comparison of their mass spectral data with an accompanying mass spectral library NIST08 Spectral Library.

The sample was prepared by diluting 0.05 mg of sample into appropriate solvent where the sample dilutes completely. In our study the sample was diluted with chloroform. It is then placed into autosampler GC-MS vials and is then subjected to GC-MS analysis using an optimal method.

3.2.3.3 TLC Analysis

Thin-layer chromatography (TLC) is one of the most commonly used technique for identification of compounds, determining their purity and separation. In the event of a separation problem, this technique comes handy in optimization of the solvent system. In this study, some of the compounds were further confirmed by their Rf values from the TLC analysis by comparison with authenticated compounds. TLC precoated plates (silica gel 60 F_{254}) of 20-25 mm thickness were used and a solvent system consisting of chloroform with a few drops (3 drops) of methanol was used. The solvent system that was initially used was chloroform and methanol which is a more polar solvent was added drop by drop, using a dropper pipette until an optimal resolution and height of the spot (Rf value) was achieved. The Rf value of chalepin in 100% chloroform (which contains 1-2% ethanol) is low. Thus it was necessary to increase the polarity of the developing solvent with a small percentage of methanol. This would increase the Rf value and enable a better resolution of separation and an increased Rf value for the compund. It is also possible to detect any impurities in the sample containing chalepin via increasing the Rf value through addition of methanol. The samples were spot approximately 1.0 cm above the bottom of the TLC plate using a fine capillary tube and allowed to dry. After the spot has dried, the TLC plate was placed into a TLC developing tank containing the developing solvent. When the TLC plate was developed to the solvent front, the plate was then removed from the developing tank. The plate was allowed to dry and was viewed under short (254 nm) and long (365 nm) ultra violet (UV) wavelength visible light. The spots that were seen in UV light is marked using a pencil. Following this, the TLC plate is placed into an iodine vapour chamber to stain the chemical compounds.

All the compounds were identified through their mass spectral data and some of the compounds were identified via nuclear magnetic resonance (NMR) data, however, only the NMR data of chalepin was shown.

3.2.4. Purification Through Recrystallization Method

Chalepin was purified to its purest form through recrystalization method. Chalepin is a polar compound and hence dilutes completely in polar solvents. A solvent in which it partially dissolves i.e. hexane was chosen to be used as the mother liquor. Chalepin was dissolved in hexane with a few drops of chloroform and was heated up using a water bath at approximately 50-60 °C. During heating, chalepin dissolves completely. The dissolved chalepin solution is covered with an aluminium foil with a few holes at the foil to enable slow evaporation. The solution was kept in the fridge (4 °C) for a day and examined the following day. Crystals would start to form slowly at the sides of the vial wall. The crystals were picked out and transferred into another clean vial and the recrystallisation process is repeated once again to obtain purest form of chalepin which has no impurities.

3.2.5 Preparation of Standard Drugs

The standard drugs used in this study were cisplatin and doxorubicin. These drugs were prepared by dissolving 1 mg in 1 ml of sterile PBS to make up to a stock concentration of 1 mg/ml, which would be further diluted to the desired concentration. These stock standard drugs were wrapped with aluminium foil and stored at -20 °C until further usage.

3.2.6 Cell Culture and Cytotoxicity Studies

3.2.6.1 Sulforhodamide (SRB) Cytotoxicity Assay

Concept of SRB Cytotoxicity Assay

This assay is used for cell density determination, based on the measurement of cellular protein content. The principle of the assay is based on the ability of the protein dye SRB to bind electrostatically and pH dependent on basic amino acids of cells that are fixed by trichloroacetic acids (Voigt, 2005). It depends on the intake of the negatively charged pink aminoxanthine dye, SRB by basic amino acids in the cells. Under acidic conditions, it binds and under mild basic conditions it can be expelled out from the cells and is used for absorbance measurement (Voigt, 2005). The higher the number of cells, the greater the amount of dye taken up. After fixation and cell lysis, the dye would be more intense to give a high absorbance value (Houghton et al., 2007). SRB assay is also proven to be linear with the cell number and cellular protein measured, sensitive and comparable to such as Lowry and Bradford, favourable signal to noise ratio, indefinately stable and it is an endpoint colorimetric assay which is non-destructive. These features enables SRB to be used as a preferred way of measurement of drug induced cytotoxicity even in large-scale usage (Voigt, 2005).

3.2.6.2 MTT (3-(4,5-Dimethylthiazol-2-yl)-2,5-Diphenyltetrazolium Bromide)

Concept of MTT Cell Proliferation Assay

This assay is based on the reduction of the tetrazolium salts. The yellow tetrazolium MTT (3-(4, 5-dimethylthiazolyl-2)-2, 5-diphenyltetrazolium bromide) is reduced by cells which are metabolically active, precisely by dehydrogenase enzymes, to generate reducing equivalents such as NADH and NADPH. Viable cells could convert MTT into a purple colored formazan with maximum absorbance of 570 nm. However when cells

die, they are unable to convert the dye to formazan purple hence this serves as a marker to measure only cells that are alive.

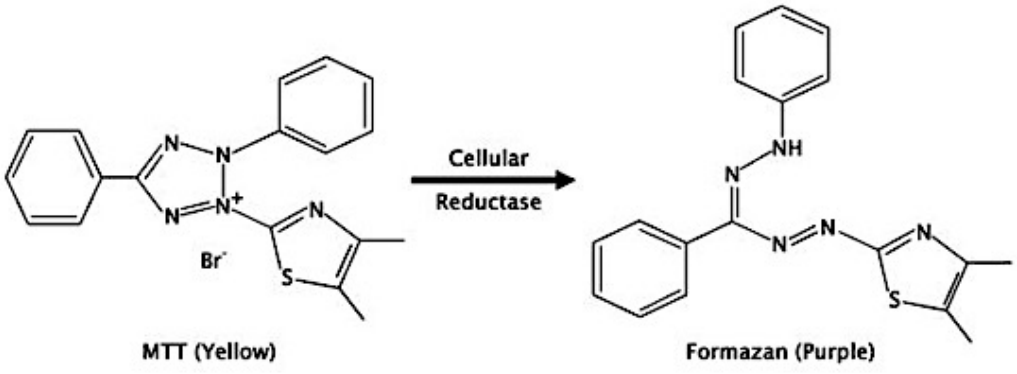

Figure 3.3: The principle of MTT Assay (Excerpted from: MTT cell proliferation assay, 2014)

The purple formazan accumulates as an insoluble precipitate inside cells and also deposited near the cell surface. It should be solubilized before absorbance reading is taken. DMSO, SDS dimethylormamide are some of the agents that could be used for solubilization purpose. The solubilizing agent should be able to stabilize the color, avoid evaporation and reduce interference of phenol red and other culture medium's components (Riss et al., 2015).

3.2.6.3 Cell Lines

The human colon carcinoma cells (HCT 116), CaSki, (a human epidermal carcinoma of cervix cell line), A549 (a human lung cancer cell line) and MRC5 (human normal lung fibroblasts) were purchased from the American Tissue Culture Collection (ATCC, USA). The viability of the cells was checked before and after treatment using tryphan blue exclusion dye method. Frozen cell stocks were stored in liquid nitrogen (-196ºC) prior to use.

3.2.6.4 Preparation of Medium

A supplemented media of 20% was prepared by adding 74.5 ml of basic media (suitable for the respective cell line used), with 20 ml of inactivated foetal bovine serum (FBS), 1 ml of L-glutamine (200 mM), 0.75 ml of sodium pyruvate (100 mM), 0.75 ml of non-essential amino acids (100x), 2 ml of penicilin/streptomycin (100x) and 1 ml amphotericin B (250 μg/ml). The medium was filtered with a 0.22 μm filter membrane and stored at 4 °C up to a month. The FBS is inactivated by placing FBS in 56 °C for 30 minutes. This is done to inactivate complement proteins that are found in newborn calf serum which might interfere with the cell culturing. The 20% media is often used during cell revival or to boost growth of cells.

The 10% RPMI 1640 medium was prepared by addition of 87 ml of pre-mixed basic media (RPMI) with 10 ml of inactivated FBS, 2 ml of penicilin/streptomycin, 1 ml of Amphotericin B. The media was then filtered with a 0.22 μm filter membrane and stored at 4 °C up to a month.

10% McCoys 5A medium was prepared by adddition of 86 ml of pre-mixed basic media with 10 ml of inactivated FBS, 1 ml of L-glutamine, 2 ml of penicilin/streptomycin and 1 ml of amphotericin B. The media was filtered with a 0.22 μm filter membrane and stored at 4 °C up to a month.

10% of Eagle's minimum essential media (EMEM) was prepared by addition of 79.5 ml of pre-mixed basic media (EMEM) with 10 ml of inactivated FBS, 7.5 ml of sodium pyruvate, 2 ml of penicilin/streptomycin and 1 ml of amphotericin B. The media filtered with a 0.22 μm filter membrane and stored at 4 °C up to a month.

3.2.6.5 Cryopreservation of Cells

When the cells are not needed, they were frozen for later use. A cryopreservation solution consisting of 50% of FBS, 20% of DMSO and 30% of Basic Medium were prepared by mixing 5.0 ml of FBS, 2.0 ml of DMSO and 3.0 ml of basic medium suitable for the cell line intented to be cryopreserved. The cryopreservation solution is filter sterilized by filtering it using a syringe filter with a 0.22 μm filter membrane. Cryopreservation solution is also known as freezing medium. Cells that were exponentially growing was detached from the tissue culture flask and added to sterile centrifuge tube where it was spun down at 1000 rpm for 5 minutes using a bench centrifuge. The cells were re-suspended in 3-6 ml of fresh cryopreservation solution and aliquotted into sterile provials (Falcon, USA), in 1 ml volumes and labelled. The provials were left to stand in ice and placed in a polystyrene cup and kept in -70ºC vapour phase of liquid nitrogen tank for about 4-24 hours. The vials were then transferred into cryocane of liquid nitrogen (-196ºC) and stored in cold room (4ºC).

3.2.6.6 Revival of Cells

The provial of cells was removed from liquid nitrogen and plunged into a beaker of ice. It was then, transferred to a 37^{o}C water bath for quick thawing. The cells were transferred into 1 ml of 20% supplemented basic media in a polypropylene tube (Falcon, USA) and spun at 100% for 5 minutes. The supernatant was discarded and the pellet re-suspended in 1 ml of 20% supplemented basic medium and incubated in a 25 ml tissue culture flask (Falcon, USA) at 37^{o}C in a 5% CO_2 incubator (Esco).

3.2.6.7 Maintenance of Cells

CaSki and A549 cell was maintained in RPMI media supplemented with 10% feotal bovine serum. HCT-116 was maintained in 10% supplemented McCOY'S 5A media containing 10% fetal bovine serum. MRC5 cells were maintained in EMEM basic media containing 10% feotal bovine serum The culture was incubated in a 5% CO_2 incubator (Esco) kept at 37^{o}C in a humidified atmosphere. The culture was sub-cultured every 2 or 3 days and routinely checked under an inverted microscope (Carl Zeiss) for any contamination. Sub-culturing was done when the cell growth was heavy.

3.2.6.8 Subcultivation of Cells

Adherent cells were attached and formed a single layer in the culture flask. Confluent cells were washed twice using phosphate buffer saline (PBS, Nacalai, Japan). The cells were detached from the flask by incubating in 1 ml of Accutase® cell detachment solution and 3 ml of PBS solution for 5-10 minutes at 37^{o}C and then sharply tapped to release the cells from attachment. The floating cells were transferred into a centrifuge tube (Falcon, USA), which contained 1 ml of 10% supplemented medium and centrifuged for 5 minutes at 1000 rpm. The supernatant was discarded carefully and 2 ml of 10% supplemented medium was added to the pellet. The cells were split and transferred into different flasks containing 7 ml of culture media each. The flask was then further incubated.

3.2.6.9 Cell Plating and Treatment of Cells with Crude Plant Extract or Isolated Compounds

Medium in tissue culture flask was initially discarded. PBS (5 ml) was then added into the flask. The solution was used to rinse the internal surfaces of flask gently. PBS was drained away carefully. Another batch of 5 ml of PBS was added again into the tissue culture flask. The flask was rinsed gently again. Later, PBS was drained away

carefully. Three (3 ml) PBS and 1 ml Accutase® cell detachment solution were added into the tissue flask and mixed well. The flask was later incubated in a 5% CO_2 incubator at 37 ^{o}C for 10 minutes. The cells were observed under inverted microscope.

The concentration of a cell suspension may be determined by placing the cells in an optically flat chamber under a microscope. The cell number within a defined area of known depth was counted and the cell concentration was derived from the count. A monolayer culture is detached with Accutase® cell detachment solution and a sample from suspension culture is taken. The viable cells were counted by 0.4% tryphan blue exclusion in a haemocytometer chamber. This was done by taking 10 µl of the cell suspension and 90 µl of 0.4 trypan blue solution, mix both of this solution in a microcentrifuge tube and then take out 15 µl of the mixture and pipetted into the heamocytometer. The cells were counted under a phase contrast microscope and cell concentration was calculated using the $M_1V_1 = M_2V_2$ formula. Cell count can also be performed by using an automated cell counter which is available commercially. Then, the desired number of cells were plated in 96-well microtiter plate (Nunc) in a volume of 100 µl. The plate was incubated in a CO_2 incubator at 37 ^{o}C for 24 hours to allow the cells to adhere and achieve 60-70% confluence at the time of the addition of the test agents. After 24 hours, the media in the wells were first discarded and replaced with fresh media containing extracts of *R. angustifolia* or isolated compounds at various concentrations of 1.56, 3.13, 6.25, 12.5, 25, 50 and 100 µg/ml with serum free media which contains 0.5% DMSO. The plates were incubated with the cells for 24, 48 and 72 hours. The negative control was treated with 0.5% of DMSO in 10% supplemented media. Cisplatin was used as the positive control.

3.2.6.10 SRB Dye Addition and Absorbance Reading

The cytotoxicity of the extracts and isolated compounds were screened using the Sulforhodamide B (SRB) assay. This assay was first described by Houghton in 2007 (Houghton et al., 2007). The incubation was halted by gentle addition of 50 µl ice cold 4% trichloroacetic acid (TCA) to each well and the plates were incubated at 4 ^{o}C for 1 hr. Then, the supernatant was discarded and the plates were washed with distilled water for 5 times and then air dried. SRB dye, (50 µl, 0.4% w/v) was added into each well and the treated cells and control were incubated at room temperature for 30 minutes. The unbound dye was removed by rapid washing four times with 1% acetic acid. The plates were then air dried and 100 µl of tris base (10 mM unbuffered, pH 10.5) was added and the plates were shaken at 500 rpm for 5 minutes to solubilize the bound SRB stain. The plates were then read with an ELISA reader (Synergy H1 Hybrid) at an absorbance of 492 nm.

Three replicate plates were used to determine the cytotoxicity activity of each extract. The average data from triplicates were expressed in terms of killing the percentage relative to negative control.

3.2.6.11 MTT Dye Addition and Absorbance Reading

The antiproliferative assay was also performed using the 3-(4,5-dimethylthiazol-2-yl)-2,5-diphenyltetrazolium bromide (MTT) according to the method of Ho et al. (2013) with some modifications. Cells that were plated into sterile 96-well culture plates at a density of 6.0×10^4 cells/mL were incubated in 5.0% CO_2 in an air-jacketed incubator at 37.0°C for 24 hours for the cells to adhere. The media was removed after 24 hours incubation, and 150.0 µL of fresh medium containing various concentrations of the extracts of *R. angustifolia* and chalepin were added. The plates were further incubated

for 24, 48 and 72 hours. At the end of the incubation period, 20.0 µL (5 mg/ml) of MTT solution (Sigma-Aldrich, USA) was added to each well, and the plates were again incubated for 4 hours. Medium containing MTT was discarded, and 150.0 µL of DMSO was added into each well to dissolve the formazan crystals. The absorbance of each well was measured at 570 nm using a microplate reader (Synergy H1 Hybrid Multi-Mode Microplate Reader, USA). The IC_{50} values were determined by the interpolation of the dose-response curve for each cell line.

3.2.6.12 Calculation of Percentage of Inhibition

The percentage of inhibition of each of the test samples was calculated according to the formula:

$$\% \text{ of Inhibition} = \frac{\text{OD control} - \text{OD sample}}{\text{OD control}} \times 100\%$$

The concentration of extract and isolated compounds which causes 50% inhibition or cell death is determined by calculating the IC_{50}. IC_{50} values (concentration of the test agent that causes 50% inhibition or cell death) were determined based on the extrapolation of the dose-dependent response curves of each extract and isolated compound. The experiments were performed in triplicates. The plant extracts that gave IC_{50} of 20 µg/ml or less were considered active (Lee et al., 2005).

3.2.6.13 Cell Enumeration

Haemocytometer was used to determine the number of cells per unit volume of a suspension. Haemocytometer is a type of counting chamber. Preparation of the haemocytometer begins with cleaning it with a lens paper. The coverslip is also cleaned.

Coverslips for haemacytometer are made especially a bit thicker than the conventional coverslips for microscopy. This is because they must be durable enough to overcome the surface tension of a drop of liquid. The coverslip would be placed over the counting surface prior to putting on the cell suspension. The suspension is placed into one of the V-shaped wells with a pipet. The area under the coverslip fills by capillary action. Enough liquid should be placed so that it covers properly. Haemocytometer is then placed on the microscope and counting grid is brought into focus at low power. Cells in the centre grid (with the smallest boxes) are counted for calculation.

A drop of diluted cell suspension (1:10) was placed on a haemocytometer. The dead cells were stained blue (tryphan blue) while the living cells were not stained. The haemocytometer was placed under a microscope and then unstained living cells were counted under the 20X objective.

The number of living cells in 1ml of the culture media was calculated using the following formula:

N (Number of cells in Tissue Culture Flask) = n x D x 10^4

n = Number of cells in box Grid 3 (centre grid in haemacytometer) (1mm^2 box)

D = Dilution Factor of cell and stain = 100µl: 900µl

3.2.7 Trypan Blue Dye Exclusion Assay

Concept

It is an assay used to determine the number of viable cells present in a cell suspension. It works on the concept where the viable cells have intact cell membrane and resists penetration of certain dyes such as the trypan blue, propidium iodide and Eosin. However, this is not the case for dead cells where it enables the influx of the dye

in the cells. When the cell suspension is mixed with trypan blue dyes, viable cells would show clear cytoplasm whereas non-viable cells would have blue colored cytoplasm.

Method

The A549 cells (1 x 10^6 cells) treated with chalepin (36 µg/ml i.e. the concentration selected based on apoptosis analysis as the optimal concentration for western blotting study) were collected into cell suspension at 24, 48 and 72 hours in a microcentrifuge tube. A volume of 10 µl of cell suspension was aliquoted out into a new sterile microcentrifuge tube and 10 µl of trypan blue dye, 0.40 % solution from Biorad was added into the cell suspension and mixed using a micropipette. From the mixture, 10 µl of the mixture was aliquoted out and inserted into the Biorad counting slide chamber. This slide was then inserted into TC10® Biorad Automated Cell counting device and the percentage of viable cells at various time points were recorded. This process was repeated three times to get results in replicates.

3.2.8 Apoptosis Studies

3.2.8.1 Morphological Studies

3.2.8.1.1 Phase Contrast Microscopy

Concept

Phase contrast microscopy brings contrast to unstained biological material by changing differences in refractive index between cellular components into differences in amplitude of light, i.e., light and dark areas, which can be observed. When dealing with transparent and colorless components in a cell, dyeing can be done but it stops all process. The phase contrast microscope has made it possible to study living cells, and cell division is an example of a process that has been examined in detail with it.

Method

A549 cells were seeded at a density of 5000-7000 cells into a tissue culture dish (6cm) and left overnight to adhere. Then, the cells were treated with chalepin at various concentrations (18, 27, 36 and 45 μg/ml) for 24, 48, and 72 hours at 37˚C and 5% CO_2. Changes in cytomorphology of the cells which include shrinkage, detachment, rounding, spiking, blebbing and formation of apoptotic bodies were observed using phase contrast microscopy (Zeiss Axio Vert. A1).

3.2.8.1.2 Hoechst/PI Fluorescent Staining

Concept

This method is done to examine the morphological changes in the cell nuclei using a fluorescence microscope. Hoechst 33342 is a blue fluorescent dye which is permeable to the nucleus. It emits blue fluorescence when bound to the double strand DNA. It is used to identify chromatin condensation and fragmentation as it stains the condensed nuclei of cells undergoing apoptosis. Propidium iodide is a cell impairment DNA binding dye which can only stain the cells when there is a loss of plasma membrane integrity. Hence, propidium iodide (PI) is a small fluorescent molecule that binds to DNA but it is unable to penetrate into cells that has an intact plasma membrane. It stains cells which undergoes late apoptosis and necrosis (Crowley et al., 2016).

Method

This study was carried out to observe changes in cell nucleus. 5000-7000 cells were seeded into each 6 cm culture dish and allowed to adhere overnight. The cells were subsequently treated with various concentrations of chalepin for 48 and 72 hours. At the end of the incubation period, the media in the culture dishes were discarded and the cells were washed twice with PBS, after which 1mL of PBS was added to each culture

dish. To stain the cells with fluorescent dyes, 100 µL of Hoechst solution (100 µg/ml) and 25 µL of PI solution (100 µg/mL) were added to each culture dish and incubated for 15 min. Finally, the cells were photographed using Leica DM-16000B fluorescent microscope.

3.2.8.2 Biochemical Analysis of Apoptosis

3.2.8.2.1 Apoptosis Detection by Annexin V-FITC/PI Staining

Concept

In healthy cells, phospholipids of the cell membrane are in an asymmetric pattern where the distribution between the inner and outer leaflet of the membrane is not similar. Phosphatidylcholine and sphingomyelin are exposed to the outer leaflet of the lipid bilayer whereas phosphatidylserine is located at the inner leaflet. Upon apoptosis this asymmetry is disrupted as phosphatidylserine translocate to the outer leaflet of the plasma membrane. Phosphatidylserine (PS) translocation from the inner side of the plasma membrane to the outer side surface is an indication of the initiation of apoptosis. Annexin V is a Ca^{2+} dependent phospholipid-binding protein, which has a high affinity towards PS. It is therefore used to detect exposed PS using the flow cytometry. Annexin V is conjugated to a fluorochrome i.e. FITC which would serve as a sensitive probe that would assist in the detection of PS. Following PS translocation, loss of membrane integrity follows which indicates the later stage of apoptosis or necrosis. Propidium iodide functions to distinguish between early and late apoptosis in a cell. Viable cells, which possess intact membranes, would hinder PI from permeating the cell whereas membranes of dead or damaged cells would enable PI to permeate and stain its nucleus. Cells that are viable would be both Annexin V and PI negative. Cells that are in early apoptotic stage would be stained Annexin V positive and PI negative. Cells that has undergone late apoptosis or is dead would be stained Annexin V positive and PI

positive. Cell death through necrosis or apoptosis is unable to be determined through this assay however if a cell has undergone apoptotic cell death, hence there would be a shift from Annexin V and PI negative (viable, or no measurable apoptosis), to Annexin V positive and PI negative (early apoptosis with intact membranes), and finally to Annexin V and PI positive (end stage apoptosis and death) over a time period. If a cell only shows a result of Annexin V and PI positive, hence the mode of cell death could not be determined by this assay.

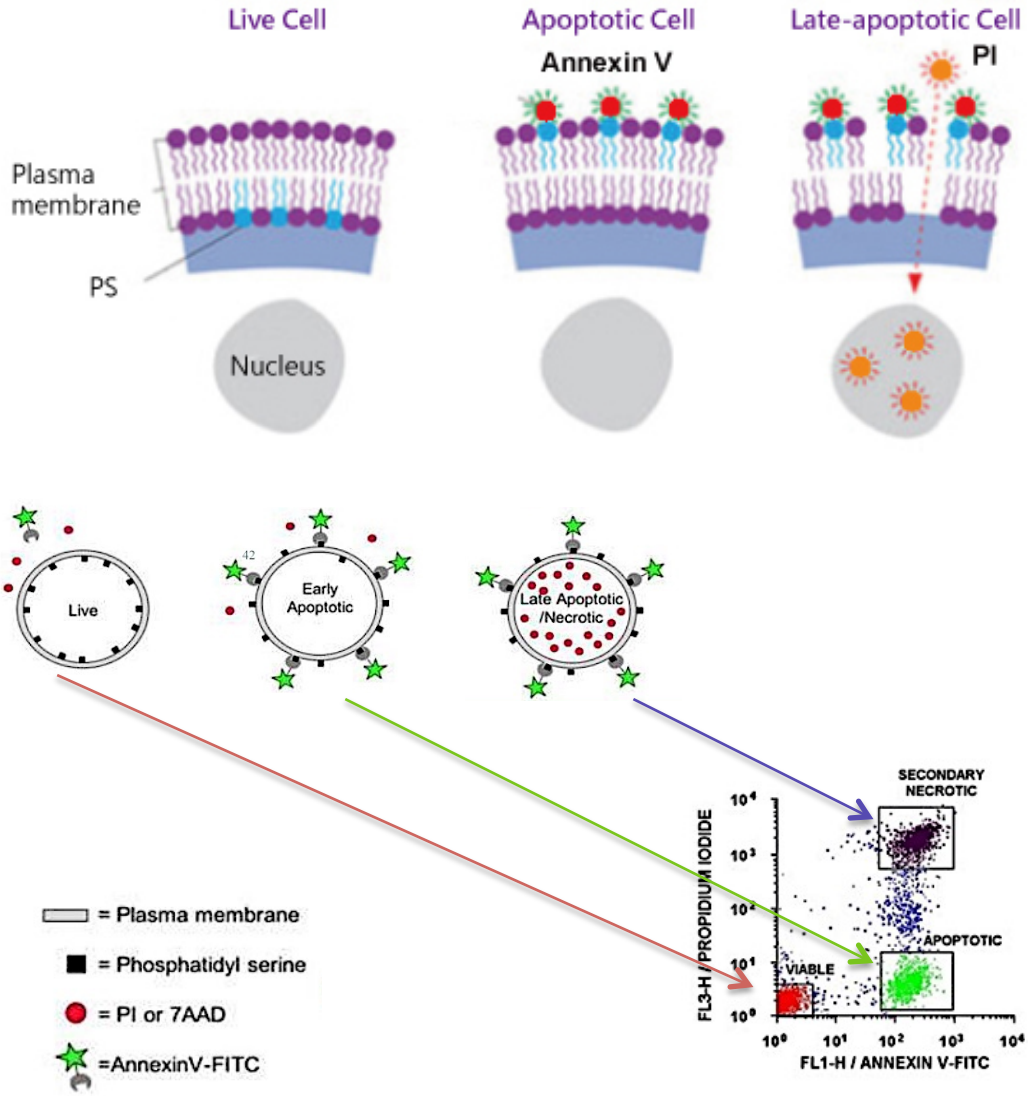

Figure 3.4: Graphical representation of the principle of the Annexin V/PI assay. Image Excerpted from: Flow cytometry (FCM)/FACS application apoptosis, n.d.

Method

FITC annexin V apoptosis detection kit (BD) was used to detect apoptosis. Cells were seeded in tissue culture dishes (5000-7000 cells/dish) and allowed to adhere overnight. Next, the cells were treated with various concentrations of chalepin for 48 and 72 hours. The cells were harvested, washed, and resuspended in 1x binding buffer according to the manual provided in the kit. In the next step, the cells were stained in the ratio of per 100,000 cells; staining of cells with 5 µL of FITC-annexin V and 5 µL of propidium iodide was done for 15 minutes. Then, 200 µL of 1x binding buffer was added to each sample. Unstained and single-stained untreated cells were also included as controls. A minimum number of 10,000 events was acquired for each replicate using Accuri C6 flow cytometer. A quadrant statistic was used to measure the population of viable, early apoptotic, late apoptotic and secondary necrotic cells. The determination between these different populations were obtained by estimating quantitatively the cells that were AnnexinV/PI stained.

3.2.8.2.2 DNA Fragmentation Measurement by TUNEL Assay

Concept

The activation of endonucleases that would cleave chromosomal DNA is a hallmark of apoptosis. These endonucleases are activated by a family of protein that executes cell death, which is known as caspases. Significant DNA fragmentation which generates large number of DNA double strand breaks and nicks is a characteristic of the event of apoptosis (Darzynkiewicz et al., 2008). TUNEL assay works on the capability of the enzyme terminal deoxynucleotidyl transferase to attach labeled dUTP into free 3'-hydroxyl terminal that is generated by the fragmentation of the genomic DNA into low molecular weight DNA strands in which the fluorescence would be detected using a flow cytometer. TUNEL has almost globally been accepted as a method of preference to

detect the apoptosis in situ, however, the detection of DNA fragmentation is not only limited to DNA damage that is associated to apoptosis, it could also detect non-apoptotic events such as necrosis and other types of cell deaths (Loo, 2011).

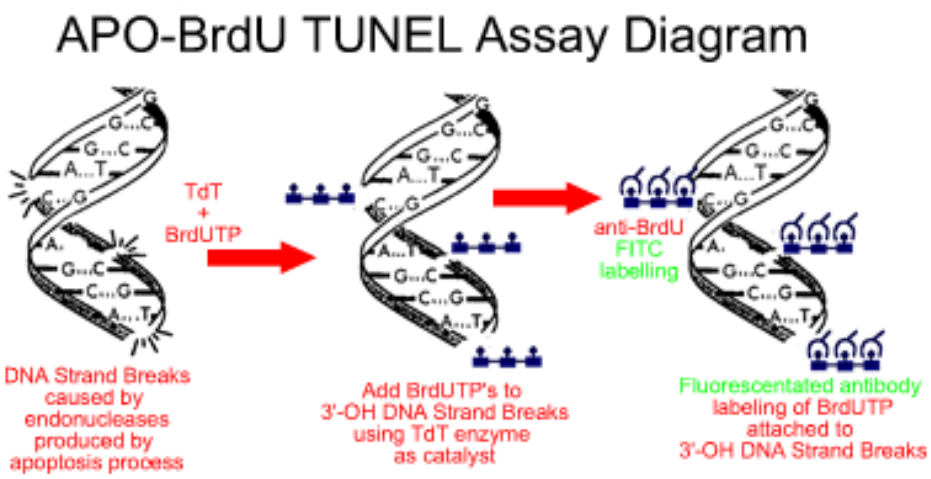

Figure 3.5: The principle of TUNEL assay. Image excerpted from: Phoenix flow systems, n.d.

Method

DNA strand breaks in apoptotic cells caused by the activation of endonucleases, were detected by APO-BrdU TUNEL assay kit. After incubation with various concentrations of chalepin at 48 and 72 hrs, cells were harvested and washed with PBS. Next, the cells were fixed with 1% (w/v) paraformaldehyde for 15 mins, then washed with PBS, and fixed with 70% (v/v) ethanol overnight. Ethanol was removed by centrifugation and DNA labeling steps were performed according to the manual provided in the kit. Samples were analyzed by flow cytometer and a minimum of 10,000 events were acquired for each replicate.

3.2.8.2.3 Mitochondrial Membrane Potential Assay

Concept

Energy that is produced in the mitochondrial respiratory chain is stored as an electrochemical gradient, which has a transmembrane electrical potential. It is about 180-200 mV negative inside and a unit of proton gradient. This energy is crucial to drive the synthesis of ATP which maintains various intracellular processes (Cossarizza et al., 1998). JC-1 is a cyanine dye which is also known as 5,5′, 6,6′-tetrachloro-1, 1′, 3,3′-tetraethylbenzimidazolocarbo-cyanine iodide (Perelman et al., 2012). JC-1 could selectively enter into mitochondria and reversibly change color from red/orange to green as the membrane potential decreases. In healthy cells, there would be high mitochondrial membrane potential. In this condition, JC-1 would form complexes known as J-aggregates with intense red fluorescence (emission wavelength 590 nm). In apoptotic cells, the mitochondrial membrane potential would decrease and JC-1 would remain in monomeric form, which would give green fluorescence (emission wavelength 530 nm). This could be viewed using a fluorescent microscope or quantified with flow cytometer. Both the colors could be detected using the filters that are commonly available in the flow cytometers. The green emissions could be analysed using the fluorescence channel 1 (FL1) and greenish orange emission could be analysed in FL2. The benefit of using JC-1 is that it can be used for qualitative and quantitative research purpose (Cossarizza et al., 1998).

Flow cytometric analysis

A lipophilic and cell-permeable fluorochrome JC-1 (5,5', 6,6'-tetrachloro-1, 1', 3,3'-tetraethyl benzimidazolyl carbocyanine iodide) was used to measure mitochondrial membrane potential ($\Delta\psi m$) according to the manufacturer's instructions (BD MitoScreen Kit). The cells ($1x10^6$) were seeded in tissue culture plates and were treated

with 18, 27, 36, and 45 μg/ml of chalepin for 48 hours incubation. The cells were then harvested, washed with PBS twice and incubated with JC-1 dye for 15 mins at 37 ^{o}C. At the end of the incubation, the cells were washed and resuspended with 500 μl of 1x assay buffer (provided in the kit). The intracellular fluorescence signals of JC-1 in the cells were then measured with Accuri C6 flow cytometer. Approximately 10,000 events were recorded per analysis. In healthy cells, JC-1 accumulates as aggregates in the mitochondria and emits red fluorescence. In cells, which have undergone apoptosis, JC-1 remains in monomeric form in the cytoplasm and emits green fluorescence. The red and green fluorescence were detected at FL-2 and FL-1 channels respectively in the flow cytometer. Ratio of mean fluorescence intensity between the FL1 and FL2 channels were calculated and this is used to determine the changes in the mitochondrial membrane potential. The results were analysed by calculating the ratio of JC-1 dimers to JC-1 monomers. A higher ratio indicated a higher membrane depolarization of mitochondria in cells (BD MitoScreen Flow Cytometry Mitochondrial Membrane Potential Detection Kit Instruction Manual). Cells that was untreated in 0.5% DMSO acted as the control.

Fluorescence microscope imaging

JC-1, mitochondrial membrane potential assay kit by Abcam was used to stain the A549 cells to view the mitochondrial membrane potential (Δψm) changes in cells. Prior to the JC-1 staining initiation, 1x dilution buffer were prepared by adding 10 mL 10x dilution buffer to 90 mL deionized water. The solution was mixed gently and thoroughly. JC-1 stock (1mM) was diluted to 20 μM working JC-1 solution. This was done by adding 200 μl of JC-1 stock solution into 10 mL of 1x dilution buffer. The cells ($1x10^{6}$) were seeded in tissue culture plates and were treated with 18, 27, 36, and 45 μg/ml of chalepin for 48 and 72 hours incubation. The cells were then harvested,

washed with PBS twice and incubated with JC-1 dye for 20 mins at 37°C. At the end of the incubation, the cells were washed and resuspended with 1000 µl of 1x dilution buffer. The cells were viewed using a fluorescence microscope at an excitation wavelength of 475 ± 20 nm and emission wavelength of 530 ± 15 nm and 590 ± 17.5 nm.

3.2.8.2.4 Intracellular Reactive Oxygen Species (ROS) Measurement

Concept

ROS is recognized as a central mediator in deciding the fate of a cell, depending on the extent of oxidative damage. 2′,7′-Dichlorofluorescin diacetate (DCFH-DA) is a non-polar dye i.e. converted into DCFH by cellular esterases. DCFH is non-fluorescent but switched to highly fluorescent DCF when oxidised by ROS. DCF could then be quantified with a flow cytometer or visualised by a fluorescent microscope and this gives an insight on the amount of ROS present intracellular.

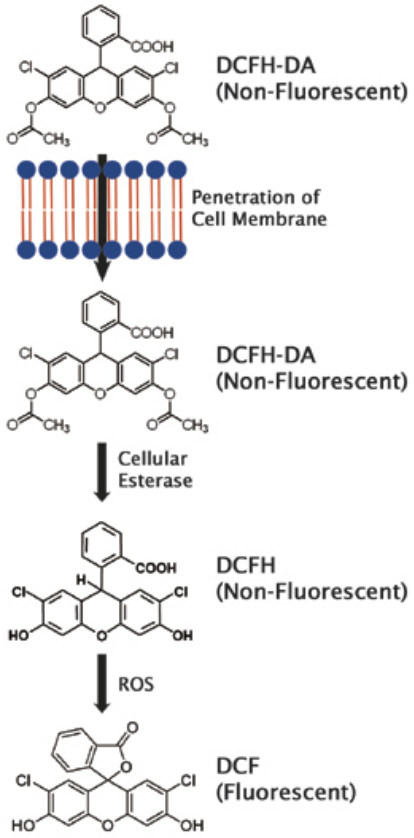

Figure 3.6: Graphical representation of the principle of intracellular ROS measurement using DCFH-DA dye. Image excerpted from: Intracellular ROS assay, n.d.

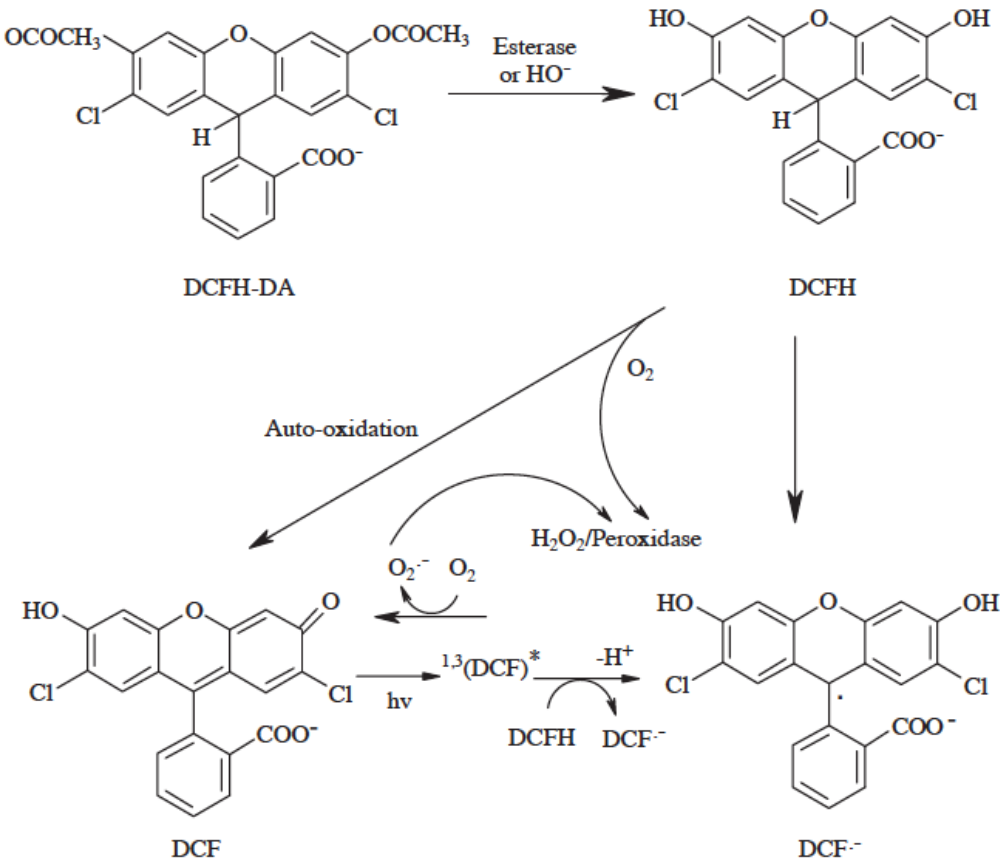

Figure 3.7: Mechanism of 2,7-dichlorodihydrofluorescein diacetate (DCFH-DA) de-esterification to 2,7-dichlorodihydro- fluorescein (DCFH) and further conversion into $DCF^{\cdot -}$. Image excerpted from Gomes et al. (2005).

Method

The assay was conducted as described by Ling et al. (2011) with some minor modifications. The ROS measurement was done using the fluorescent probe 2',7'-dichlorofluorescein diacetate (DCFH-DA) that enabled the monitoring of intracellular accumulation of ROS. The A549 cells were seeded into a 96 well plate with a density of $2x10^4$ cells per well and allowed to attach overnight. Treatment with chalepin at various concentrations were done the next day and incubated for different time periods. At the end of the incubation period, the media was removed and 5 µM of DCFH-DA which is diluted in media was added to the cells and incubated for 40 minutes at 37 ^{O}C. The cells were then washed three times with clear media and the fluorescence intensity

(excitation = 485 nm and emission = 530 nm) was measured using a microplate reader. The morphology of the cells were observed using a fluorescence microscope.

3.2.8.2.5 Caspase-3, 8 and 9 Activation Activity Assay

Concept

The caspase family are cysteine proteases which have been evolutionarily conserved. It plays a central role as executioners of the apoptotic pathway. The apoptotic role of caspases occur in the embryogenesis process and in maintaining cellular homeostasis. Caspases also play non-apoptotic roles such as in inflammation, cell differentiation, motility and neuronal functions (Kaushal et al., 2014). Activation of caspases is a tightly controlled mechanism. It is present as inactive zymogens (procaspase) and it is activated upon proteolytic cleavage to the activated caspase. Activation of caspases results generation of a cascade of signalling events that permits controlled abolishment of cellular components (McIlwain et al., 2013).

The CaspILLUME Fluorescein caspase staining kit utilises caspase inhibitors such as DEVD-FMK for caspase 3, IETD-FMK for caspase 8 and LEHD-FMK for caspase 9, conjugated to FITC as a marker. FITC-DEVD-FMK (caspase 3), FITC-IETD-FMK (caspase 8) and FITC-LEHD-FMK (caspase 9) is cell permeable, non toxic and binds irreversibly to activated respective caspases in the apoptotic cells. The fluorescence that is emitted by cells that have undergone apoptosis, which has absorbed these markers, could be quantified with a flow cytometer.

Method

Caspase activity assays were performed according to the instructions in the manual (CaspILLUME, Genetex). Cells were seeded at a density of $1x10^6$ cells per culture dish. After being subjected to treatment for 48 and 72 hours, the cells were detached with accutase, washed, and resuspended in PBS. Next, 300 μL of each sample was aliquoted into centrifuge tubes, after which 1 μL of fluorescent substrate (FITC-DEVD-FMK for caspase 3, FITC-IETD-FMK for caspase 8 and FITC-LEHD-FMK for caspase 9 activity) was added to each tube and incubated for 1 h at 37°C incubator. At the end of the incubation period, the cells were centrifuged at 3000 rpm for 5 minutes and the supernatant was removed. After that, the cells were resuspended in 0.5 mL wash buffer (provided in the kit) and centrifuged at 3000 rpm for 5 minutes. This step was repeated before performing the analysis with flow cytometer (Accuri C6) with wavelength Ex. = 485 nm and Em. = 535 nm and a minimum of 10,000 events were acquired for each replicate.

3.2.9 Cell Cycle Analysis

Concept

Cell cycle analysis is a method of quantification of DNA content using flow cytometry. The DNA is stained with DNA binding dyes such as propidium iodide and the amount of DNA present in the cell is proportional to the amount of dye that is present. Cells in S phase would have more DNA than cells in G1 phase. Hence, more dye would be taken up and more fluorescent signal would be detected. The cells in G2 phase would approximately be twice as bright as cells in G1 phase. Fixation of cells with alcohol allows cells to be dehydrated and permeable to the dye that is present. Alternatively, Triton X-100 (0.1%) which is a detergent is used to permeablize the cell (Flow cytometric analysis of cell cycle, n.d.).

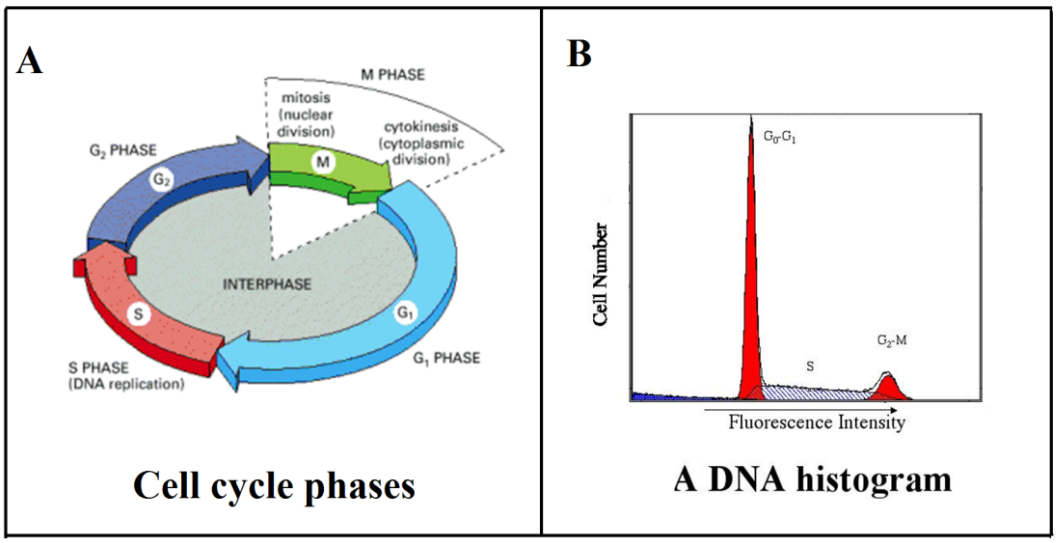

Figure 3.8: Graphical representation of principle of cell cycle analysis. Image excerpted from Tabll et al. (2011).

Method

After 48 and 72 hours of treatments with chalepin, adherent and floating cells were collected, centrifuged and fixed in 70% ethanol overnight. All samples were centrifuged to remove ethanol and the cell pellets were washed with cold PBS. The cells were subsequently resuspended in 300 µL of staining solution containing concentrations of 50 µg/mL propidium iodide, 50 µg/mL Rnase, 0.1% Triton X-100, 1 mg/mL sodium citrate and distilled water. Following 30 minutes incubation at room temperature, the cells were analysed with a flow cytometer and data analysis was performed by Modfit LT software.

3.2.10 Proteomic Studies (Western Blot Analysis)

Concept

Western blotting is a common technique used in research to separate and identify proteins in a sample of tissue homegenate or extract (Yang et al., 2009). A mixture of proteins would be separated based on molecular weight through gel electrophoresis followed by a transfer to a membrane (PVDF or nitrocellulose) which would result in band for each protein. The membrane would then be incubated with the antibody of the protein of interest and the protein bands could be detected and viewed via secondary antibody which could react with chemilumisence. The thickness of a band would usually correspond to the amount of protein that was present (Mahmood et al., 2012).

3.2.10.1 Sample Preparation for Western Blot

Preparation of whole cell lysate

Approximately $0.5x10^6$ of A549 cells were plated into 60 mm tissue culture dishes and allowed to adhere overnight. The next day, the existing media in the culture dish is discarded and fresh media containing chalepin at a concentration of 36 μg/ml were added. The culture dishes were incubated for 2, 4, 8, 12 and 24 hours. At the end of the treatment time, the cells were washed by addition of cold PBS and gentle rocking. The PBS was aspirated and the washing step is repeated several times. Radioimmunoprecipitation (RIPA) lysis buffer was prepared by mixing 1ml lysis buffer with 10 μl of protease inhibitor and EDTA each. The RIPA buffer is kept in ice before using. When the washing with PBS step has been completed, ice cold RIPA lysis buffer cocktail was added into the tissue culture dish. The cells were incubated with the lysis buffer for 20 minutes on ice. The cells would detach in a mucus form. The cells were gently agitated using a pipette to detach it or cell scraper was used if necessary. The cell

suspension was transferred into a microcentrifuge tube and centrifuged at 13,000 rpm for 10 minutes at 4 °C. After centrifugation, the clear supernatant was transferred into a fresh tube and kept in -80 °C until further usage.

Preparation of nuclear and cytoplasm extracts

Nuclear extract and cytoplasmic extract from A549 cells were prepared to determine the expression of p65 and phosphorylated p65 protein for the NF-κB pathway. These cell fractions were prepared using the nuclear extraction kit from Active Motif. For preparation of nuclear extracts, the cells were first collected in ice-cold PBS in the presence of phosphatase inhibitors to limit further protein modifications (expression, proteolysis, dephosphorylation, etc.). The cell suspension was centrifuged at 2000 x g at 4°C and the supernatant were discarded. Then, the cells were resuspended in hypotonic buffer to swell the cell membrane and make it fragile by incubating for 15 minutes on ice. A volume of 25 µl of detergent was added for every 100 µl of hypotonic buffer and it was vortexed for 10 seconds at the highest speed. Addition of the detergent causes leakage of the cytoplasmic proteins into the supernatant. A small amount of cells were taken and checked under microscope to ensure that the cells have been efficiently lysed and that nuclei have been released. If the cells are not well lysed, an ice-cold dounce homogenizer was used to lyse. The lysate was then centrifuged at 14,000 x g for 30 seconds in a microcentrifuge tube, which have been pre-cooled. The supernatant which is the cytoplasmic fraction was transferred into a pre-chilled microcentrifuge tube and stored in -80 °C until further use. After collection of the cytoplasmic fraction, the pellet was used for the nuclear fraction collection. The nuclei were lysed using the complete lysis buffer provided in the kit and the nuclear proteins were solubilized in detergent-free lysis buffer in the presence of the protease inhibitor cocktail. The suspension was incubated for 30 minutes on ice on a rocking platform set at 150 rpm. It was then

vortexed for 30 seconds at the highest setting and next, centrifuged for 10 minutes at 14,000 x g in a microcentrifuge tube which has been pre-cooled at 4 °C. The supernatant which was the nuclear fraction was transferred into another pre-chilled microcentrifuge tube and the aliquot was stored at -80 °C until further used.

3.2.10.2 Bradford Assay to Determine Protein Concentration

Quickstart Bradford Assay Kit from Biorad was used to determine the protein concentration in the sample. Bradford reagent is thawed to room temperate and aliquoted into a 50 ml tube for usage. The standard bovine serum albumin (BSA) curve was prepared. In a 96 well plate, 250 µl of Bradford reagent was mixed with 5 µl of various concentration of of BSA. For each concentration of BSA, a triplicate is prepared. The Bradford reagent would immediately change to bright blue upon addition of BSA. Blank used was 250 µl of Bradford reagent added with 5 µl of distilled water. The test materials were mixed well and incubated for 5 minutes at room temperature. Following this, absorbance was read using a spectrophotometer at 595 nm. The standard curve was plotted with absorbance value against concentration of BSA. An equation was derived from the straight line with R^2 value near to 1. This equation was used to determine the concentration of protein in our protein samples. The same method as described above was employed to determine the protein samples. Samples were cold thawed by taking them out of -80 °C and placing them into 4 °C fridge. The samples were added to Bradford reagent and absorbance values were taken as described above. The absorbance value was extrapolated into the standard curve to determine the concentration of protein present in the sample. Approximately 40 µg of protein was loaded in each lane of the gel as each well could accommodate only a maximum of 30 µl of sample and loading buffer. However, if the protein sample is concentrated,

consideration could be given into loading more amount of protein as the higher the amount of protein added, the higher would be the intensity of the bands viewed.

3.2.10.3 Protein Estimation Calculation

The absorbance value of the protein samples are adjusted with the absorbance value of the blank sample. The protein concentration (mg/ml) is determined through extrapolation of the absorbance value to the respective concentration in the BSA standard curve. The concentration from the extrapolation is converted into μg/ml. This is done by multiplying the value obtained from graph with 1000x. Then, the volume required for an amount of 40 μg of protein is determined and this is done by dividing the value to 1000 and then multiplying with 40. This value obtained would be the volume of sample that needs to be loaded to obtain a loading amount of 40 μg of protein. An example on the above calculation is as below:

Absorbance of sample = 0.880

Absorbance of blank = 0.300

Absorbance of sample – Absorbance of blank = 0.580

y=0.3646x (equation derived from BSA standard curve)

Protein concentration (mg/ml) = 0.580/0.3646

=1.5908

Protein concentration in μg/ml = 1.5908 x 1000

= 1590.8

Volume for 40 μg of protein = 1590*40/1000

= 63.63 μl of protein lysate of same

3.2.10.4 Protein Denaturation

Loading buffer (4x) which consists of 250 µl of 1M Tris-HCl, pH 6.8, 320 µl of 25% SDS, 100 µl of β-mercaptoethanol, 300 µl of 100% Glycerol and 30 µl of 1% bromophenol blue was prepared. One part of 4x loading buffer was mixed with 3 parts of protein samples. This is to ensure that the final concentration of loading sample is 1x. The protein sample and loading buffer were mixed with slight vortex to ensure proper mixing. The sample is boiled at 100 °C for 5 minutes on a heating block. After heating period, the sample is taken out from the heating block and let to cool to room temperature. The sample was vortexed and spinned down prior to loading.

3.2.10.5 Preparation of Running Gel and Stacking Gel

Ammonium persulfate solution 10% (w/v) was prepared by dissolving 10 mg of APS into 100 µl of distilled water. The glass plates were wiped with 70% ethanol to ensure there are no old gel residues and assembled into the casting stands. The casting stands are then attached to the casting frame and the glass plates were filled with distilled water to ensure there is no leakage and once no leakage detected, the distilled water is discarded. Resolving gel solution was prepared according to the volume described at the table below and approximately 5 ml of the solution was pipetted into the glass plates. Immediately, a layer of distilled water is topped up into the glass plate apart from the resolving gel solution. This is to ensure that the resolving gel front polymerises into a straight line. Once the resolving gel has polymerised, the casting stand is inverted to discard the excessive distilled water and the gel surface is rinsed with distilled water to remove any debris on the gel and to give a good interface between stacking and resolving gels. The stacking gel is prepared according to the recipe given below and was loaded on top of the resolving gel. Immediately combs were inserted and the stacking

solution is allowed to polymerise. Upon polymerisation, the comb is removed and the glass plates were detached from its casting frame and casting stands and attached to the gel holder cassettes and placed into the running tank and running buffer was added immediately till it fills the wells in the gel completely. This step is done to ensure that the excessive gel residue in the well is washed off and polymerisation stops. It is noteworthy that the percentage of 30% acrylamide in the gel could be varied, most commonly used percentage would be 10-12%. This depends on the size of the protein that is expected to be detected. In the case of larger proteins, a lower percentage of gel was used and in the case of lower molecular weight protein detection, higher percentage of gel was used. The recipe for the resolving gel and stacking gel is as described below:

Table 3.2: Recipe for resolving and stacking gel

10%

For 2 gels

Ingredients	10% Running gel	4% Stacking gel
30% Acrylamide	6.64ml	1.33ml
Water	8.04ml	6.00ml
1.5M Tris-HCl pH8.8	5.00ml	-
0.5M Tris-HCl pH6.8	-	2.52ml
10% SDS	200µl	100µl
10% Ammonium Persulfate (APS)	120µl	60µl
TEMED	30µl	15µl

12%

For 2 gels

Ingredients	12% Running gel	4% Stacking gel
30% Acrylamide	8.00ml	1.33ml
Water	6.70ml	6.00ml
1.5M Tris-HCl pH8.8	5.00ml	-
0.5M Tris-HCl pH6.8	-	2.52ml
10% SDS	200µl	100µl
10% Ammonium Persulfate (APS)	120µl	60µl
TEMED	30µl	15µl

3.2.10.6 Preparing Gel Cassette and Gel Tank and Initiation of Electrophoresis

After placing the gel casettes into the gel tank and filling the middle portion of the gel cassette holder with running buffer (refer appendix for recipe), the gel is now ready to be loaded with protein samples. The gel is loaded with molecular weight ladder markers followed by the protein samples accordingly. In our case, the first lane was loaded with protein ladder followed by negative control (untreated sample) and then followed by samples with 2 hours exposure of chalepin, samples with 4 hours, 8 hours, 12 hours and 24 hours exposure of chalepin at 36 μg/ml. All the lanes were loaded with same amount of protein as earlier calculated using the Bradford protein estimation assay. In our experiment, 50 μg protein was loaded. Empty wells were loaded with loading buffer and this is to ensure that all the wells would be resolved with same resolving power. After the loading of sample, the outer portion of the gel cassettes were filled with running buffer and the tank was closed with the tank lid and connected to the power pac. Electrophoresis was initiated with a setup of 100 V for approximately one hour or until the loading marker reaches 0.5 cm above the bottom of the gel. The electrophoresis was stopped and the glass plates were removed carefully.

3.2.10.7 Transfer of Proteins to a Membrane (Wet Transfer Method)

The glass plates rinsed with distilled water and pry opened using a plastic knife provided with the Biorad tools. The stacking gel was cut and discarded and the gel was rinsed with distilled water on a shaker with mild shaking (10 rpm) for 3 minutes to remove the SDS residue in the gel. The nitrocellulose membrane (0.45 μm, Biorad) was cut according to the size of the gel and placed carefully into the transfer buffer (refer appendix for recipe) and left to equilibrate for about 10 minutes. Apart from the membrane, same was done for filter paper, fiber pads and gels. After equilibrating the components in the transfer buffer, gel sandwich was prepared. The cassette with the

black side down is placed on a clean surface. One pre-wetted fiber pad was placed on the black side of the cassette. Next, a sheet of filter paper is placed on the fiber pad followed by the equilibrated gel. The nitrocellulose membrane is placed on top of the gel followed by another filter paper and a fiber pad. It is noteworthy that at the placement of each component, it is necessary to roll using a roller to ensure no air bubbles are trapped in between the stacks. The cassette is closed firmly by being careful not to move the gel or the filter paper in the sandwich and locked with the white latch. The cassette is placed in the module. The frozen blue cooling unit and the module was placed into the transfer tank and completely filled with iced-cold transfer buffer. The transfer tank's lid was assembled and connected to the power pack the proteins were transferred at 200 V for 2 hours. After 2 hours, the transfer was halted and the membrane is carefully removed from the cassette.

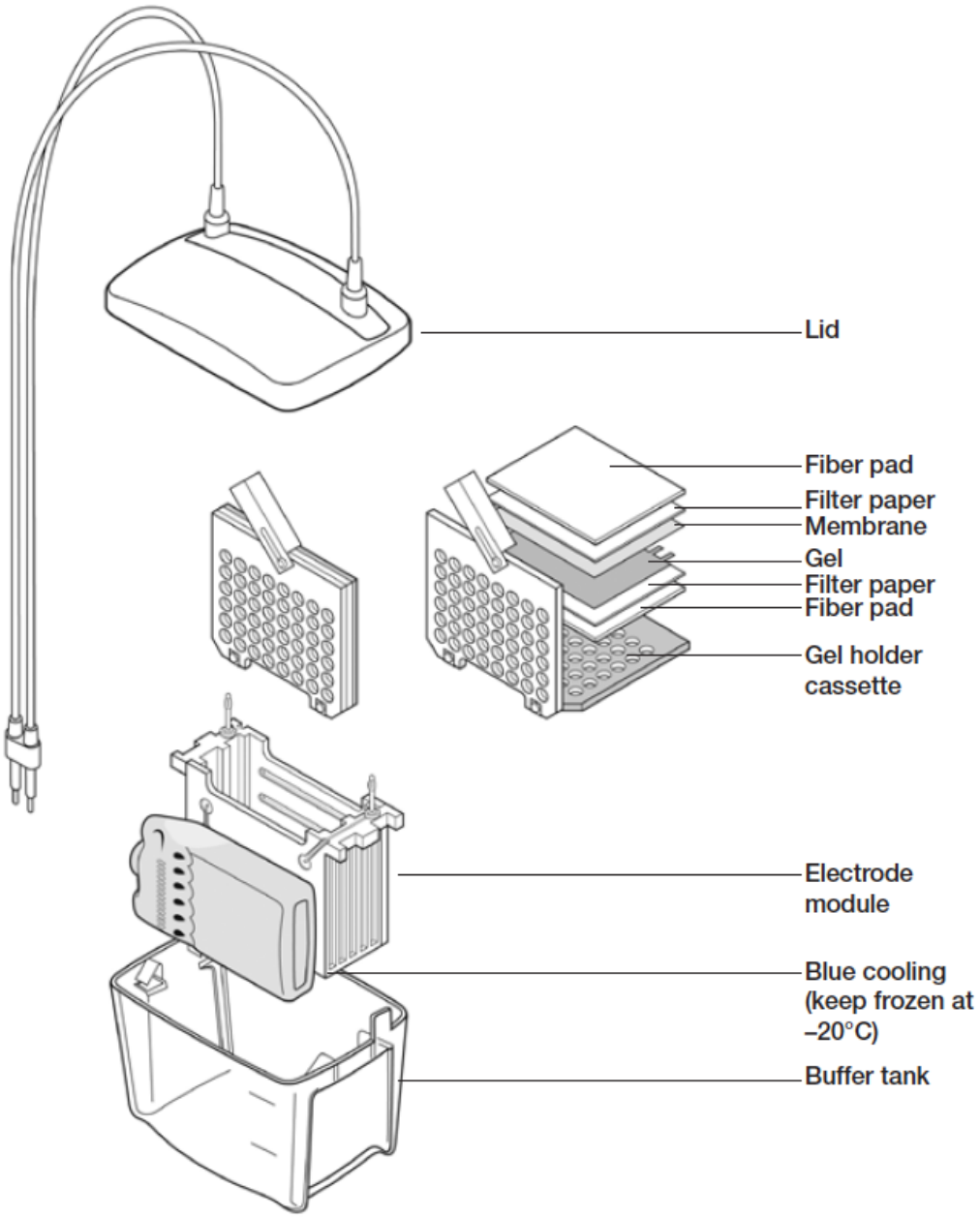

Figure 3.9: The assembly of wet transfer. Image excerpted from: Manual Bio-Rad.

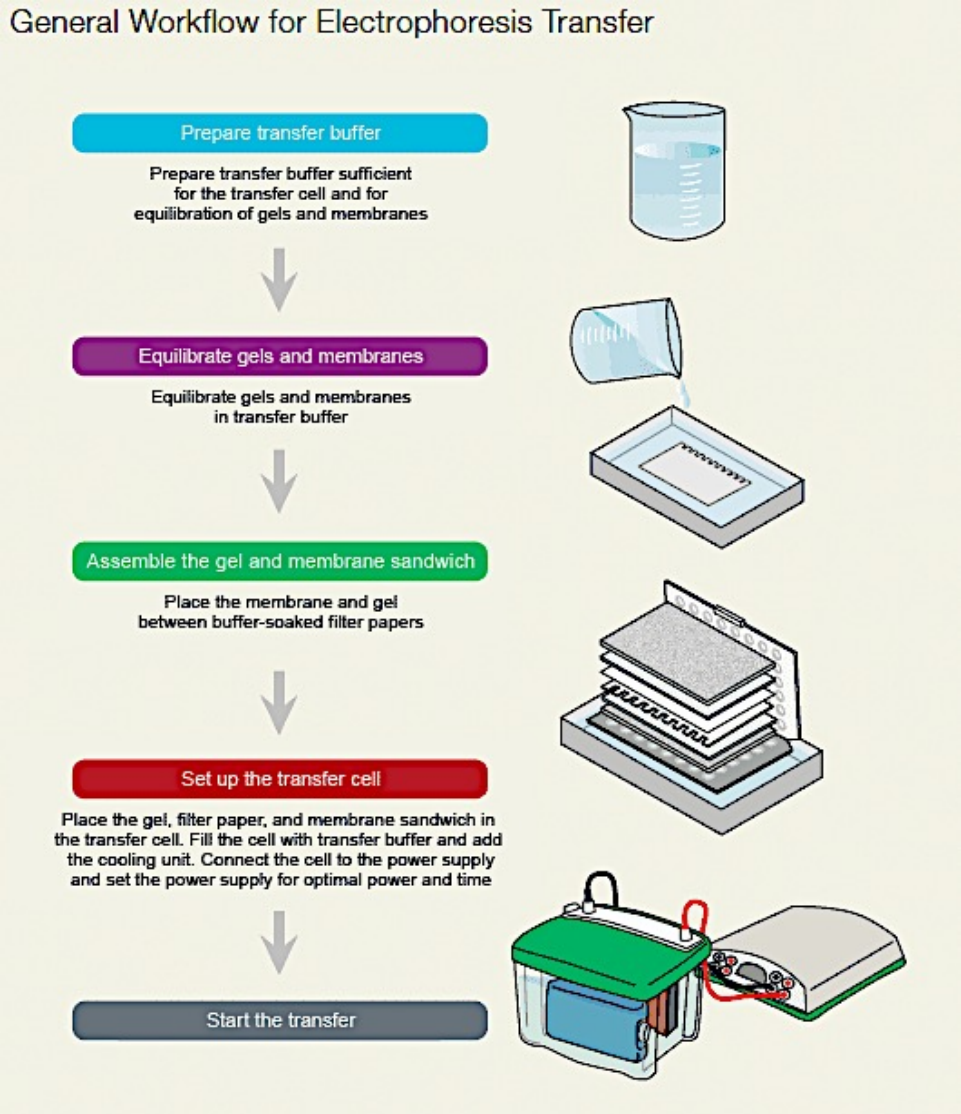

Figure 3.10: Overview of the wet transfer procedure. Image excerpted from: Introduction to Protein Electrophoresis Bio-Rad, n.d.

3.2.10.8 Membrane Blocking and Primary and Secondary Antibody Incubation

The membrane with transferred proteins was blocked with blocking buffer known as Blocking One (Nacalai) for one hour with slow shaking at room temperature. Primary antibody was prepared with 1:1000 dilutions with blocking buffer. Example, 10 µl of primary antibody is diluted into 10 ml of blocking buffer. After 1 hour blocking, the membrane was probed with specific primary antibody overnight at 4 °C on a slow shaker. After primary antibody probing, the membrane was washed 3 times with 1x TBS-T (refer appendix for recipe) with 5 minutes incubation each time on a fast shaker.

The HRP conjugated-secondary antibody was prepared with blocking buffer with 1:10 000 times dilution. Example 1 µl of secondary antibody was diluted in 10 ml of blocking buffer. After the primary antibody-washing step, the membrane was incubated with HRP conjugated-secondary antibody for 1 hour at room temperature. After the incubation period, the membrane was washed 3 times with 1x TBS-T with 5 minutes incubation each time on a fast shaker.

3.2.10.9 Enhanced Chemiluminescence Viewing of Protein Bands

After the washing step, the membrane was immersed in the enhanced chemiluminesence (ECL) solution (Advansta) and protein bands were visualized and captured on a ChemiDoc XRS Imaging System. The membrane was exposed to different periods of luminescence to detect the ideal intensity of protein bands. The images were captured and saved to be further quantified using ImageJ software.

3.2.10.10 Stripping and Re-probing of Membrane

The membrane was stripped using a stripping buffer (refer appendix for recipe) under fast shaking for 15 minutes. The stripped membrane is washed once with TBS-T under fast shaking for 5 minutes. The blocking, primary antibody and secondary antibody step is repeated on the membrane. A membrane can be ideally stripped twice.

3.2.10.11 Quantification of the protein bands

The image of the band is cropped and quantified using the densitometry quantification software ImageJ. The values obtained via densitometry quantification is normalised with the β-actin and then normalised again with the negative control to obtain the fold increase or decrease in a protein expression.

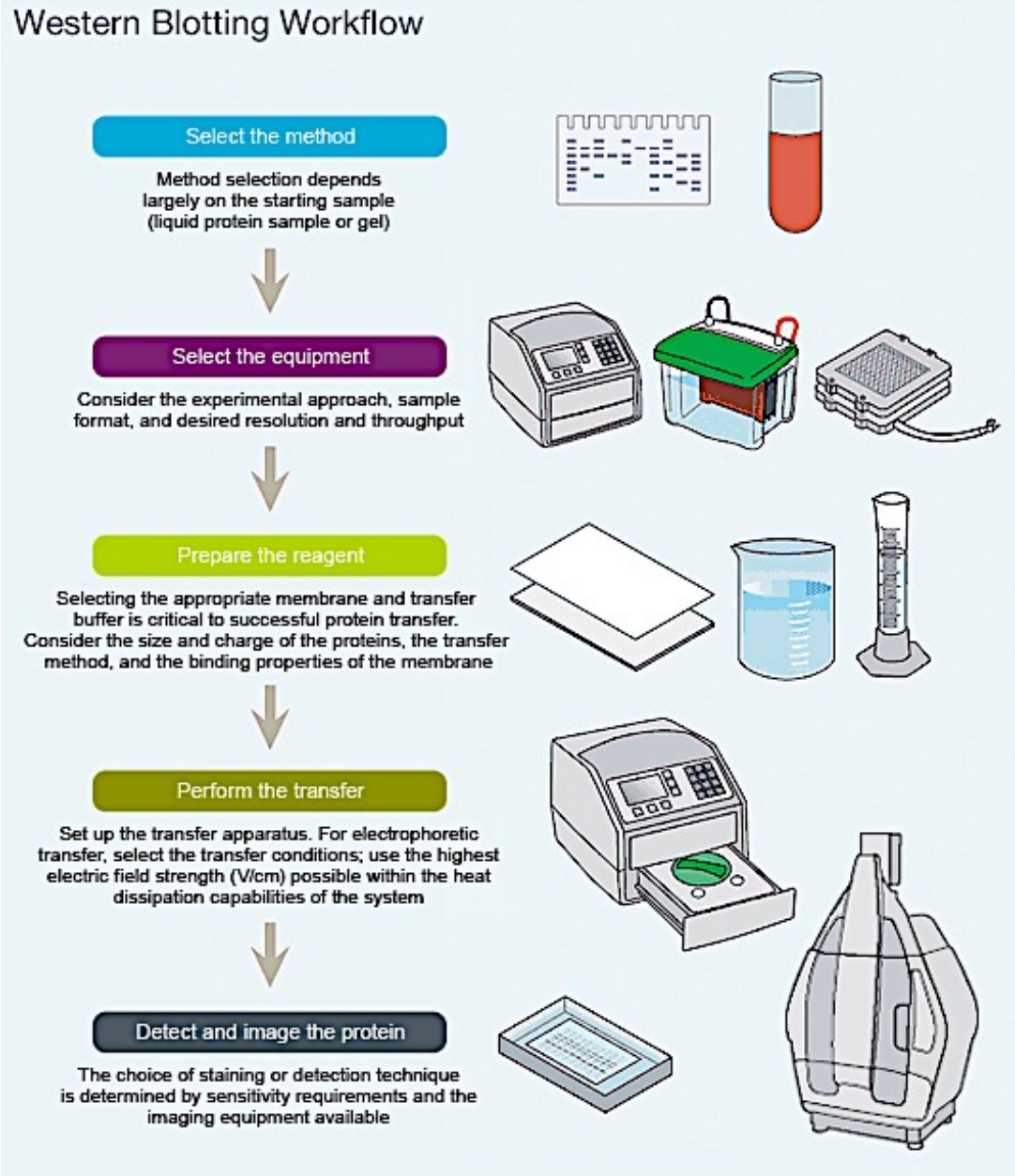

Figure 3.11: Overview of the western blot workflow. Image excerpted from: Introduction to Western Blotting Bio-Rad, 2017.

3.2.11 Metastasis Inhibition Studies

3.2.11.1 Cell Attachment Assay

Concept

Cell attachment is an important factor for the maintenance of the structure of the tissue, to promote migration of cells. Cell attachment is also essential for the transduction of microenvironment information across the plasma membrane. Cells that are unable to attach by themselves are vulnerable to cell death. This assay measures the ability of treated cells to re-attach on the treated surface of the tissue culture dishes. The ability of the cells to attach is important for it to inhabit a new location.

Method

Briefly, cells were seeded at $1x10^5$ cells/well in a 24-well microtiter plate, treated with methanol and chloroform extracts of *R. angustifolia* at concentrations 10, 20, 50 μg/ml and chalepin was treated at concentrations of 18, 36 and 45 μg/ml. The treated cell were then incubated at 0, 6, 12 and 24 hours. After that, the treated cells were detached using 0.5% trypsin-EDTA and plated back onto a new culture plate. After each incubation period of 0 to 24 hours, the cell attachment status and morphology were observed and photographed with a phase contrast microscope.

3.2.11.2 Scratch Motility Assay

Concept

The basic concept of this experiment is to create a scratch in a cell monolayer and to capture images at the initial stage and at regular intervals which results in the subsequent closure of the scratch that is due to cell migration. In comparison with other methods, the *in vitro* scratch assay is particularly suitable for studies on the effects of

cell–matrix and cell–cell interactions on cell migration, mimic cell migration during wound healing *in vivo* (Liang et al., 2007).

Method

A total of 1 x 10^5 cells/well were seeded into 24-well microplates. It was allowed to attach and grow overnight. The following day, the cell monolayer was scratched with a yellow pipette tip, making the scratch into a single straight line. It was of importance to create scratches of approximately similar size in the assessed cells and control cells to minimize any possible variation caused by the difference in the width of the scratches. It was then washed with PBS twice to remove cells that are floating and these cells were treated with 10, 20, 50 μg/ml of methanol and chloroform extracts of *R. angustifolia* and chalepin was treated at concentrations of 18, 36 and 45 μg/ml in a serum free media. These cells were incubated at various time points (0, 6, 12, 24 hours) and viewed under a phase contrast microscope and the image of the scratched region was recorded.

3.2.11.3 Cell Migration Assay

Concept

This experiment is based on the Boyden chamber principle where treated cancer cells are placed in the inserts of the transwell and the chemotaxic response is monitored through the movement of the cell through the membrane pore. Migration is an important cellular function such as wound healing, inflammation, angiogenesis and others. Malfunction in this process results in disorders such as cancer, tumor formation and metastasis.

The Boyden chamber assay was introduced by Boyden and is based on a chamber which has two medium-filled compartments. These compartments are separated by microporous membrane. The cells which are placed in the upper compartment are

allowed to migrate and move through the pores on the membrane towards the lower compartment. Chemotaxic agents usually FBS is placed at the lower compartment. At the end of an incubation period, the cells are fixed and stained at the amount of cells that has migrated to the lower compartment is calculated (Chen, 2005).

Method

Approximately 1 x 10^6 cells were seeded into 35 mm tissue culture dishes and allowed to adhere for a day. On the next day, the cells were treated with various concentrations of extracts of *R. angustifolia* (10, 20, and 50 µg/ml) and chalepin (18, 36, and 45 µg/ml) in serum free media. The extracts and compound were incubated for 48 hours. The next day, the cells were washed and harvested using Accutase®. The cells (300 000 cells) were counted using hemacytometer and then re-plated into the upper chamber of the transwell of 24 well plates provided in the Merck ECM 508 QCM™ 24-well cell migration assay kit. The kit provided inserts of 24 well plates which an 8 mm pore size polycarbonate membrane, as this is appropriate for most cell types. This pore size supports optimal migration of A549 cell, as it is a fibroblast cell. The bottom portion of the transwell was filled with the serum supplemented media. At the end of 24 hours incubation time, the media at the upper chamber was carefully aspirated out. The cells that have migrated through the membrane pore would be at the outer bottom of the transwell insert. This insert was removed from the well plate using a sterilized forcep and then placed a in a new well containing 400 µL of cell stain solution. It was then incubated for 20 minutes at room temperature. At the end of incubation period, the cell stain solution is aspirated out. Then, by using a cotton tip the non-migratory cell layer at the interior of the insert was swabed to remove all the cells in the inward perimeter. This step was repeated once more. The insert was air dried and then the image of the migrated cells was captured using a phase contrast microscope. The insert of the well

was placed on a glass slide and the image was captured. After that, the stained inserts were placed in a clean well containing 200 µL of extraction buffer solution provided in the kit for 15 minutes at room temperature. The insert was removed and a volume of 100 µL of the mixture is then transferred into 96-well plate and the absorbance was read using a microplate reader at a wavelength of 560 nm. The calculation is done based on the formulae below.

$$\text{Percentage of Migrated Cells} = \frac{[\text{Total number of treated (migrated) cells}]}{[\text{Total number of untreated (migrated) cells}]} \times 100\%$$

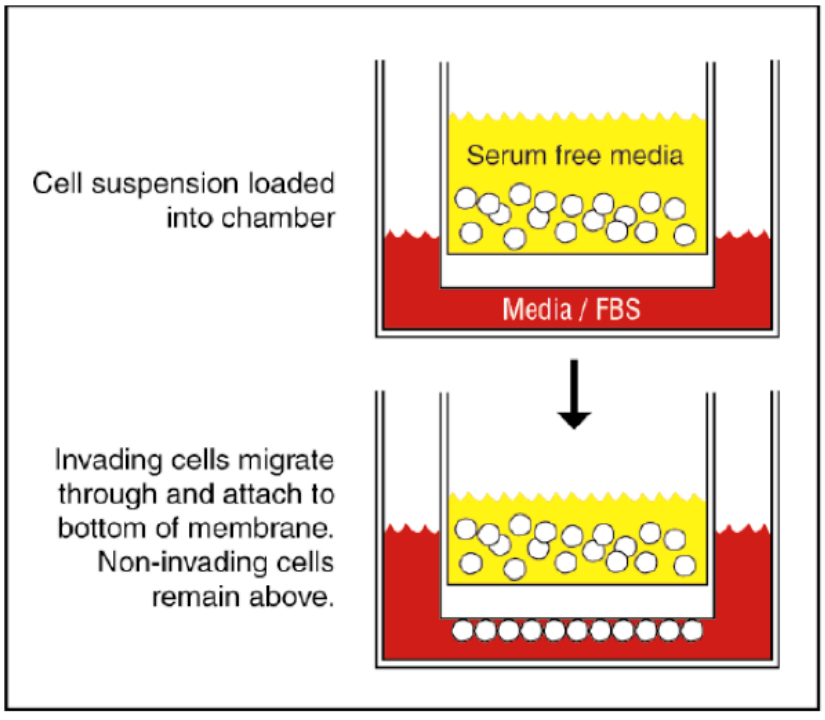

Figure 3.12: Overview on the cell migration assay. Image excerpted from: QCM™ 24-Well Fluorimetric Cell Migration Assay (Manual), 2009.

3.2.11.4 Cell Invasion Assay

Concept

Cancer cells starts invasion through adhesion and spreading along the blood vessel wall. The proteolytic enzymes such as MMP collagenases assists in lysing tiny holes in the basement membrane surrounding the blood vessel wall to allow cancer cells to invade through. Invasion through the extracellular matrix (ECM) is an important step in tumor metastasis. To study this criteria, microporous membrane inserts coated with reconstituted basement membrane matrix of proteins derived from the Engelbreth Holm-Swarm (EHS) mouse tumor which was already provided in the ECM 554 Kit was used. This coating mimics the environment of the blood vessel which the cancer cells would evade. Most commonly used method in this study is the Boyden Chamber assay which has been optimised and simplified using the kit. Boyden Chamber assay is based on the concept where a chamber of two medium-filled compartment which is separated by membrane was used. The cells were placed in the upper chamber and was allowed to move to the lower chamber in the presence of a chemotaxic agent according to the set incubation time and at the end of the experiment the percentage of moved cells was calculated.

Method

Cells that have been passaged 2-3 times before the assay were used and ideally they should attain 80% confluency. Approximately 1 x 10^6 cells were seeded into 35 mm tissue culture dishes and allowed to adhere for a day. On the next day, the cells were treated with methanol and chloroform extracts of *R. angustifolia* at concentrations 10, 20, 50 µg/ml and chalepin was treated at concentrations of 18, 36 and 45 µg/ml in serum free media. The extracts and compound were incubated for 48 hours. The next day, the cells were washed and harvested using Accutase®. The cells (300 000 cells) were

counted using hemacytometer and then re-plated into the upper chamber of coated transwell of 24 well plates provided in the Merck ECM 554 QCM^{TM} 24-well cell invasion assay kit. The bottom portion of the transwell was filled with the serum supplemented media. The treated cells were allowed to invade across the coated membrane for 24 hours. After 24 hours, the percentage of invaded cells were measured. Prior to measurement, the invaded cells which is at the outer bottom part of the transwell were dislodged in cell detachment buffer provided in the kit. The transwell insert was removed from the well . The detached cells were then lysed using the cell lysis buffer and the dye solution which was provided in the kit was prepared according to the instruction and added to the lysed cells. The mixture was incubated for 15 minutes at room temperature and then 200 µl of the mixture were transferred to a 96-well plate which is suitable for fluorscence measurement and it was read using a fluorescence plate reader using 480/520 nm filter set. The calculation is done based on formulae below:

$$\text{Percentage of Invaded Cells} = \frac{[\text{Total number of treated (invaded) cells}]}{[\text{Total number of untreated (invaded) cells}]} \times 100\%$$

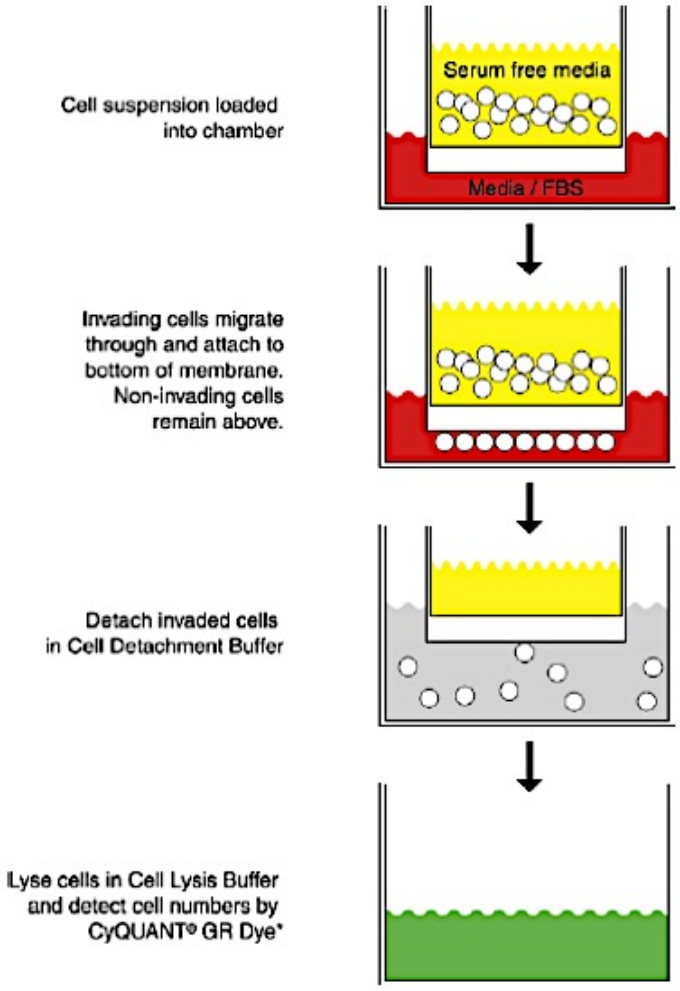

Figure 3.13: Overview of the cell invasion assay. Image excerpted from QCM™ 24-Well Cell Invasion Assay (Fluorometric) manual, 2003.

3.2.11.5 Cell Adhesion Assay

Concept

This kit studies the adhesion capacity of the cancer cells on 7 different types of extracellular matrix proteins (ECM) i.e. Collagen I, Collagen II, Collagen IV, Fibronectin, Laminin, Tenascin, Vitronectin and a negative control which is the BSA coat. This kit uses a colorimetric detection method. Cell adhesion is an important factor to be studied upon on cancer cells because various molecules participates in the extracellular matrix adhesion of cancer cells and promotes recurrent, invasive and

metastatic cancer. Besides progression of cancer, these proteins also play a major role in cell growth, cell motility, wound healing, inflammation and etc. In this experiment, the ability of the compounds and extracts to inhibit cancer cells from attaching to these various ECM proteins was studied. The importance of this assay is to test the ability of a certain type of cell or cell line to adhere to a specific adhesive substrate and to test the ability of certain cell- adhesive substrate interaction inhibitors (Humphries, 2009).

Method

Cells that have been passaged 2-3 times before the assay were used and ideally they should attain 80% confluency. Approximately 1 x 10^6 cells were seeded into 35 mm tissue culture dishes and allowed to adhere for a day. On the next day, the cells were treated with various concentrations of extracts of *R. angustifolia* and chalepin in serum free media. The extracts and compound were incubated for 48 hours. The next day, the cells were washed and harvested using Accutase®. The detached cells were counted with a haemocytometer. The appropriate number of plate strips that is provided in the kit (Merck ECM 540 QCM^{TM} 96-well cell adhesion assay kit) was rehydrated with 200 uL of PBS per well for 10 minutes at room temperature. Before the cells were added, PBS was removed from the strips. A single cell suspension was prepared and 7000 cells in 100 uL of media were added per well of strips in the ECM array plate. Each test samples were tested in triplicate. The plates were incubated for 2 hours at 37°C in a CO_2 incubator. At the end of the incubation period, the media is gently aspirated from the well and discarded. The wells were washed 2-3 times with 200 uL of Assay Buffer per well. After the washing process, 100 uL of Cell Stain solution were added to each well and incubated for 5 minutes at room temperature. Then, the stains were removed from the wells and washed gently with deionized water for 3-5 times. The final wash was discarded and the wells were air dried for a few minutes. A volume of 100 uL of

Extraction Buffer was added to each well and the strips were incubated on an orbital shaker with a gentle rotation at room temperature for about 10 minutes. The absorbance value was read on a microplate reader at the wavelength 560 nm. The percentage of inhibition of the adhesion of the cell resulted from the treatment of compound or extract was calculated.

$$\text{Percentage of Adherent Cells} = \frac{[\text{Mean OD of the test cells} - \text{Mean OD of the blank}]}{[\text{Mean OD of the untreated cells} - \text{Mean OD of the blank}]} \times 100\%$$

3.2.11.6 Gelatin Gel Zymography

Concept

Gelatin zymography is a powerful way to detect proteolytic enzymes, which are capable of degrading gelatin from various biological sources. It detects members of matrix metalloproteinase family that is MMP-2 and MMP9. This is due to their gelatin degrading capacity (Toth et al., 2012). The aim of this technique is to study the extracellular matrix-degrading proteases such as matrix metaloproteases (MMPs), which is present in the cell cultures. The method identifies the MMPs based on its molecular weight and substrate specificity. Zymography is a technique for studying hydrolytic enzymes on the basis of substrate degradation. In the presence of the proteolytic enzyme, MMP2, it would cleave the substrate (gelatin), which is present in the mixture of the gel to produce a white opaque band at location of the molecular weight of MMP2 on the gelatin gel that would be visible after staining. This method can be used to study the factors that regulate the expression of gelatin and modulate

zymogen activation in experimental models. This system gives an insight on the expression of gelatinase and activation in human cancer tissues and its relatability in cancer progression (Toth et al., 2012).

Method

Approximately 1 x 10^5 cells/well were seeded into 24 well plates and then treated with methanol extract, chloroform extract and chalepin at various concentrations. After 48 hours incubation period, the supernatants were collected and centrifuged to remove the debris. Then, the supernatant were stored at -20°C to be used as the conditioned media. The media was then mixed with one part of 5x Tris-Glycine SDS sample buffer. It was then incubated for 10 minutes at room temperature. The sample was then loaded onto a 12.5% SDS-polyacrylamide gel that has been added together with 0.1% gelatin. The gel was then run with 1x Laemmli buffer (running buffer) at 125V for 60 minutes. When the proteins were completely resolved, the gel was removed and washed twice with renaturing buffer on a shaker at room temperature for each washing. After that, the gel was incubated with developing buffer overnight at 37°C. It was then stained with 0.1% Coomasie blue for 1 hour. Finally the gel was destained with destaining solution I and then destaining solution II and the presence of matrix metalloproteinase enzyme was observed as an opaque unstained band against a dark blue background. The gel was then scanned with a gel scanner and recorded.

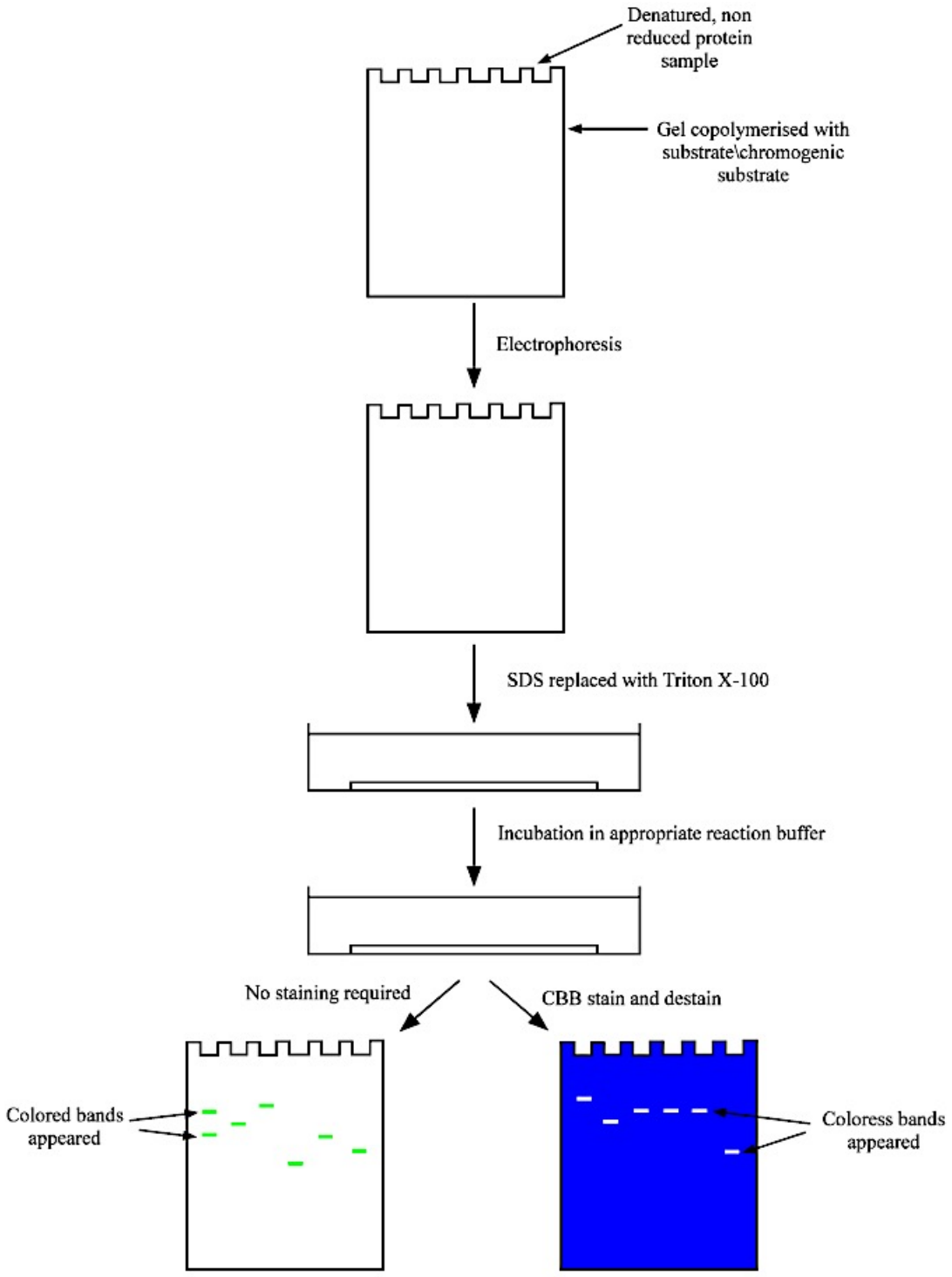

Figure 3.14: Overview of the gelatin zymography technique. Image excerpted from Zymography: Enzymes in action, n.d.

3.2.12 Statistical Analysis

All the values reported are shown as mean ± standard error of the mean and all the experiments were conducted at least twice using sample triplicates. Figures from morphological studies, flow cytometry plots, Western blot analyses and anti-metastasis assays are representative of the experiment replicates. Comparison between control and treated groups were performed using one-way ANOVA with post hoc Tukey test (*$p<0.05$ considered statistically significant). Statistical analysis were performed using SPSS 20.0 software and calculations were done using the Microsoft Excel. Quantification of the bands in the western blot analysis was done using the ImageJ software.

CHAPTER 4: RESULTS

4.1 Extraction, Fractionation and Screening for Cytotoxicity

Extraction and fractionation was done on the leaves of *Ruta angustifolia* Pers. The yield of the methanol extract was 55.0 g which is 31.4% of the total dried ground leaves. The methanol extract was further partitioned with solvents of different polarity. Water extract gave the highest yield followed by chloroform extract. Ethyl acetate extract had the lowest yield from methanol extract, as compared to the other fractions. The percentage of the partitioned extracts (hexane, chloroform, ethyl acetate and water) were calculated based on the methanol extract.

Table 4.1: The yield of extracts of *R. angustifolia* from 175.0 g of dried ground leaves

Extracts	Yield (g)	Percentage (%)
Methanol	55.0	-
Hexane	2.96	5.33
Chloroform	11.85	21.35
Ethyl Acetate	0.87	1.57
Water	30.08	54.20

About 1.0 g of chloroform extract yielded to about 700 mg of chloroform extract without chlorophyll upon removal of chlorophyll in the extract by using the activated charcoal. From this amount, 500 mg of chloroform extract without chlorophyll was utilized for isolation via HPLC.

4.1.2 Cytotoxicity Screenings of the Crude and Fractionated Extracts of *R. angustifolia*

Selected cancer cell lines (A549, CaSki and HCT-116) were used in the screening of the crude and fractionated extracts of *R. angustifolia* for their cytotoxic potency. Toxicity towards normal cells was tested against MRC5 cell line. All the extracts

showed no toxicity towards MRC5 with an IC_{50} value of more than 100.00 µg/ml. The chloroform extract (without chlorophyll), showed slight toxicity with an IC_{50} value of 65.7 ± 0.5 µg/ml. It was found that the activity of all the extracts were time and concentration dependent in which the lowest IC_{50} value was observed when treatment was done over 72 hours. The methanol extract exhibited good cytotoxic activity in all the cancer cell lines tested and without toxicity to normal cells. The chloroform extract showed the highest activity and the cytotoxicity was even better when chlorophyll was removed; however it exhibited slight toxicity to MRC5 cell. The chloroform extract without chlorophyll exhibited the best cytotoxicity in A549 cell line with an IC_{50} of 8.8 µg/ml; hence it was chosen as a candidate for further isolation of the chemical components.

Table 4.2: The IC_{50} values of *in vitro* cytotoxicity screening with SRB assay upon various extracts of *R. angustifolia* against selected cell lines

Cell Line	Incubation Time	A549	CaSki	HCT-116	MRC5
Extract		IC_{50} (µg/ml)			
Methanol	72	7.02 ± 0.36	10.6 ± 0.09	14.5 ± 0.93	>100
	48	51.2 ± 1.85	35.0 ± 1.13	50.1 ± 0.36	>100
	24	85.6 ± 0.85	>100.0	>100.0	>100.0
Hexane	72	33.1 ± 1.667	41.2 ± 0.23	36.4 ± 2.01	>100.0
	48	>100.0	>100.0	88.0 ± 2.65	>100.0
	24	>100.0	>100.0	>100.0	>100.0
Chloroform	72	10.1 ± 0.35	9.4 ± 0.49	11.8 ± 0.1	>100.0
	48	22.67 ± 4.31	29.00 ± 0.46	14.2 ± 0.2	>100.0
	24	72.0 ± 0.5	>100.0	26.8 ± 0.8	>100.0
Ethyl Acetate	72	35.1 ± 1.00	18.1 ± 0.15	23.3 ± 0.4	>100.0
	48	>100.0	46.00 ± 0.76	>100.0	>100.0
	24	>100.0	>100.0	>100.0	>100.0
Water	72	73.9 ± 8.30	92.2 ± 2.58	>100.0	>100.0
	48	>100	>100.0	>100.0	>100.0
	24	>100	>100.0	>100.0	>100.0
Chloroform without chlorophyll	72	8.8 ± 0.32	13.9 ± 1.23	10.8 ± 0.70	65.7 ±0.5
	48	23.2 ± 0.90	22.1 ± 0.21	14.6 ± 0.46	>100.0
	24	88.0 ± 0.5	>100.0	22.6 ± 0.45	>100.0

Tabulated values are mean ± standard deviation (SD) of three replicates

(A)

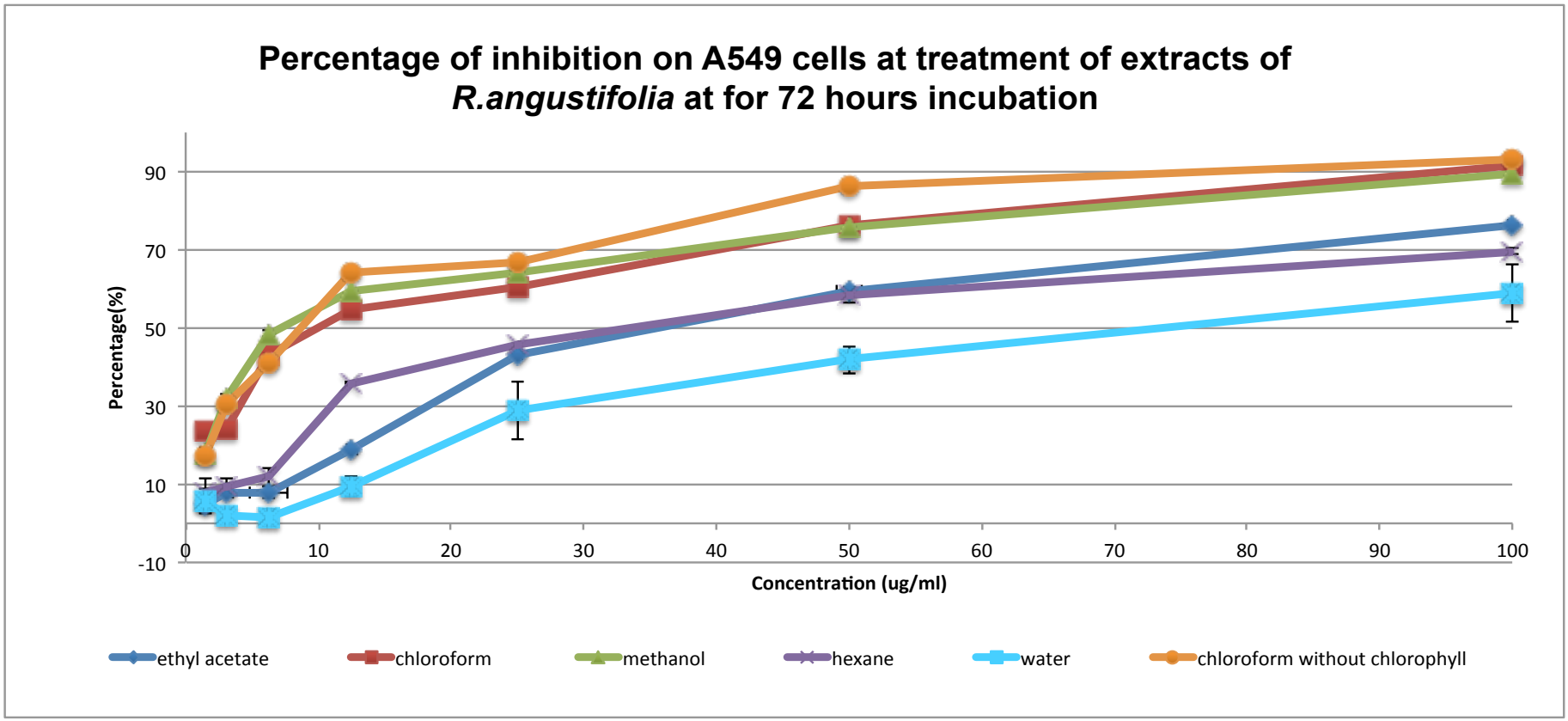

Figure 4.1(A): The percentage of inhibition of various extracts of *R. angustifolia* against A549 cell line at 72 hours incubation. The data expressed as mean ± S.D. of three independent replicates (n=3).

(B)

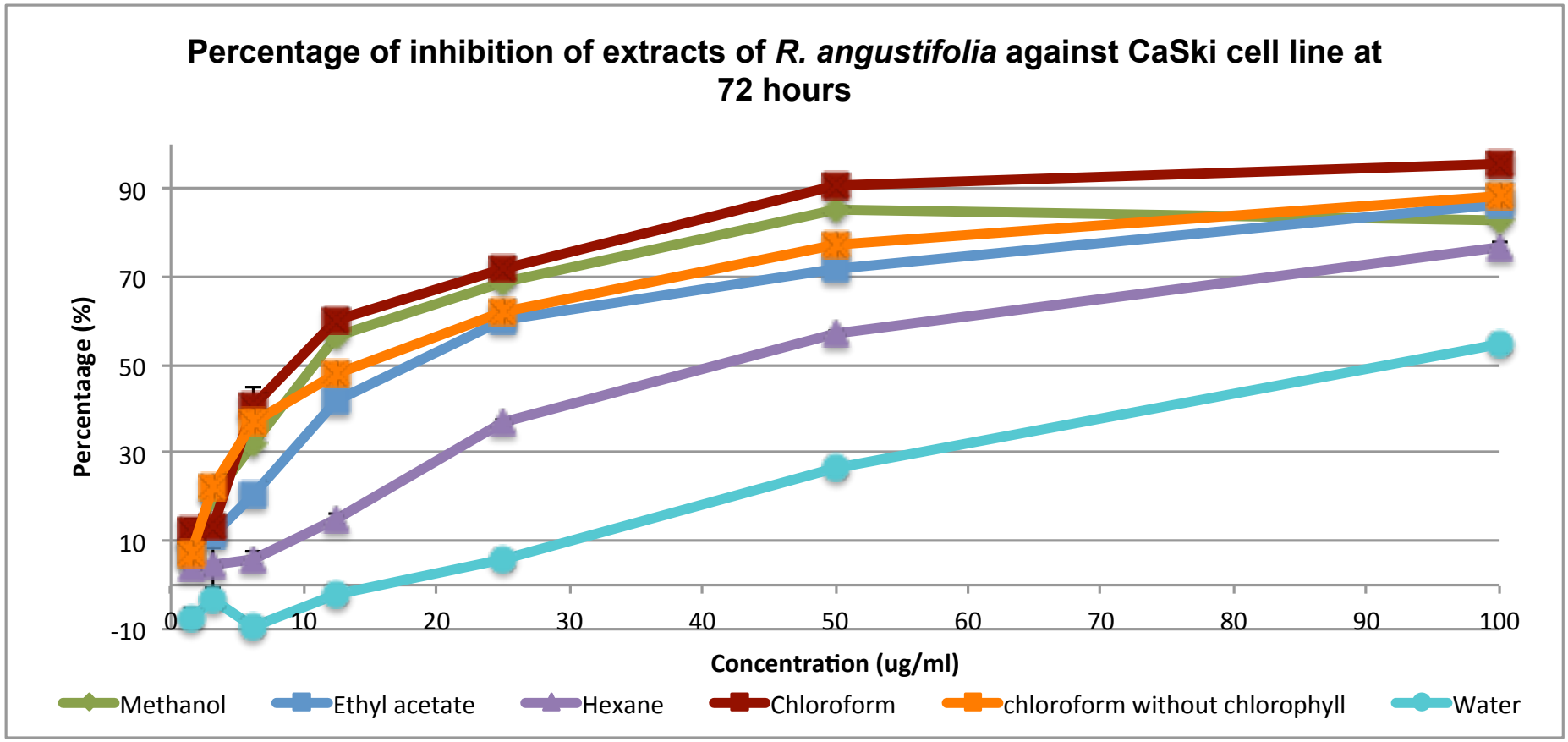

Figure 4.1(B): Graph shows the percentage of inhibition of various extracts of *R. angustifolia* against CaSki cell line at a range of concentrations in 72 hours incubation. The data expressed as mean ± S.D. of three independent replicates (n=3).

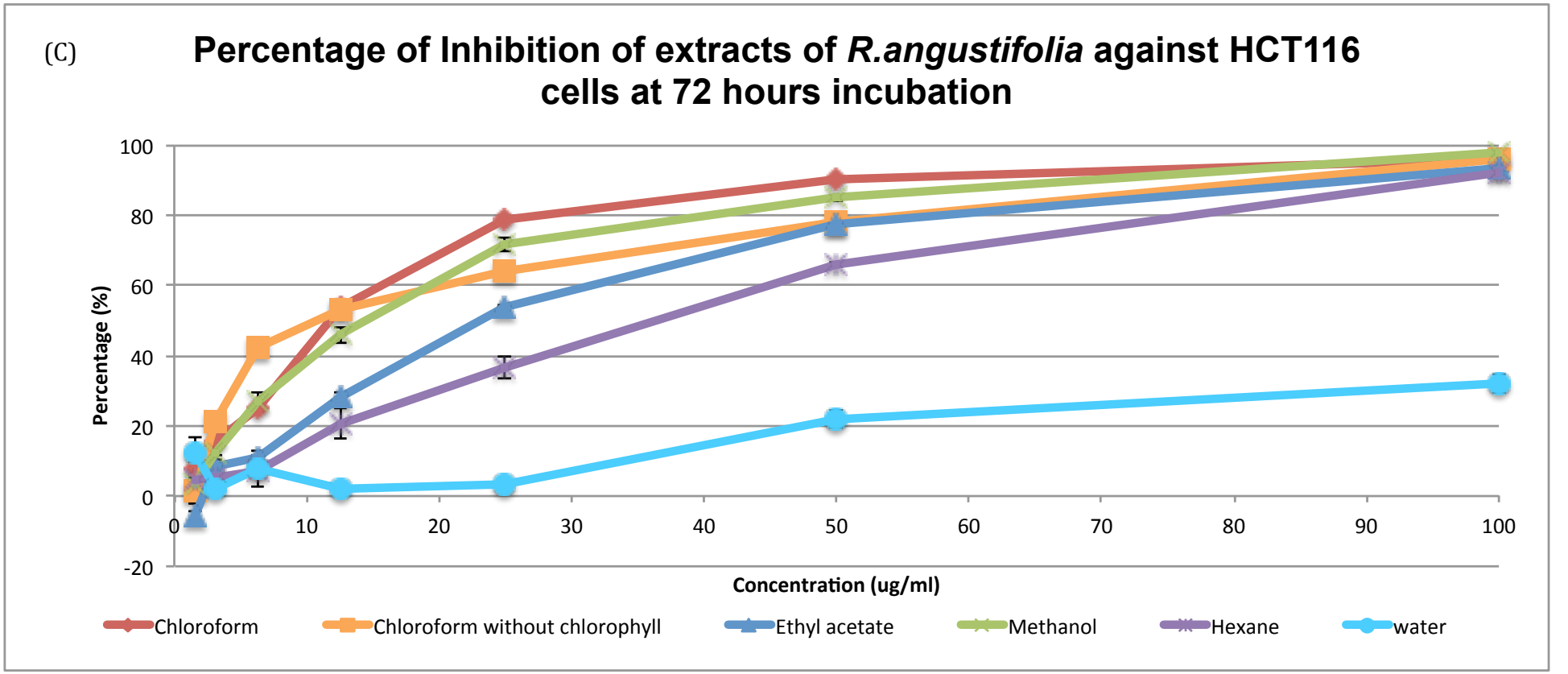

Figure 4.1 (C): Graph shows the percentage of inhibition of various extracts of *R. angustifolia* against HCT 116 cell line at a range of concentrations in 72 hours incubation. The data expressed as mean ± S.D. of three independent replicates (n=3).

(D)

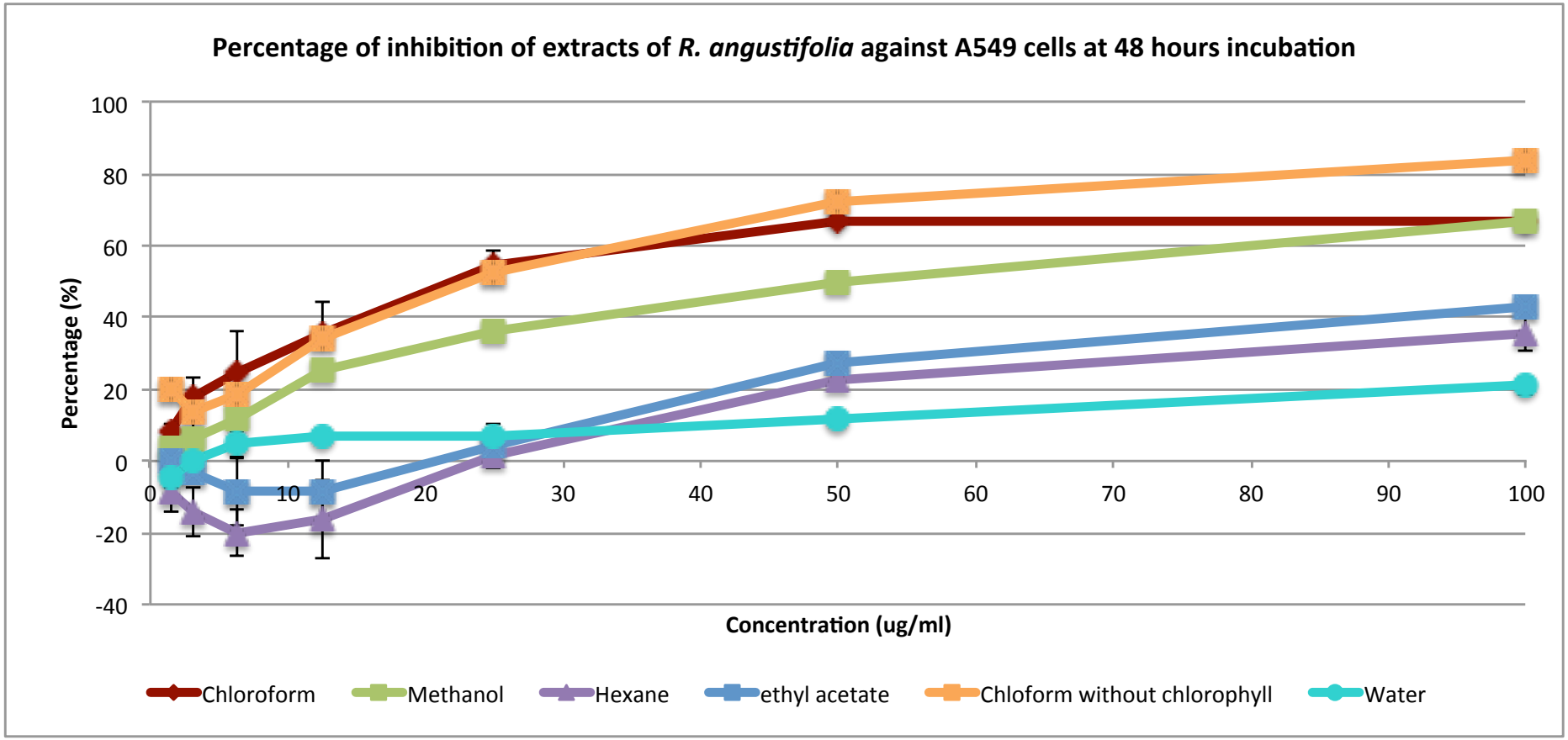

Figure 4.1(D): The percentage of inhibition of various extracts of *R. angustifolia* against A549 cell line at 48 hours incubation. The data expressed as mean ± S.D. of three independent replicates (n=3).

(E)

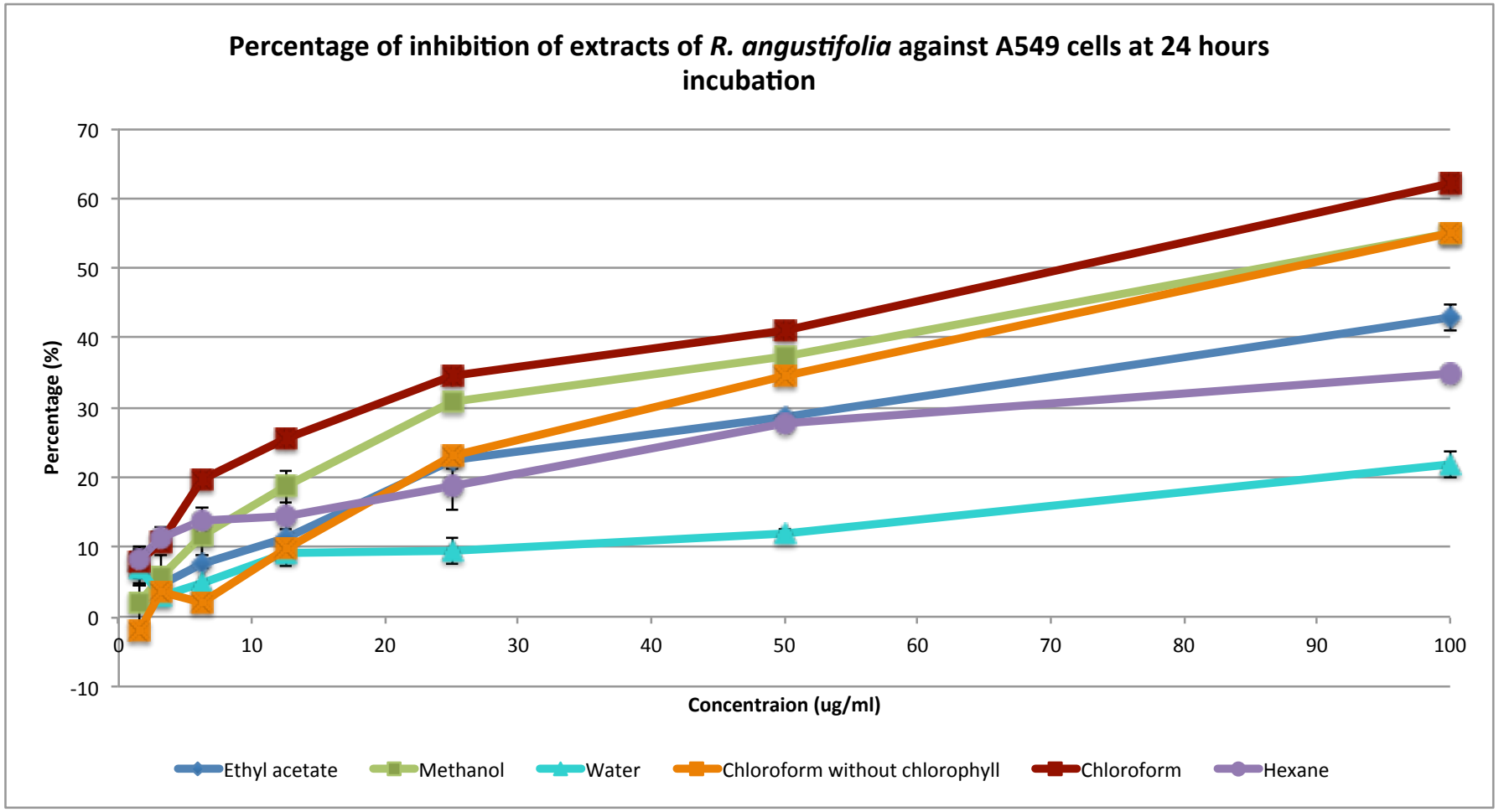

Figure 4.1(E): The percentage of inhibition of various extracts of *R. angustifolia* against A549 cell line at 24 hours incubation. The data expressed as mean ± S.D. of three independent replicates (n=3).

4.1.2 Criteria of Selection on the Active Extract & Cancer Cell Line to be Further Studied On

Chloroform extract was selected to be further chemically isolated based on the criteria that it exhibited the highest cytotoxicity against all the tested cancer cell lines. Chloroform extract exhibited the lowest IC_{50} value in comparison to other extracts i.e. 10.1 ± 0.35, 9.4 ± 0.49 and 11.8 ± 0.1 μg/ml for A549, CaSki and HCT-116 cancer cell line, respectively (Table 4.2). Chloroform extract has chlorophyll in which the chlorophyll would interfere with the isolation of compounds by giving many unwanted peaks in the total ion chromatogram of HPLC. In order to avoid problems with interference during chemical isolation, chlorophyll was removed from the extract prior to subjecting it to the isolation via HPLC. The chloroform extract without chlorophyll was against tested against various cancer cell lines to determine its cytotoxicity. The IC_{50} obtained were 8.8 ± 0.32, 13.9 ± 1.23 and 10.8 ± 0.70 for A549, CaSki and HCT-116 cancer cell line, respectively (Table 4.2). Based on these results, it is clear that the A549 cell showed the highest potency against the chloroform extract without chlorophyll. Hence, A549 cell line was chosen as the cell line to be use in further downstream biological studies.

4.2 Chemical Isolation of Active Compounds from the Chloroform Extract (without chlorophyll) of *R. angustifolia* Leaves

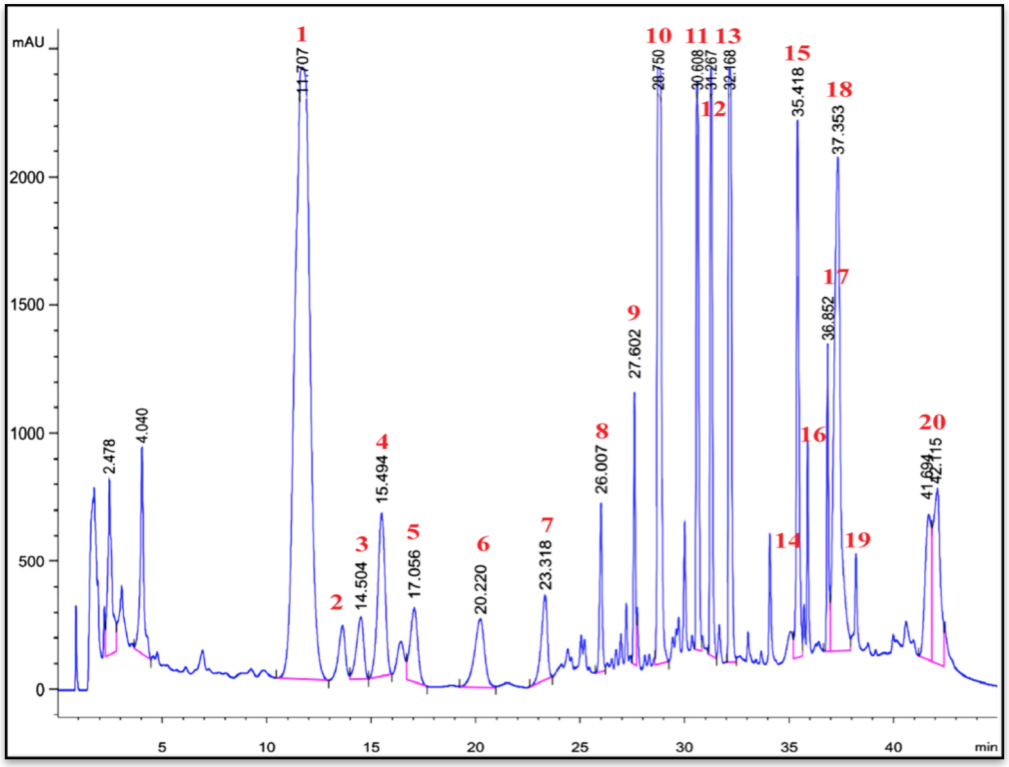

Figure 4.2: High Performance Liquid Chromatography (HPLC) chromatogram of the chloroform extract (without chlorophyll) of *R. angustifolia*

The chloroform extract (without chlorophyll) was subjected to isolation and purification using HPLC. Fractions were repeatedly collected using preparative HPLC method. The HPLC profile of the chloroform extract was shown in Figure 4.2. Twenty fractions were collected and twelve compounds were successfully identified using GCMS analyses. The mass spectral data of the isolated compounds obtained were found to be consistent with previous reports (Del Castillo et al., 1986; Orlita , Sidwa - Gorycka , Kumirska , et al., 2008; Orlita , Sidwa - Gorycka , Paszkiewicz , et al., 2008; Wu et al., 2003; Yang et al., 2007). The compounds which has been successfully identified are graveoline (1), psoralen (3), kokusaginine (4), methoxsalen (5), bergapten (7), arborinine (8), moskachan B (9), chalepin (10), moskachan D (12), chalepensin (13), rutamarin (14) and neophytadiene (16). The chemical structures of these compounds are illustrated in Figure 4.18

Table 4.3: Yield of isolated compounds (from 500 mg sample of chloroform without chlorophyll) from HPLC

Peak No.	Identification	Method of Identification	Yield (mg)	Percentage Yield (%)
1	Graveoline	GCMS	19.3	3.86
2	Unidentified	-	0.5	0.10
3	Psoralen	GCMS	2.0	0.40
4	Kokusaginine	GCMS	6.7	1.34
5	Methoxsalen	GCMS	2.8	0.56
6	Unidentified	-	0.2	0.04
7	Bergapten	GCMS	1.4	0.28
8	Arborinine	GCMS	2.7	0.54
9	Moskachan B	GCMS	0.1	0.02
10	Chalepin	TLC, GCMS, NMR	31.1	6.22
11	Unidentified	-	1.1	0.22
12	Moskachan D	GCMS	5.2	1.04
13	Chalepensin	NMR, GCMS	7.6	1.52
14	Rutamarin	GCMS, TLC	14.8	2.96
15	Unidentified	-	2.4	0.48
16	Neophytadiene	GCMS	7.1	1.42
17	Unidentified	-	2.9	0.58
18	Mixture of acids, stigmasterol and vitamin E	GCMS	27.9	5.58
19	Phenol, 9,12,15-octadecatrienoic acid, vitamin E, γ-sitosterol	GCMS	13.0	2.60
20	Phenol, 12-docosenamide	GCMS	6.6	1.32

4.3 Identification of Chemical Components

The twelve compounds namely graveoline, psoralen, kokusaginine, methoxsalen, bergapten, arborinine, moskachan B, moskachan D, chalepensin, chalepin, rutamarin and neophytadiene were identified through their mass spectral data (Figures 4.3 – 4.15) obtained from GC-MS analysis which were found to be consistent with published data (Del Castillo et al., 1986; Orlita , Sidwa ‑ Gorycka , Kumirska , et al., 2008; Orlita , Sidwa ‑ Gorycka , Paszkiewicz , et al., 2008; Wu et al., 2003; Yang et al., 2007). However chalepin was identified through its mass spectral obtained from GC-MS analysis which were consistent with published data (Orlita , Sidwa ‑ Gorycka , Paszkiewicz , et al., 2008), TLC analysis and also NMR spectral data (Figure 4.11). Some peaks collected from HPLC were not identified due to insufficient amount. The following compounds analysed were identified from their EI mass spectra by their m/z values:

(a)

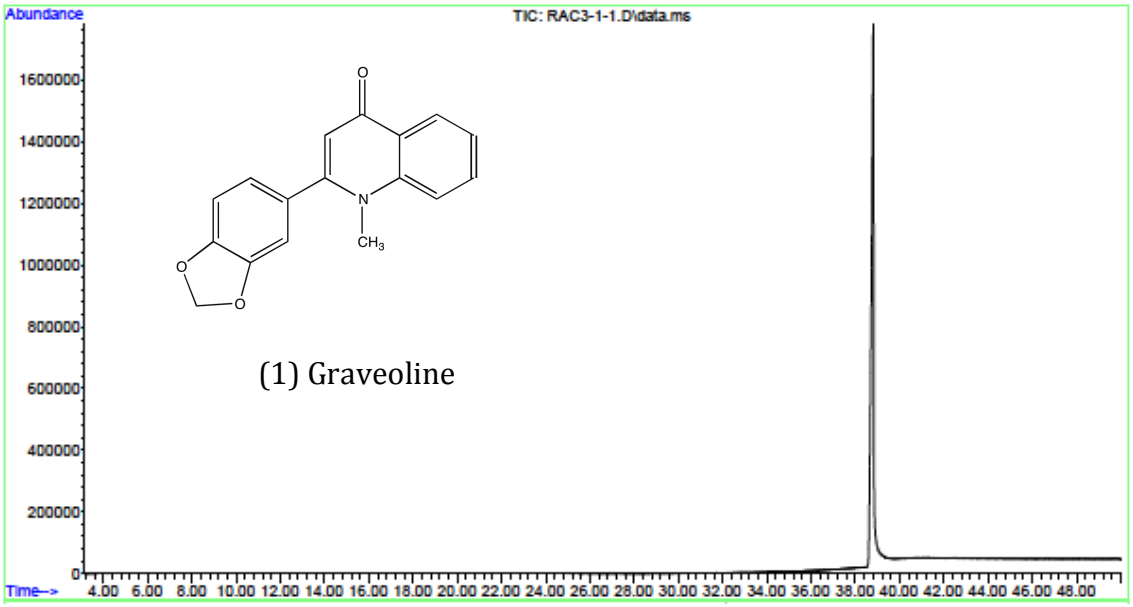

(b)

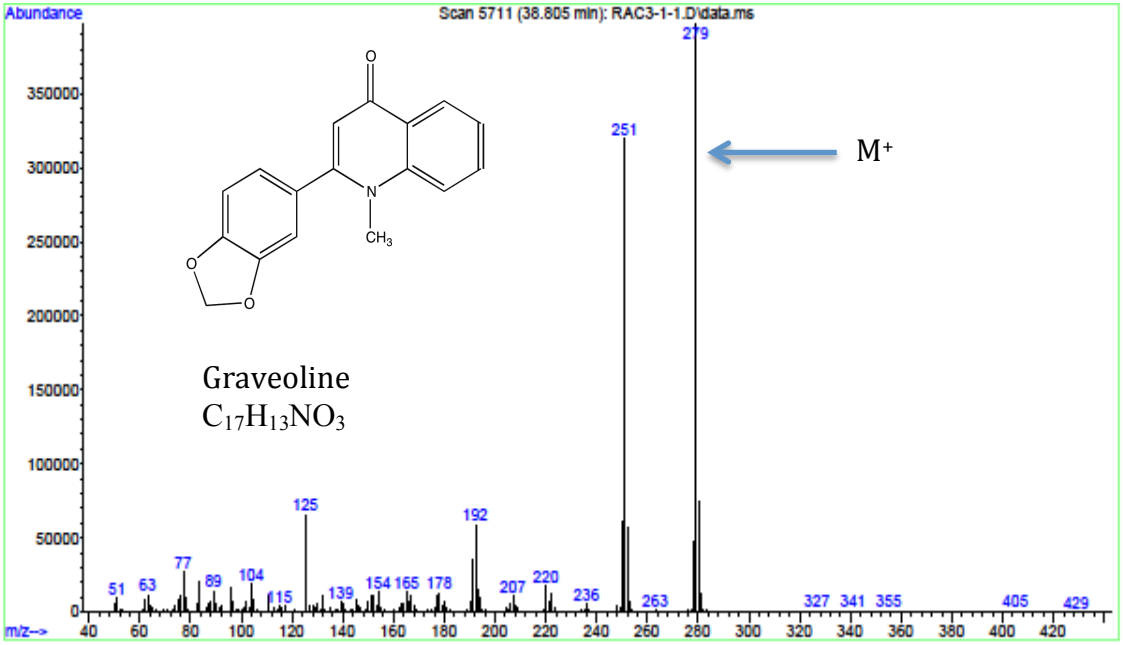

Figure 4.3: GC-MS analysis of graveoline (a) Total ion chromatogram (b) Mass spectrum

Graveoline, ($C_{17}H_{13}NO_3$), white powder, EIMS *m/z* (% intensity), 279 ($[M]^+$, 100), 251 ($[M\text{-}CO]^+$, 92), 192 (22), 125 (25). The mass spectral data obtained was in agreement with published data (Wu et al., 2003).

(a)

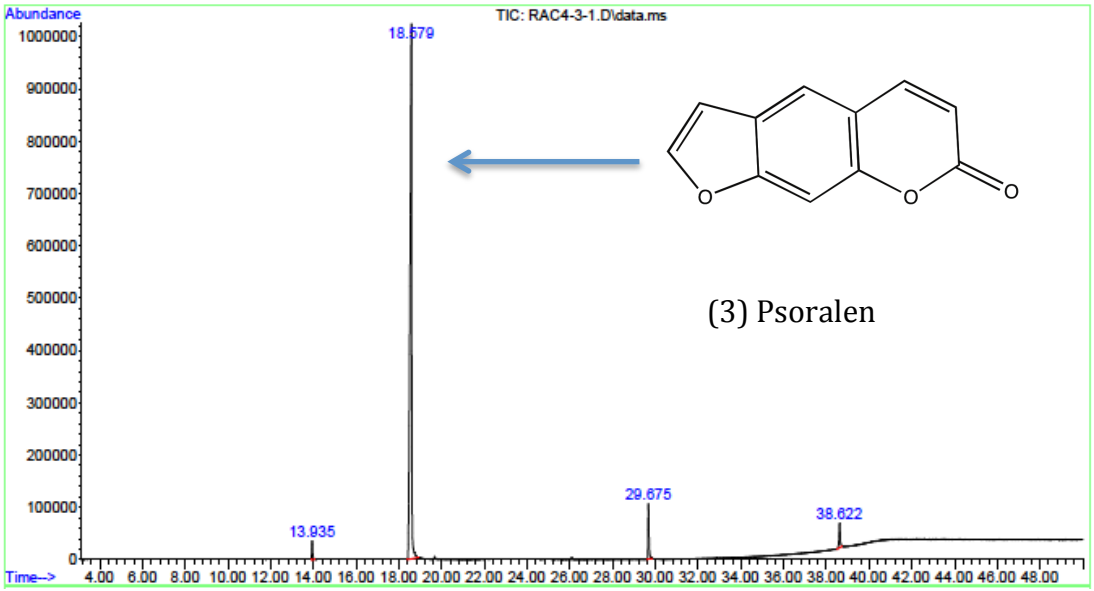

(b)

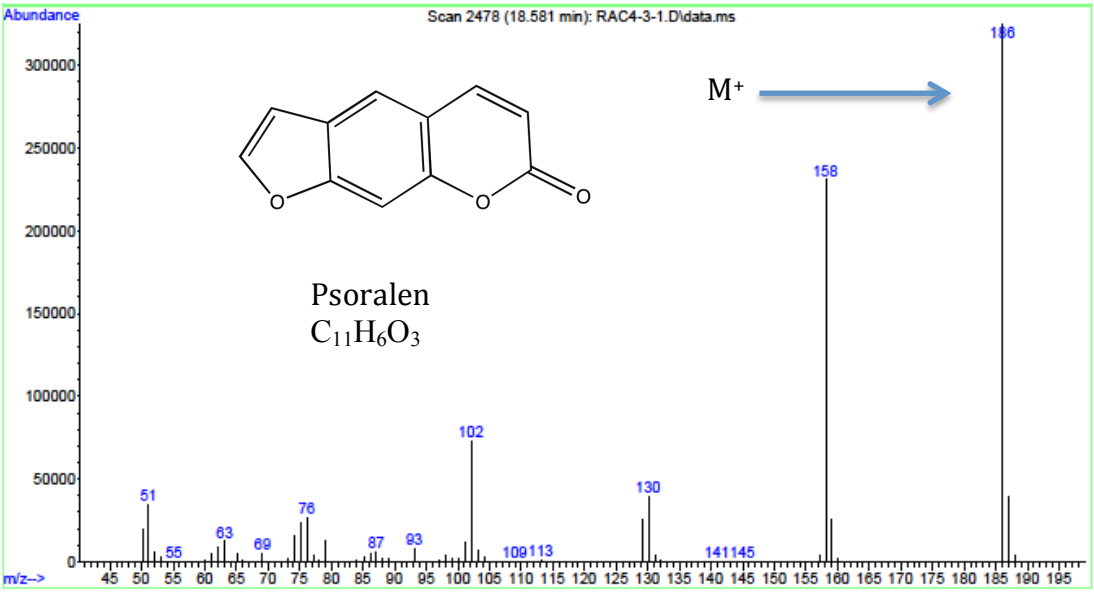

Figure 4.4: GC-MS analysis of psoralen (a) Total ion chromatogram (b) Mass spectrum

Psoralen, ($C_{11}H_6O_3$), yellowish powder, EIMS *m/z* (% intensity), 186 ($[M]^+$, 100), 158 ($[M\text{-}CO]^+$, 65), 130 ($[M\text{-}CO\text{-}CO]^+$, 19) and 102 ([M-CO-CO-CO], 32). The mass spectral data was in agreement with published data of psoralen (Orlita , Sidwa - Gorycka , Kumirska , et al., 2008; Wu et al., 2003).

(a)

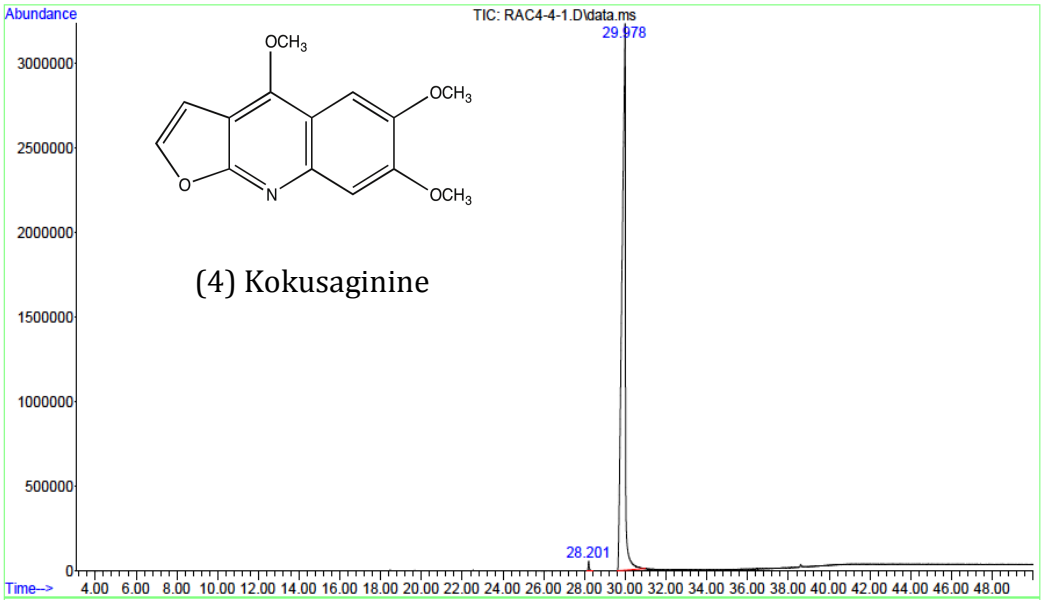

(b)

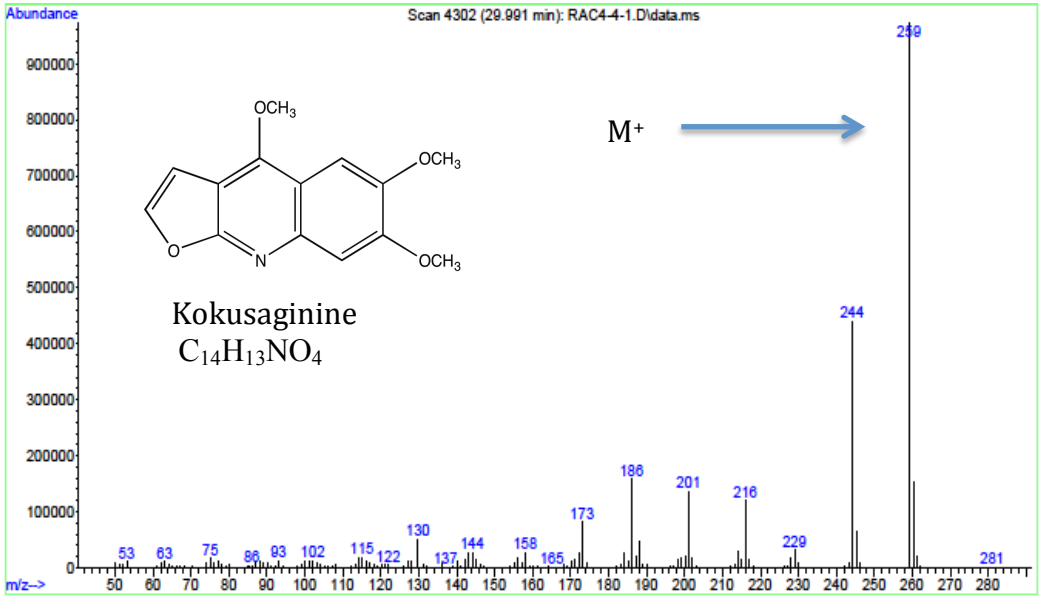

Figure 4.5: GC-MS analysis of kokusaginine (a) Total ion chromatogram (b) Mass spectrum

Kokusaginine, ($C_{14}H_{13}NO_4$), white crystals, EIMS *m/z* (% intensity), 259 ($[M]^+$, 100), 244 ($[M\text{-}Me]^+$, 43), 216 ($[M\text{-}Me\text{-}CO]^+$, 15), 201 ($[M\text{-}Me\text{-}CO\text{-}Me]^+$, 19), 186 ($[201\text{-}Me]^+$, 25) and 173 ($[186\text{-}CH]^+$, 16). The obtained mass spectral data is in agreement with published data (Wu et al., 2003).

(a)

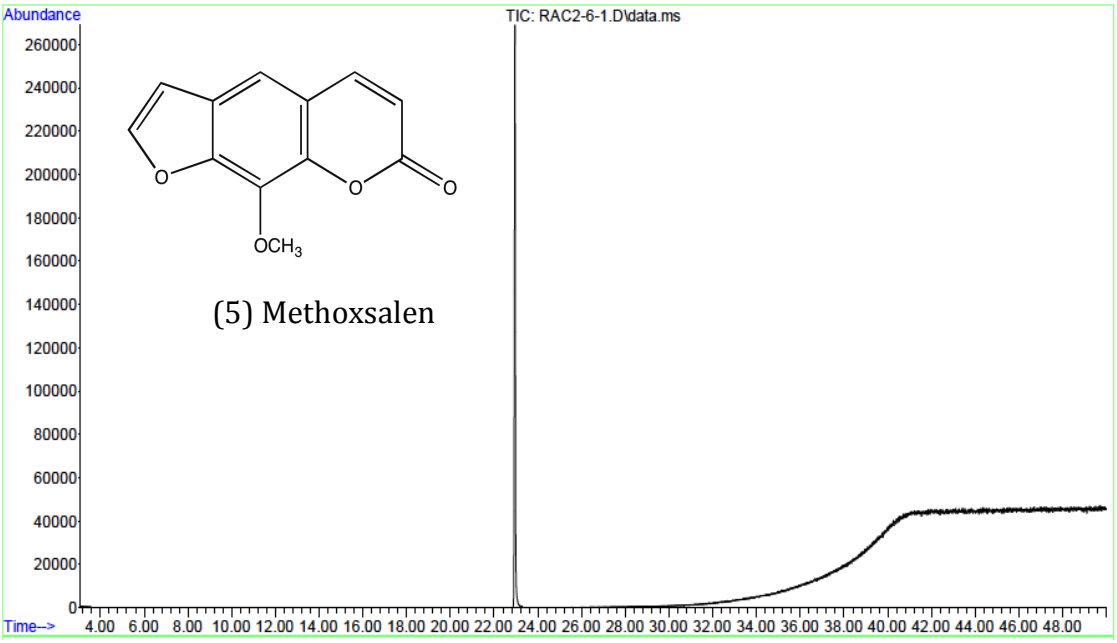

(b)

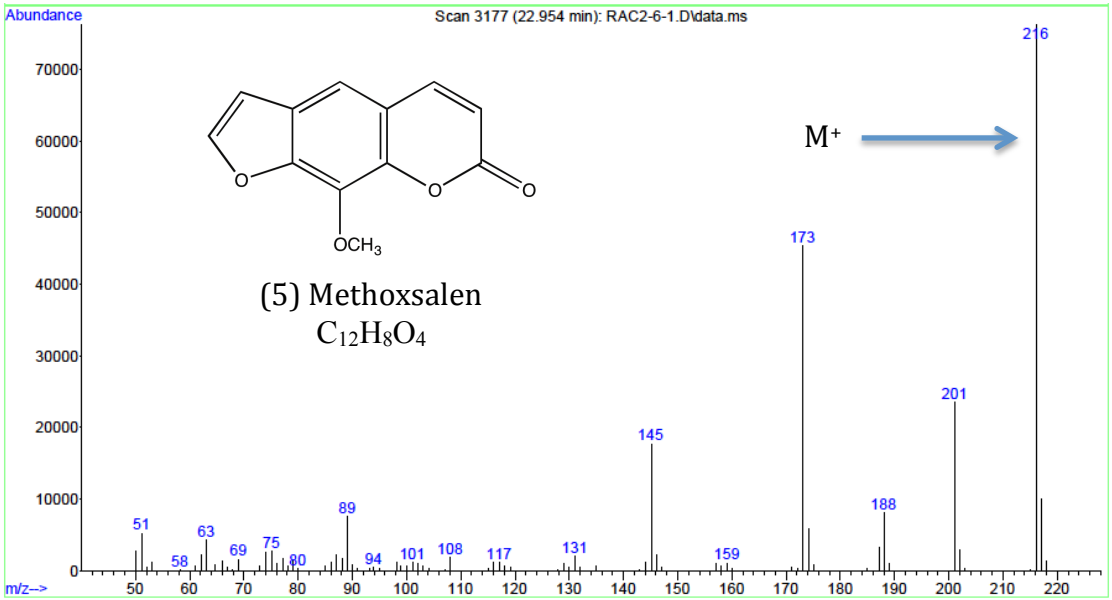

Figure 4.6: GC-MS analysis of methoxsalen (a) Total ion chromatogram (b) Mass spectrum

Methoxsalen, ($C_{12}H_8O_4$), yellowish oil, EIMS *m/z* (% intensity), 216 ($[M]^+$,100), 201 ($[M-Me]^+$, 35), 188 ($[M-CO]^+$,14), 173 ($[188-CO]^+$, 54) and 145 ($[173-CO]^+$, 21). The data obtained was consistent with the mass spectral data of methoxsalen from NIST webbook.

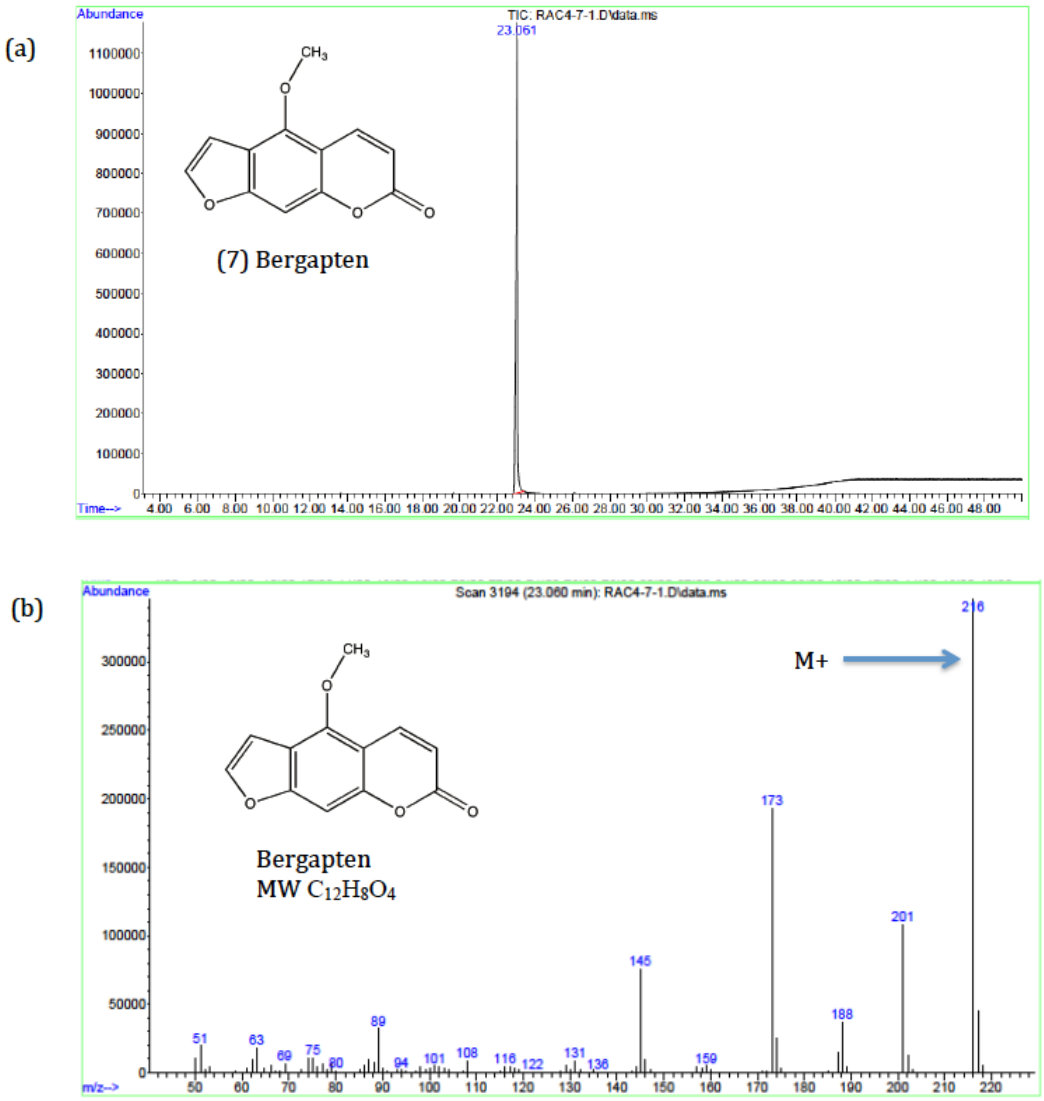

Figure 4.7: GC-MS analysis of bergapten (a) Total ion chromatogram (b) Mass spectrum

Bergapten, ($C_{12}H_8O_4$), white powder, EIMS *m/z* (% intensity), 216 ($[M]^+$, 100), 201 ($[M\text{-}Me]^+$, 35), 188 ($[M\text{-}CO]^+$, 15), 173 ($[M\text{-}Me\text{-}CO]^+$, 64) and 145 ($[M\text{-}Me\text{-}CO\text{-}CO)]^+$, 21). The data obtained was consistent with published data (Orlita , Sidwa ‐ Gorycka , Paszkiewicz , et al., 2008).

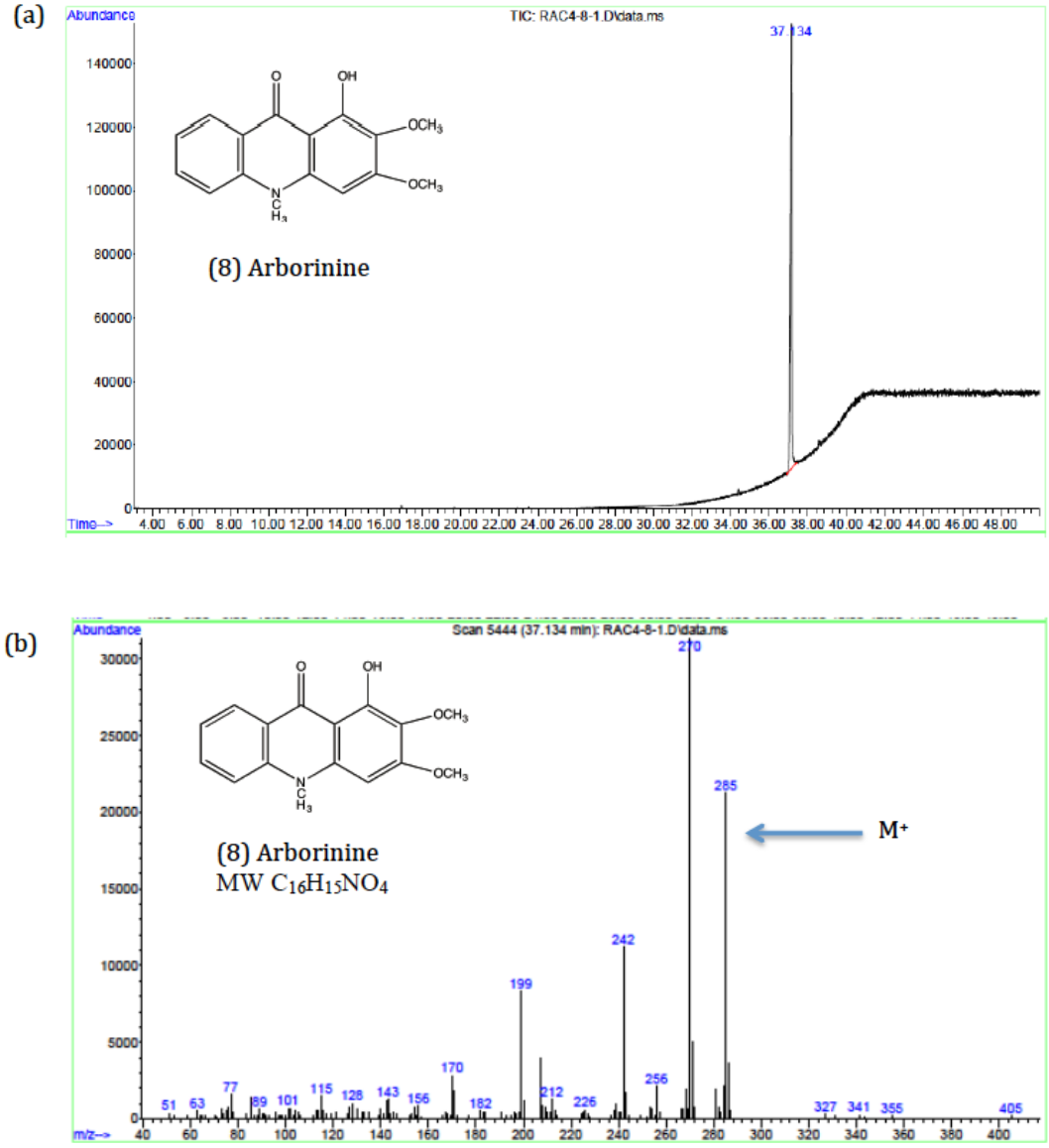

Figure 4.8: GC-MS analysis of arborinine (a) Total ion chromatogram (b) Mass spectrum

Arborinine, ($C_{16}H_{15}NO_4$), yellow crystal, EIMS *m/z* (% intensity), 285 ($[M]^+$, 66), 270 ($[M\text{-}Me]^+$, 100), 242 ($[M\text{-}Me\text{-}CO]^+$, 49). The mass spectra was in agreement with published data (Orlita , Sidwa ‐ Gorycka , Kumirska , et al., 2008).

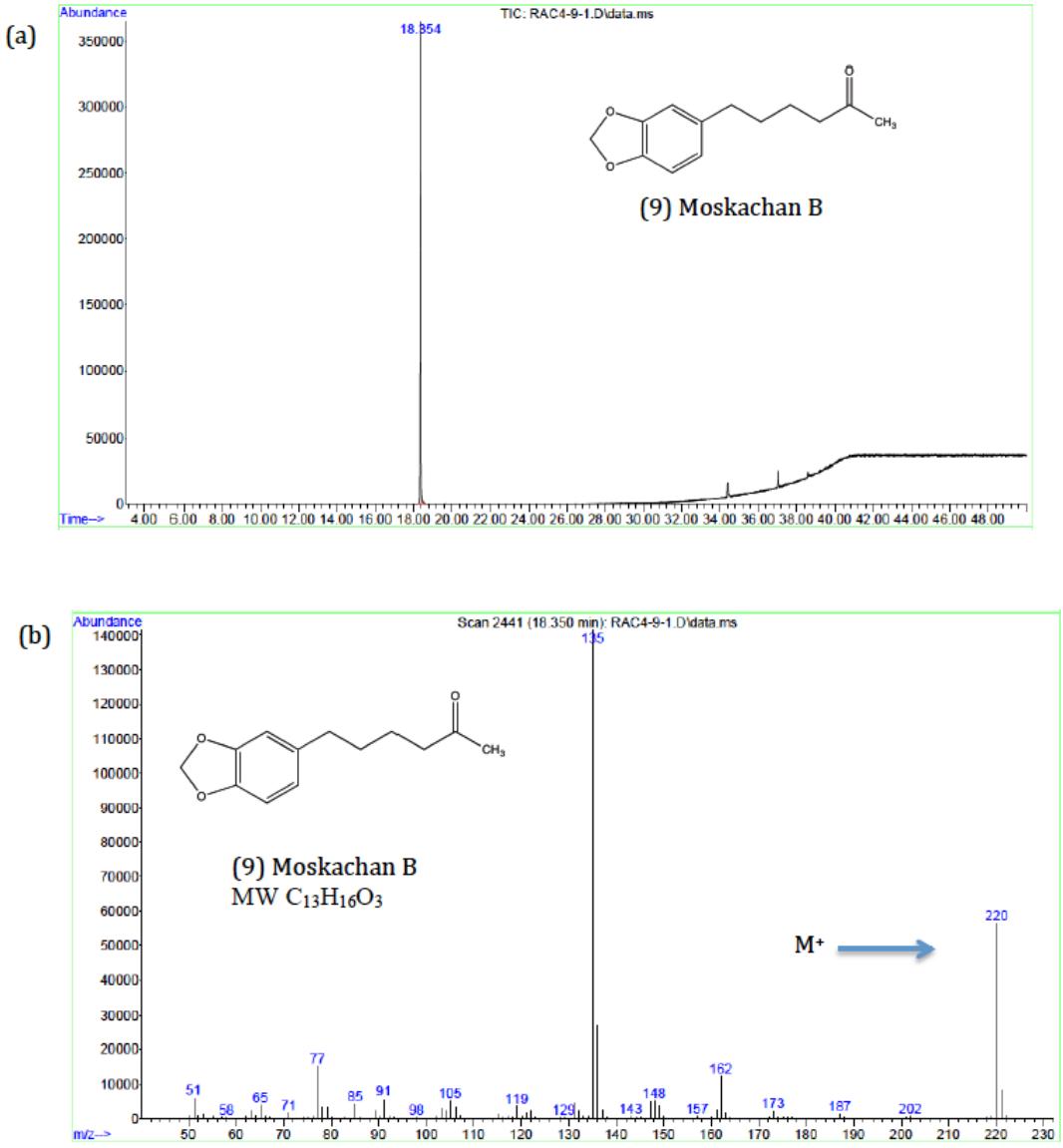

Figure 4.9: GC-MS analysis of moskachan B (a) Total ion chromatogram (b) Mass spectrum

Moskachan B, ($C_{13}H_{16}O_3$), brownish oil, EIMS *m/z* (% intensity), 220 ($[M]^+$, 21), 135 ($[M\text{-}CH_2CH_2CH_2COCH_3]^+$, 100). The mass spectra was in agreement with published data (Del Castillo et al., 1986).

(a)

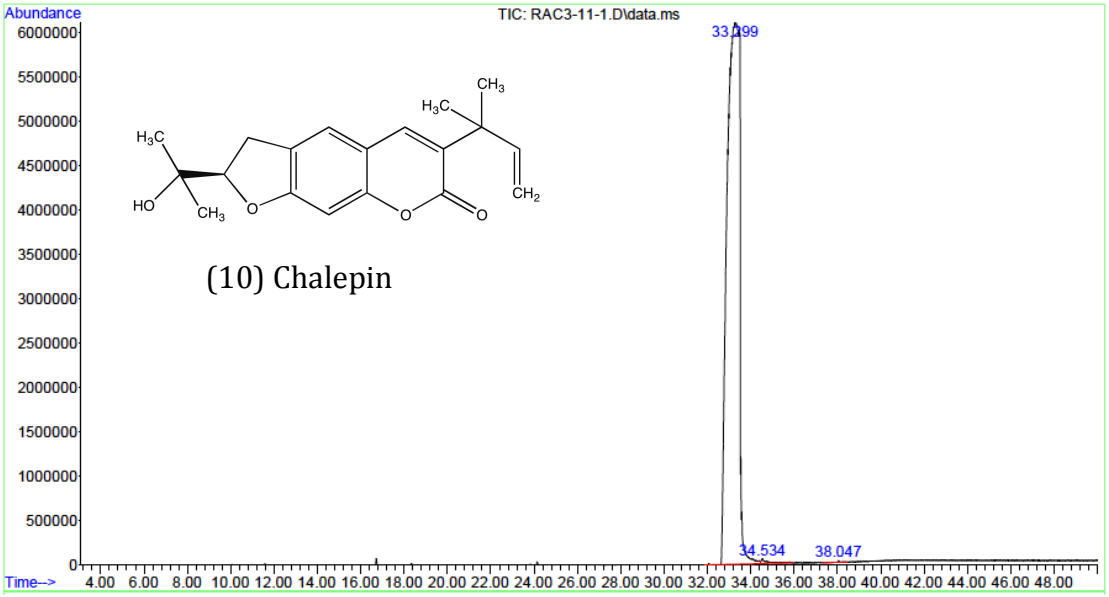

(b)

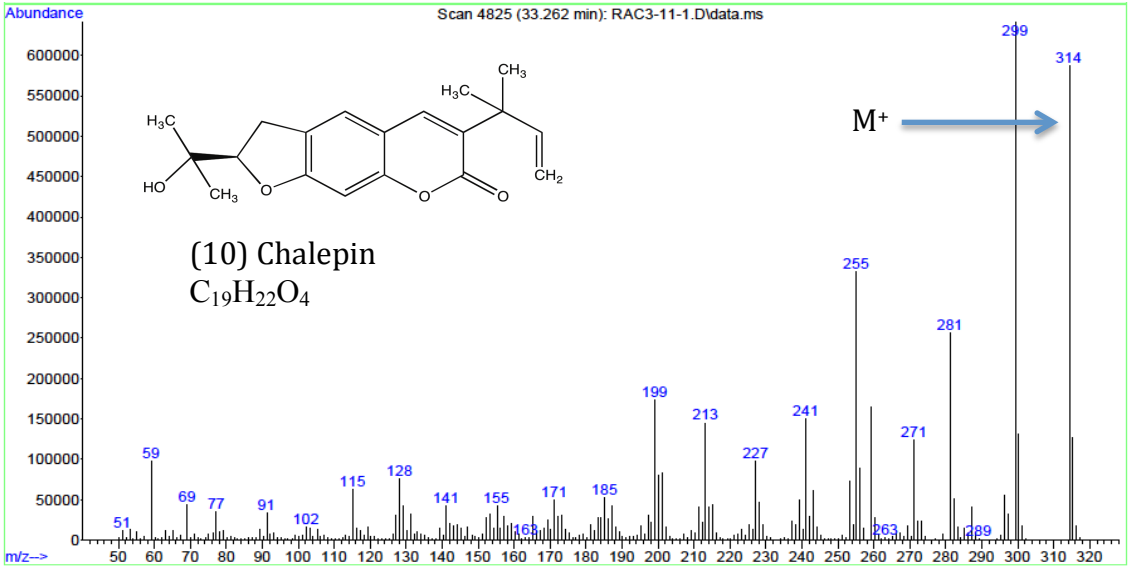

Figure 4.10: GCMS analysis of chalepin (a) Total ion chromatogram (b) Mass spectrum

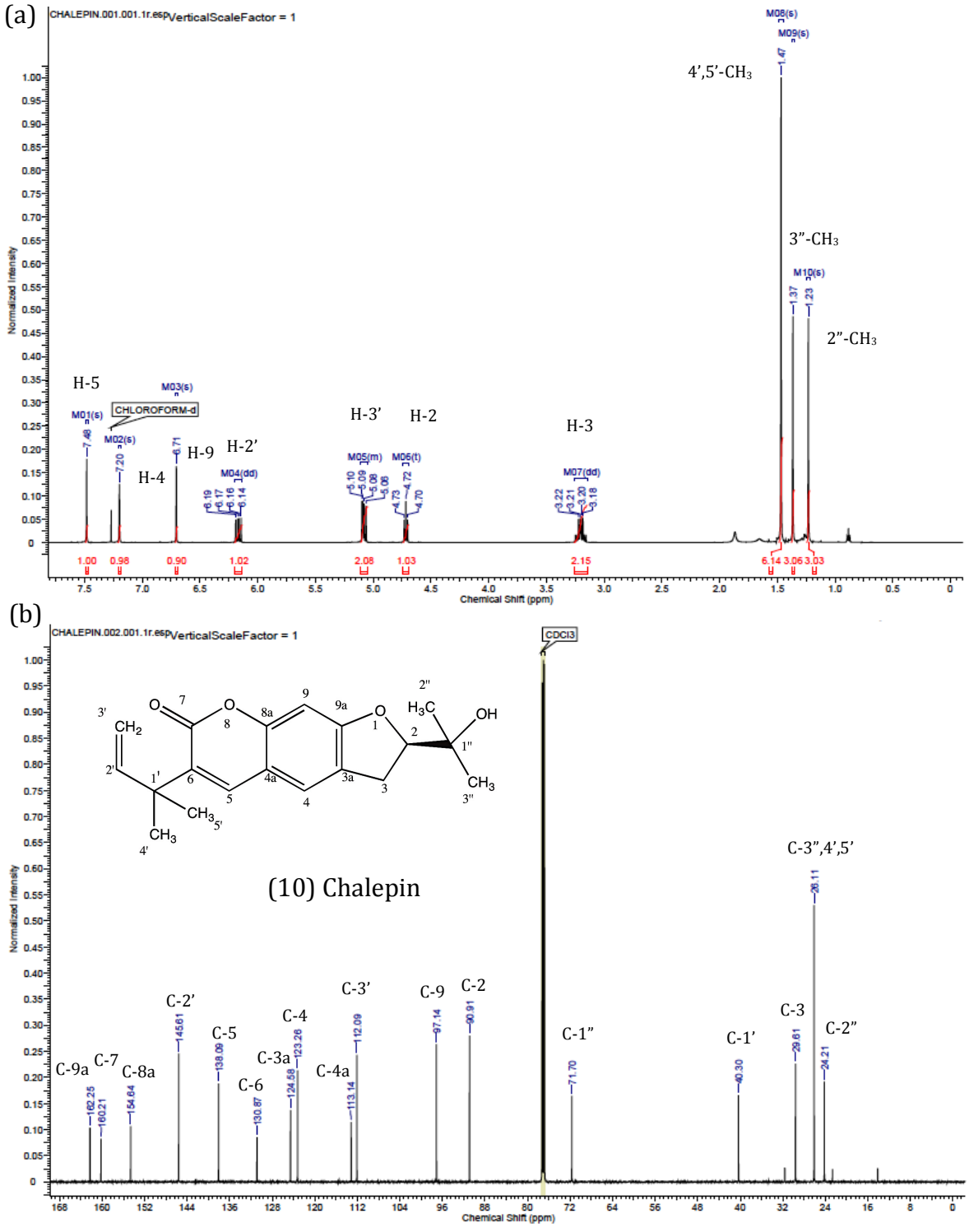

Figure 4.11 : NMR spectra of isolated chalepin. (a) Proton (^{1}H) NMR spectrum and (b) ^{13}C NMR spectrum

Chalepin, ($C_{19}H_{22}O_4$), white crystals, EIMS *m/z* (% intensity), 314 ($[M]^+$, 88), 299 ($[M\text{-}Me]^+$, 100), 281 ($[M\text{-}Me\text{-}H_2O]^+$, 34) and 255 ($[M\text{-}(CH_3)_2COH]^+$. The mass spectral data in the present study corresponds to the data reported in a published data (Orlita , Sidwa ‐ Gorycka , Paszkiewicz , et al., 2008). The GCMS analysis of chalepin is shown in Figure 4.10. ^1H NMR data (600 MHz, $CDCl_3$): δ 7.48 (1H, *s*, H-5), δ 7.20 (1H, *s*, H-4), δ 6.71 (1H, *s*, H-9), δ 6.17 (1H, *dd*, J = 18.00, 12.00 Hz, H-2'), δ 5.09 (2H, overlapping *dd*, H-3'), δ 4.72 (1H, *t*, J = 9.00 Hz, H-2), δ 3.21 (2H, overlapping *dd*, J= 18.00, 12.00, 6.00 Hz, H-3), δ 1.47 (6H, *s*, 4',5'-CH_3), δ 1.37 (3H, *s*, 3"-CH_3), δ 1.23 (3H, *s*, 2"-CH_3). The ^{13}C NMR data (600 MHz, $CDCl_3$): δ 162.25 (C-9a), δ 160.21 (C-7), δ 154.64 (C-8a), δ 145.61 (C-2'), δ 138.09 (C-5), δ 130.87 (C-6), δ 124.58 (C-3a), δ 123.26 (C-4), δ 113.14 (C-4a), δ 112.09 (C-3'), δ 97.14 (C-9), δ 90.91 (C-2), δ 71.70 (C-1"), δ 40.30 (C-1'), δ 29.61 (C-3), δ 26.11 (C-3",4',5'), δ 24.21 (C-2"). The NMR spectra of isolated chalepin is shown in Figure 4.11.

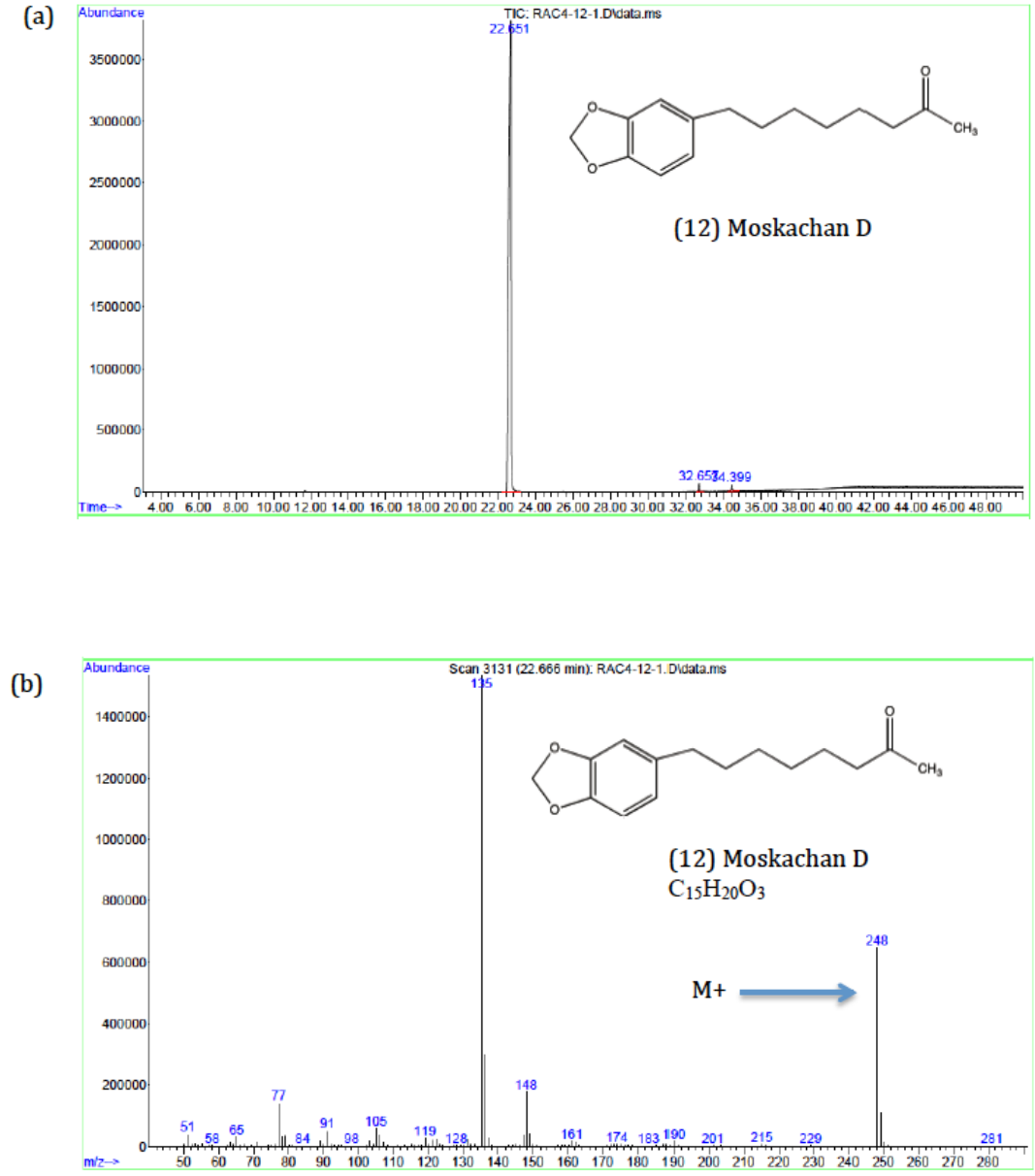

Figure 4.12: GC-MS analysis of moskachan D (a) Total ion chromatogram (b) Mass spectrum

Moskachan D, ($C_{15}H_{20}O_3$) yellowish oil, EIMS *m/z* (% intensity), 248 ($[M]^+$, 30), 148 ($[M\text{-}CH_2\text{-}CH_2\text{-}CH_2\text{-}CH_2\text{-}COCH_3]^+$, 15), 135 ($[M\text{-}CH_2\text{-}CH_2\text{-}CH_2\text{-}CH_2\text{-}COCH_3\text{-}CH]^+$,100),91($[M\text{-}CH_2\text{-}CH_2\text{-}CH_2\text{-}CH_2\text{-}COCH_3\text{-}CH\text{-}COO]^+$,3), 77($[C_6H_5]^+$, 11). The obtained data is consistent with published data (Del Castillo et al., 1986).

(a)

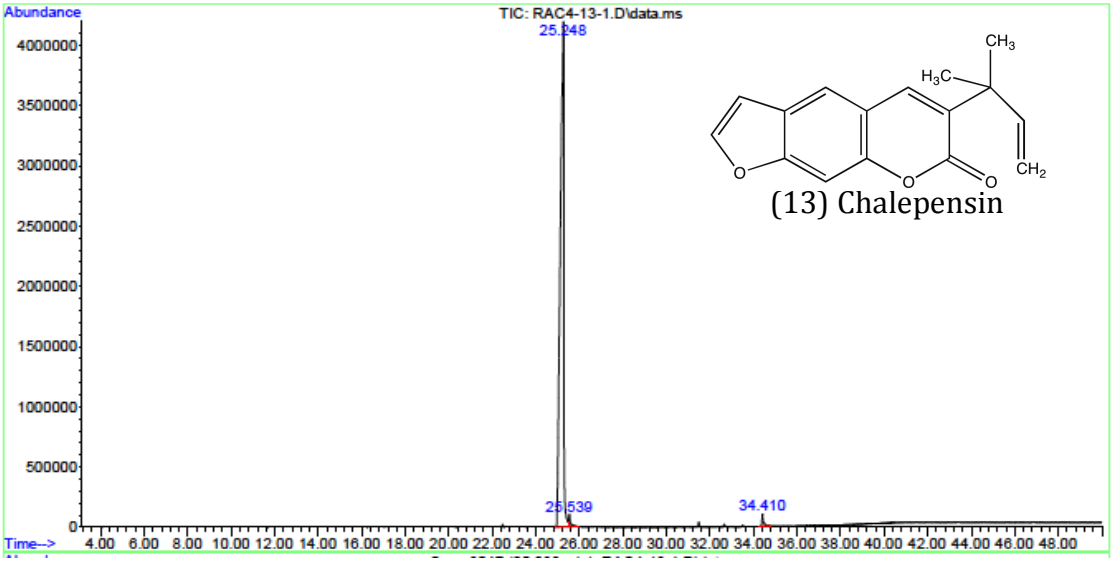

(b)

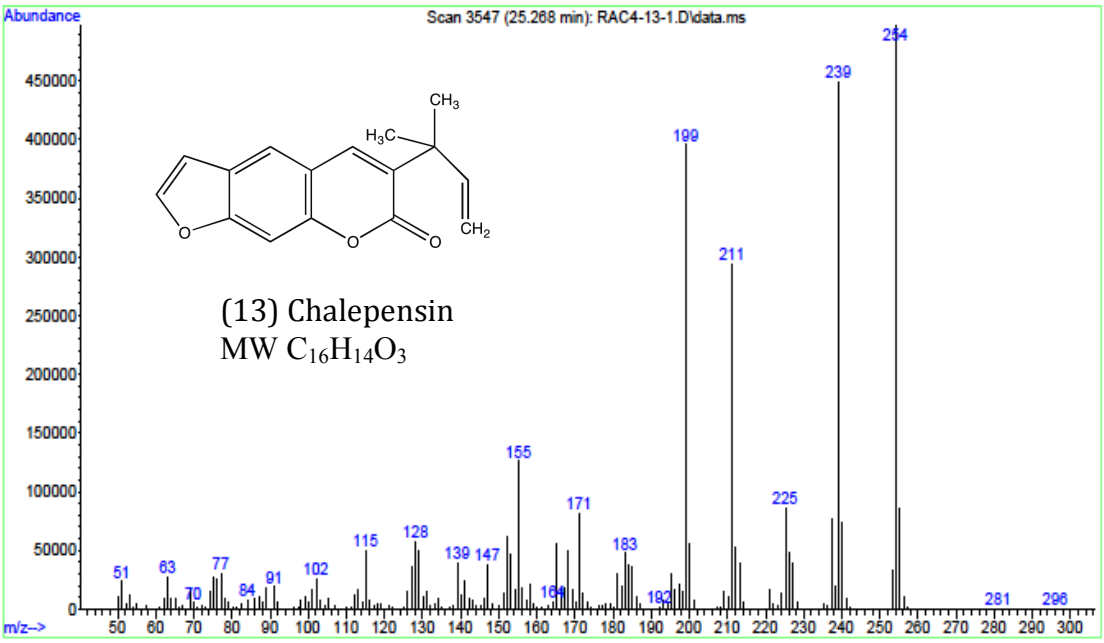

Figure 4.13: GC-MS analysis of chalepensin (a) Total ion chromatogram (b) Mass spectrum

Chalepensin, ($C_{16}H_{14}O_3$), yellowish solid, EIMS *m/z* (% intensity), 254 ($[M]^+$, 100), 239 ($[M\text{-}CH_3]^+$, 95), 211 ($[M\text{-}CH_3\text{-}CH\text{-}CH_3]^+$, 70), 199 ($[M\text{-}CH_3\text{-}CH\text{-}CH3\text{-}C]^+$, 85). The mass spectra is in agreement with published data (Wu et al., 2003).

(a)

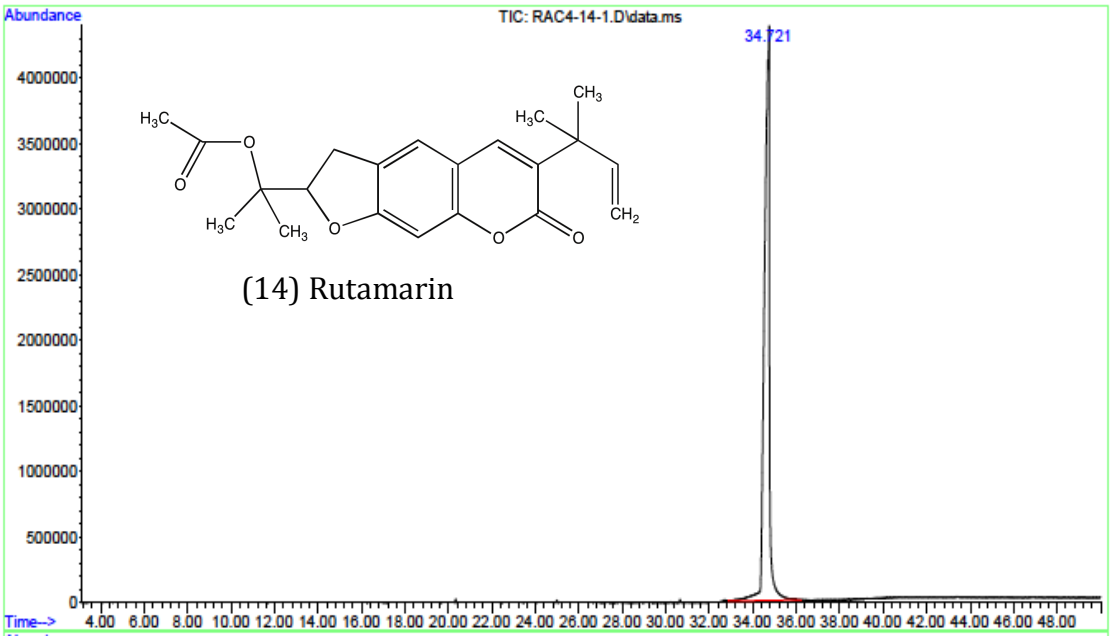

(b)

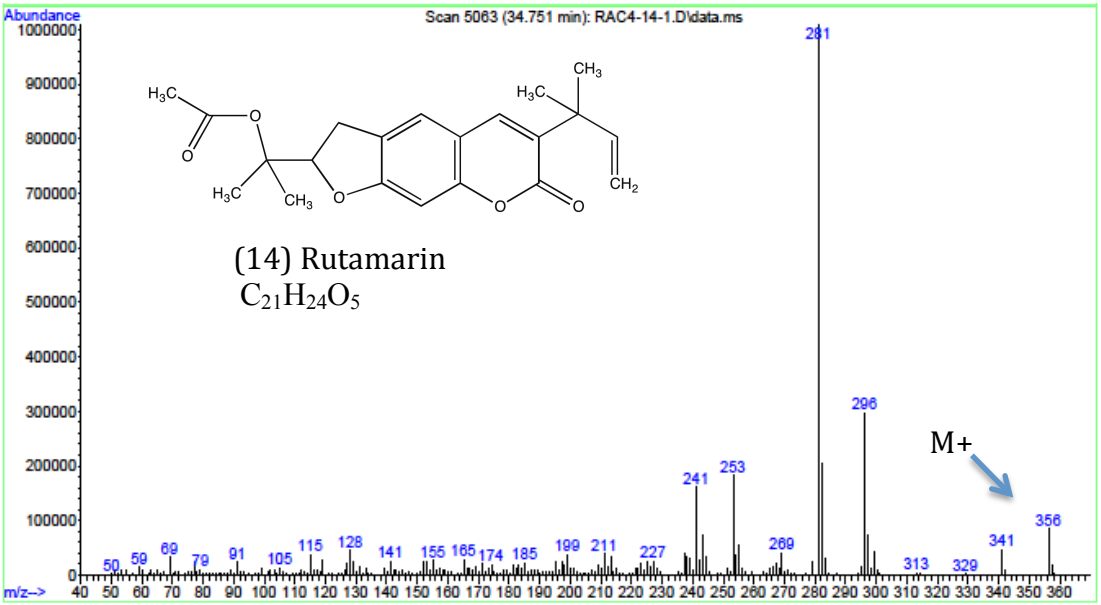

Figure 4.14: GC-MS analysis of rutamarin (a) Total ion chromatogram (b) Mass spectrum

Rutamarin, ($C_{21}H_{24}O_5$), colorless crystals, EIMS *m/z* (% intensity), 356 ($[M]^+$, 8), 341 ($[M\text{-}CH_3]^+$, 4), 296 ($[M\text{-}CH_3\text{-}COO]^+$, 19), 281 ($[M\text{-}CH_3\text{-}COO\text{-}CH_3]^+$, 100), 253 ($[M\text{-}CH_3\text{-}COO\text{-}CH_3\text{-}CO]^+$, 14). The mass spectral data is in agreement with published data (Wu et al., 2003).

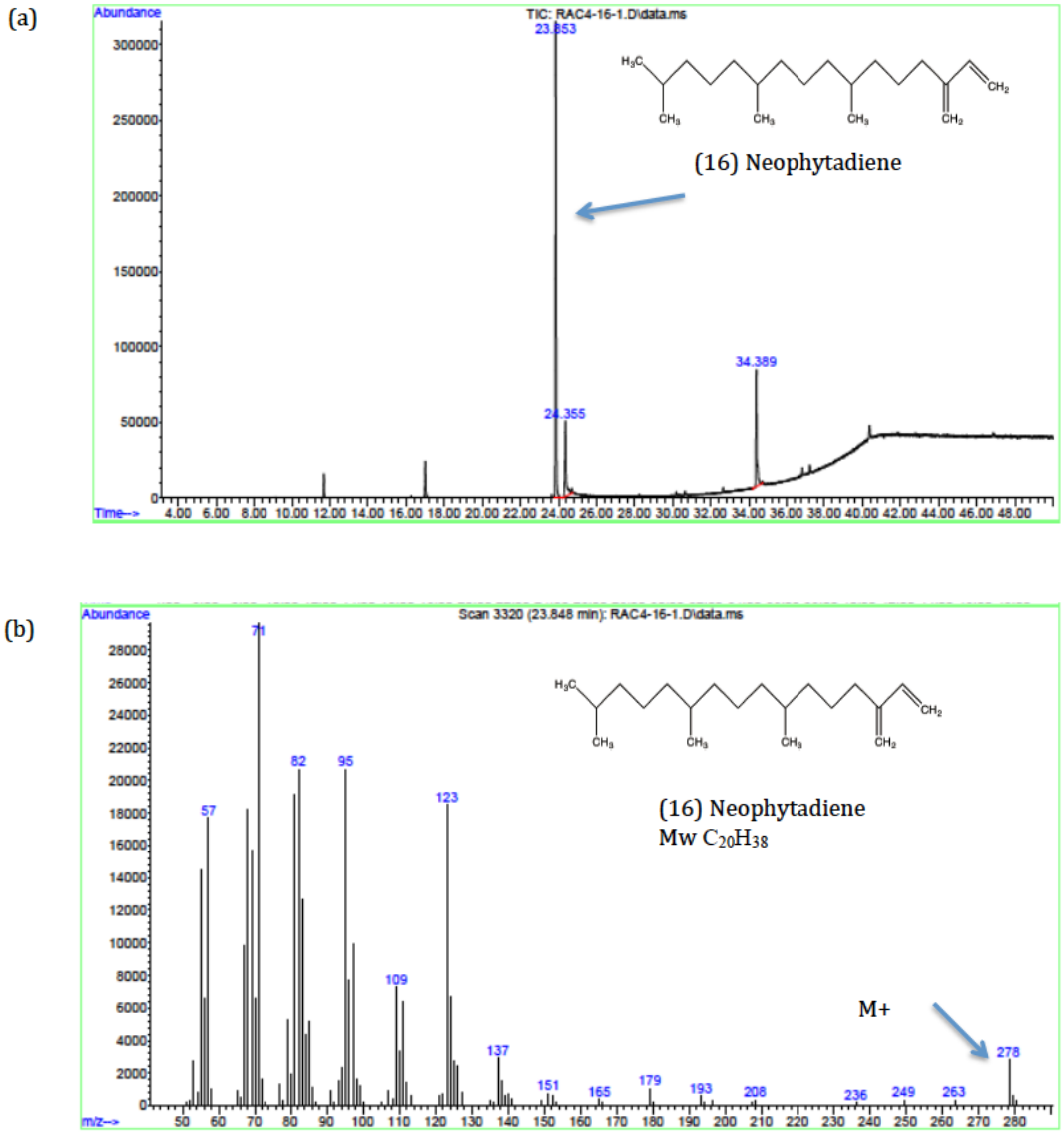

Figure 4.15: GC-MS analysis of neophytadiene (a) Total ion chromatogram (b) Mass spectrum

Neophytadiene, ($C_{20}H_{38}$), light yellow oil, EIMS *m/z* (% intensity), 278 ($[M]^+$, 15), 137 (14), 123 (68), 109 (42), 95 (71), 82 (70) and 71 (100). The mass spectral from GCMS analysis is identified through comparison with NIST MS Library data.

Table 4.4: Identified isolated chemical compounds using GC-MS

Peak No.	Compounds	Molecular Weight	Molecular Formula	Retention Time (s)
1	Graveoline	279	$C_{17}H_{13}NO_3$	39.22
2	Unidentified	-	-	-
3	Psoralen	186	$C_{11}H_6O_3$	18.46
4	Kokusaginine	259	$C_{14}H_{13}NO_4$	29.98
5	Methoxsalen	216	$C_{12}H_8O_4$	22.54
6	Unidentified	-	-	-
7	Bergapten	216	$C_{12}H_8O_4$	23.06
8	Arborinine	285	$C_{16}H_{15}NO_4$	37.13
9	Moskachan B	220	$C_{13}H_{16}O_3$	18.35
10	Chalepin	314	$C_{19}H_{22}O_4$	33.26
11	Unidentified	-	-	-
12	Moskachan D	248	$C_{15}H_{20}O_3$	22.65
13	Chalepensin	254	$C_{16}H_{14}O_3$	25.65
14	Rutamarin	356	$C_{21}H_{24}O_5$	34.72
15	Unidentified	-	-	-
16	Neophytadiene	278	$C_{20}H_{38}$	23.85
17	Unidentified	-	-	-
18	Mixture of acids, Stigmasterol and Vitamin E	-	-	-
19	9,12,15-octadecatrienoic acid, Vitamin E, **γ**-sitosterol	-	-	-
20	12-docosenamide	-	-	-

TLC Analysis on the Isolated Compound Chalepin

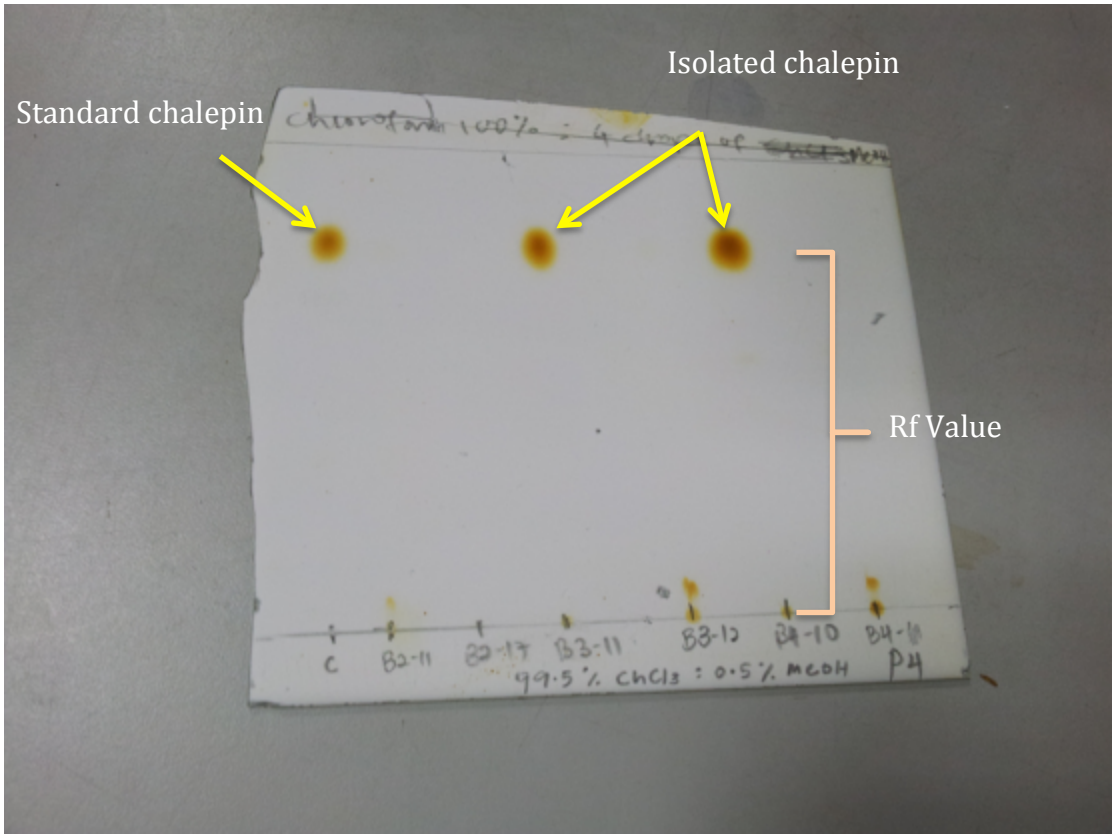

Figure 4.16: TLC analysis on isolated chalepin with comparison with a standard chalepin.

TLC was done to confirm the purity and identity of the major compound, chalepin. A comparison was done with the identified standard chalepin. The Rf value of the isolated compound was found to be same with the Rf value of the identified standard. This further confirms the identity of the compound isolated to be chalepin.

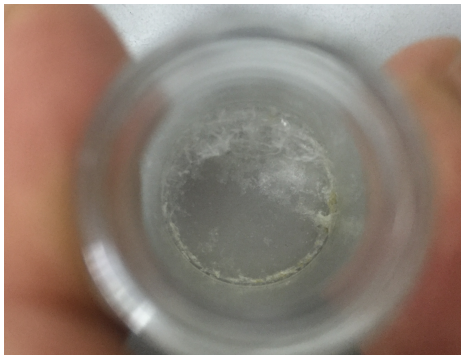

Figure 4.17: Morphology of isolated chalepin crystals

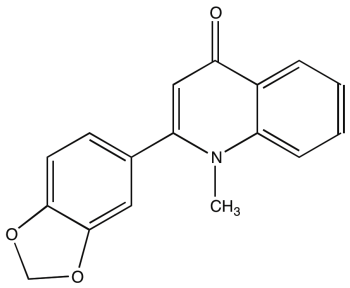

(1) Graveoline
(white powder)

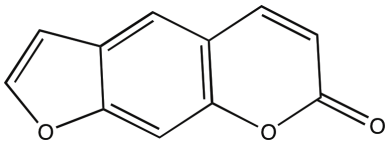

(3) Psoralen
(yellowish powder)

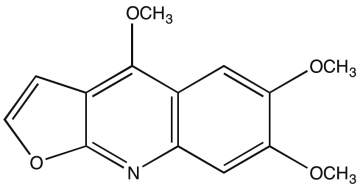

(4) Kokusaginine
(white crystals)

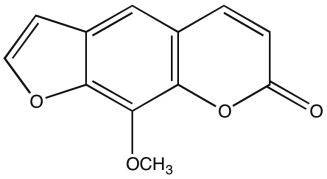

(5) Methoxsalen
(yellow oil)

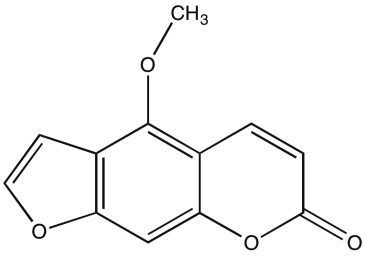

(7) Bergapten
(white powder)

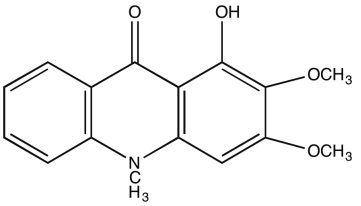

(8) Arborinine
(yellow solid)

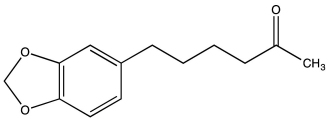

(9) Moskachan B
(brownish oil)

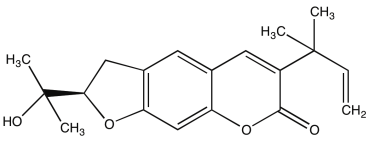

(10) Chalepin
(yellowish solid)

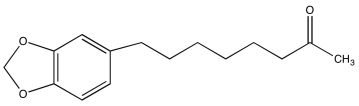

(12) Moskachan D
(orange colored oil)

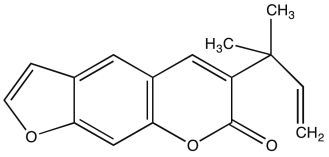

(13) Chalepensin
(yellowish solid)

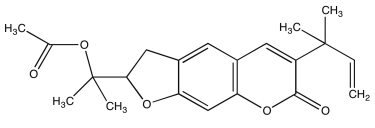

(14) Rutamarin
(yellow oil)

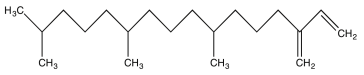

(16) Neophytadiene
(light yellow oil)

Figure 4.18: Chemical structures of isolated compounds from chloroform extract of *R. angustifolia.*

Table 4.5: Classification of compounds isolated and identified from chloroform extract of *R. angustifolia* (without chlorophyll) to its functional group

Classification of Isolated Compounds	
Alkaloids	Arborinine
	Kokusaginine
	Moskachan B and Moskachan D
	Graveoline
Furanocoumarins	Bergapten
	Psoralen
	Methoxsalen
Dihydrofuranocoumarins	Chalepin
	Rutamarin
	Chalepensin

4.4 Cytotoxicity of Isolated Compounds

A total of ten (10) isolated compounds that had sufficient amount for further testing such as moskachan D, bergapten, moskachan B, neophytadiene, graveoline, kokusaginine, chalepin, chalepensin, arborinine and rutamarin were tested for their cytotoxicity effect against A549 human lung carcinoma cells and the normal human lung fibroblasts MRC5 cells. Results showed that the cytotoxicity effect against A549 cell was dose and time dependent. Chalepin exhibited the highest cytotoxicity against A549 cell line after 72 hours incubation with a IC_{50} value of 8.69 ± 2.43 µg/ml. It was also mildly toxic to the normal cell line with a IC_{50} value of 23.4 ± 0.6 µg/ml.

Arborinine, chalepensin and also moskachan D also exhibited promising cytotoxic property against A549 cell line with IC_{50} values of 13.1 ± 0.06, 14.0 ± 0.15 and 18.5 ± 0.65 µg/ml respectively. However, arborinine and chalepensin showed moderate toxicity towards MRC5 normal human lung fibroblast cell line with IC_{50} values of 20.8 ± 0.15 and 23.3 ± 0.55 µg/ml respectively. Moskachan D was non-toxic towards normal cell with an IC_{50} value of 90.8 ± 0.8 µg/ml. Other isolated compounds showed no toxicity towards the normal cells with IC_{50} values ranging more than 50.0 µg/ml.

The positive control that was employed in this study is cisplatin. Cisplatin is a commonly used chemotherapeutic drug for the treatment of non-small cell lung carcinoma. It's mode of action is to cause DNA damage in the carcinoma cell and thus induce apoptosis. In our study, cisplatin showed an IC_{50} value of 24.5± 1.8 µg/ml at 72 hours incubation time against A549 cells. However it showed no signs of toxicity towards MRC5 normal lung fibroblast cells. Chalepin (8.69 ± 2.43 µg/ml), arborinine (13.1 ± 0.06 µg/ml), chalepensin (14.0 ± 0.15 µg/ml) and moskachan D (18.5 ± 0.65 µg/ml) showed an IC_{50} value lower as compared to cisplatin. This showed us that these isolated compounds are more potent than the standard cisplatin. Among these isolated compounds, chalepin showed the best cytotoxicity with an IC_{50} value of 8.69 ± 2.43 µg/ml. Chalepin could be a promising chemotherapeutic drug.

(A)

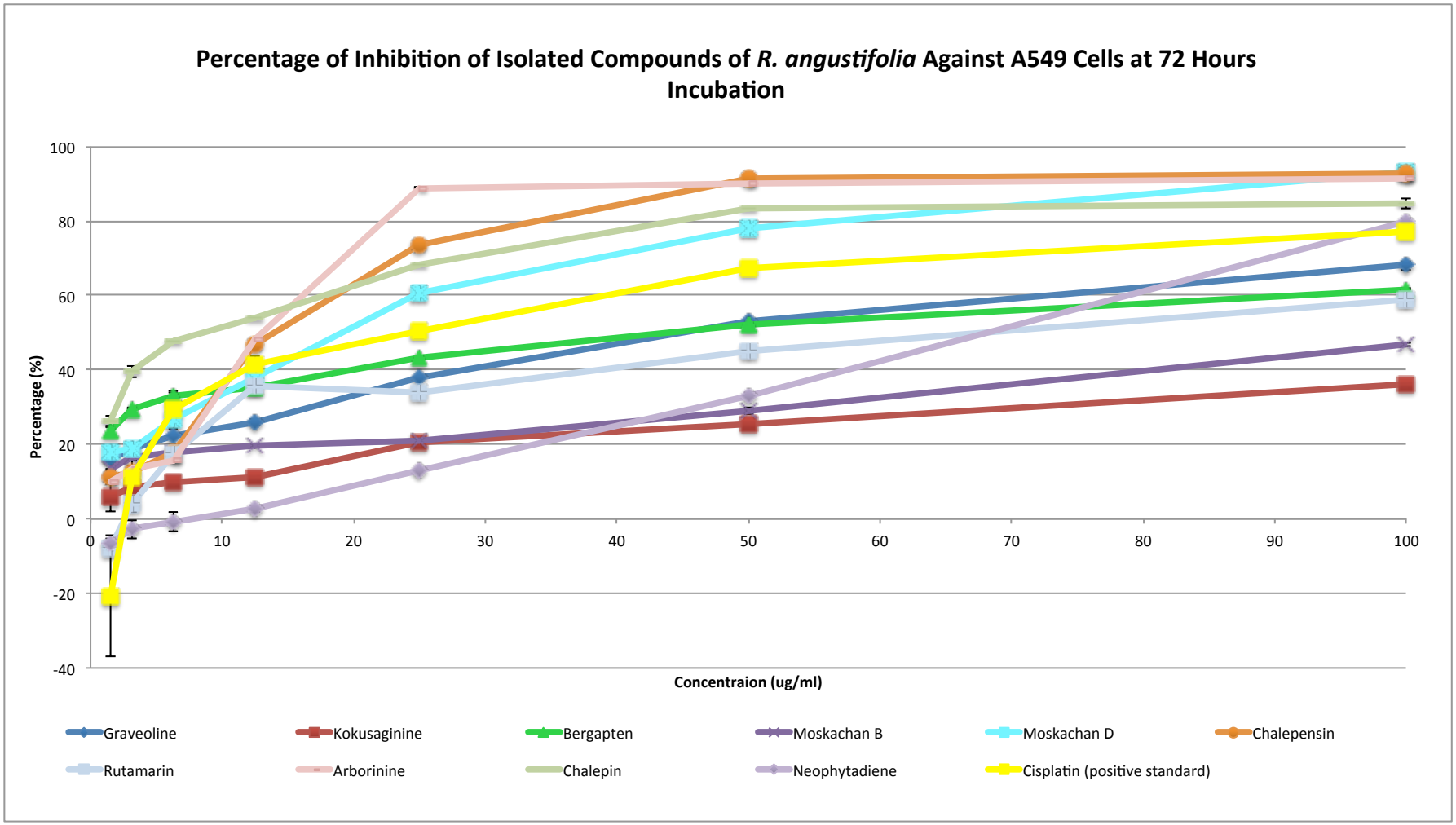

Figure 4.19(A): The percentage of inhibition of isolated compounds of *R. angustifolia* against A549 cell line at 72 hours incubation. The data expressed as mean ± S.D. of three independent replicates (n=3).

(B)

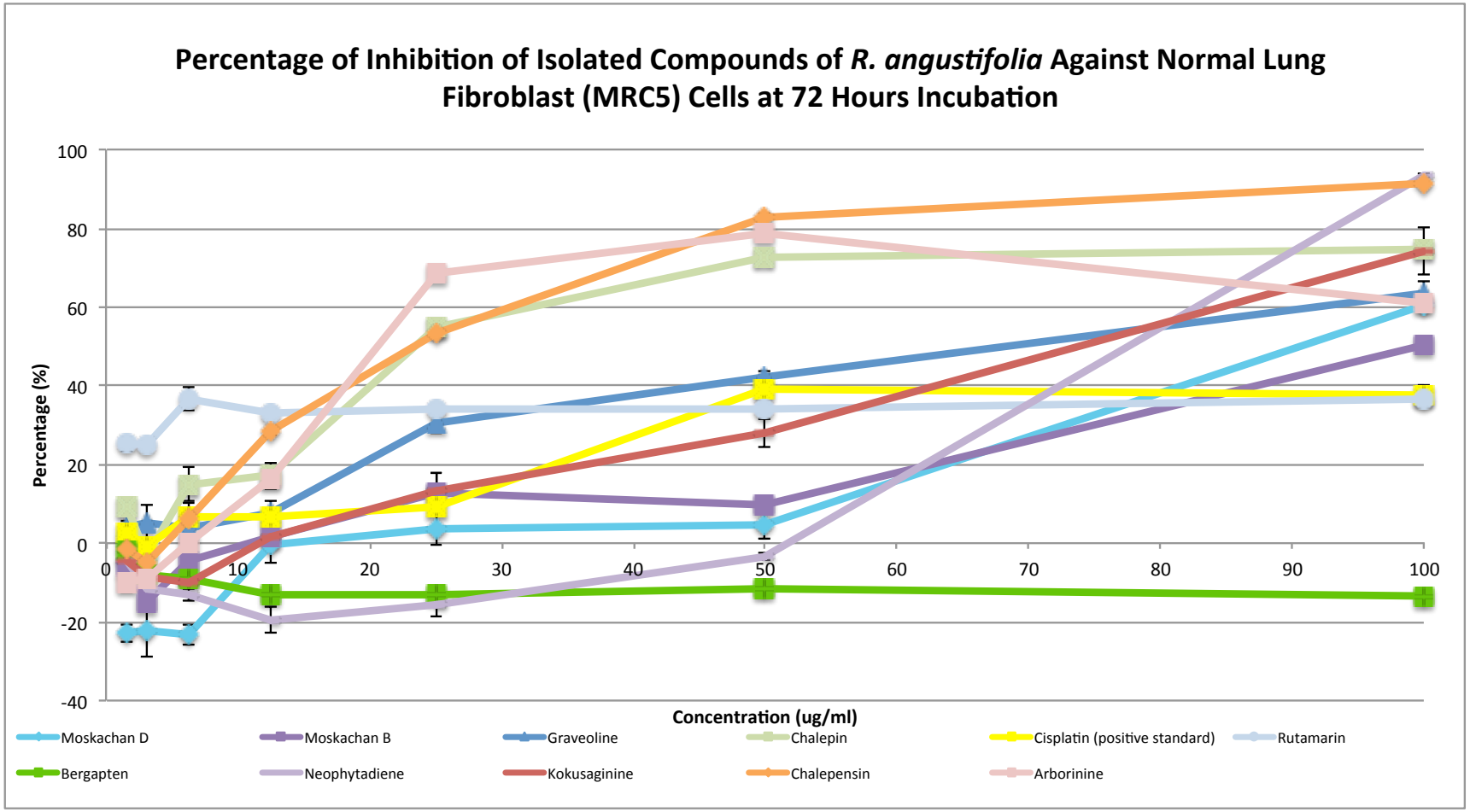

Figure 4.19(B): The percentage of inhibition of isolated compounds of *R. angustifolia* against MRC5 cell line at 72 hours incubation. The data expressed as mean ± S.D. of three independent replicates (n=3).

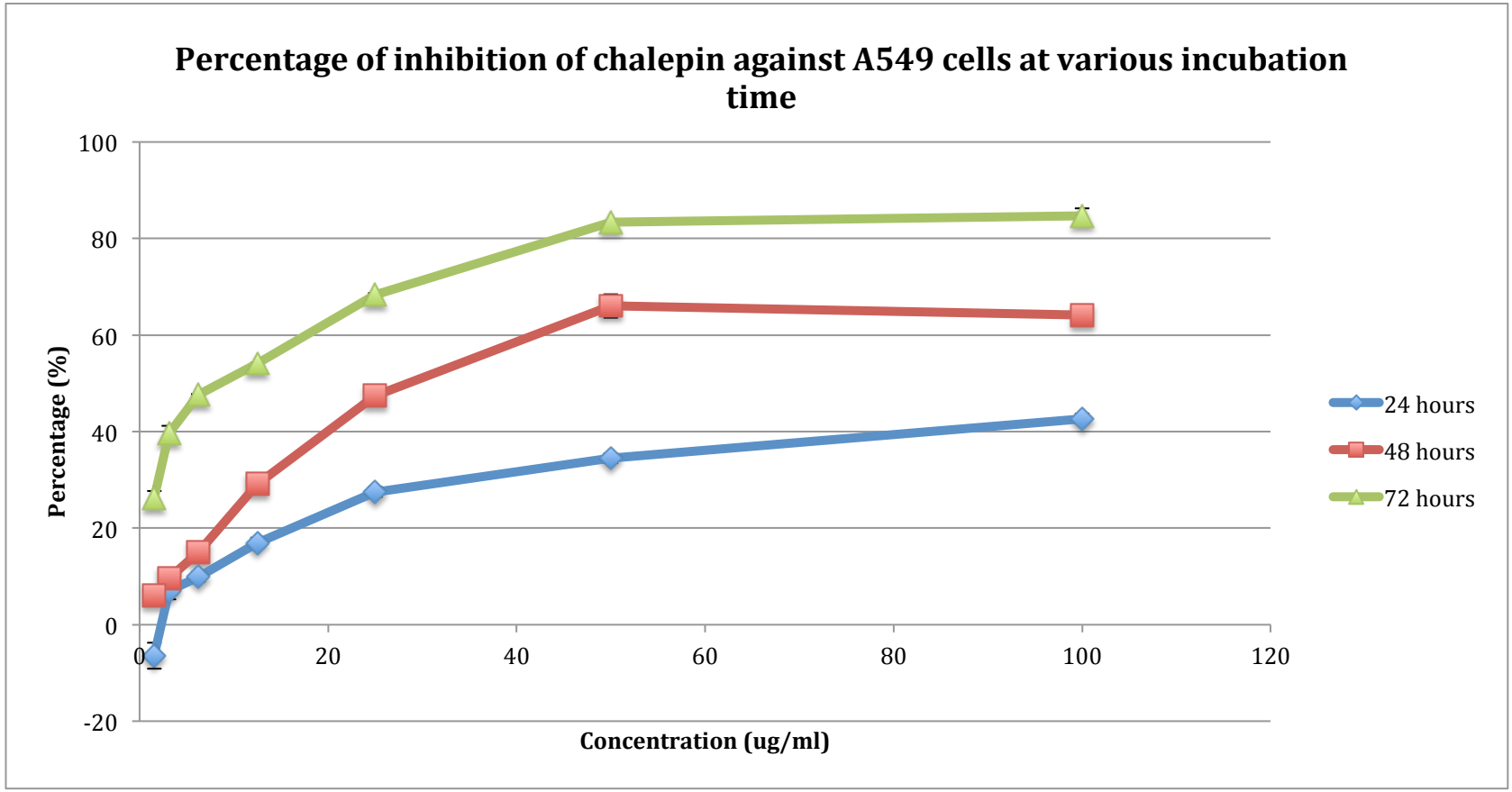

Figure 4.20: The percentage of inhibition of chalepin isolated from *R. angustifolia* against A549 cell line at various incubation times. The data expressed as mean ± S.D. of three independent replicates (n=3).

Table 4.6 : IC_{50} value of isolated compounds against A549 cell lines at 48 and 72 hours incubation and MRC5 cell line at 72 hours treatment.

Isolated Compounds	IC_{50} in µg/ml (µM) (A549)		(MRC5)
	48 hrs	**72 hrs**	**72 hrs**
Graveoline	76.3 ± 2.08 (273.5)	44.6 ± 0.47 (159.9)	69.7 ± 2.5 (249.8)
Kokusaginine	87.4 ± 7.08 (337.5)	>100 (>386.1)	74.8 ± 0.82 (288.8)
Bergapten	>100 (>463.0)	43.53 ± 1.81 (201.5)	>100 (>463.0)
Moskachan B	>100 (>454.5)	>100 (>454.5)	>100 (>454.5)
Moskachan D	77.5 ± 3.0 (312.5)	18.5 ± 0.65 (74.6)	90.8 ± 0.8 (366.1)
Chalepensin	30.5 ± 1.30 (120.1)	14.0 ± 0.15 (55.1)	23.3 ± 0.55 (91.7)
Rutamarin	56.3 ± 1.53 (158.1)	68.5 ± 3.06 (192.4)	>100 (>281.0)
Arborinine	27.7 ± 0.26 (97.2)	13.1 ± 0.06 (46.0)	20.8 ± 0.15 (73.0)
Chalepin	28.3 ± 1.06 (90.1)	**8.69 ± 2.43 (28.0)**	23.4 ± 0.6 (74.5)
Neophytadiene	69.2 ± 1.06 (248.9)	68.00 ± 2.43 (244.6)	77.4 ± 0.98 (278.4)
Cisplatin*	-	24.5± 1.8 (81.67)	>100 (>333.33)

*Cisplatin was used as the positive standard reference. Tabulated values are mean ± standard deviation (SD) of three replicates.

4.5 Criteria for the selection of the isolated compound for further study

The compound chalepin exhibited an IC_{50} value which showed most cytotoxicity towards A549 cells at 72 hours incubation i.e. 8.69 ± 2.43 µg/ml. Chalepin was also found to be the major compound present (6.22%) in the chloroform extract of *R.angustifolia* (Table 4.3). Hence it was selected to be further studied on in the apoptosis analysis and proteomic studies.

4.6 Morphological changes induced by chalepin

4.6.1 Phase contrast microscopy studies

Morphological changes in the A549 cells treated with different concentrations of chalepin were observed using the inverted phase contrast microscope. Typical morphological features of apoptosis such as plasma membrane blebbing, cell vacuolisation, echinoid spiking, chromatin condensation, formation of apoptotic bodies, cell shrinkage, nuclear fragmentation and others were observed. Untreated cells appeared to be thriving healthily in the culture. After 48 hours of incubation, formation of apoptotic bodies and cell vacuolisation were observed whereas after 72 hours, most of the cells were floating and there was a shrinkage and also decrease in the cell number. At 40x magnification, alteration in condensation of chromatin and in shape of cells were observed.

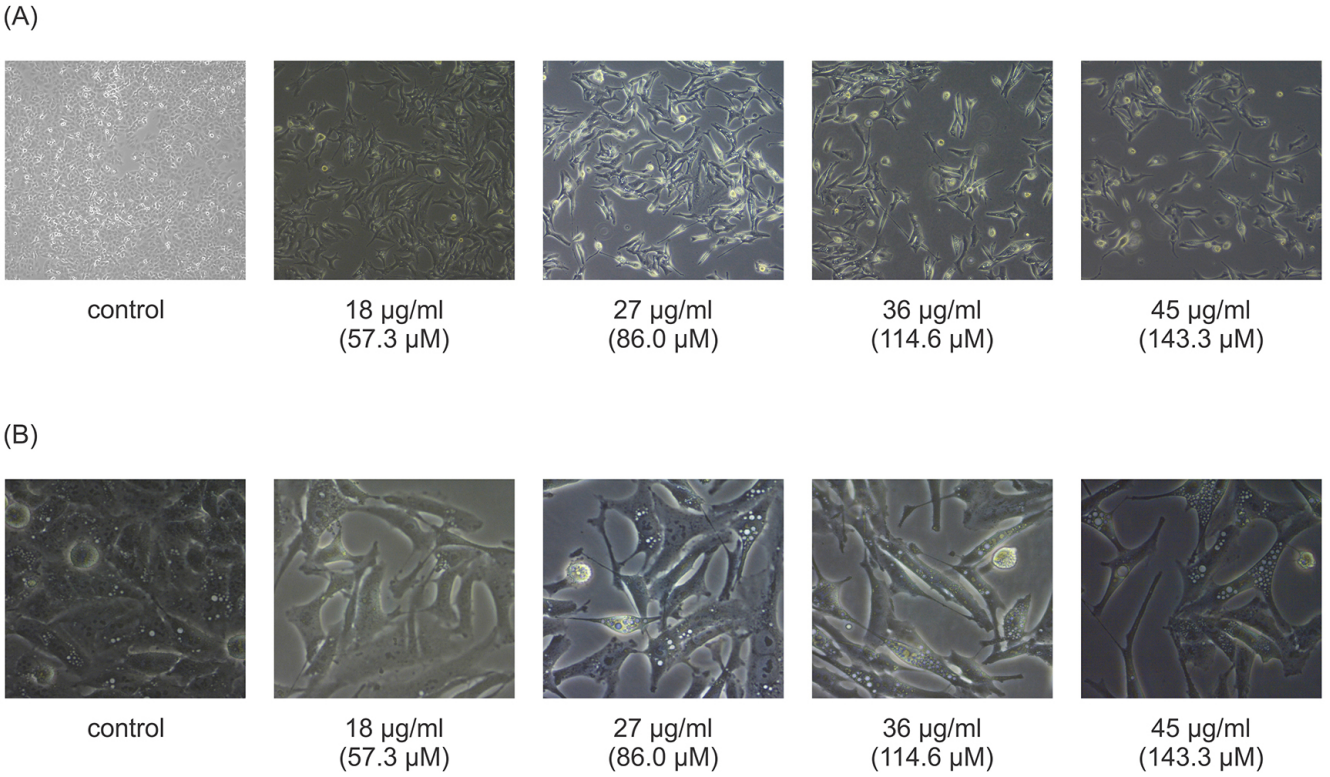

Figure 4.21: Untreated control was compared with A549 cells treated at different doses and time. The morphological changes in the cells were observed under phase-contrast microscopy at 10x and 40x magnification. **(A)** A549 cells treated with different concentrations of chalepin for 48 hours and observed at 10x magnification. **(B)** A549 cells treated with different concentrations of chalepin for 48 hours and observed at 40x magnification.

(C)

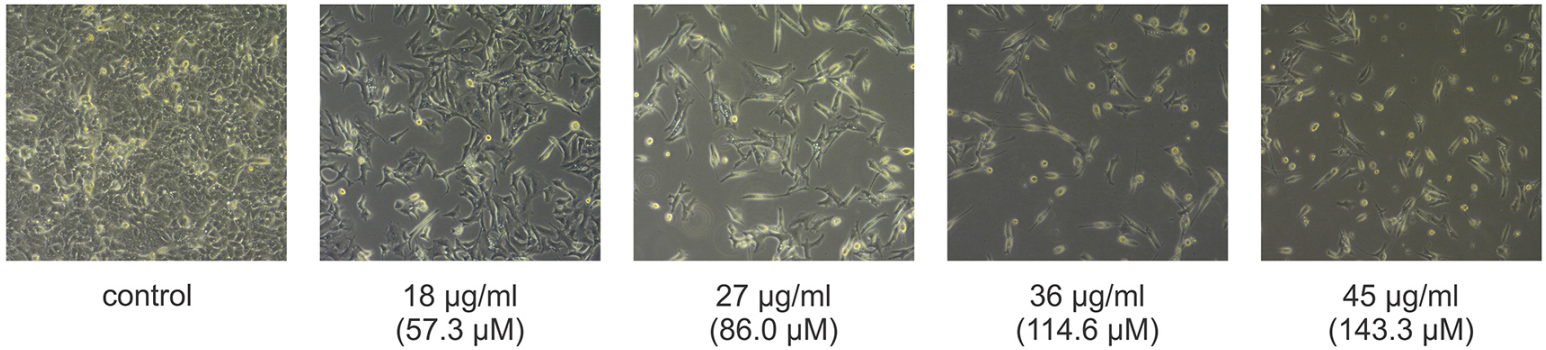

(D)

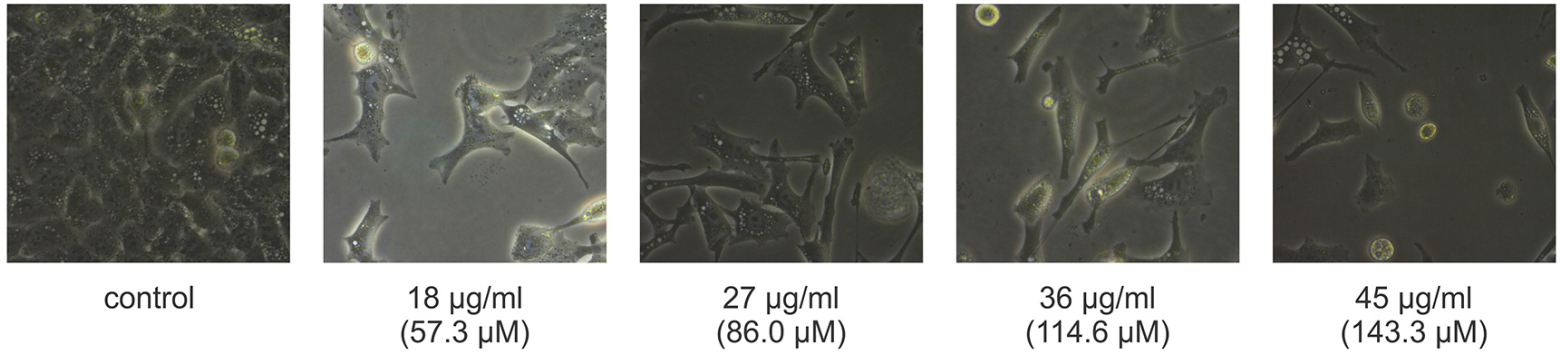

Figure 4.21: Untreated control was compared with A549 cells treated at different doses and time. The morphological changes in the cells were observed under phase-contrast microscopy at 10x and 40x magnification. **(C)** A549 cells treated with different concentrations of chalepin for 72 hours and observed at 10x magnification. **(D)** A549 cells treated with different concentrations of chalepin for 72 hours and observed at 40x magnification. Cells shrinkage, formation of echinoid spikes, vacuolisation, formation of apoptotic bodies and rounding were observed clearly

4.6.2 Hoechst 33342 and PI nuclear staining

The nuclear morphological changes after treatment with chalepin at various concentrations were observed using Hoechst 33342 and propidium iodide (PI) dye, and was observed under a fluorescent microscope. The control showed only low blue color. After treatment of chalepin for 72 hours at various concentrations, observation of cells fluorescing bright blue colored nucleus was observed. The higher the concentration of chalepin, the higher the number of cells that emits a bright blue signal. In a 40x magnification, chromatin condensation and nuclear cleavage were observed. Hoechst 33342 is a dye with small molecules which could pass through the membrane and bind to DNA of apoptotic cells to emit a bright blue fluorescence. At higher concentrations and incubation time, some cells emit pink or red fluorescence. This is due to the factor that some cells have undergone late apoptosis (pink) or necrosis (red) where the nuclear membrane has been compromised and thus enabled the propidium iodide dye to penetrate and stain the nuclear DNA.

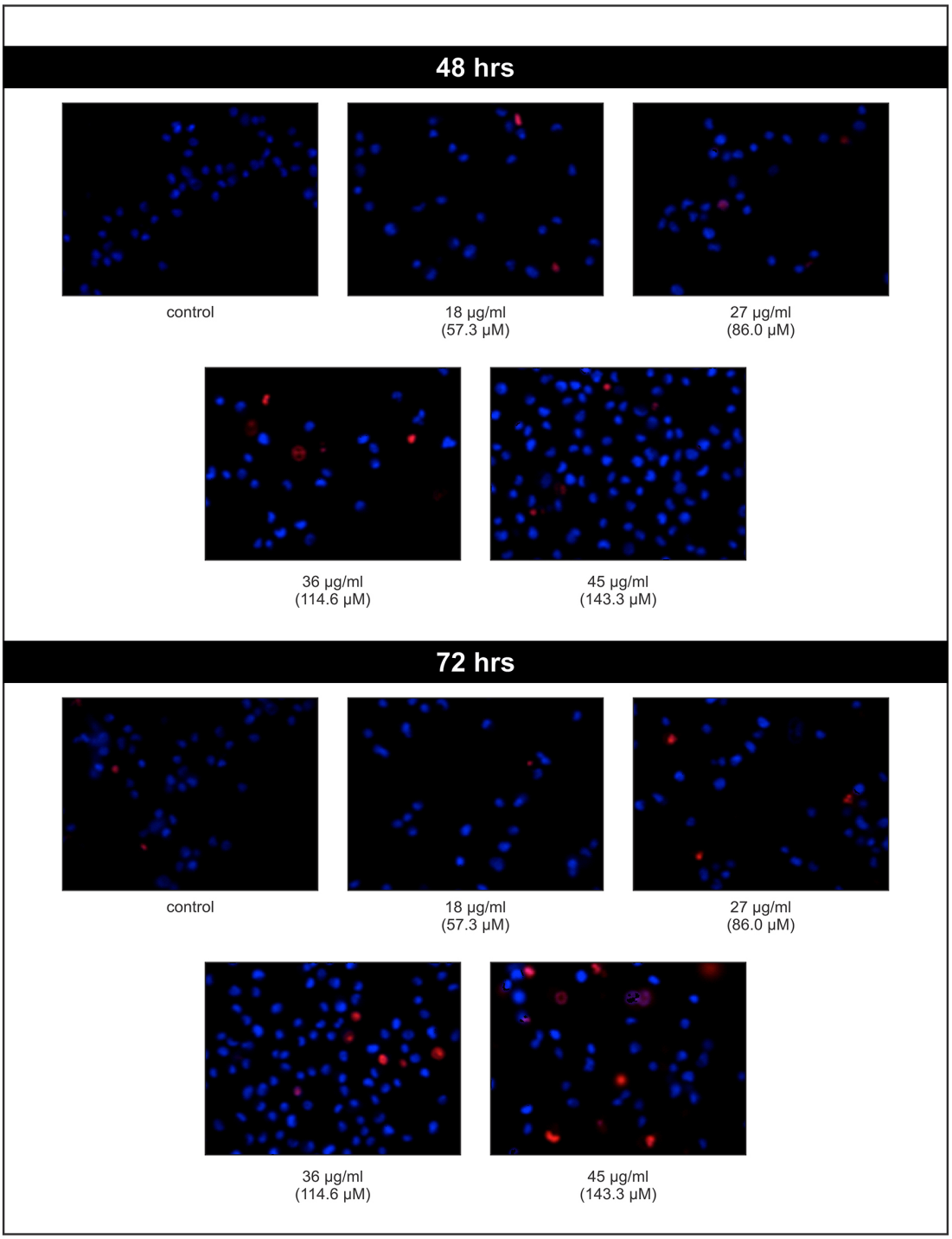

Figure 4.22: Effects of chalepin at different concentrations on nuclear morphological changes of A549 cell line at 48 h and 72 h incubation. After the incubation period, the cells were stained with Hoechst 33342 and PI and were examined with a fluorescent microscope under magnification of 400x to observe the chromatin condensation, nuclear fragmentation and cell shrinkage.

4.7 Biochemical Apoptotic Analysis

4.7.1 Annexin V-FITC/PI apoptotic analysis

The phosphatidylserine (PS) exposure on the outer leaflet of the plasma membrane is a hallmark of apoptosis. Annexin V is a protein which has high affinity for PS. Thus the binding of Annexin V to PS provides a very sentitive method for detecting cellular apoptosis. A population of cells undergoing apoptosis may contain necrotic cells due to their damaged plasma membrane. To distinguish between Annexin V positive apoptotic and necrotic cells, the fluorescent dye propidium iodide was used. Membranes of damaged cells are permeable to propidium iodide. Thus, using Annexin V conjugated to FITC (a fluorescent dye) enables apoptotic cells to be identified and quantified on single cell basis by flow cytometry. In this study, it can be observed that as the treatment concentration of chalepin increased, the density plot showed increase in the cell population at the lower right quadrant (Q1-LR) which represents the early apoptotic cells and also subsequently towards the upper right quadrant (Q1-UR) which represents population of late apoptotic/secondary necrotic cells. Comparison between 48 hours and 72 hours showed that at longer incubation, the cell population in early, late apoptosis/secondary necrosis (upper right quadrant – Q1-UL) increased with dose. But the highest increase was observed in the late apoptosis quadrant represented by upper right quadrant in the density plot. The untreated, control cells which stayed at lower left quadrant (Q1-LL) showed low staining with both annexin V and PI showing viable cells. The total Annexin V positive cells represents a total of early and late apoptotic cells in A549 cells, shows an increase in dose and time dependant manner. The Annexin V positive cells showed an increase from 7.27 ± 0.16 % at 9 µg/ml to 20.6 ± 0.53 % at 45 µg/ml of chalepin. The population of Annexin V positive cells observed was significantly higher after 72 hours incubation.

(A)

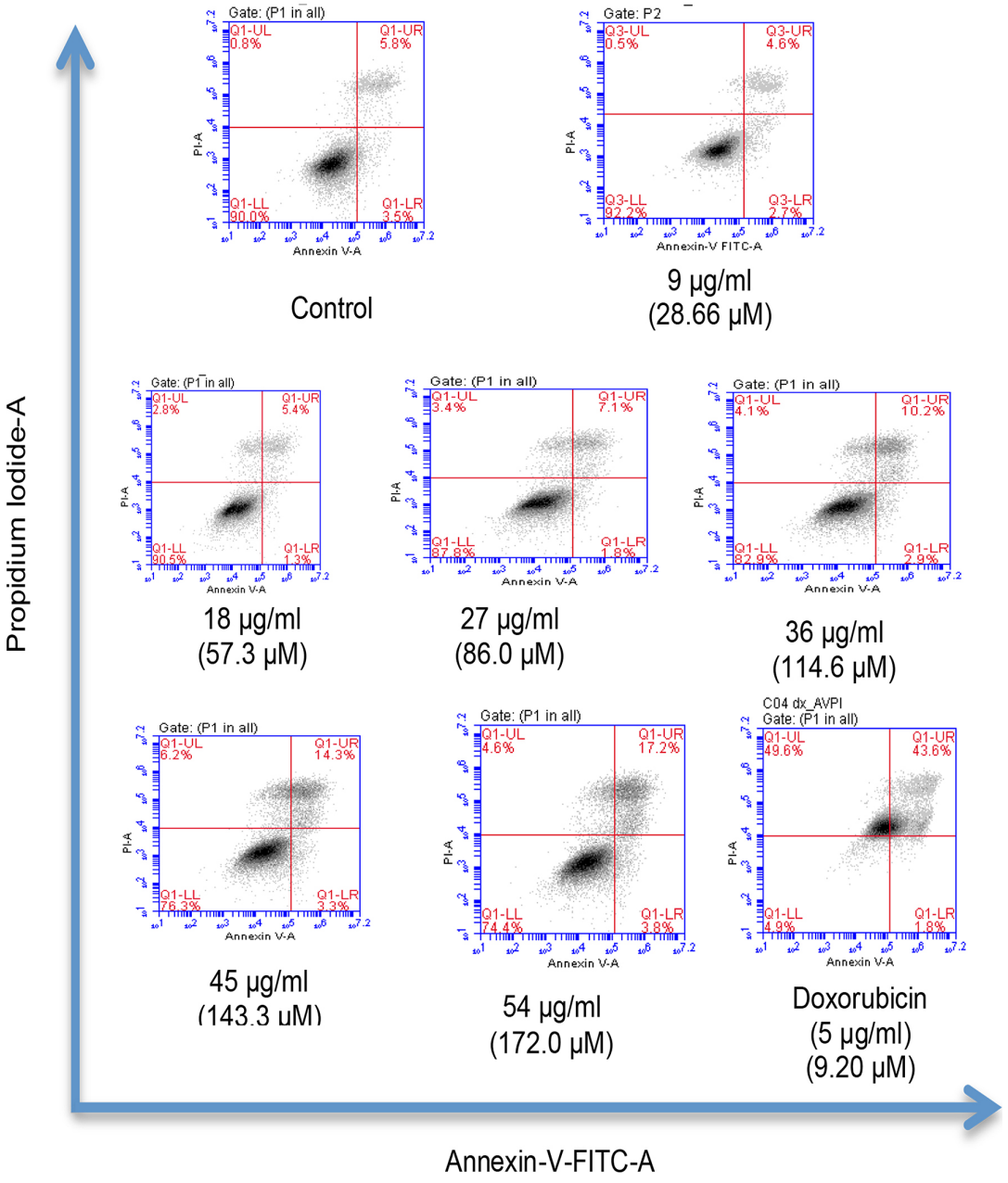

Figure 4.23(A): Induction of early and late apoptosis by chalepin at various concentrations in A549 cell line. (A) shows the flow cytometric density plot of Annexin V-FITC/PI staining in A549 cells when treated with different concentrations of chalepin (18.0-45.0 ug/ml) at 48 hours incubation.

(B)

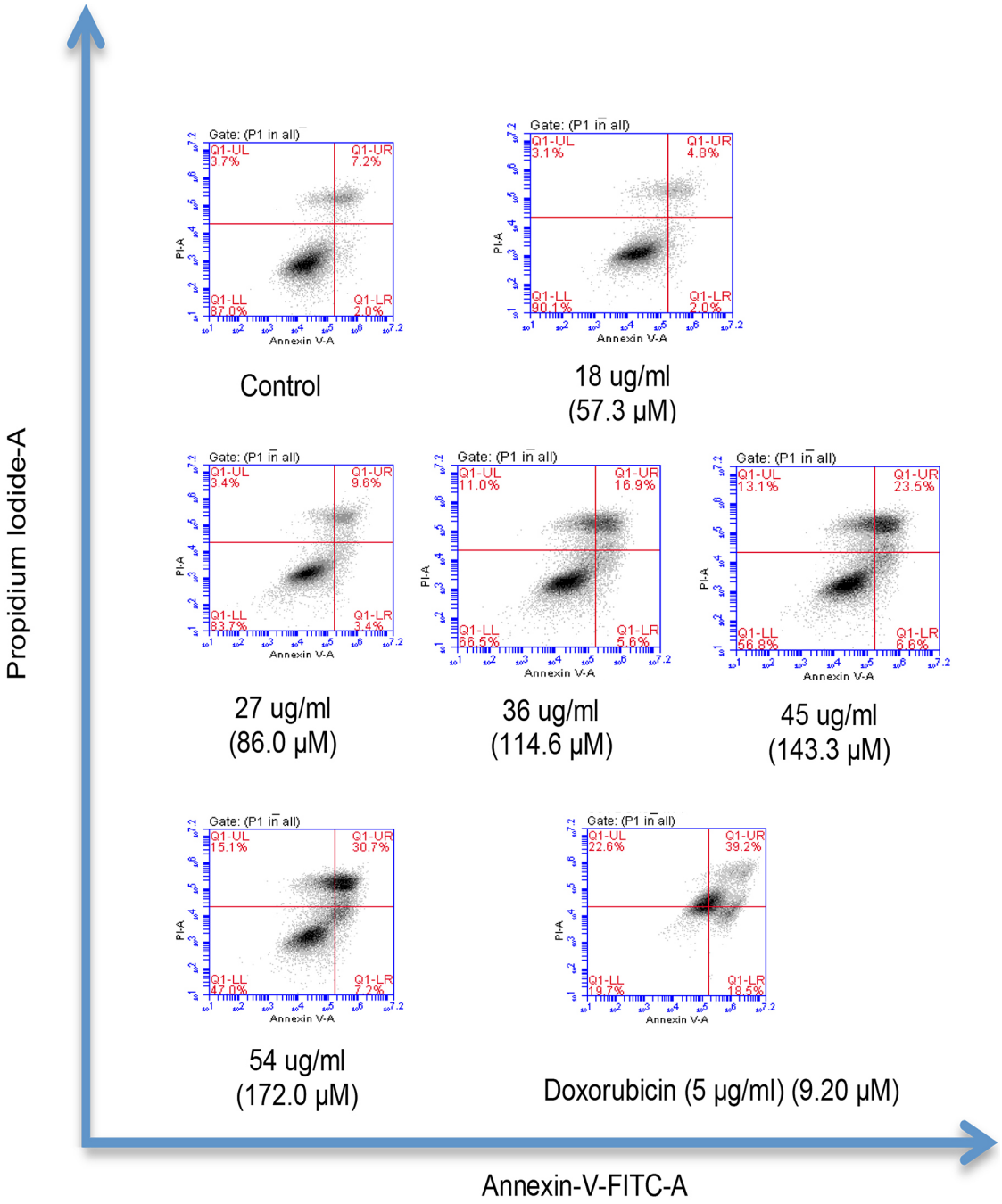

Figure 4.23(B): Induction of early and late apoptosis by chalepin at various concentrations in A549 cell line. Image shows the flow cytometric density plot of Annexin V-FITC/PI staining in A549 cells when treated with different concentrations (18.0 - 45.0 ug/ml) at 72 hours incubation time.

(C)

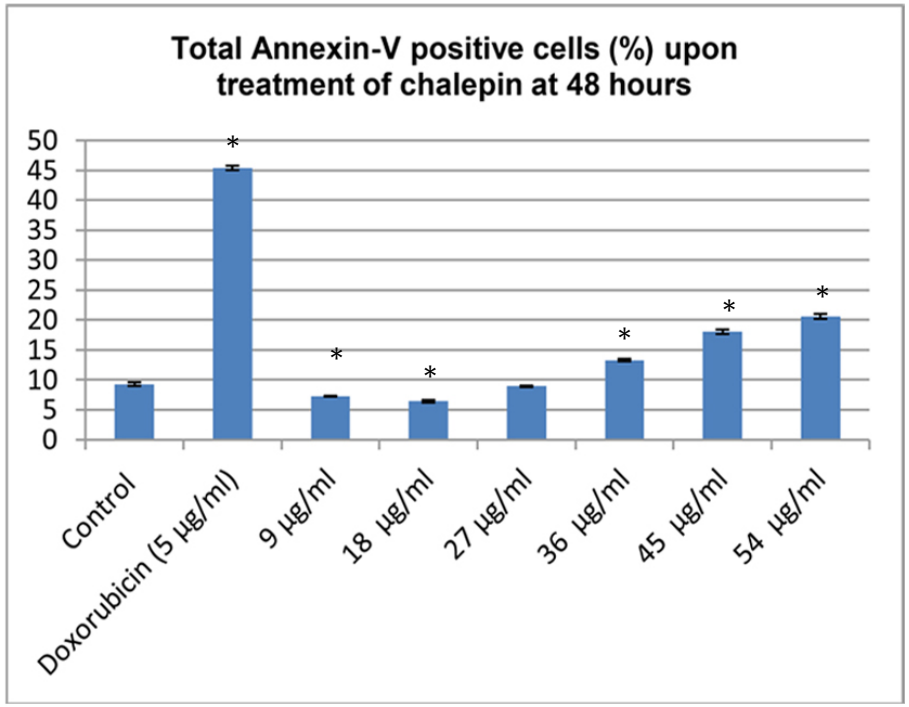

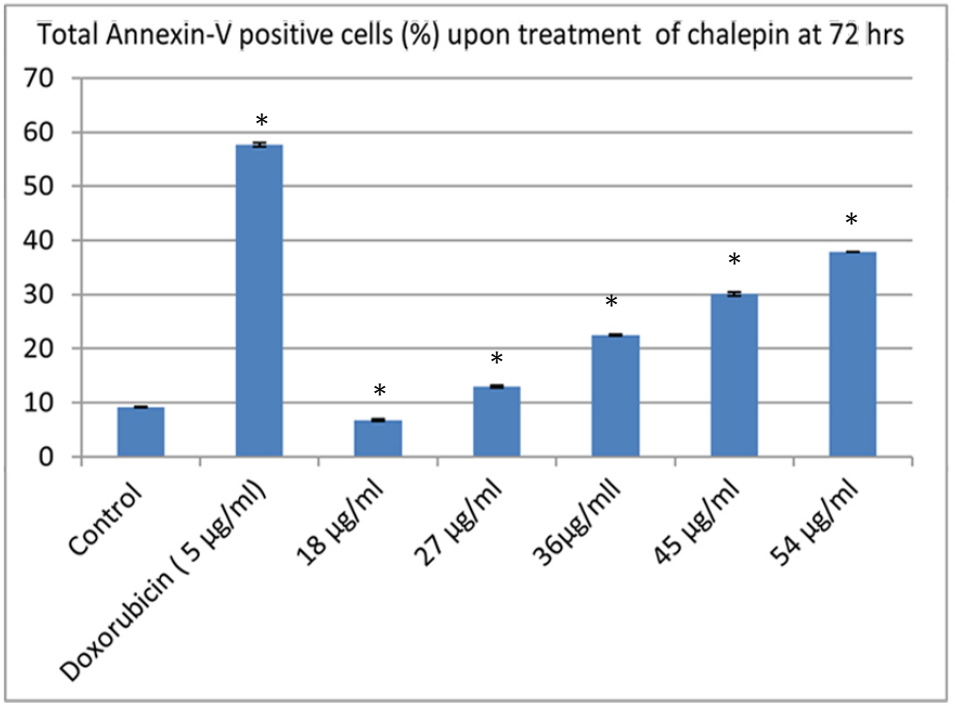

Figure 4.23(C): The bar chart shows the total annexin V positive cells. Doxorubicin served as the positive control. The data is expressed as mean ± S.D. from three replicates. Asterisks indicates significantly different value as compared to control (*$p<0.05$).

(D)

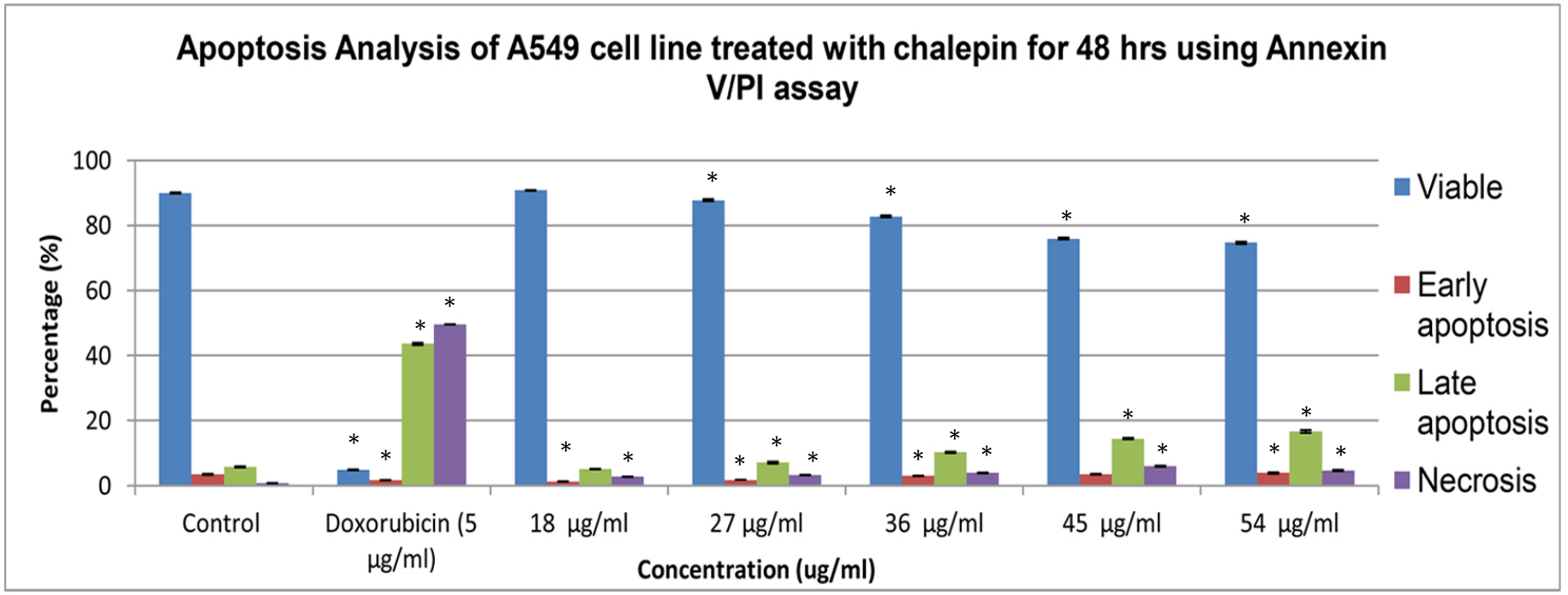

Figure 4.23(D): The bar charts shows the distribution of cells in viable, early apoptosis, late apoptosis and secondary necrosis phase in 48 hours incubation. Doxorubicin served as the positive control. The data is expressed as mean ± S.D. from three replicates. Asterisks indicates significantly different value as compared to control (*$p<0.05$).

(E)

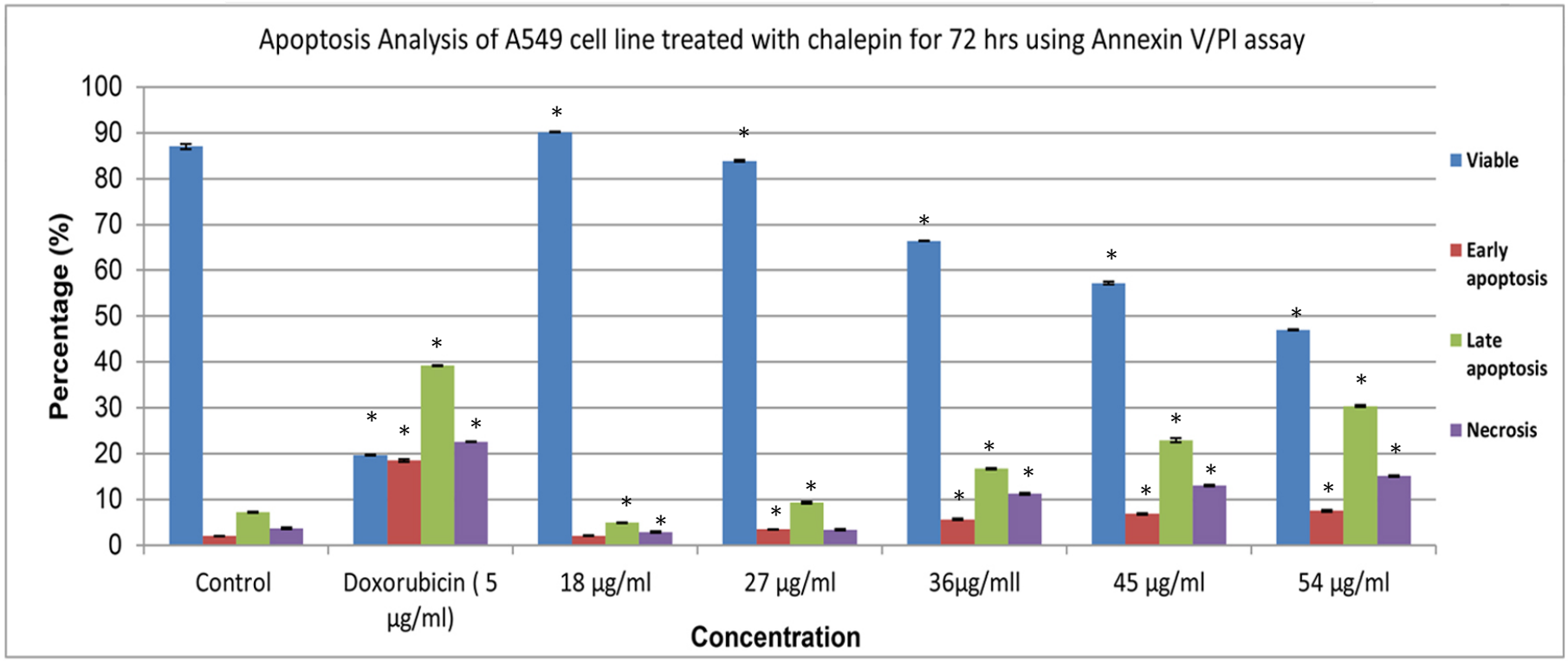

Figure 4.23(E): The bar charts shows the percentage of distribution of the treated cell population in viable, early apoptosis, late apoptosis or secondary necrosis phase in 72 hours incubation. Doxorubicin served as the positive control. The data is expressed as mean ± S.D. from three replicates. Asterisks indicates significantly different value as compared to control (*$p<0.05$).

4.7.2 DNA fragmentation induced by chalepin on A549 cell

DNA fragmentation is one of the main distinctive feature of apoptosis. DNA fragmentation is activated by nucleases which would degrade the nuclear DNA into fragments of about 200 base pairs in length. This feature is measured by using APO-BrDU TUNEL assay kit. In this study, chalepin was treated at various concentrations and incubated for 48 and 72 hours to measure the ability to induce DNA fragmentation. It was found that chalepin induces DNA fragmentation in A549 cell in a dose and time dependent manner. DNA fragmentation is represented in the density plot above with R3 representing percentage of cells that has nuclear DNA fragmentation for treatment at 48 hours and 72 hours. The cell population would move to the upper region in the density plot when DNA fragmentation is labelled. Upper region in the density plot represents cells with fragmented DNA. Based on the results obtained, after 48 hours incubation, the DNA fragmentation increased from 1.0 ± 0.08 % for untreated control cells to 38.5 ± 0.70 % for cells treated with chalepin at 45 μg/ml. At 72 hours, the DNA fragmentation increased from 1.50 ± 0.35 % for untreated control cells to 73.50 ± 0.20 % at 36 μg/ml however, a drop was observed at 45 μg/ml to 66.50 ± 0.29 %. This result indicates that upon treatment of chalepin, DNA fragmentation is initiated in the cell by endonucleases to enable cells to undergo apoptosis. With increasing concentration of treated chalepin, the percentage of DNA fragmentation in the treated cells increases. This trend is also true for higher incubation time. The DNA fragmentation that occurs in the cells is dependent on the concentration of chalepin and the incubation hours.

(A)

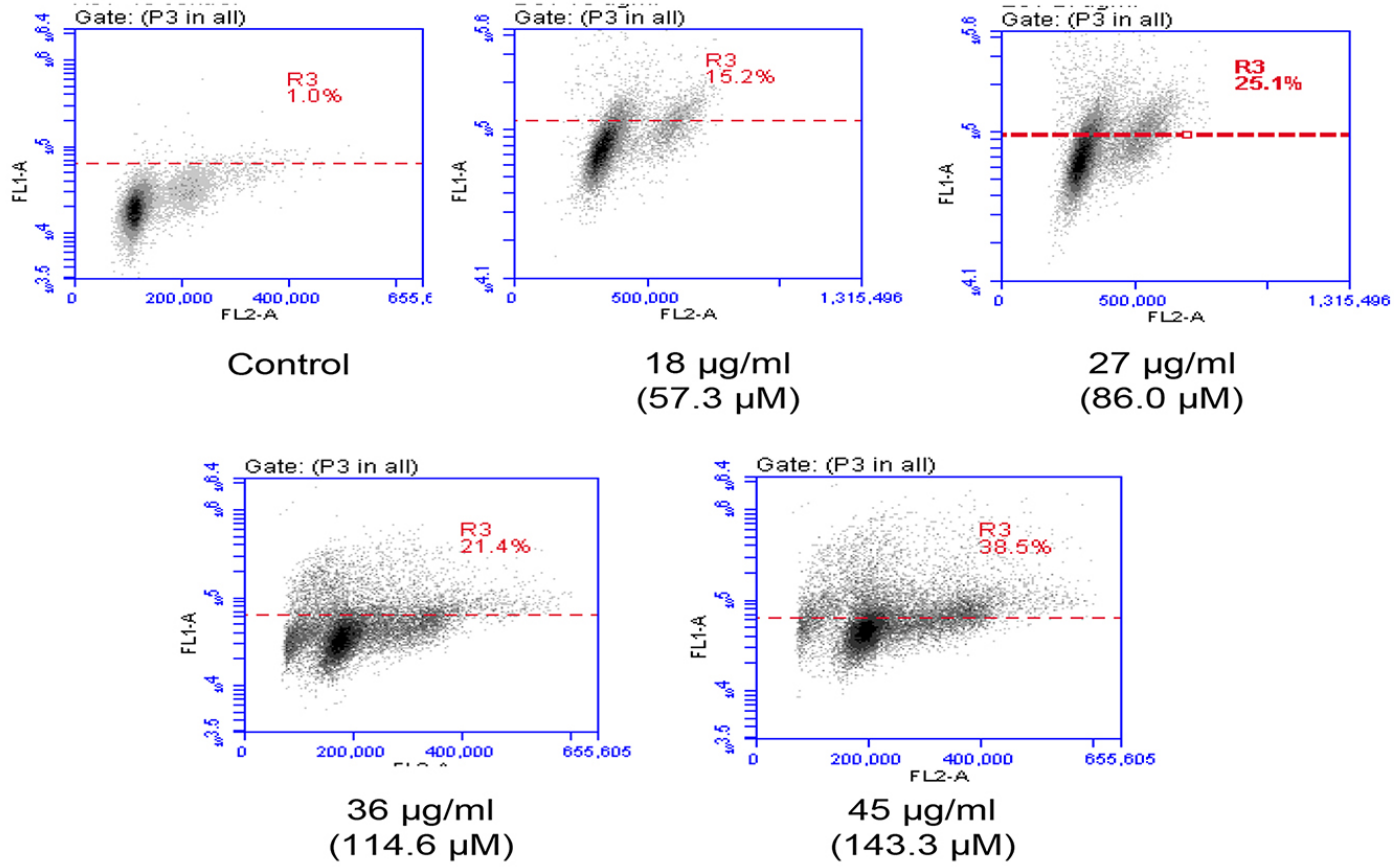

Figure 4.24(A): DNA fragmentation based on TUNEL assay on A549 cells treated with chalepin at various concentrations at 48 hour incubation. R3 region in the dot plots obtained from flow cytometry represents TUNEL positive staining in which cells were stained with FITC-conjugated anti-BrdU antibody which resulted from treatment of chalepin.

(B)

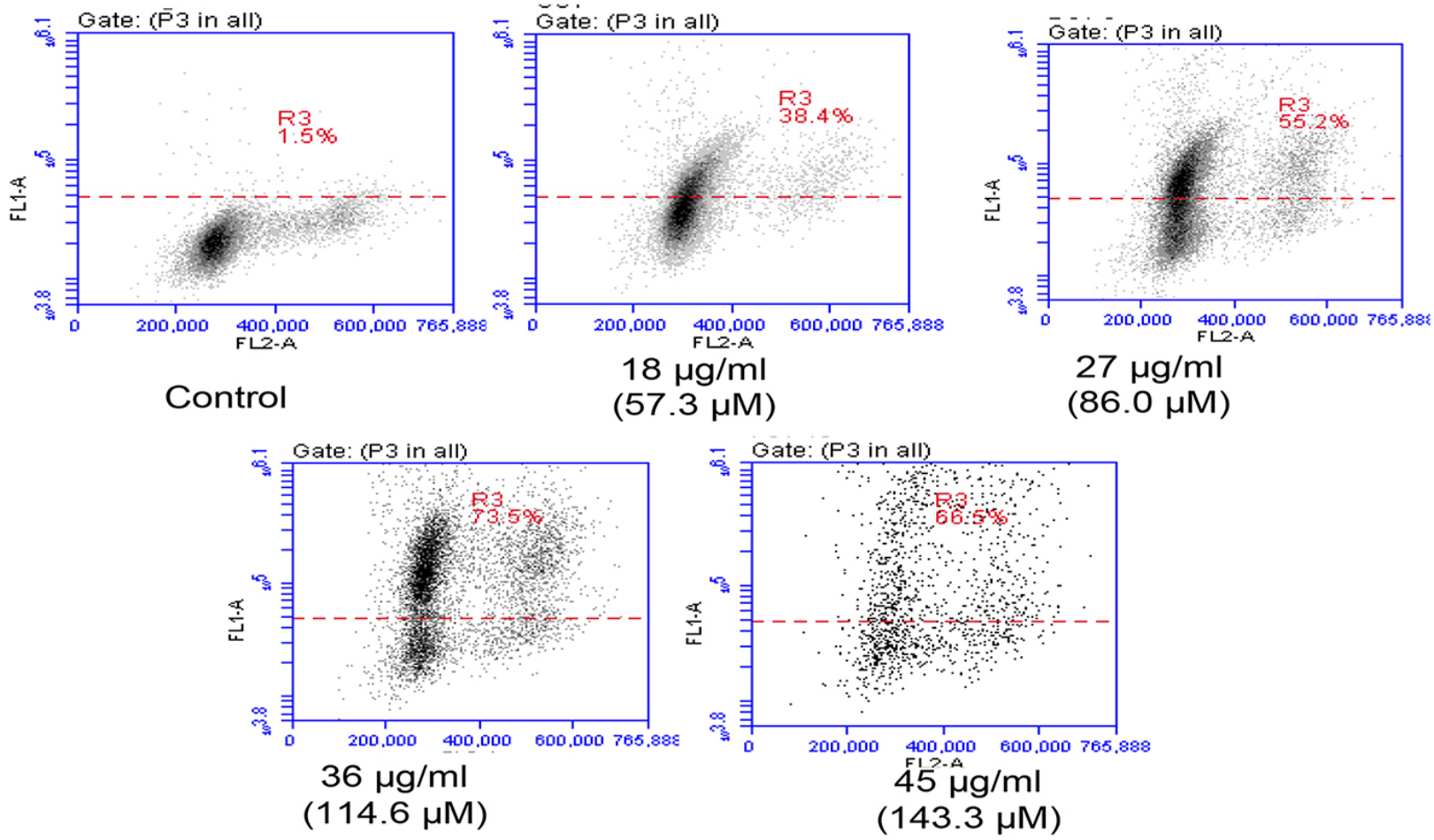

Figure 4.24(B): DNA fragmentation based on TUNEL assay on A549 cells treated with chalepin at various concentrations at 72 hour incubation. R3 region in the dot plots obtained from flow cytometry represents TUNEL positive staining in which cells were stained with FITC-conjugated anti-BrdU antibody which resulted from treatment of chalepin.

(C)

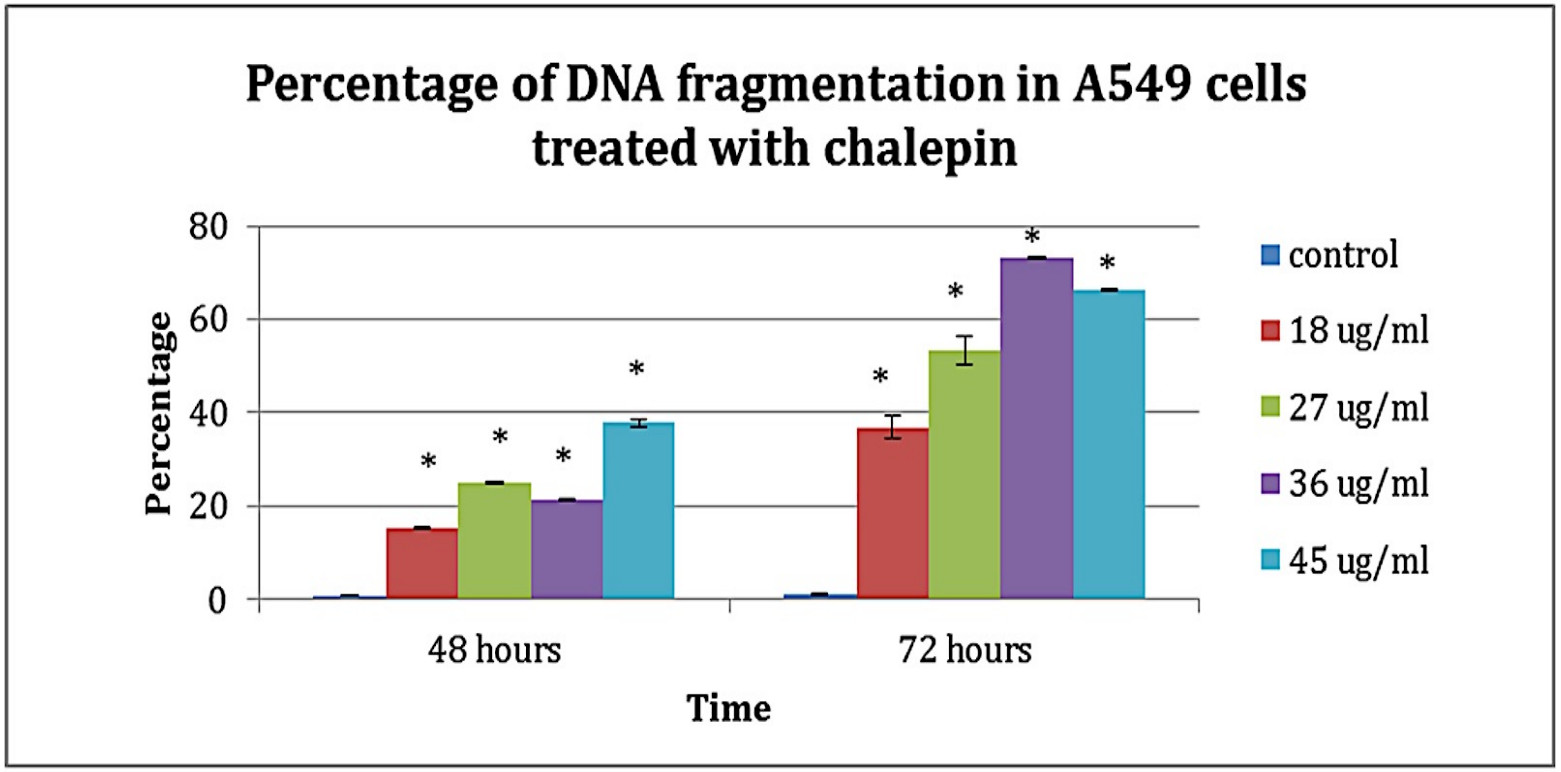

Figure 4.24(C): Bar chart represents the percentage of TUNEL positive cells. Histograms are representative of three separate experiments (n=3). Asterisks indicate significantly different value from control (*$p<0.05$).

4.7.3 Measurement of mitochondrial membrane potential

Mitochondrial membrane potential (MMP) may be disrupted during early apoptosis. The loss of MMP in A549 cells which were treated with various concentrations of chalepin was observed using the JC-1 dye. During the early stage of apoptosis, mitochondrial depolarisation occurs and this enabled fluorescence of JC-1 to turn from red aggregates to green monomers. Figure 4.25(A) showed untreated control cell did not show any increase in green monomer formation. Upon treatment with chalepin at different concentrations, the percentage of green monomer increases in cytoplasm Figure 4.25(B). This shows that, chalepin significantly induced reduction of mitochondrial membrane potential in A549 cells in a concentration dependent manner. Figure 4.25(C) shows that at 48 hours incubation time, the untreated cells gives red fluorescence which indicates that there is high membrane potential in the mitochondrial membrane which enables the JC-1 dye to pass through the mitochondrial membrane and form aggregates which could give the red fluorescence. This shows that the cells are healthy. As the cells are treated with chalepin, there is an increase in the presence of the green fluorescence as the concentration of chalepin treated is increased. When a cell undergoes apoptosis, the mitochondrial membrane potential would drop and this would inhibit the influx of JC-1 dye into mitochondria. It would remain in its initial monomeric form at cytoplasm which would give the green fluorescence that is observed in cells that were treated with high concentration of chalepin i.e. 36 μg/ml and 45 μg/ml. This observation is similar at 72 hours incubation time with a difference of more fluorescence intensity at higher treatment time (Figure 4.25(D)). We observed that the cells at 45 μg/ml treatment dosage at 72 hours, almost all gives a green fluorescence. This indicates that almost all the cells that were observed are undergoing apoptosis.

(A)

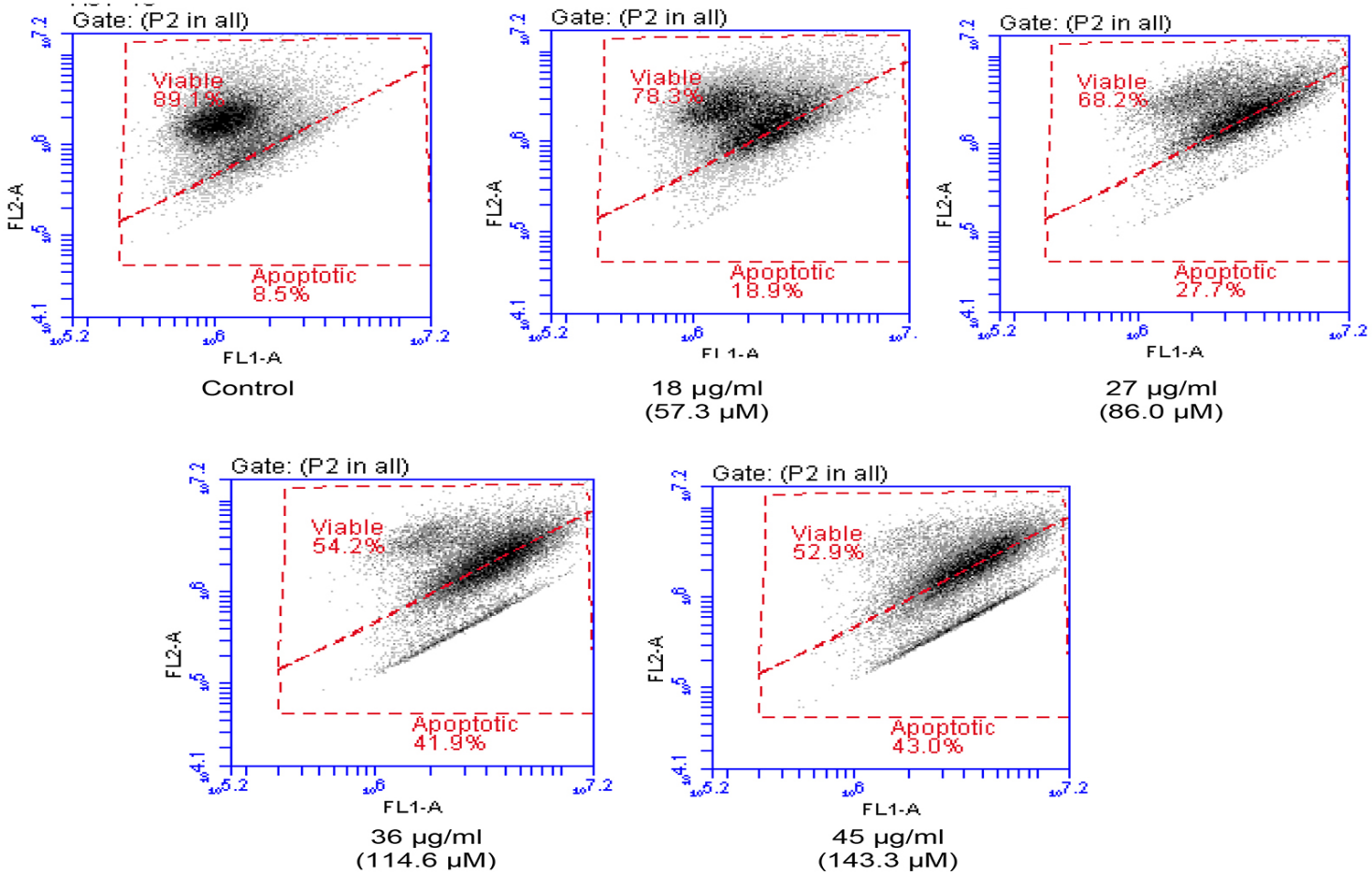

Figure 4.25(A): Dot plots obtained from flow cytometer shows the attenuation of mitochondrial membrane potential (MMP) in A549 cells treated with chalepin at various concentrations and incubated at 48 hours.

(B)

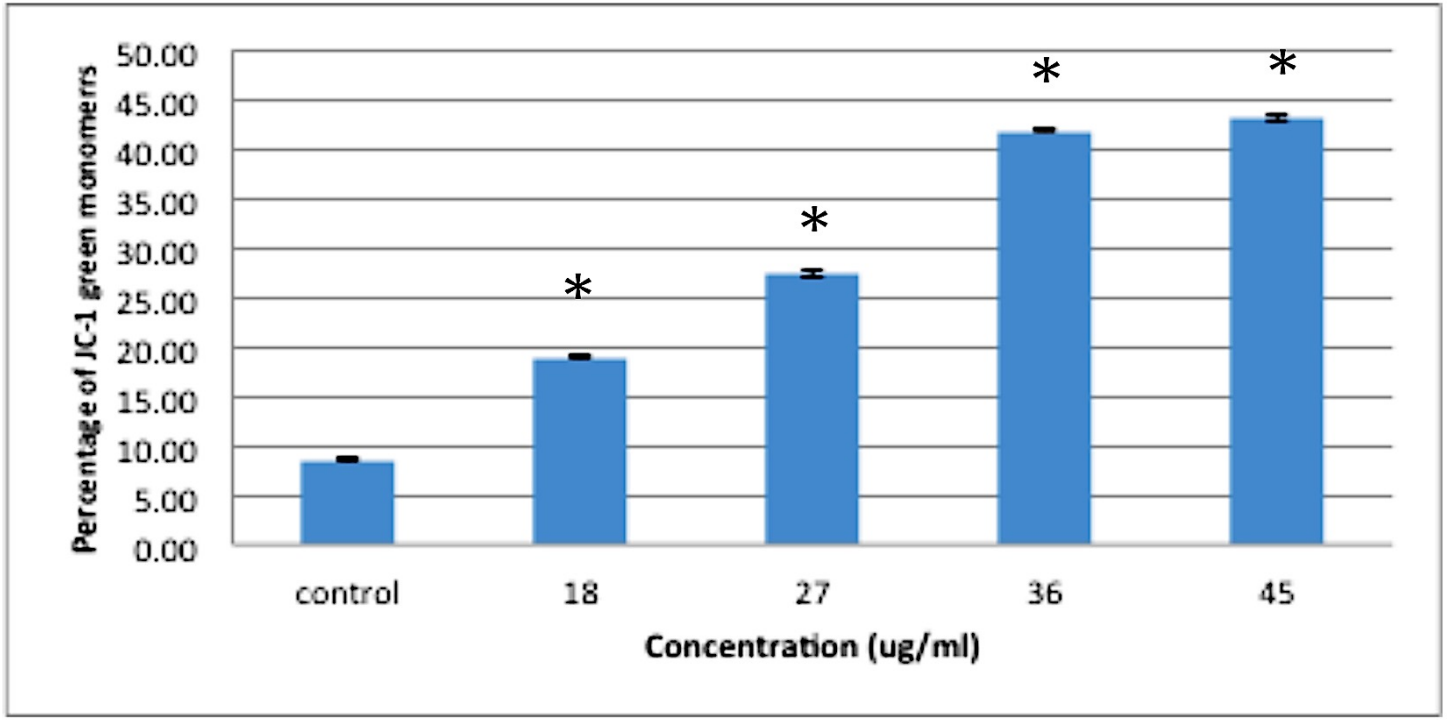

Figure 4.25(B): Bar chart represents the percentage of JC-1 that remained as green monomer which shows the apoptotic cells with compromised mitochondrial membrane potential upon treatment of chalepin in dose dependent manner. The data expressed as mean ± S.D from triplicates in experiment. Asterisks indicates significantly different value from control (*$p<0.05$).

(C)

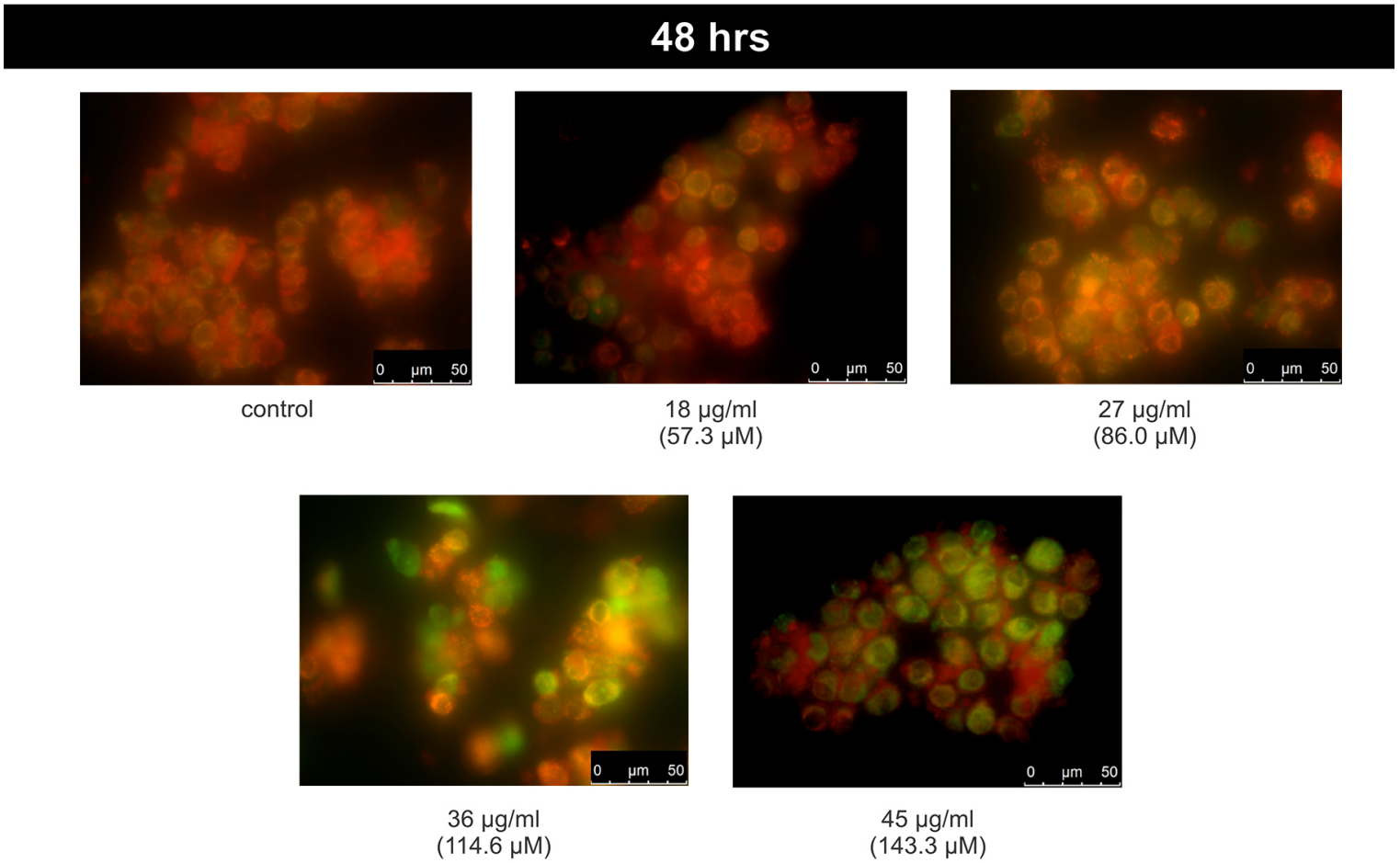

Figure 4.25(C): Effects of chalepin at different concentrations on mitochondrial membrane potential changes of A549 cell line at 48 h treatment time. After the incubation period, the cells were stained with JC-1 dye and were examined with a fluorescent microscope under magnification of 630x to observe whether the JC-1 aggregates in mitochondria (healthy cells) or JC-1 remains in monomer form at cytoplasm (apoptotic cells)

(D)

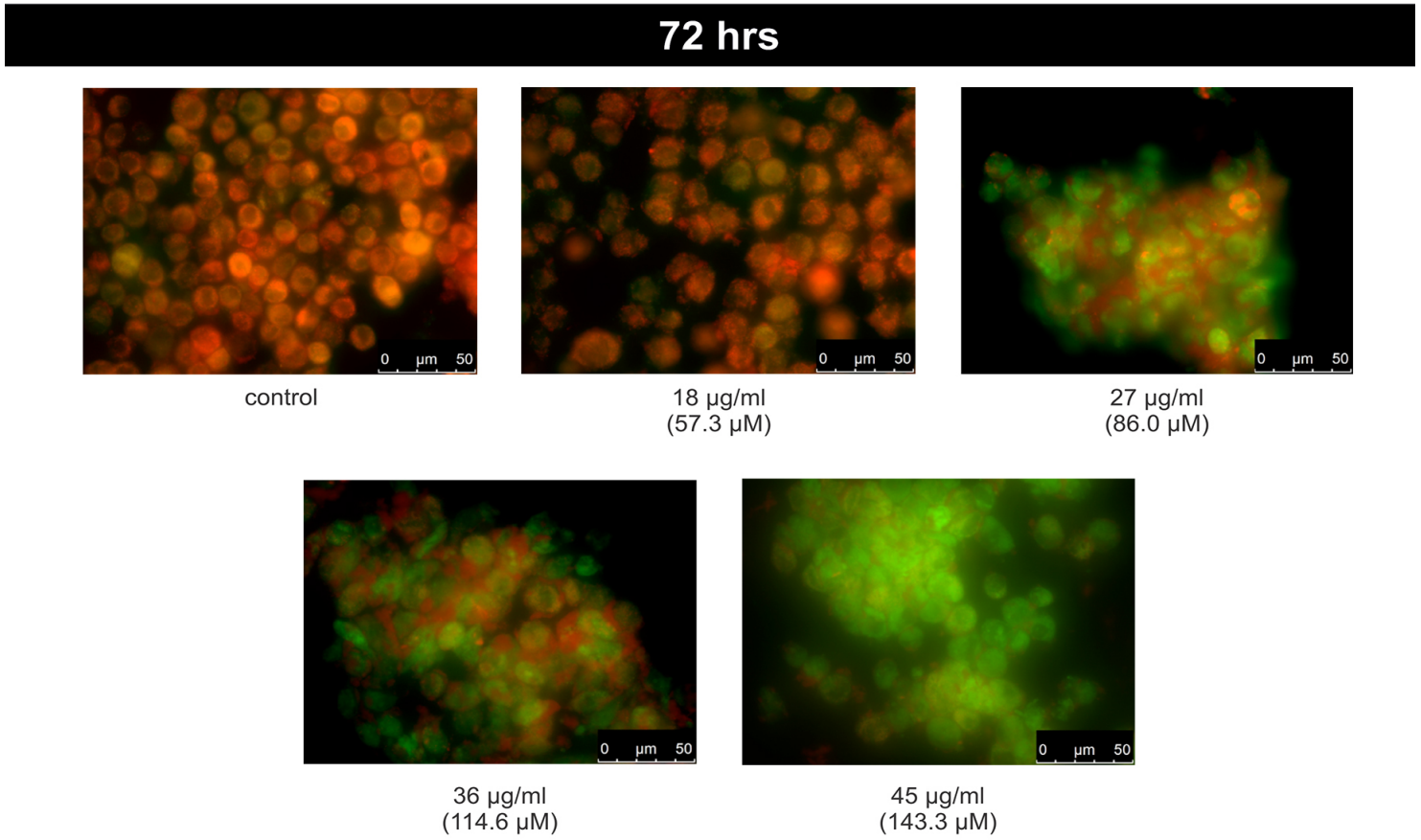

Figure 4.25(D): Effects of chalepin at different concentrations on mitochondrial membrane potential changes of A549 cell line at 48 h and 72 h treatment time. After the incubation period, the cells were stained with JC-1 dye and were examined with a fluorescent microscope under magnification of 630x to observe the JC-1 aggregates in mitochondria (healthy cells) or JC-1 remains in monomer form at cytoplasm (apoptotic cells).

4.7.4 Measurement of the intracellular ROS generation by chalepin

The effect of chalepin in inititating the generation of intracellular ROS in A549 cells was detected using the DCFH-DA dye. Observation through fluorescent microscope was done on lung carcinoma cells after treatment of chalepin for 24 and 48 hours showed an increase in intensity of green fluorescence of DCF in a dose and time dependent manner in Figure 4.26(A &B). It was observed that, as the concentration of chalepin that was treated to the cells increased, there was an increase in the intensity of green fluorescence by the DCFH-DA dye. This trend was also true for an increase in the incubation time. The DCFH-DA is a non-polar dye which would be converted into DCFH by cellular esterases. DCFH is non-fluorescent but is switched to fluorescent DCF when it is oxidized by ROS in the cell. Hence, the qualitative imagining showed that the increase in the intracellular ROS content is dependent upon the concentration of chalepin and also the incubation time of the treatment. Besides the qualitative imaging, the quantification of the intracellular content of ROS by measurement of the fluorescence of the DCF was also conducted. The fluorescence were then calculated in the ratio of fold increase of the fluorescence intensity in the treated cells as compared to the untreated negative control cells. The fold increase of intracellular ROS was calculated based on fluorescence value obtained from microplate reader. It was observed that in comparison to the control, the treated cells showed a gradual increase in the fold increase of intracellular ROS content starting at 2 hours up till 6 hours. This increase was time and dose dependent. However at 8 hours, there was a drop in the fluorescent measurement of the treated cells (Figure 4.24(C)). This observation could be due to the reason where cell death has commenced and thus there is a drop.

(A)

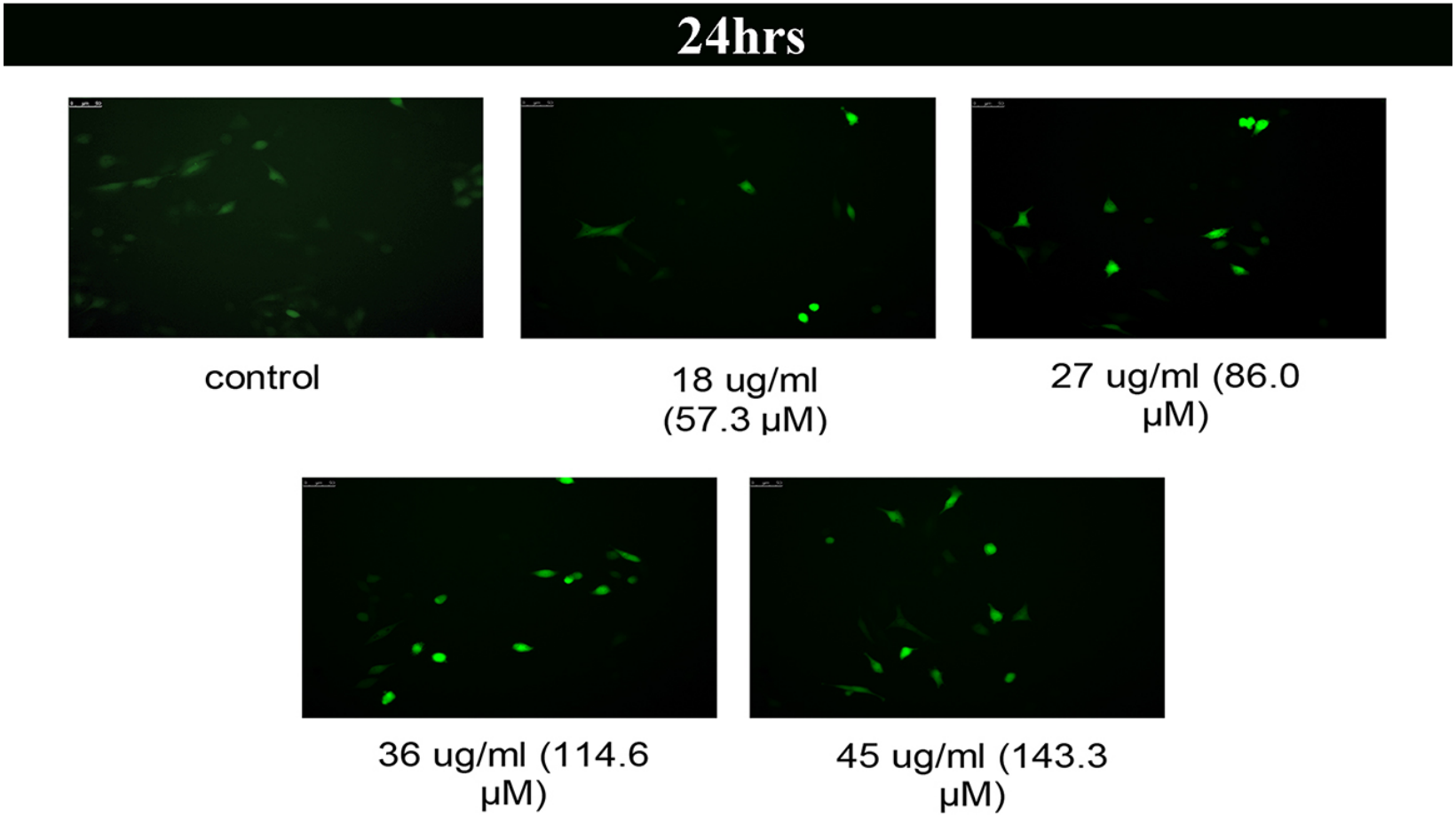

Figure 4.26(A): Elevation of the intracellular reactive oxygen species (ROS) level was observed qualitatively through observation of the cells after incubating with DCFH-DA dye and examining the changes using a fluorescent microscope. Induction of ROS in A549 cells treated with chalepin at various concentrations and incubated for 24 hours.

(B)

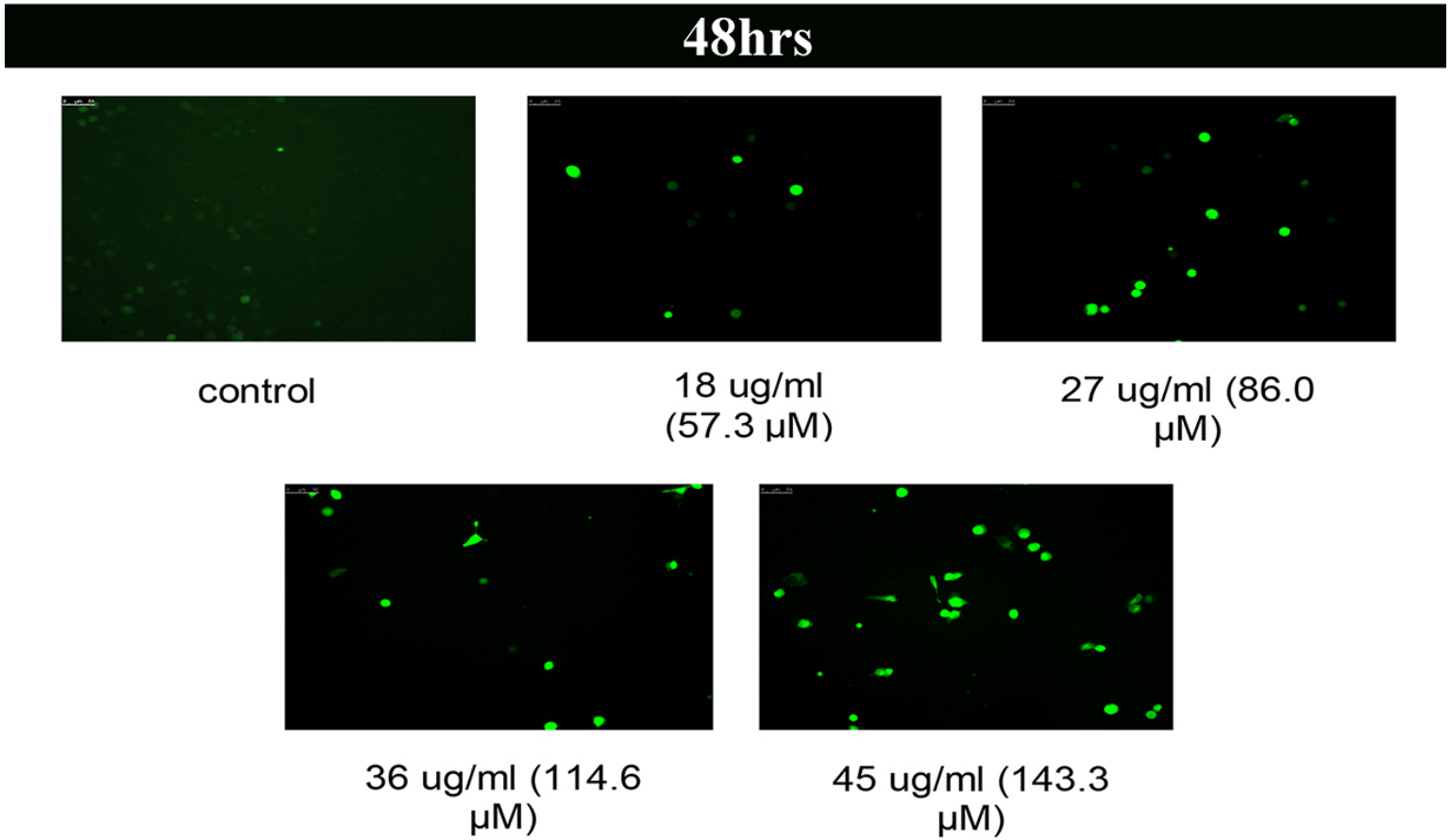

Figure 4.26(B): Elevation of the intracellular reactive oxygen species (ROS) level was observed qualitatively through observation of the cells after incubating with DCFH-DA dye and examining the changes using a fluorescent microscope. Induction of ROS in A549 cells treated with chalepin at various concentrations and incubated for 48 hours.

(C)

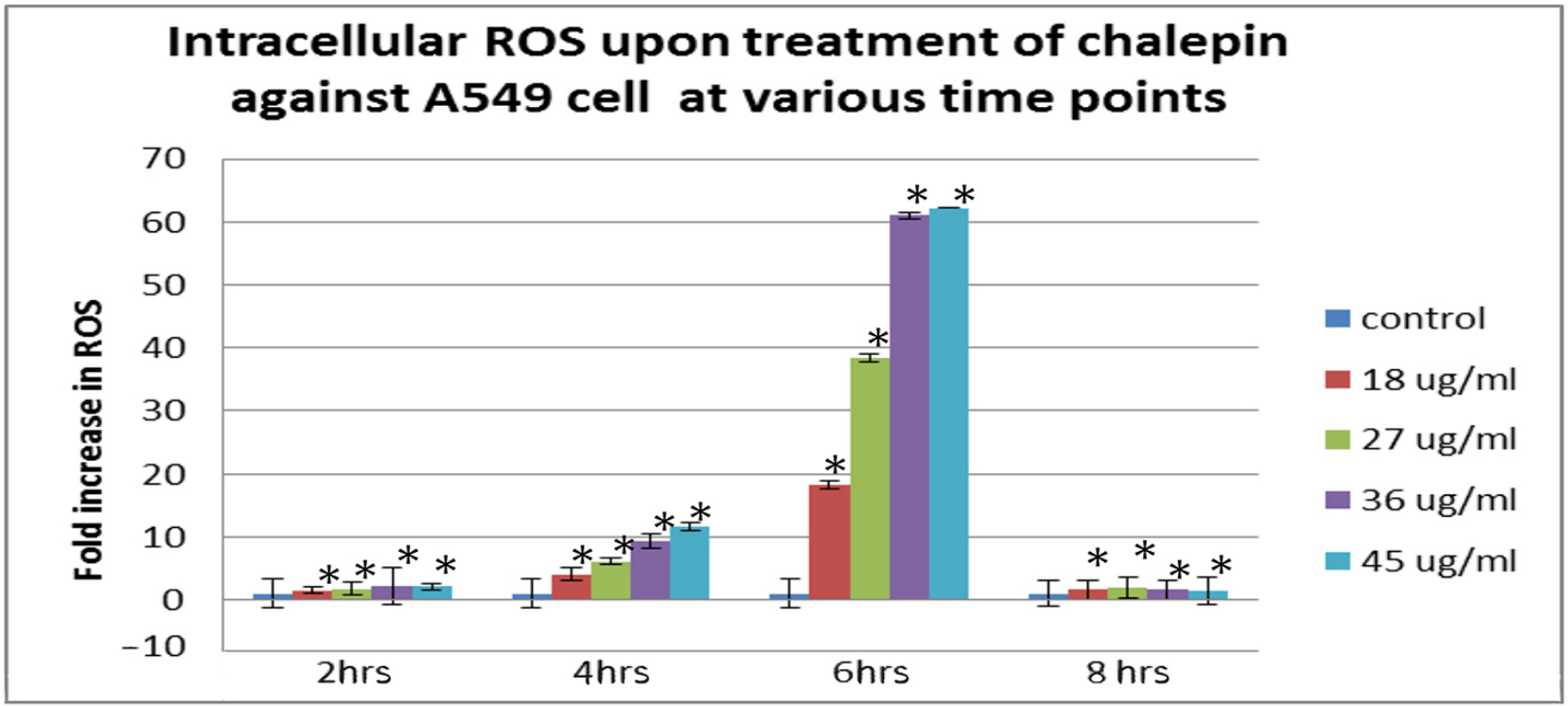

Figure 4.26(C): Elevation of the intracellular reactive oxygen species (ROS) level was observed qualitatively through observation of the cells after incubating with DCFH-DA dye and quantified using a fluorescence plate reader. Bar chart represents the fold increase of Intracellular ROS level in A549 cells treated with different concentrations of chalepin as compared to untreated negative control cells. The data expressed as mean ± S.D. from three replicates. Asterisks indicates significantly different value from control (*$p<0.05$).

4.7.5 Caspase 9 Activation Analysis

Caspase 9 is associated with the activation of the intrinsic mitochondrial mediated pathway. CaspILLUME fluorescein active caspase 9 staining kit was used to determine the caspase 9 activity in regards to the treatment of chalepin in A549 cells. Cells with activated caspase 9 would move to the right side (V1-R) of the density plot. The results shows that there is a remarkable increase in the caspase 9 activity of cells treated with chalepin as compared to the control. It was observed that after 48 hours of incubation period there is a five-fold increase in activation of caspase 9 from 4.5 ± 0.35 % in untreated control to 22.57 ± 0.21 % in cells treated with 45 μg/ml of chalepin. As for the 72 hours incubation period, there was an increase from 3.97 ± 0.15 % for untreated control cells to 33.5 ± 0.35 % for treated cells with 45 μg/ml of chalepin and this is a 8.44 fold increase. When cells receive apoptotic stimuli, the mitochondria releases cytochrome c which then binds to Apaf-1, together with dATP. The resultant complex recruits caspase 9 leading to its activation. Activated caspase 9 cleaves downstream caspases such as caspase-3, -6 and -7 initiating the caspase cascade (Kuida, 2000). This results shows that chalepin treated cells undergo apoptosis through the mitochondrial pathway.

(A)

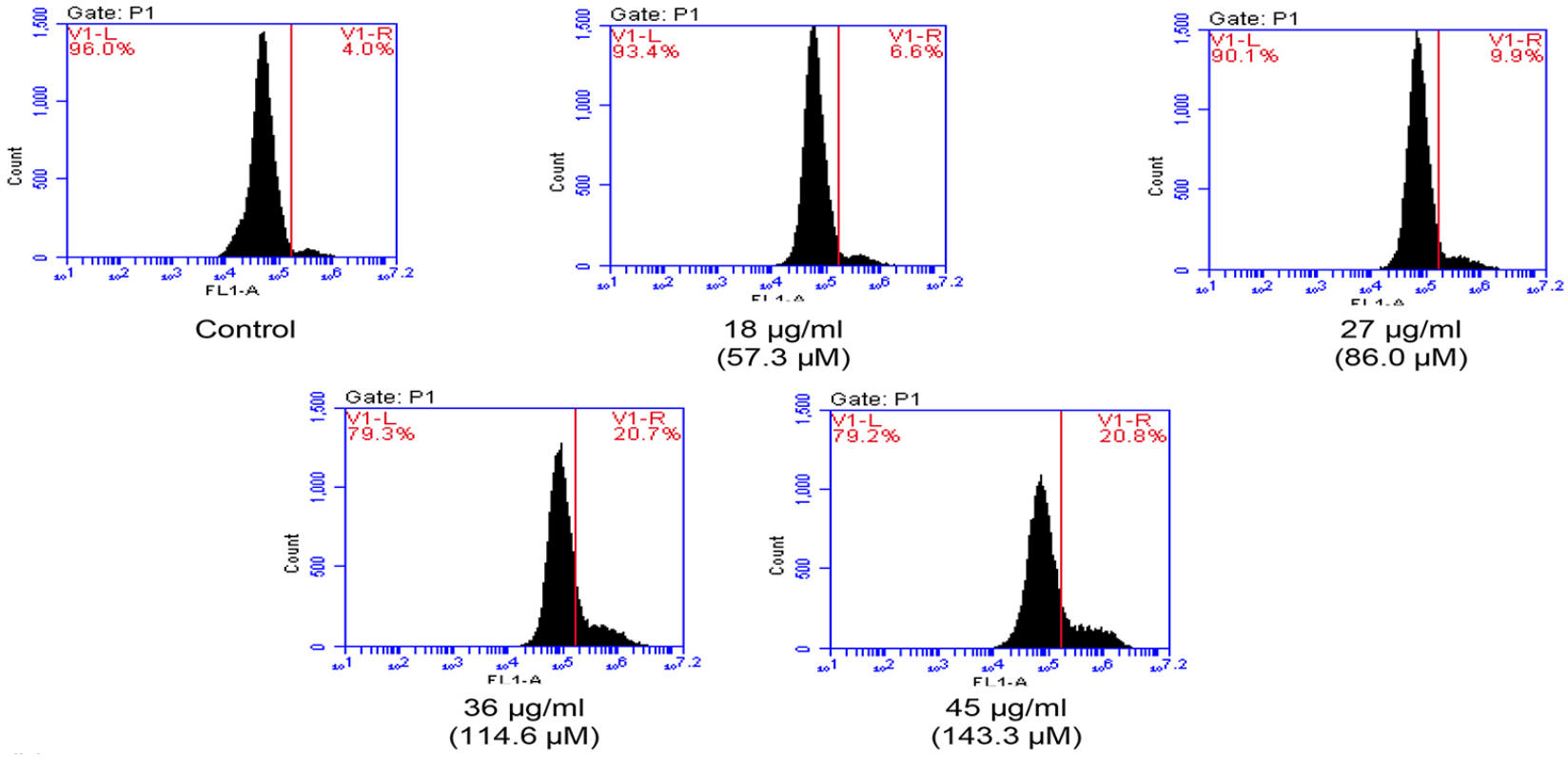

Figure 4.27(A): Caspase 9 activity of A549 cells treated with various concentrations of chalepin and incubated for 48 hours incubation. Flow cytometric analysis of apoptotic (V1-R) and non-apoptotic populations (V1-L) for active caspase 9 activity for untreated A549 cells and A549 cells treated with chalepin at various concentrations.

(B)

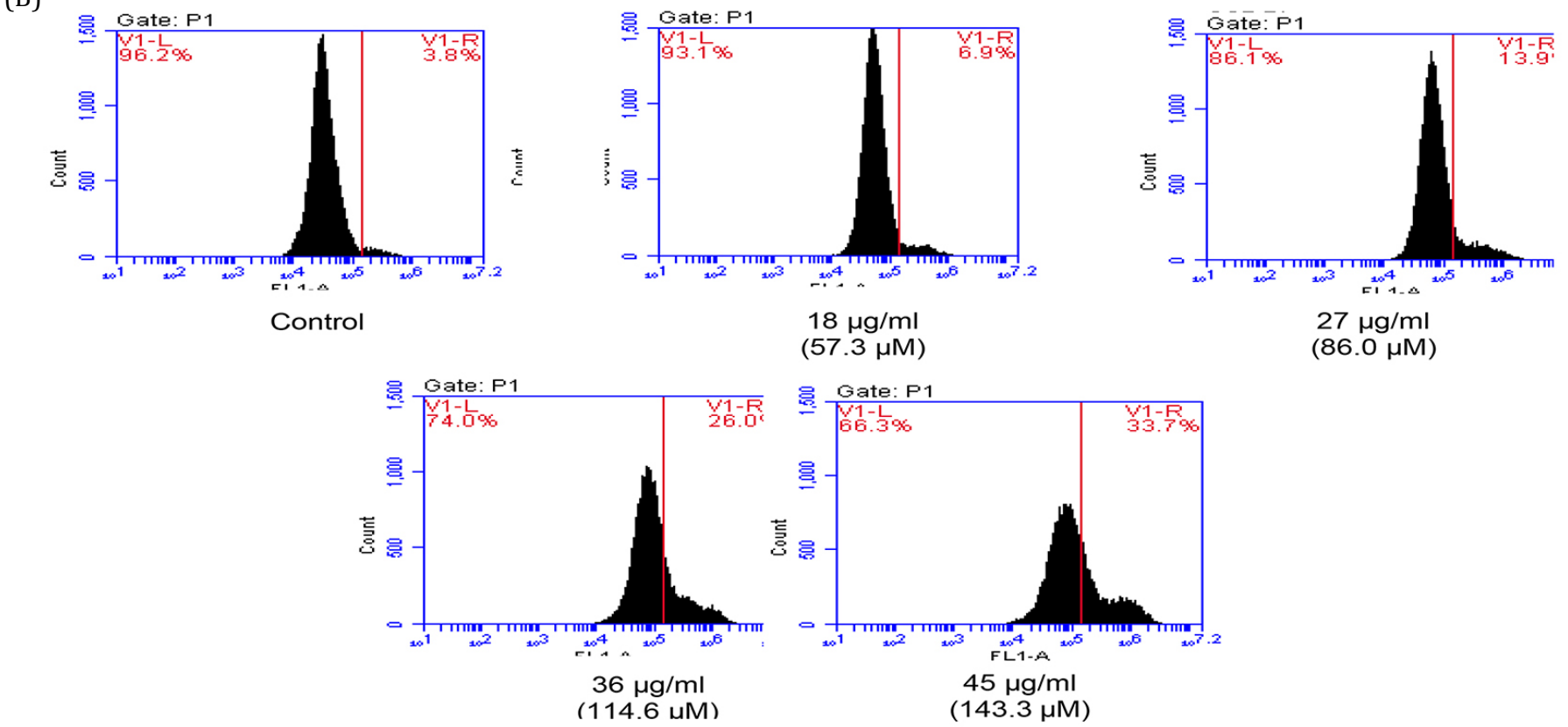

Figure 4.27(B): Caspase 9 activity of A549 cells treated with various concentrations of chalepin and incubated for 72 hours incubation. Flow cytometric analysis of apoptotic (V1-R) and non-apoptotic populations (V1-L) for active caspase 9 activity for untreated A549 cells and A549 cells treated with chalepin at various concentrations.

(C)

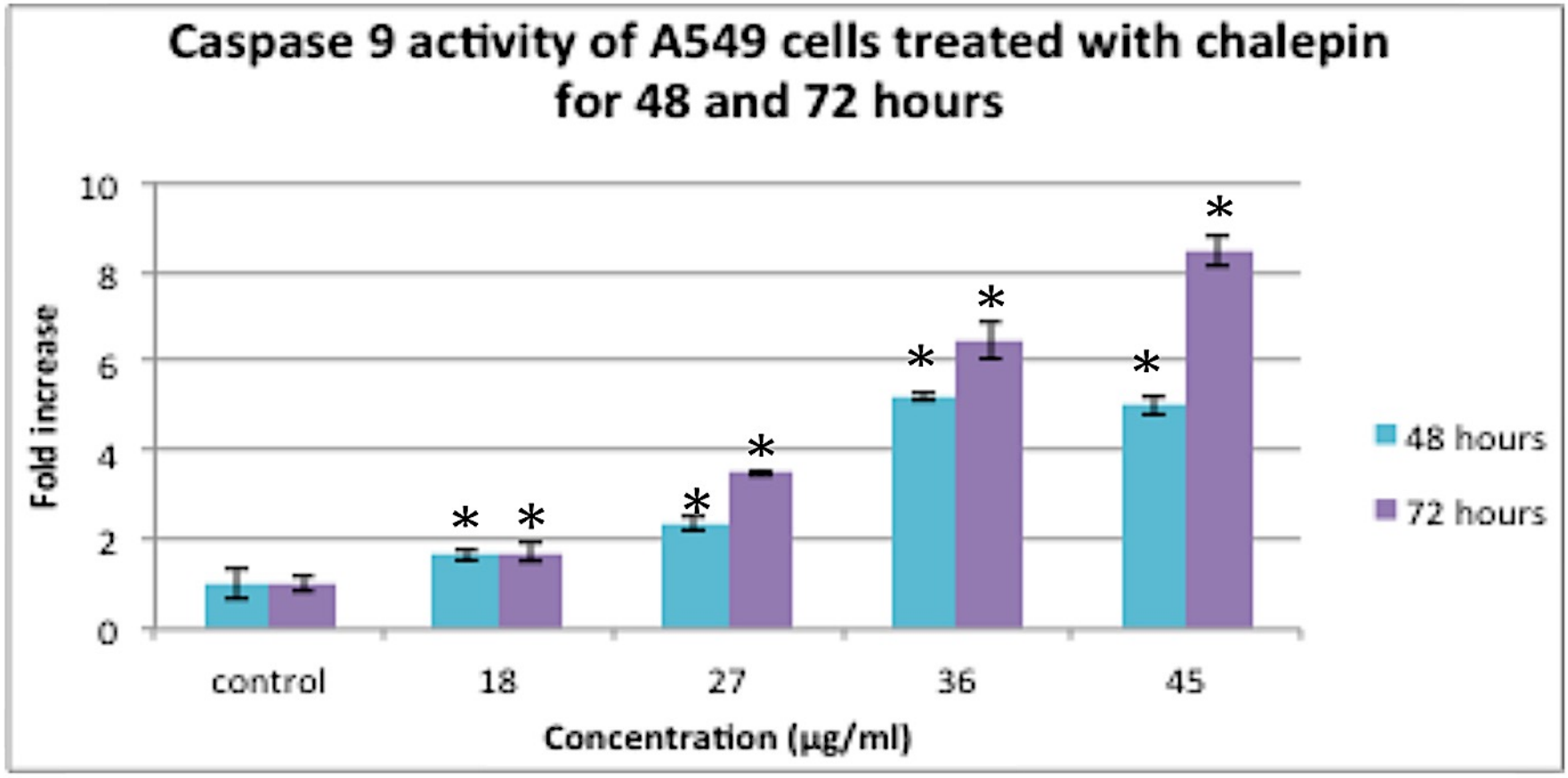

Figure 4.27(C): Caspase 9 activity of A549 cells treated with various concentrations of chalepin and incubated for 48 h and 72 h incubation. Bar chart representing a comparison of fold increase between chalepin treated A549 cells at different incubation times (48 & 72 h). The data expressed as mean ± S.D. of three replicates. Asterisks indicates significantly different value from control (*$p<0.05$).

4.7.6 Caspase 3 Activation Analysis

Caspase 3 is a downstream caspase signal also known as the effector caspase. Upon activation of caspase 9, a signal cascade results in an activation of caspase 3 which in turn results in the hydrolysis of more than 100 target protein that subsequently results in apoptosis. Defect in caspase 3 activity results in cancer. In this study, it was observed that A549 cells treated with chalepin induces caspase 3 activation. CaspILLUME fluorescein active caspase 3 staining kit was used and the cell population was analysed using a flow cytometer. In the event of caspase 3 activation, the cell population would move to the right hand side (V1-R) of the density plot. It is observed that after 48 hours of incubation period, there is an increase of 2.83 ± 0.06 % for untreated control to 26.40 ± 0.79 % for cells treated with 45 μg/ml of chalepin and this is a 9.32 fold increase. As for the 72 hours incubation period, there was an increase from 5.63 ± 0.21 % for untreated control cells to 49.07 ± 0.63 % for treated cells with 45 μg/ml of chalepin and this is a 8.71 fold increase. Caspase 3 is required for some typical characteristics of apoptosis, and is crucial for apoptotic chromatin condensation and DNA fragmentation in all cell types. Caspase 3 is essential for certain processes associated with the dismantling of the cell and the formation of apoptotic bodies, but it may also function before or at the stage when commitment to loss of cell viability is made (Porter et al., 1999). Therefore activation of caspase 3 in chalepin treated A549 cells therefore is an evidence that apoptosis has commenced.

(A)

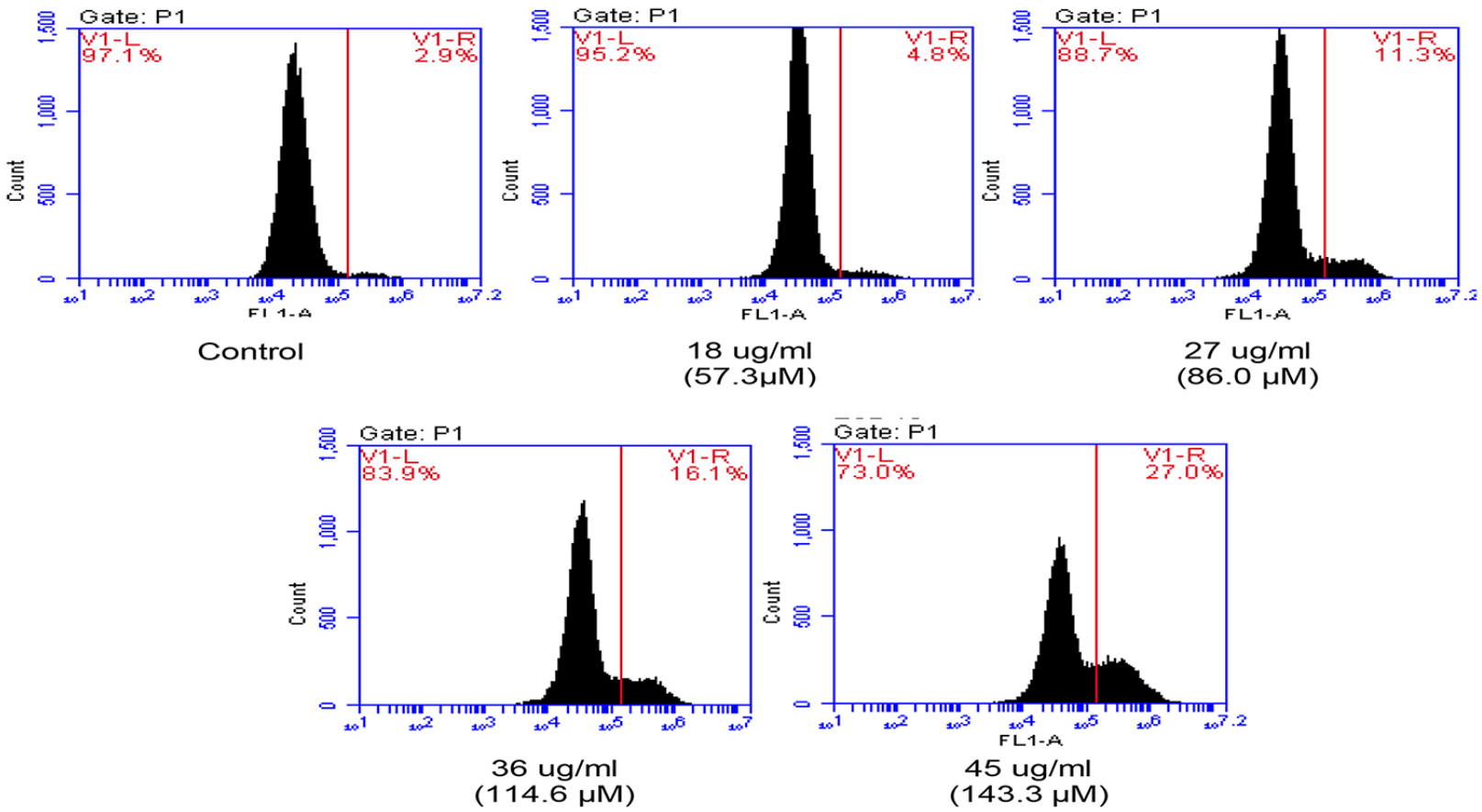

Figure 4.28(A): Caspase 3 activity of A549 cells treated with various concentrations of chalepin and incubated for 48 hours. Flow cytometric analysis of apoptotic (V1-R) and non-apoptotic populations (V1-L) for active caspase 3 activity for untreated A549 cells and A549 cells treated with chalepin at various concentrations for 48 hours.

(B)

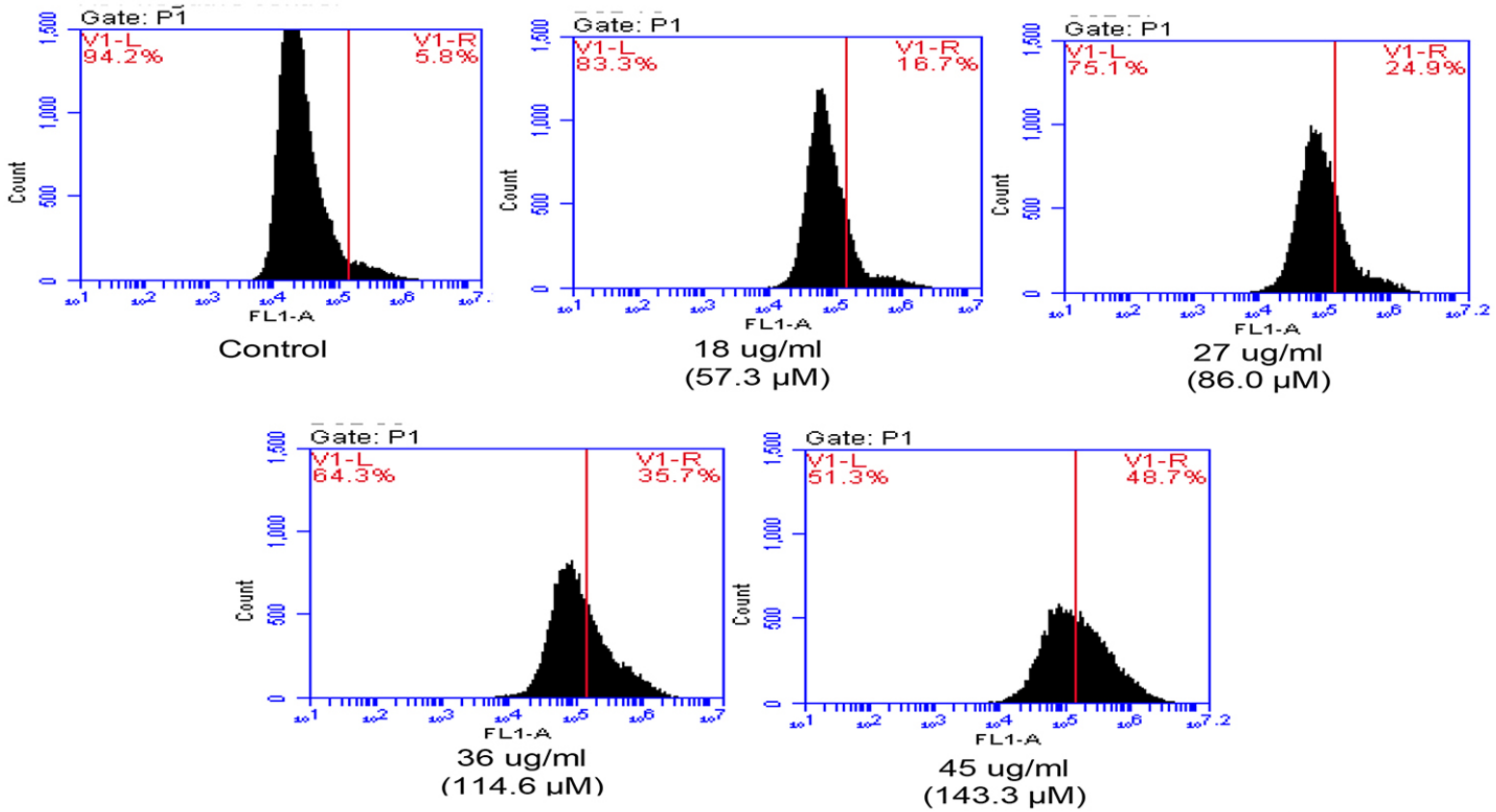

Figure 4.28(B): Caspase 3 activity of A549 cells treated with various concentrations of chalepin and incubated for 72 hours. Flow cytometric analysis of apoptotic (V1-R) and non-apoptotic populations (V1-L) for active caspase 3 activity for untreated A549 cells and A549 cells treated with chalepin at various concentrations.

(C)

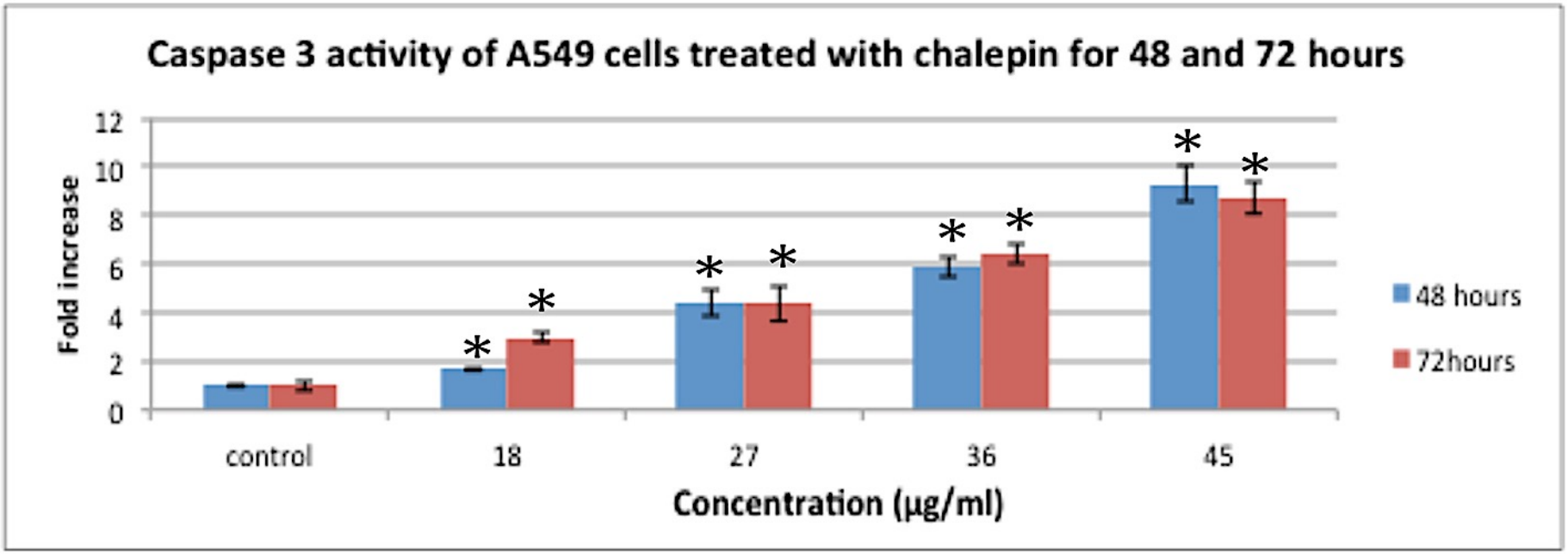

Figure 4.28(C): Bar chart representing the fold increase of caspase 3 activity in A549 cells treated with chalepin at various concentrations and different incubation time as compared to the untreated control cells. The data expressed as mean ± S.D. of three replicates. Asterisks indicates significantly different value from control (*$p<0.05$).

4.7.7 Caspase 8 Activation Analysis

Caspase 8 is associated with the activation of the extrinsic apoptotic pathway. CaspILLUME fluorescein active caspase 8 staining kit was used to determine the caspase 8 activity in regards to the treatment of chalepin in A549 cells. Cells with activated caspase 8 would move to the right side (V1-R) of the density plot (Figure 4.29(A)). The results show that there is a remarkable increase in the caspase 8 activity of cells treated with chalepin as compared to the control. It was observed that after 48 hours of incubation there is a five-fold increase in the activation of caspase 8 from 4.93 ± 0.15 % in untreated control to 26.0 ± 0.36 % in cells treated with 45 μg/ml of chalepin. As for the 72 hours incubation period, there was an increase from 6.43 ± 0.12 % for untreated control cells to 53.7 ± 0.31 % for treated cells with 45 μg/ml of chalepin which corresponds to a 8.33 fold increase. Caspase 8 is a member of the cysteine protease family, which is involved in apoptosis. Caspase 8 is synthesised as an inactive procaspase 8 which will then undergo proteolytic cleavage to be activated. Ligand binding to death receptors induced trimerisation of the death receptors, which results in recruitment of receptor specific adaptor proteins such as Fas-associated death domain (FADD), which will in turn recruit caspase 8. Activated caspase 8 starts an apoptotic signal cascade which activates downstream caspases such as caspase 3 or caspase 7 or on the other hand may also cause the cleavage of Bcl-2 protein which can lead to the release of cytochrome c from the mitochondria and to trigger mitochondrial mediated intrinsic apoptotic pathway (Kruidering et al., 2000).

These results show that chalepin treated cells undergo apoptosis through the activation of caspase 8.

(A)

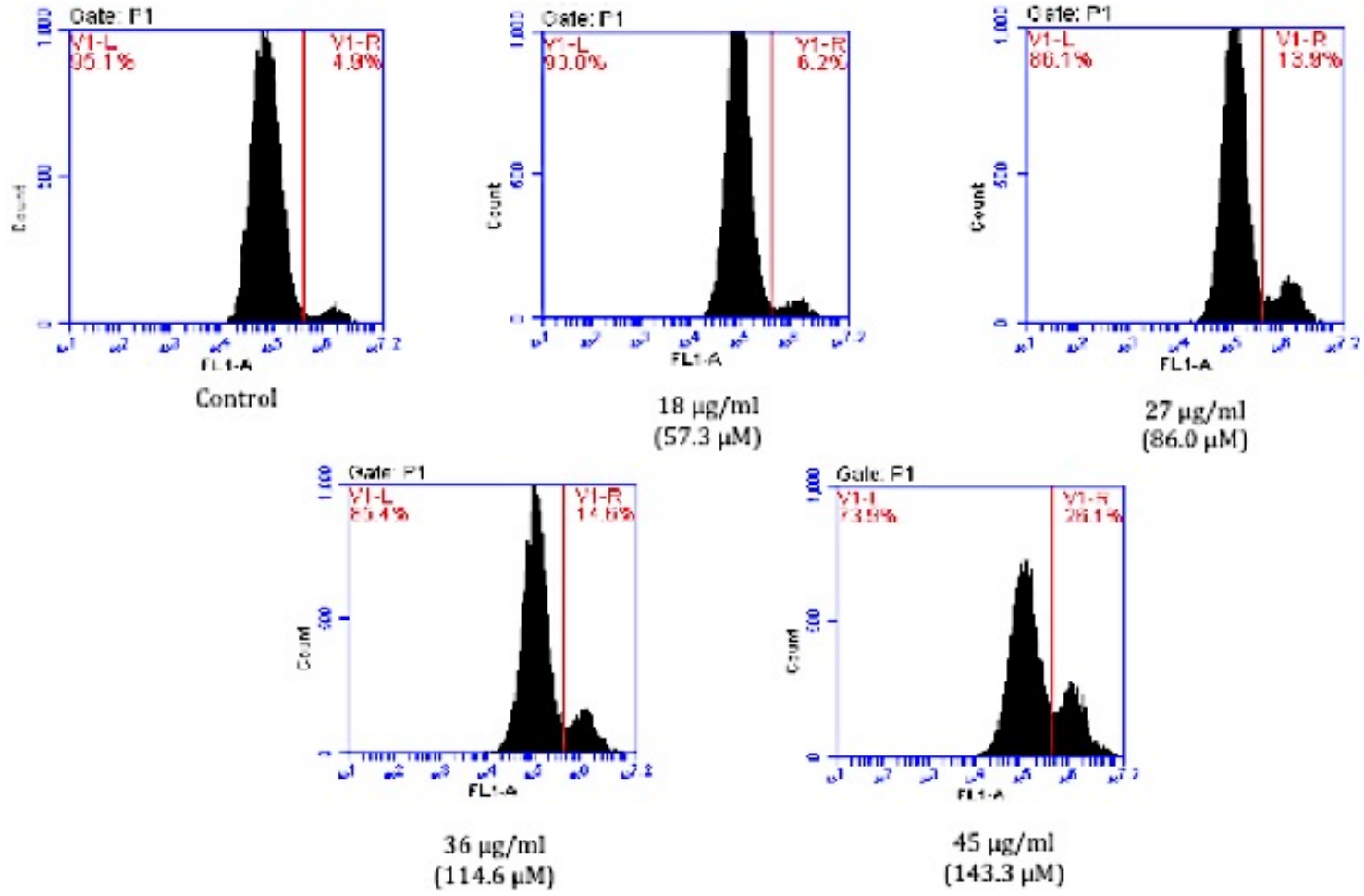

Figure 4.29(A): Caspase 8 activity of A549 cells treated with various concentrations of chalepin and incubated for 48 hours. Flow cytometric analysis of apoptotic (V1-R) and non-apoptotic populations (V1-L) for active caspase 8 activity for untreated A549 cells and A549 cells treated with chalepin at various concentrations for 48 hours.

(B)

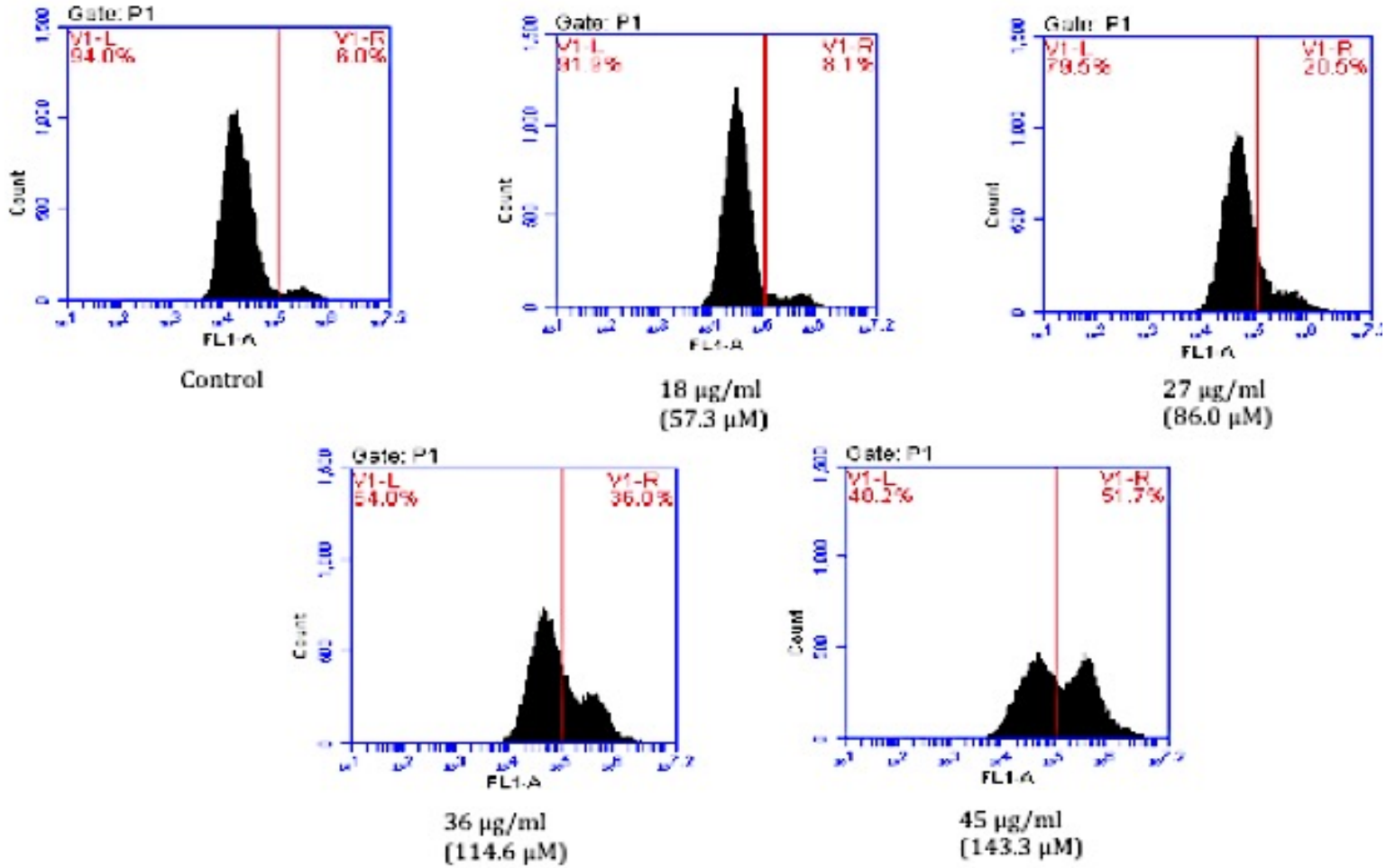

Figure 4.29(B): Caspase 8 activity of A549 cells treated with various concentrations of chalepin and incubated for 72 hours. Flow cytometric analysis of apoptotic (V1-R) and non-apoptotic populations (V1-L) for active caspase 8 activity for untreated A549 cells and A549 cells treated with chalepin at various concentrations for 72 hours.

(C)

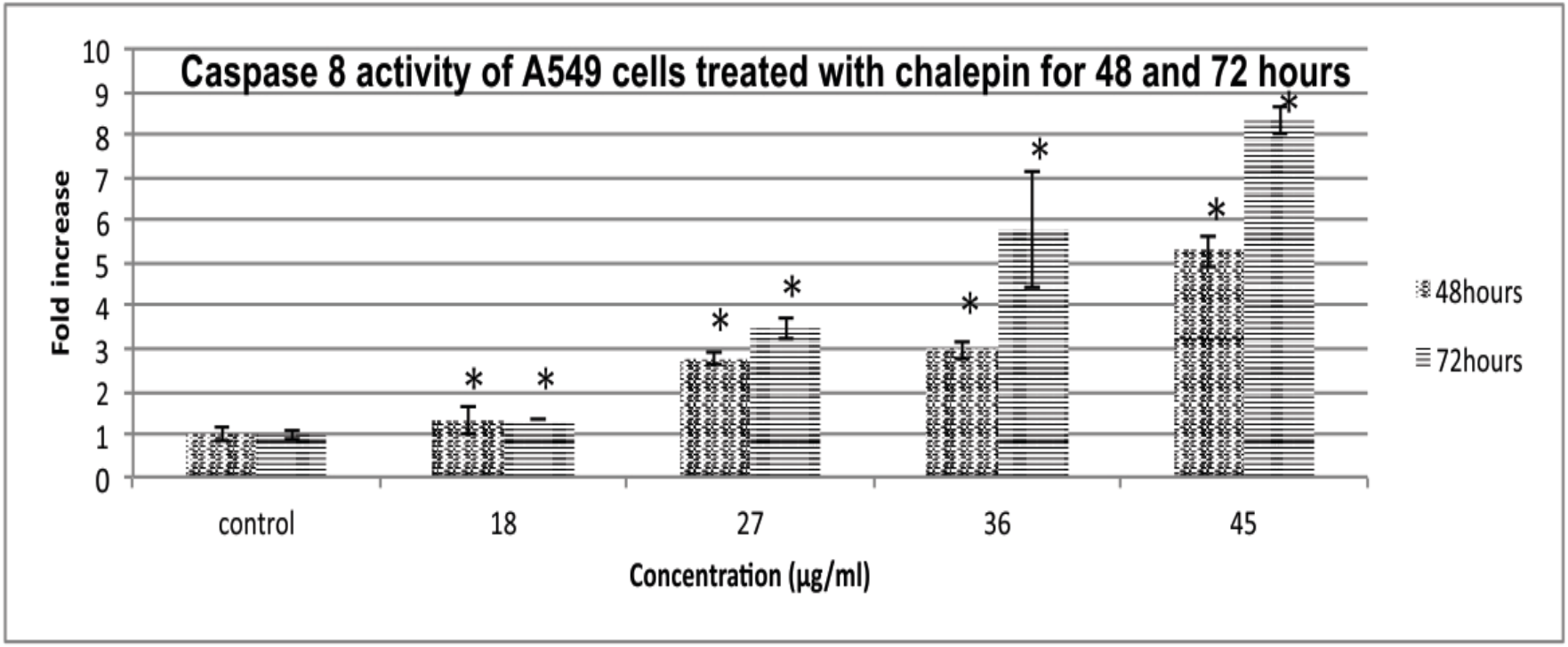

Figure 4.29(C): Bar chart representing a comparison of fold increase between chalepin treated A549 cells at different concentrations and incubation times (48 & 72 h). The data expressed as mean ± S.D. of three replicates. Asterisks indicates significantly different value from control (*$p<0.05$).

4.8 Cell Cycle Analysis

Cell cycle analysis was conducted in order to understand the ability of chalepin to affect cell proliferation was conducted. The A549 cells were labelled with propidium iodide and were evaluated with a flow cytometer to determine the phase in which the cells were accumulated post treatment of chalepin. There was a significant accumulation of cells in the S phase after treatment of chalepin for 48 and 72 hours (Figure 4.30). The accumulation was 27.73% at 48 hours and 25.38% at 72 hours after treatment with 45 μg/ml of chalepin. For the control (untreated) cells, the number of cells at the S phase was only about 4.02%. Accumulation of cells at a certain phase indicates that the cell cycle is arrested at that particular point. It was also observed that there was a slight increase in the G2/M phase at 72 hours, however the increase was neither dose dependent nor consistent. From the cell cycle analysis, it is apparent that chalepin arrests A549 cells at the S phase which is the synthesis phase where DNA replication occurs.

(A)

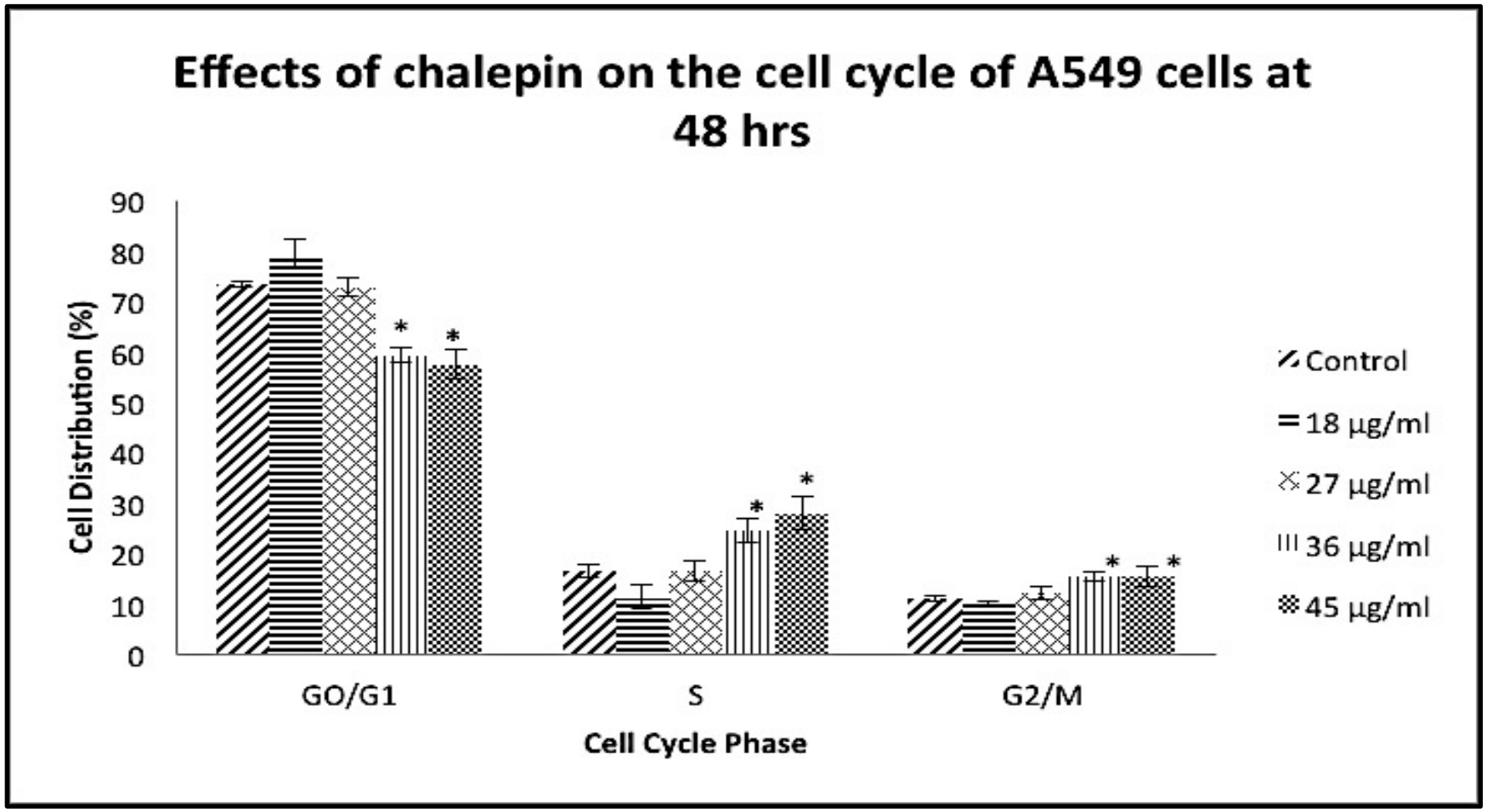

Figure 4.30(A): Bar chart representing cell distribution of A549 cells treated with various concentrations of chalepin for 48 hours at various cell cycle phases. Asterisks indicate significantly different value from control (*$p<0.05$). The data expressed as mean ± S.D. of three replicates.

(B)

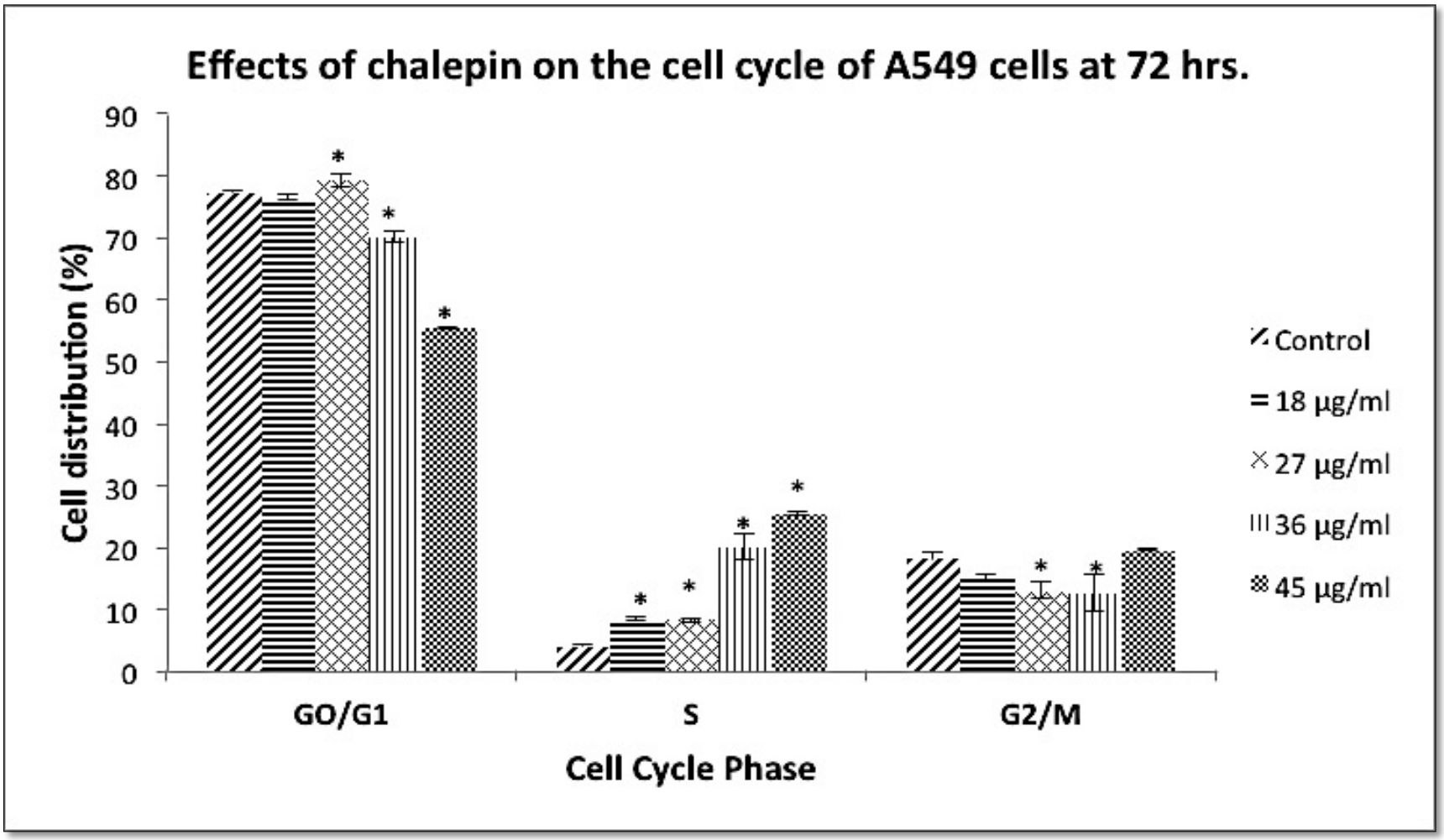

Figure 4.30(B): Bar chart representing cell distribution of A549 cells treated with various concentrations of chalepin for 72 hours at various cell cycle phases. Asterisks indicate significantly different value from control (*$p<0.05$). The data expressed as mean ± S.D. of three replicates.

(C)

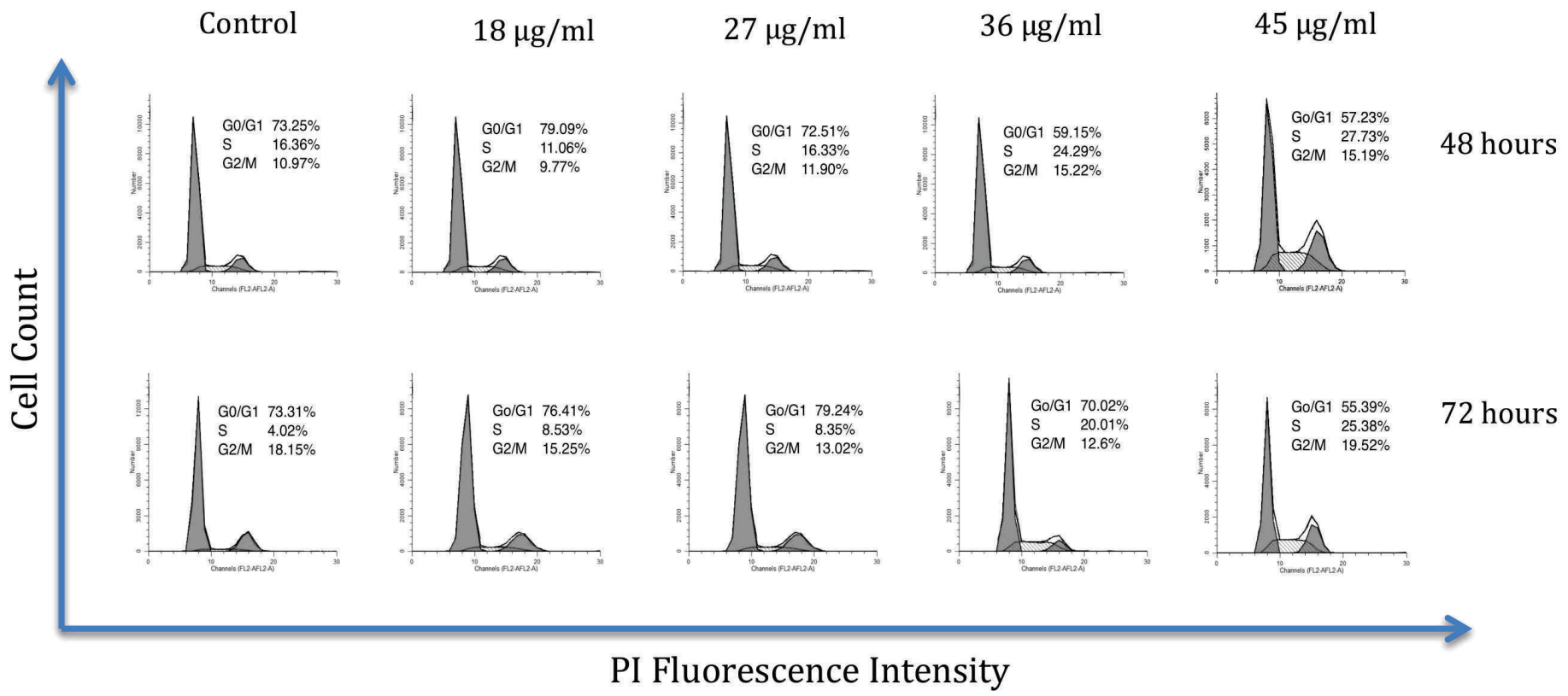

Figure 4.30(C): Flow cytometric cell cycle analysis of A549 cells treated with chalepin for 48 and 72 hours at various concentrations

4.9 Trypan Blue Dye Exclusion Assay

The results shows that at 24 hours, about 91.17 ± 1.53 % of viable cells were observed. The percentage of viable cells dropped sharply to 39.67 ± 1.89 % at 48 hours and to 12.0 ± 1.57 % at 72 hours.

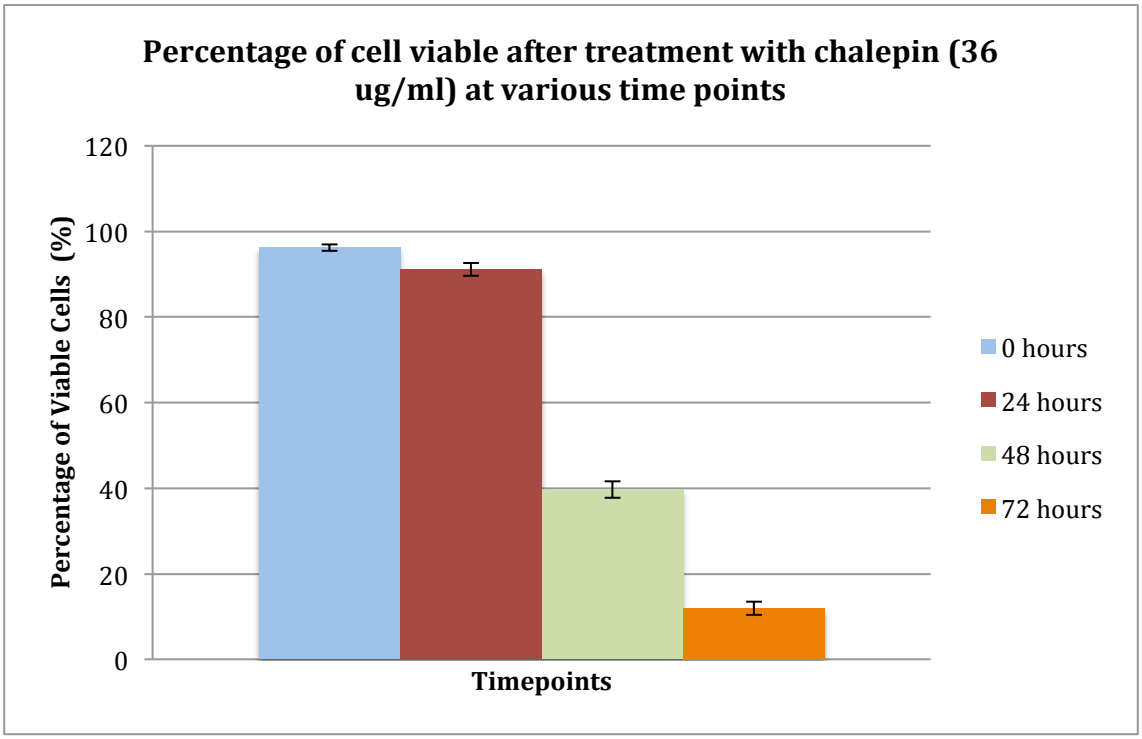

Figure 4.31: Trypan blue dye exclusion assay of A549 cells treated with chalepin (36 µg/ml) for various incubation time. Data showing the percentage of viable cells at different incubations of chalepin. The data expressed as mean ± S.D. of three replicates. Asterisks indicate significantly different value from control (*p<0.05).

It was observed that the treatment of the compound chalepin at 36 µg/ml results in cell death starting at 24 hours and henceforth leading to a sharp increase in the number of cell death (Figure 4.31). This was observed with the sharp decrease in the percentage of viable cells at 48 hours. Almost all cells have undergone death at the later time point which is at 72 hours. This results shows that apoptosis (cell death) commence at 24 hours. The suitable time point to study the expression of protein would be prior to 24

hours or up to 24 hours as the expression of protein after this time point might not give an accurate result.

From this assay, we have determined that the best time point to study the expression of protein for A549 cells treated with chalepin would be up to 24 hours.

4.10 Western Blot Analysis

4.10.1 Bradford standard curve for the estimation of protein concentration in samples

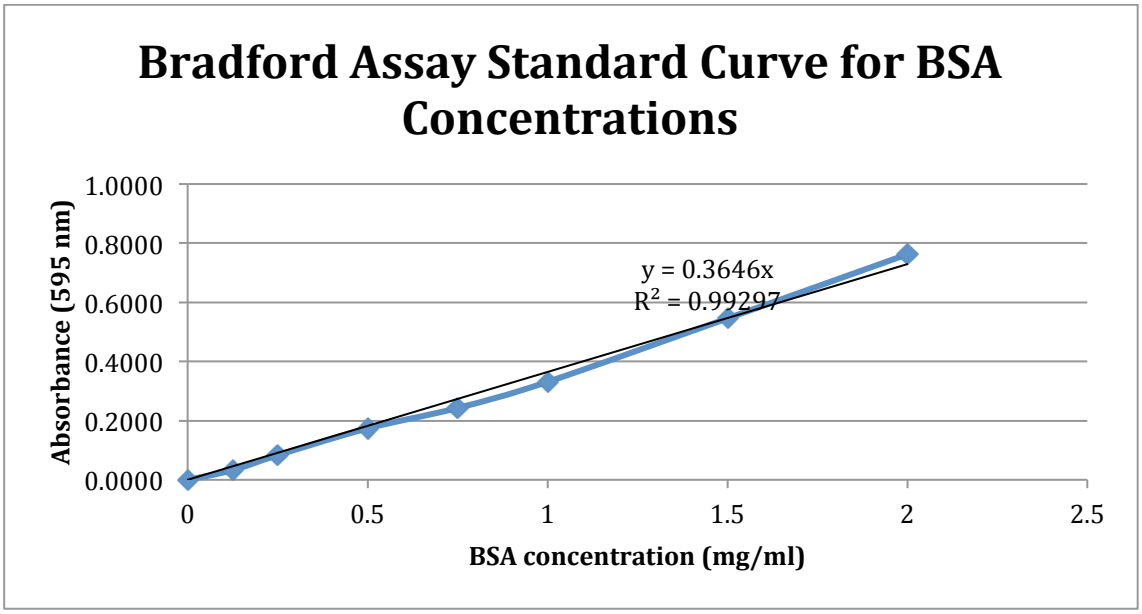

Figure 4.32: BSA standard curve of Bradford assay

The standard curve is of good data representation if the R^2 value is close to one. On our study, the R^2 value is of close proximity to 1 and thus the curve is of high accuracy. The straight line equation from the standard curve is y=0.3646x where y is the absorbance value and x is the concentration. Protein concentration was calculated by dividing the absorbance value of the sample to 0.3646.

4.10.2 Effects of chalepin on apoptotic related proteins

Changes in the expression of proteins involved in regulation of survival and cell death following chalepin treatment were examined by Western Blot analysis. Activation of caspase cascade would trigger proteolytic degradation of PARP and DNA fragmentation by endonucleases, leading to apoptosis. The expression of PARP was studied in A549 cells treated with chalepin at different incubation time. It was observed that the quantity of PARP expressed decreased with time. This shows that the level of PARP decreased with time as shown by Figure 4.33(A).

The mitochondrial mediated pathway is also known as BCL-2 regulated pathway. The balance of function between proapoptotic and antiapoptotic Bcl-2 protein family determines the fate of cells towards apoptosis (Czabotar et al., 2014). Studies have shown Bax, Bad, Bak promote the release of cytochrome c, while bcl-2 and Bcl-X_L delay this response and promote cell survival. Bcl-2 family members regulate the apoptotic response by controlling the mitochondrial membrane permeabilization (MMP). Depolarisation of MMP and the formation of MPT (mitochondrial permeability transition) pore is a result of the tranlocation of Bax from cytosol to mitochondria (Chalah et al., 2008).

Chalepin was found to downregulate anti-apoptotic gene products such as Bcl-2, survivin, XIAP, Bcl-xl and cFLIP as shown by Figure 4.33(B) This clearly shows that it downregulates proteins that play a vital role in the cell survival and thus, induces apoptosis. An upregulation in the expression of Bax was observed Figure 4.33(C). There was an upregulation in the expression of cytochrome c, Figure 4.33(C), which shows that the cytochrome c moved out of mitochondria to cytosol leading to an upregulation of cytochrome c. All these factors promotes cell cytolysis or cytostasis.

The cytochrome c release and binding with dATP and Apaf-1 results in formation of apoptosome which recruits and activates caspase-9. Activated caspase 9, results in activation of effector caspases such as caspase-3/7. These effector caspases then initiates apoptosis events. Results indicated that chalepin induces cleavage of procaspases 9 and 3 to the active cleaved form. Procaspase 9 showed a downregulation which indicated cleavage of the protein to an active form. Procaspase 3, also showed downregulation which indicated an activation. This result is further stregthened by detection of the cleaved caspase 3 which showed an upregulation. All these results are illustrated in Figure 4.33(D). This clearly indicates that the intrinsic pathway which is mediated by the mitochondria is activated. These results are consistent with earlier caspase 3 and caspase 9 activity determinations using flow cytometer.

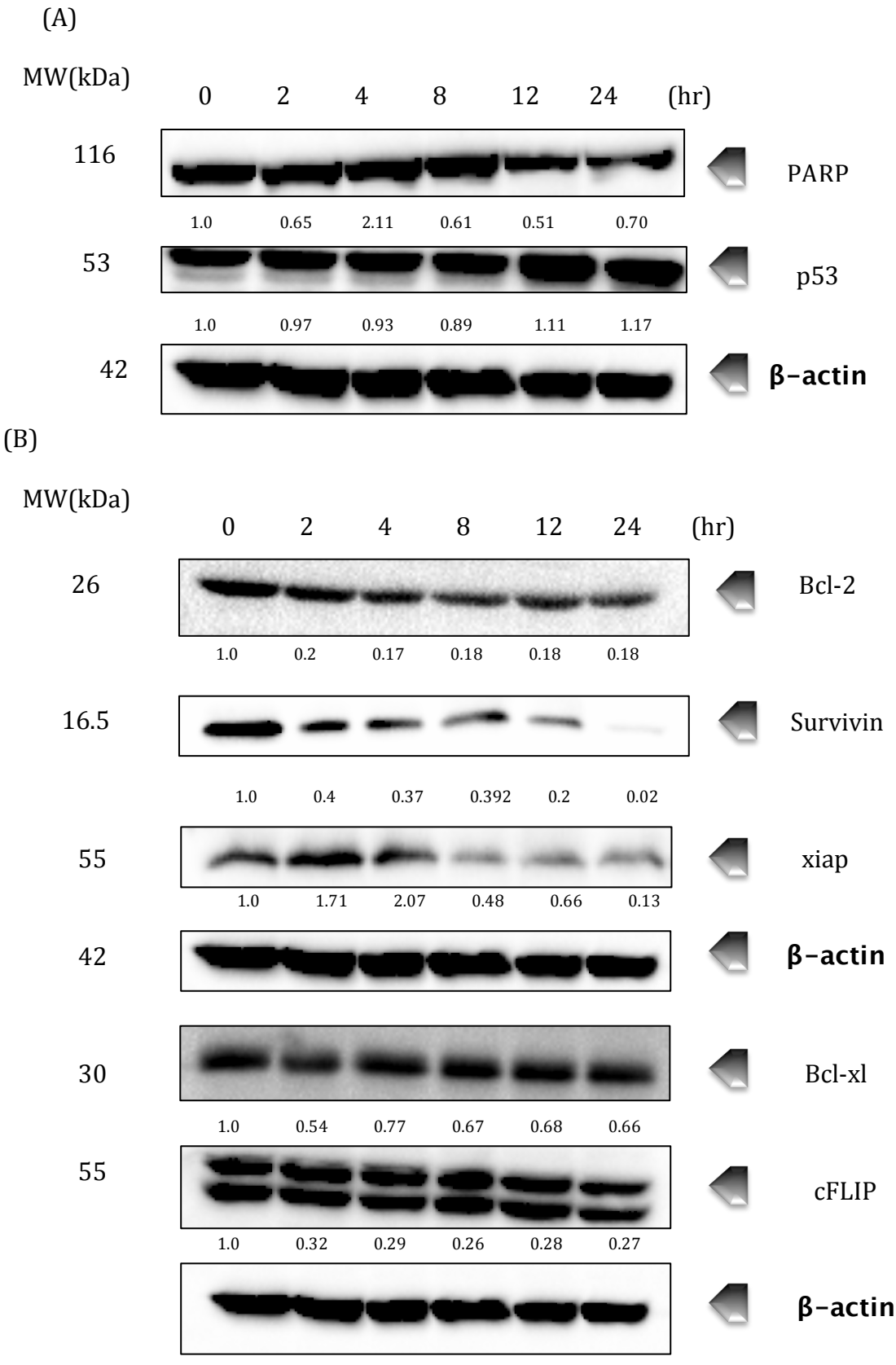

Figure 4.33: Western blot analysis of whole cell protein lysate of A549 cells treated with chalepin at concentration of (36 µg/ml) at 2,4,8,12, and 24 h. (A) Cleavage of PARP and upregulation of p53 tumor supressor factor, induced by chalepin.(B) Chalepin (36 ug/ml) inhibits anti-apoptotic gene products.

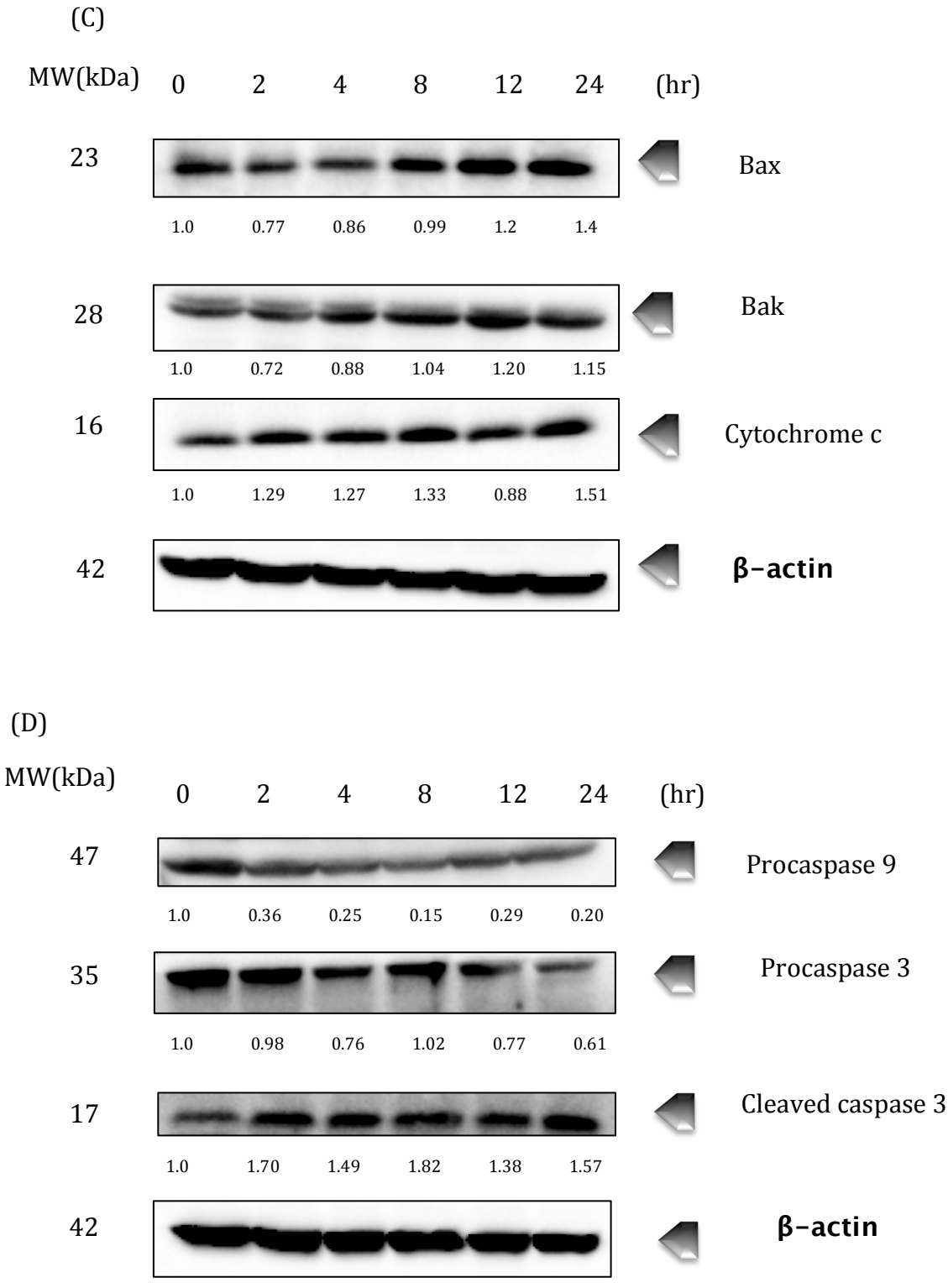

Figure 4.33: Western blot analysis of whole cell protein lysate of A549 cells treated with chalepin at concentration of (36 µg/ml) at 2,4,8,12, and 24 h. (C) Chalepin induces Bax and bak expression and cytochrome c release. (D) Chalepin activates cleavage of procaspase 9 and procaspase 3.

4.10.3 Effects of chalepin on cell cycle related proteins

Western blot analysis was conducted to determine the expression level of cell cycle related proteins as shown in Figure 4.34. Cell cycle is a process, which involves interaction between cyclins and cyclin dependant kinases (CDKs) and their inhibitors such as CDK interacting protein (CIP) and kinase inhibitory proteins (KIP). Figure 4.34 shows that cyclins i.e. cyclin E and cyclin D1 are downregulated. Cyclin D1 regulates the progression of cell cycle from phase G0/G1 to S phase wherease cyclin E regulates the progression between S phase to G2/M phase. Downregulation of both the cyclins indicates that the cell cycle is hindered at all the phases. Cyclin-dependent kinases (CDKs) are serine/threonine kinases, which are regulated by cyclins and cyclin dependent kinase inhibitors. CDKs and cyclins complexes to initiate the progression of cell cycle in a cell however the kinase activity of the CDK/cyclin complex is tightly regulated by a group of cyclin-dependent kinase inhibitors (CKIs) which would stop the cell cycle from progressing under unfavourable conditions (Lim et al., 2013). The cyclin dependent kinases, which were, studied in this experiment i.e. Cdk 2 and Cdk 4 both showed downregulation with increasing time. This is another indication that the formation of complex between cyclin and Cdks are inhibited, and thus inhibiting the cell cycle progress. Two CKIs ($p21^{(CIP)}$ and $p27^{(KIP)}$) showed slight downregulation in this study and then upregulation as treatment time of chalepin increases. This indicates that upon treatment of chalepin, the CKIs which inhibit the formation of cyclin and Cdk complex is halted in the cell. It was also observed that pRb (phosphorylated retinoblastoma protein) showed dramatic downregulation. Rb protein is responsible in inducing the E2F transcription factor into the nucleas to initiate transcription of cell cycle related genes. The hypophosphorylation indicates that this process is inhibited and cell cycle is arrested in the S phase as replication of the DNA content is blocked.

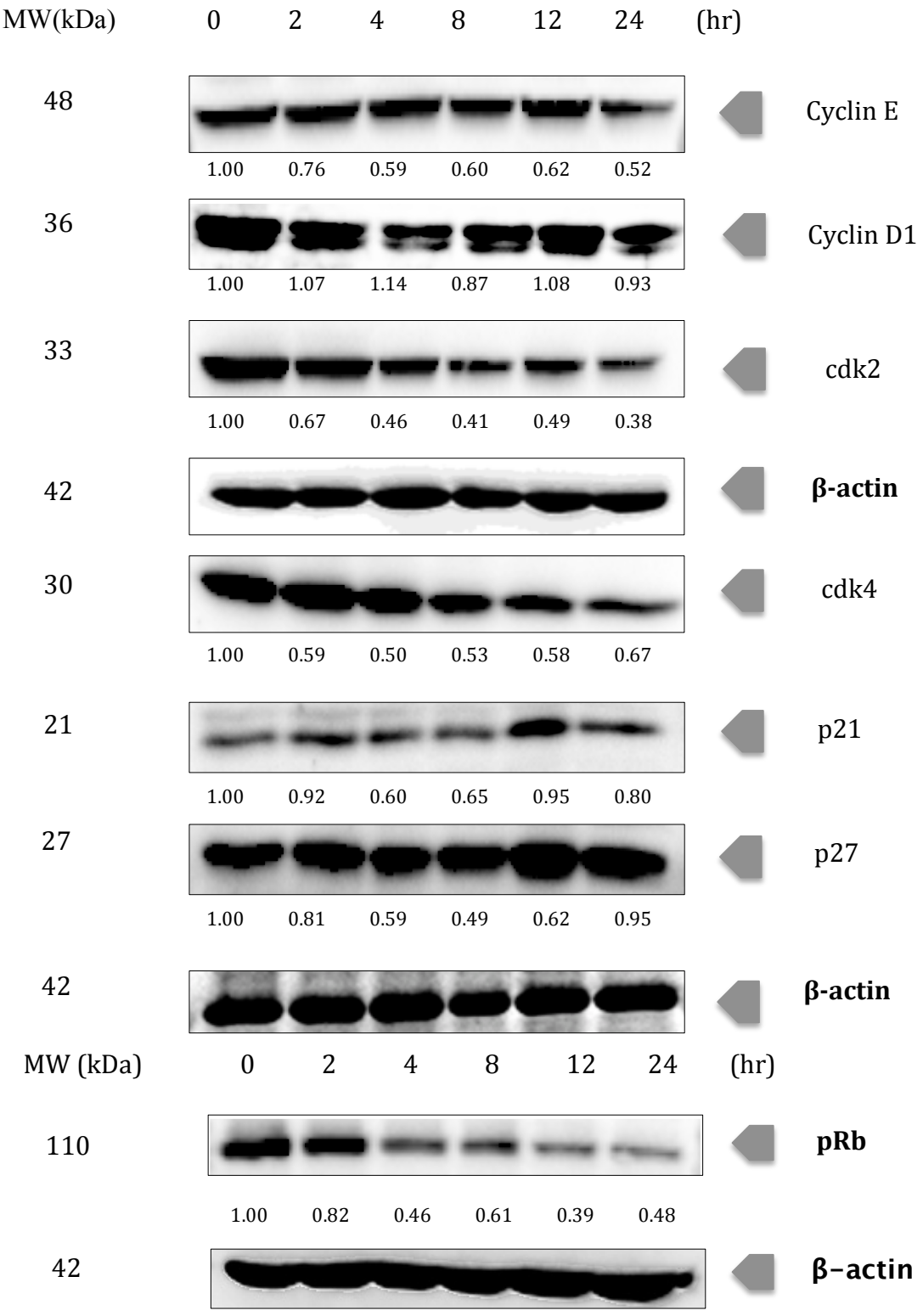

Figure 4.34 : Chalepin induces changes expression in cell cycle related proteins in a dose-dependent manner. A549 cells (2 x 10^6 mL^{-1}) were treated with 36 µg/ml of chalepin at various timepoints, after which the whole-cell extracts were prepared and 30 µg of protein was resolved by 12% SDS-PAGE gel, electrotransferred onto nitrocellulose membranes and probed for the cyclin E, cyclin D1, Cdk2, Cdk4, p21, p27 and phosphorylated Rb proteins. The experiments were conducted in triplicates.

4.10.4 Effect of chalepin on anti-apoptotic proteins

The effect of chalepin on anti apoptotic proteins such as cIAP-1, cIAP-2 and Mcl-1 was evaluated. Western blot results show that the anti apoptotic gene products are downregulated. Cellular inhibitors of apoptosis 1 and 2 (cIAP-1 and cIAP-2) can inhibit death receptor-mediated apoptosis, however they are often over-expressed in cancers. Both the anti apoptotic gene products showed downregulation upon treatment with chalepin (Figure 4.35). Mcl-1 is an anti-apoptotic Bcl-2 family member. It is important for the survival of multiple cell lineages and was found to be one of the most highly amplified genes in cancer (Perciavalle et al., 2012). In this study, Mcl-1 has been suppressed upon treatment with chalepin, which suggests that apoptosis is favoured.

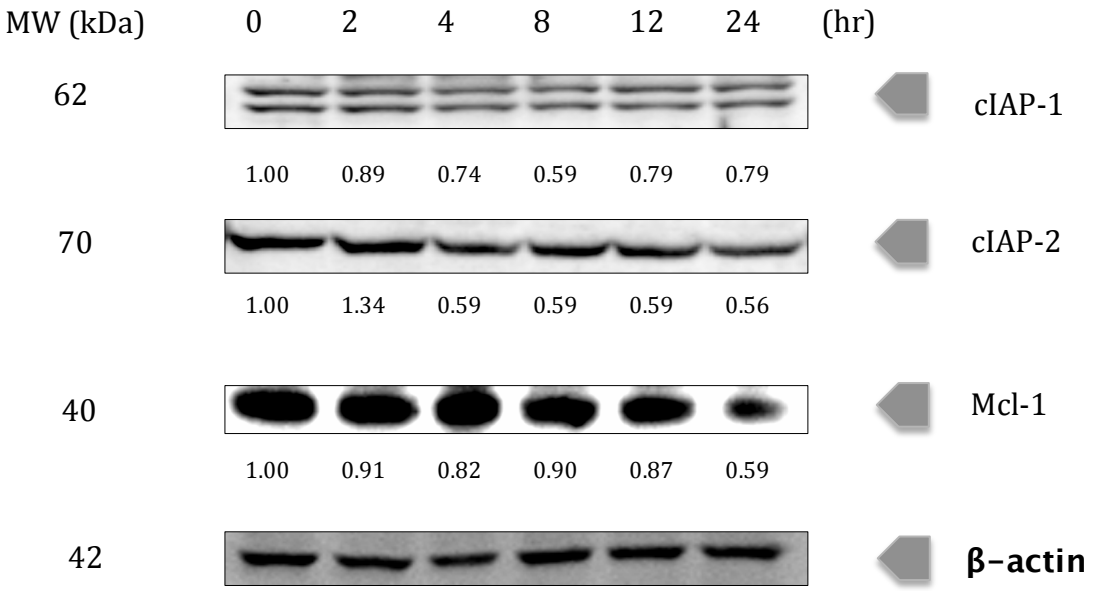

Figure 4.35: Chalepin inhibits the expression of anti-apoptotic gene products, cIAP-1, cIAP-2 and MCl-1 in a dose-dependent manner. A549 cells (2 x 10^6 mL^{-1}) were treated with 36 µg/ml of chalepin at various timepoints, after which the whole-cell extracts were prepared and 30 µg of protein was resolved by 12% SDS-PAGE gel, electrotransferred onto nitrocellulose membranes and probed for cIAP-1, c-IAP-2 and Mcl-1. The experiments were conducted in triplicates.

4.10.5 Effect of chalepin on the expression of Cox-2 and c-myc

Cox-2 and c-Myc play an important role in growth modulation. Treatment of chalepin on A549 cells resulted in downregulation of both these gene products (Figure 4.36). Cox-2 is upregulated during both inflammation and cancer. Cox-2 was discovered to modulate cell proliferation and apoptosis mainly in solid tumors, such as, colorectal, breast, and prostate cancers, and, more recently, in hematological malignancies. These findings prompted many analyses on the effects of a combination of Cox-2 inhibitors together with different clinically used therapeutic strategies in order to further improve the efficiency of future anticancer treatments (Sobolewski et al., 2010). A549 cells treated with chalepin exhibited substanstial downregulation after 24 hours of treatment. Chalepin therefore acts as a Cox-2 inhibitor. c-Myc is an oncogene which controls regulation of cellular growth and cellular metabolism. Often, c-Myc overexpression is necessary to support the the increased need for nucleic acids, proteins and lipids that are utilised in rapid cellular proliferation. In cancer cells, c-Myc is almost always overexpressed, sometimes by mutations in the gene itself or more commonly through the induction of c-Myc expression through upstream oncogenic pathways (Miller et al., 2012). The ability of chalepin to inhibit the expression of this gene product is a significant result in halting the metabolism support that is needed for the growth of the A549 human lung carcinoma cell.

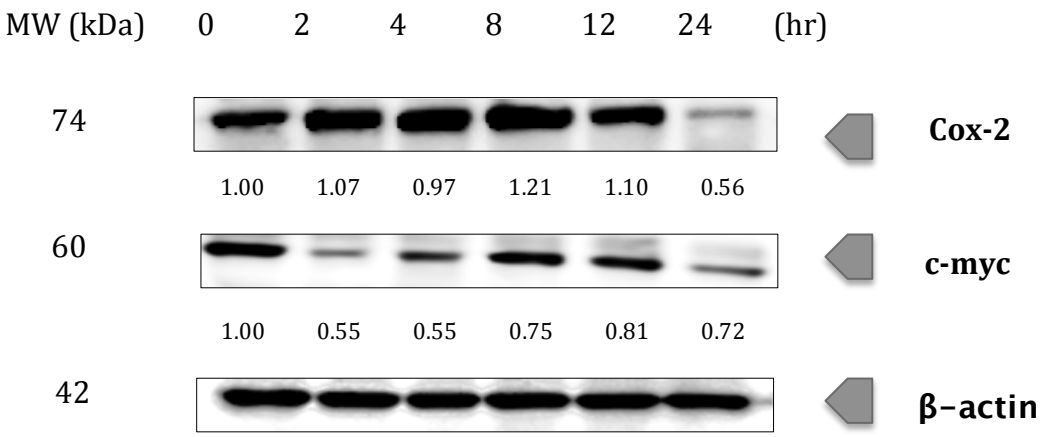

Figure 4.36: Chalepin inhibits the expression of Cox-2 and c-myc in a dose-dependent manner. A549 cells (2 x 10^6 mL^{-1}) were treated with 36 µg/ml of chalepin at various timepoints, after which the whole-cell extracts were prepared and 30 µg of protein was resolved by 12% SDS-PAGE gel, electrotransferred onto nitrocellulose membranes and probed for Cox-2 and c-Myc. The experiments were conducted in triplicates.

4.10.6 Effects of chalepin on NF-kB pathway

NF-κB or nuclear factor-kappa B is an omnipresent transcription factor. It consists of a few subunits such as p50, p65 and Iκβα, which resides in the cytoplasm. When there is external stimuli such as inflammation, environmental pollutions, prooxidants, carcinogens, stress and growth factors, these subunits are activated. External stimuli generally activates the IκB Kinase (IKK) complex. There are a few kinases which assist in this activation which is known as Iκβα kinases (IKK). The regulatory step in this pathway requires activation of Iκβ Kinase (IKK) complex that has high molecular weight. The catalysis of IKK is generally carried out by three tightly associated IKK subunits. IKKα and IKKβ serve as the catalytic subunits of the kinase and IKKγ or commonly known as NEMO serves as the regulatory subunit (Israël, 2010). The activation of IKK initiates upon phosphorylation at Ser177 and Ser181 in the activation loop of IKKβ (Ser176 and Ser180 in IKKα), which causes conformational changes, resulting in kinase activation. The increase in the activity of kinase will result in the phosphorylation of the NF-κB inhibitor, which is Iκβα that would result in dissociation

of the inhibitor from NF-κB, and ubiquitination of the Iκβα. The ubiquination would then recruit proteosome which would degrade the Iκβα, inhibitor (Karin, 1999). The free NF-κB would then move to nucleas to initiate transcription of DNA to mRNA and then further translate to proteins which would subsequent respond to the initial external stimuli by causing changes in the cell. This activation has been known to affect various gene products, which regulates inflammation, cancer, angiogenesis, metastasis, apoptosis and chemoresistance (Sethi et al., 2008). The response of chalepin towards the NF-κB pathway was studied in A549 cells. Nuclear extracts and cytoplasmic extracts were prepared and the proteins expressed were studied. Results shows that the content of p65 subunit protein in the nuclear extract was almost constant with slight upregulation and then a downregulation as the treatment time increases. Chalepin also inhibited the phosphorylation of p65, which hinders its activation. Cytoplasmic extract was used to study the degradation of Iκβα and phosphorylation of Iκβα. Results showed that chalepin inhibits the degradation of Iκβα. The expression showed an upregulation at 1 hours treatment time and showed slight downregulation and then upregulation as the incubation time is increased. However, the degradation of Iκβα is either inhibited or constant depending upon the incubation time. Phosphorylation of Iκβα was inhibited as the results showed a downregulation in the expression of pIκβα. Overall, the results indicates that the NF-κB pathway is suppressed especially at earlier incubation time. The results are represented in Figure 4.37.

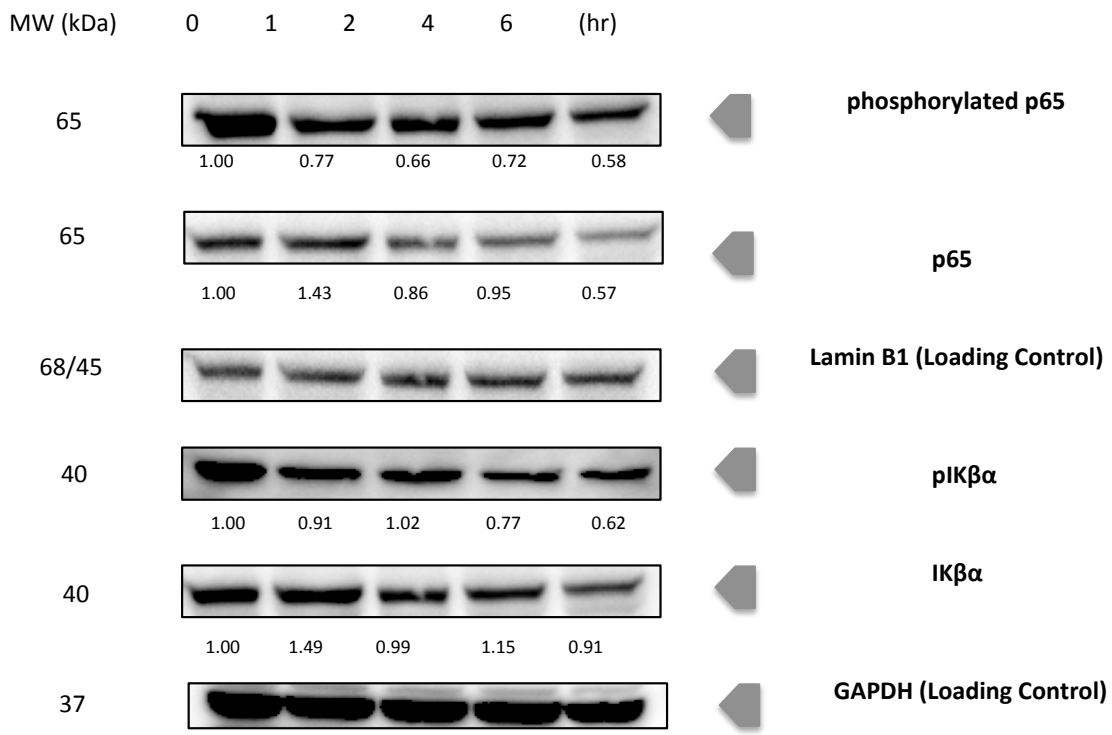

Figure 4.37: Chalepin suppresses NF-κB pathway in a time dependent manner. A549 cells (2 x 10^6 mL^{-1}) were treated with 36 μg/ml of chalepin at various timepoints (0,1,2,4 and 6 hours), after which the cell nuclear extracts and cytoplasmic extracts were prepared and 30 μg of protein was resolved by 10% SDS-PAGE gel, electrotransferred onto nitrocellulose membranes and probed for phosphorylated p65, p65, phosphorylated IKβα and IKβα. The experiments were conducted in triplicates.

4.10.7 Effects of chalepin on the STAT3 phosphorylation

Signal transducer and activator of transcription 3 (STAT3) has been linked to proliferation, survival, invasion and angiogenesis of a variety of human cancer cells. Among the family of STAT signalling proteins, STAT3 has been most closely linked to tumorigenesis. Persistent activation of STAT3 has been frequently observed in many kinds of tumor formation (Sethi et al., 2014). Upon activation by interleukins or cytokines, STAT3 becomes phosphorylated and then undergoes dimerisation, which results in nuclear translocation and DNA binding which subsequently induce gene transcription of genes, which are essential for cell growth and thus initiate

tumorigenesis. In this study, the expression of total STAT3 is almost constant whilst the expression of phosphorylated STAT3 showed considerable downregulation. This shows that chalepin has the effect of inhibiting the activation of this transcription factor by inhibiting the phosphorylation that would eventually stop the downstream gene transcription process. Results are represented in Figure 4.38.

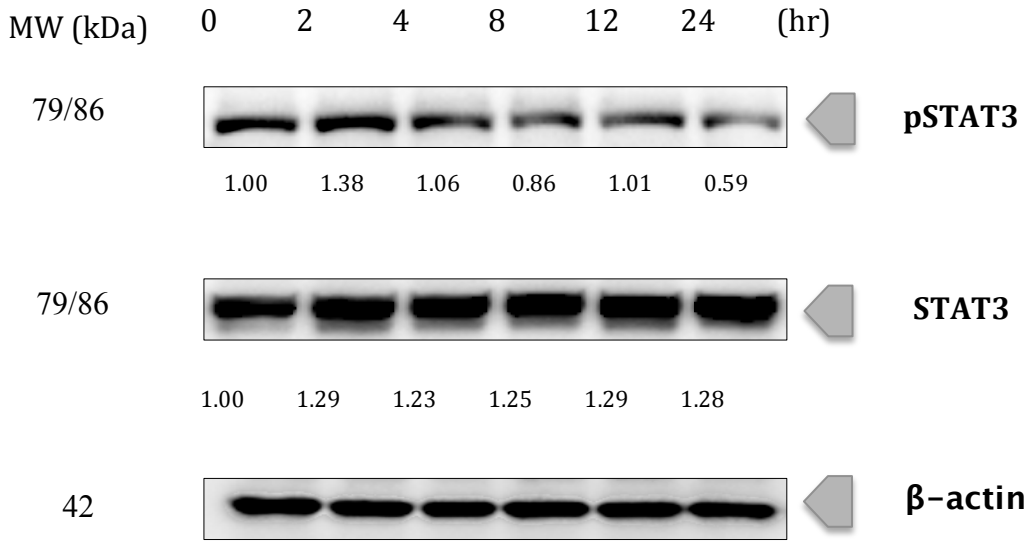

Figure 4.38: Chalepin inhibits constitutive STAT3 phosphorylation in A549 cell line in a time dependent manner. A549 cells (2 x 10^6 mL^{-1}) were treated with 36 µg/ml of chalepin at various timepoints, after which the whole-cell extracts were prepared and 30 µg of protein was resolved by 12% SDS-PAGE gel, electrotransferred onto nitrocellulose membranes and probed for phosphorylated STAT3 and STAT3. The experiments were conducted in triplicates.

4.10.8 Effects of chalepin on death receptors

Death receptors play an importat role in initiating the extrinsic apoptotic pathway. Death receptor 4 (DR4) and death receptor 5 (DR5) was downregulated upon treatment of chalepin up till an incubation time of 12 hours. Interestingly, there was an upregulation at 24 hours incubation time (Figure 4.39).

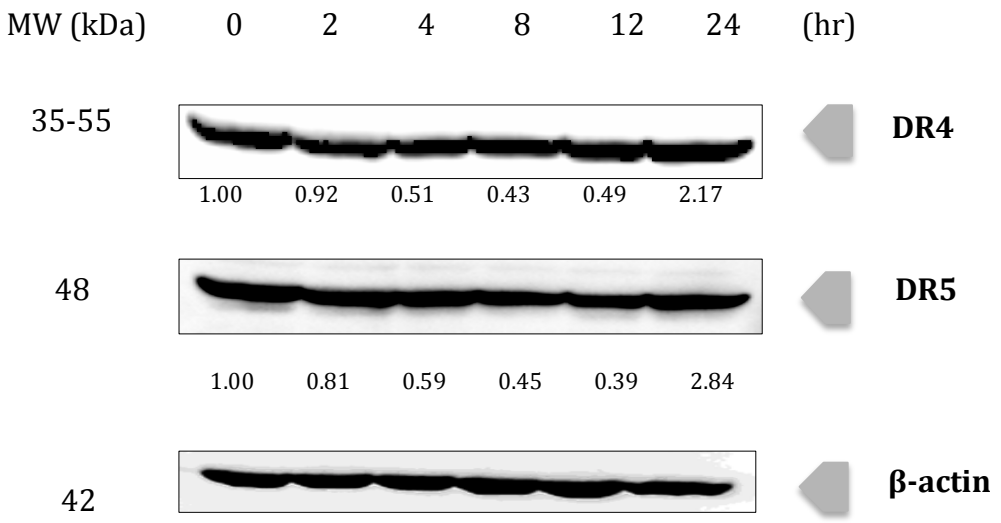

Figure 4.39: Chalepin increases expression level of death receptors in A549 cell line in a time dependent manner. A549 cells (2 x 10^6 mL^{-1}) were treated with 36 µg/ml of chalepin at various timepoints, after which the whole-cell extracts were prepared and 30 µg of protein was resolved by 12% SDS-PAGE gel, electrotransferred onto nitrocellulose membranes and probed for DR4 and DR5. The experiments were conducted in triplicates.

4.10.9 Effect of chalepin on cleavage of BID

Results showed that chalepin induces cleavage of BID. This result is consistent with the activation of caspase 8 which was shown earlier through the flow cytometry assay. BID is a BH3 domain containing proapototic Bcl-2 family member which is a substrate to the caspase 8 which is activated by death receptor mediated apoptotic signalling pathway. BID would be cleaved by caspase 8 to truncated BID (tBID) and this would translocate to mitochondrial to initiate the intrinsic/mitochondrial-mediated apoptosis (Li et al., 1998).

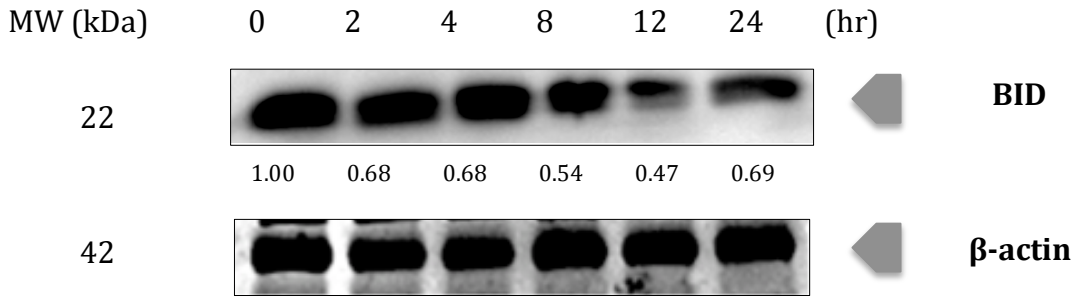

Figure 4.40: Chalepin promotes cleavage of BID in A549 cell line in a time dependent manner. A549 cells (2 x 10^6 mL^{-1}) were treated with 36 µg/ml of chalepin at various timepoints, after which the whole-cell extracts were prepared and 30 µg of protein was resolved by 12% SDS-PAGE gel, electrotransferred onto nitrocellulose membranes and probed for BID protein. The experiments were conducted in triplicates.

4.10.10 Effect of chalepin on metastasis related proteins

Intercellular adhesion molecule 1 or more commonly known as ICAM-1 is a cell surface glycoprotein and expressed in fibroblasts, leukocytes, and is commonly upregulated in the presence of inflammatory mediators and also in epithelial tumorigenesis (Rosette et al., 2005). This molecule that acts as an adhesion molecule was found to enhance metastasis of some cancer cells. Particularly, a study showed that in lung cancer, inhibition of this molecule stops the invasion. In our study, chalepin was found to inhibit this molecule in A549 cells. There was a drop up till 0.20 fold as compared to control (1.00). Vascular endothelial growth factor (VEGF) is a glycoprotein, which mediates angiogenesis and acts a key mediator in angiogenesis in cancer. Angiogenesis is an important event in cancer development and growth as cancer cells requires nutrition and oxygen to thrive (Carmeliet, 2005). A549 cells treated with chalepin showed to downregulate the expression of VEGF proteins and thus suppress angiogenesis. The downregulation was the highest at 2 hours incubation where it dropped to 0.48 fold. Subsequently this drop showed an increase as the incubation time was increased (Figure 4.41).

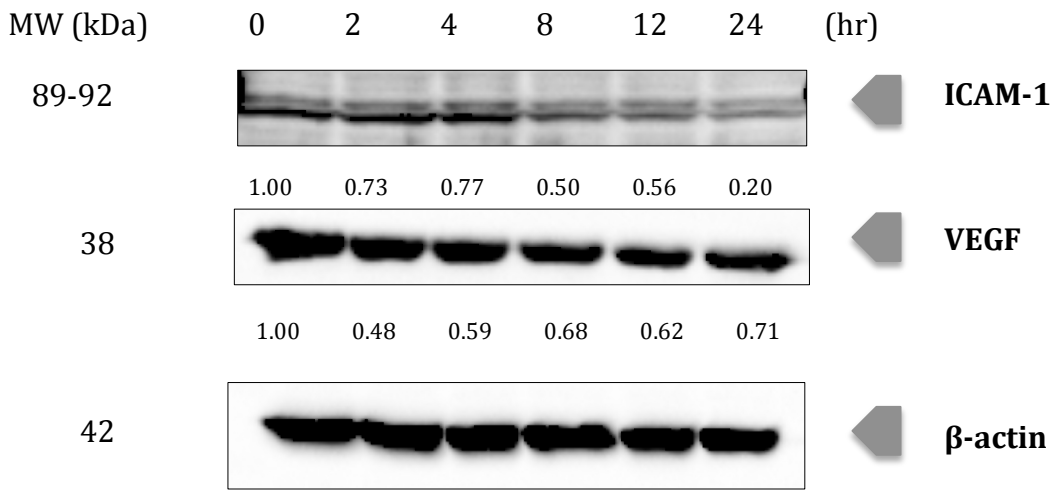

Figure 4.41: Effects of chalepin on metastasis related proteins Chalepin inhibits the expression metastasis related proteins in a dose-dependent manner. A549 cells (2 x 10^6 mL^{-1}) were treated with 36 µg/ml of chalepin at various timepoints, after which the whole-cell extracts were prepared and 30 µg of protein was resolved by 12 % SDS-PAGE gel, electrotransferred onto nitrocellulose membranes and probed for ICAM-1 and VEGF. The experiments were conducted in triplicates.

4.10.11 Effects of chalepin on EGFR pathway related proteins

EGFR or epidermal growth factor receptor is a transmembrane protein which, is activated when it binds to peptide growth factors. EGFR was found to be involved in progression of various types of cancer. In our study, chalepin was found to inhibit the expression of the EGFR receptor and also inhibites the phosphorylation of EGFR thus stops the activation of this receptor. The pEGFR showed a drop up to 0.42 while total EGFR showed a trend of decrease in the expression at the earlier incubation time and then a slight increase thereafter.

Expression of Jak 1 in cancer cells often enables it to metastasize to different site in the body through contact with individual cells. Results showed that chalepin was able to inhibit this protein upon treatment in A549 cells. A study by Song et al., 2011 showed that JAK1 (a small molecule) activated STAT3 activity in NSCLC. STAT3 has been

found to promote the formation of tumor growth particularly in NSCLC. This notion correlates with the earlier shown results where chalepin exhibits a supression (drop to ~0.7-0.8 fold) in STAT3 phosphorylation. This supression could be due to the inhibition in the Jak1. Chalepin probably acts as the small molecule inhibitor.

Extracellular signal-regulated kinase pathway or the ERK pathway determines the cellular control of various processes such as cell motility, cell differentiation, survivability and proliferation. In human tumors, this pathway is often upregulated. Blockage of this pathway was found to result in anti-proliferative, anti-metastatic and anti-angiogenic effect in tumor cells (Kohno et al., 2006). In our study, the phosphorylation of ERK showed marked inhibition i.e. up to 0.29 fold at 12 hours from the initial 1.0 fold in control (0 hours) (Figure 4.42). This shows that chalepin stops the activation of ERK.

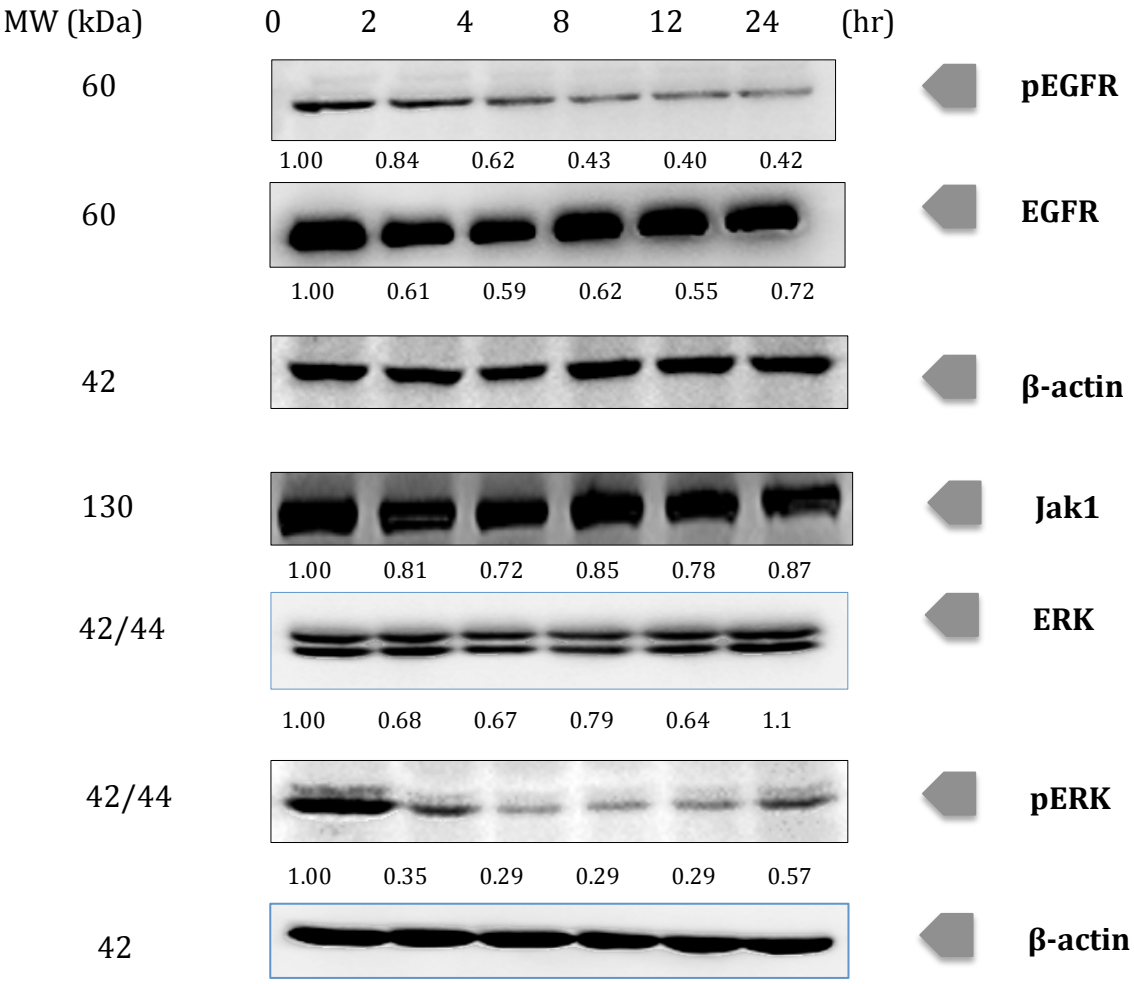

Figure 4.42: Effects of chalepin on EGFR pathway related proteins. Chalepin effects the expression of EGFR related proteins in a dose-dependent manner. A549 cells (2 x 10^6 mL^{-1}) were treated with 36 µg/ml of chalepin at various timepoints, after which the whole-cell extracts were prepared and 30 µg of protein was resolved by 12 % SDS-PAGE gel, electrotransferred onto nitrocellulose membranes and probed for respective antibodies. The experiments were conducted in triplicates.

AKT in its activated form is known to promote the survivability factor in the cell. It exerts antiapoptotic activity by preventing cytochrome c release from mitochondria. AKT also was found to phosphorylate proapoptotic factors such as Bad and procaspase 9 and thus inactivating it. A549 cells treated with chalepin showed an initial decrease in the expression of the phosphorylated AKT. However, at 24 hours incubation period, the expression of the phosphorylated Akt showed an increase i.e.1.19 fold as compared to the control (1.0 fold) (Figure 4.43). This trend is similar in the expression of AKT.

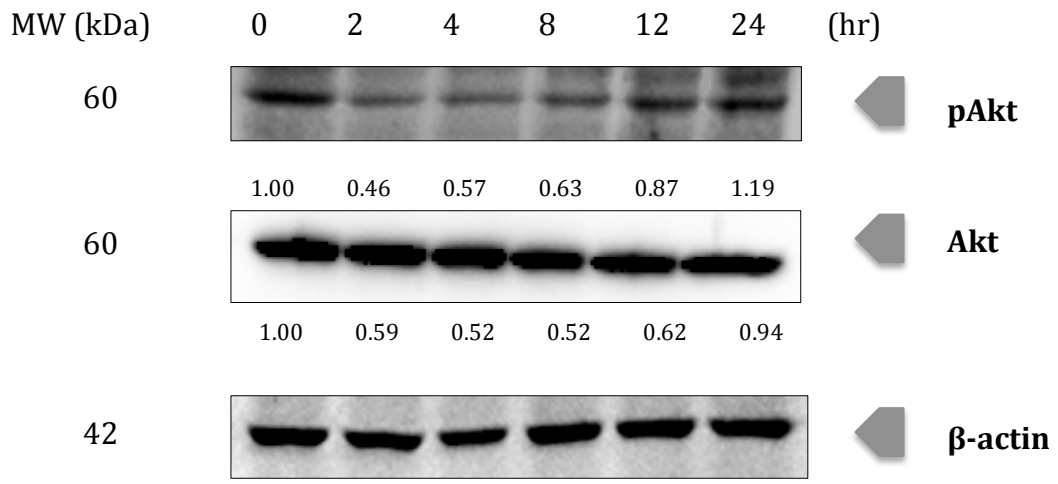

Figure 4.43: Chalepin modulates the expression of Akt and pAkt in a dose-dependent manner. A549 cells (2 x 10^6 mL^{-1}) were treated with 36 µg/ml of chalepin at various timepoints, after which the whole-cell extracts were prepared and 30 µg of protein was resolved by 12 % SDS-PAGE gel, electrotransferred onto nitrocellulose membranes and probed for phosphorylated Akt and Akt. The experiments were conducted in triplicates.

c-Raf is a proto-oncogene that is part of ERK1/2 pathway. C-Raf has been found overexpressed in various primary human cancer such as lung cancer. In order for c-Raf to be stimulated, it is phosphorylated at various sites in the presence of growth factors (Leicht et al., 2007). To activate the protein c-Raf, phosphorylation need to be commenced. C-Raf is a promising therapeutic target in cancer due to its role in mediating transformation of downstream oncogenic Ras and many other growth factors (Leicht et al., 2007). Our results showed that the expression of c-Raf was downregulated upon treatment of chalepin. Chalepin was also found to act as small molecule kinase inhibitors as we observed a downregulation in the expression of phosphorylated c-Raf upon treatment of it (Figure 4.44). Besides that, the function of c-Raf in mediating the oncogene expression of Ras was obstructed, as there was a significant decrease in the expression of Ras upon treatment with chalepin.

mTOR or the mammalian target of rapamycin, responds to various stimuli that manipulates essential signalling pathways that control cell growth, proliferation,

motility and survival such as PI3K, MAPK and AMPK. It plays a critical role in coordinating cell growth as well as cellular nutrients and energy. In cancer cells, elements of mTOR pathway were deregulated. This includes PI3K amplification, loss of function of PTEN, AKT overexpression and others (Pópulo et al., 2012). mTOR has been a promising target for cancer therapy. Chalepin treated cells showed downregulation in the expression of phosphorylated mTOR, which is the active form of the mTOR whereas mTOR showed an almost constant value of expression. Rapamycin, which is a prominent inhibitor of mTOR, acts through inhibition of mTOR phosphorylation at Ser-2448 (Chiang et al., 2005).

MEK or mitogen-activated extracellular signal-regulated kinase, which is present in the Raf-Ras-MEK-ERK pathway, is one of the best-defined kinase cascades in cancer cell biology. It is commonly activated by growth factors or mutations in the oncogene commonly Ras and Raf in this pathway. Such fiascos often lead to carcinogenesis in several types of cancer such as pancreatic cancer, lung cancer, breast cancers and colorectal cancer. Inhibiting these kinases has been a target to be considered in cancer chemotherapy (Neuzillet et al., 2014). MEK inhibitors or MEKi are promising therapeutic agents. Results indicated that treatment of chalepin acted as an inhibitor of phosphorylation of MEK. This was observed as slight downregulation in expression where the protein decreased to 0.6 fold upon treatment. This may indicate that the kinases responsible for phosphorylation of MEK were inhibited by chalepin. Earlier results, which have shown the chalepin to inhibit the upstream Ras, c-Raf, ERK also correlates with this result.

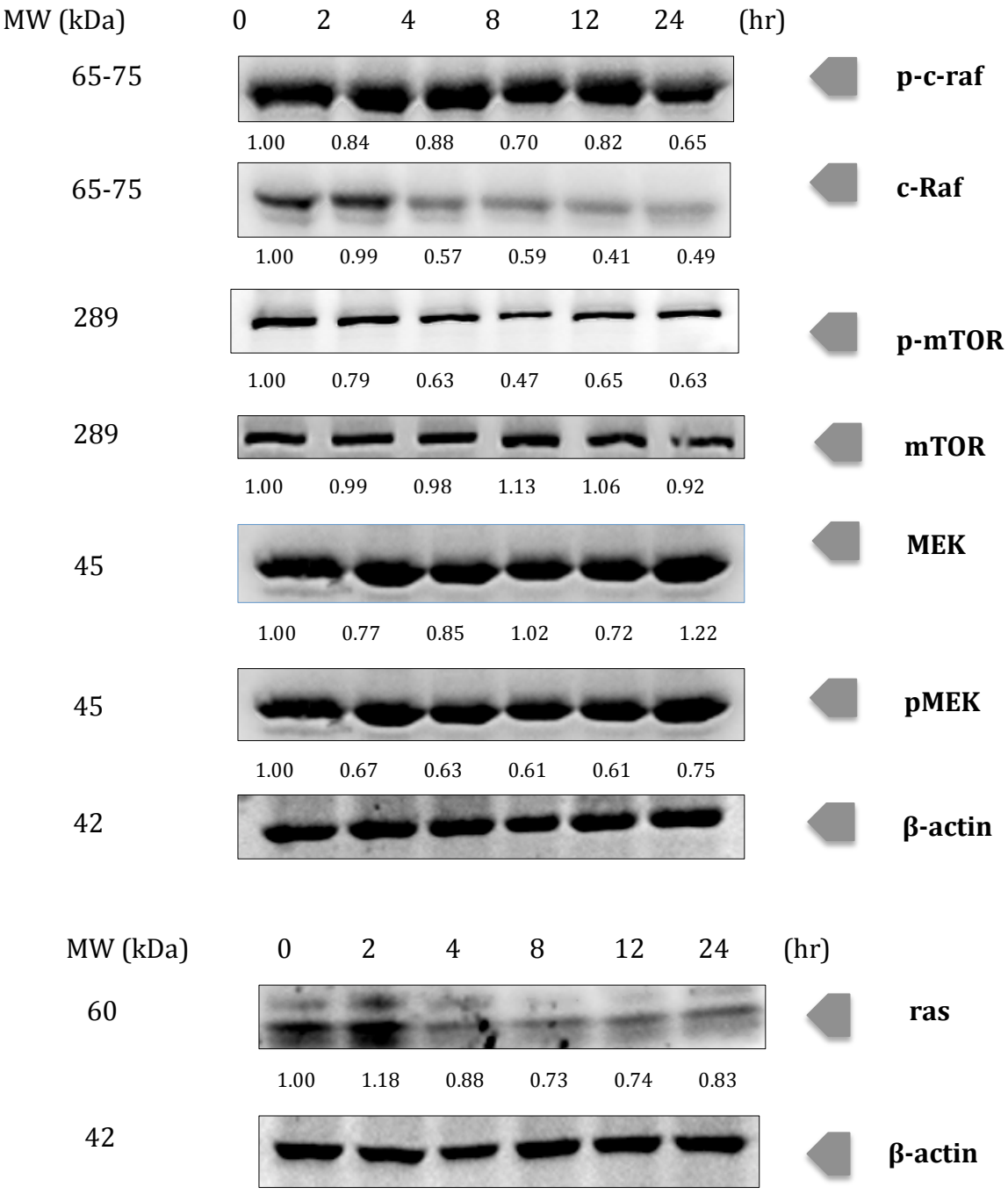

Figure 4.44: Chalepin inhibits the expression of proteins in the ERK1/2 pathway, MEK, and MAPK pathway in a dose-dependent manner. A549 cells (2 x 10^6 mL^{-1}) were treated with 36 µg/ml of chalepin at various timepoints, after which the whole-cell extracts were prepared and 30 µg of protein was resolved by 12 % SDS-PAGE gel, electrotransferred onto nitrocellulose membranes and probed for respective antibodies. The experiments were conducted in triplicates.

Results show that the expression of phosphorylated SAPK/JNK showed a remarkable decrease with a drop to 0.44 fold from 1.0 in control. This indicates that chalepin has inhibited the kinase activity which activates the SAPK/JNK via phosphorylation. Total

SAPK/JNK however showed some fluctuation and remained almost constant as to control with a fold of 1.06 as compared to control (1.0) at 24 hours incubation of chalepin. On the other hand, the expression of p38 showed a downregulation upon treatment of chalepin. It was downregulated to 0.41 at 4 hours incubation time and showed some fluctuations at higher time points. The phosphorylated p38 however showed a marked downregulation with up to 0.85 fold as compared to control 1.0, at 24 hours. This indicates that chalepin inhibits the expression of p38 and also the phosphorylation of p38.

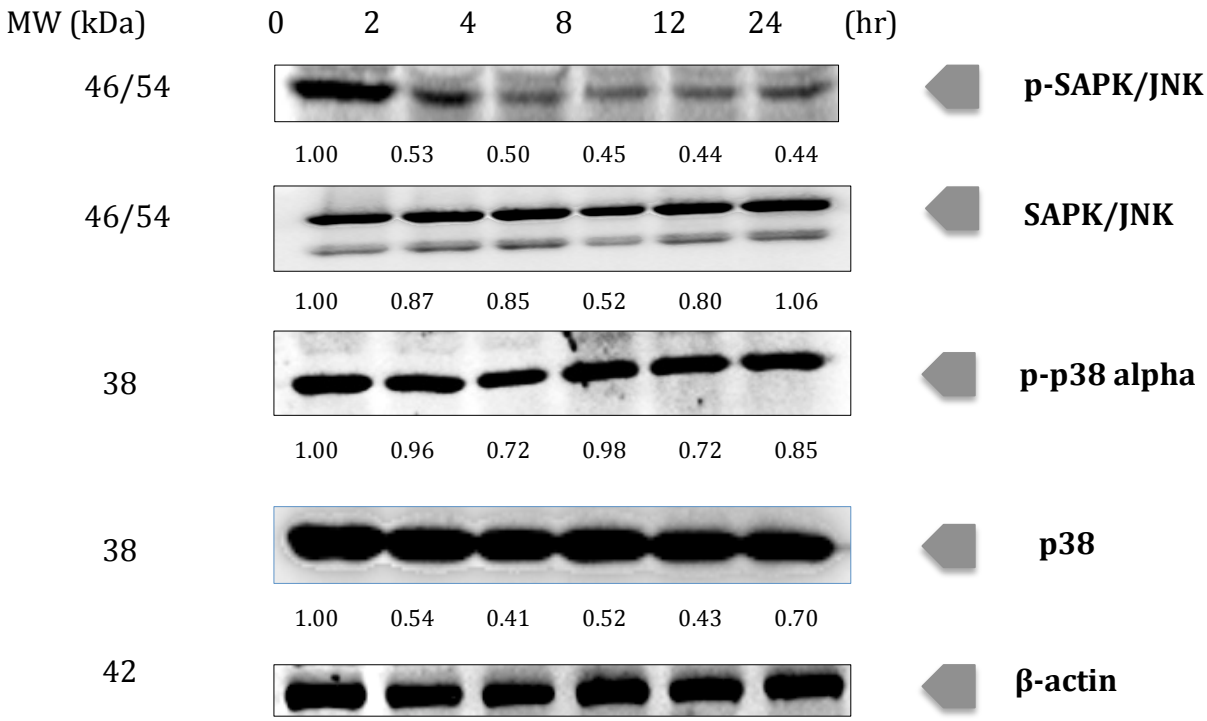

Figure 4.45: Chalepin inhibits the expression SAPK/JNK related proteins in a dose-dependent manner. A549 cells (2 x 10^6 mL^{-1}) were treated with 36 µg/ml of chalepin at various timepoints, after which the whole-cell extracts were prepared and 30 µg of protein was resolved by 12 % SDS-PAGE gel, electrotransferred onto nitrocellulose membranes and probed for respective antibodies. The experiments were conducted in triplicates.

4.11 Anti-metastatic effect of extracts of *R. angustifolia* and chalepin

One of the main reason cancer is a fatal disease is because of its ability to spread and metastasize to different parts of the body. In metastasis, cancer cells break free from the initial point of formation and travels via the blood and lymph system. It then attaches and form a secondary tumor at a different site in the body. Metastasis involves a series of events which includes cell invasion, migration, adhesion, establishment of tumor at secondary site and the ability of expression of matrix metalloproteinase enzymes. Effects of methanol extract, chloroform extract and chalepin from *R. angustifolia* on these series of events in metastasis was evaluated.

4.11.1 Cell growth inhibition assay on methanol extract, chloroforom extract and chalepin from *R. angustifolia* against A549 cells (MTT assay)

The methanol extract, chloroform extract and chalepin isolated from *R. angustifolia* were tested for their ability to inhibit cell growth through the MTT assay. MTT assay is a colorimetric assay which assesses the cell's metabolic activity. A549 cells were treated with various concentrations of the test samples and the viable cells were measured using the MTT dye. Percentage of inhibition was calculated in comparison with the control untreated cells. A graph was plotted with percentage of inhibition against concentration and IC_{50} value was evaluated to measure the concentration at which 50% inhibition occurs. Figure 4.46(A-C) shows the differences in the percentage of inhibition of the test samples at different measured time points. The percentage of inhibition of chloroform extract was found to be the highest as compared to methanol extract and chalepin. Table shows the IC_{50} value which was extrapolated from the graph. Lowest IC_{50} value was observed from methanol extract at 72 hours incubation

2.5 ± 0.28 µg/ml. Among the tested samples, methanol extract possessed the lowest IC_{50} (highest cytotoxicity) as compared to chloroform extract and chalepin at all the incubation time. However, chalepin showed the highest IC_{50} value i.e. lowest cytotoxicity in comparison with the extracts at the various time points tested. Since the least cell death was observed at 24 hours sample incubation, hence 24 hours incubation was chosen as the optimal time point for anti-metastatic study. All the assays were conducted at 24 hours incubation. The same test samples exhibited negative percentages of inhibition. This occurs when the test samples at lower concentrations fail to inhibit the cancer cells effectively and was overcomed by the high rate of proliferation of the cell. This leads to cells in the particular well to have proliferated more in number compared to the amount plated. This is the reason for negative inhibition to occur at certain instances especially at lower concentrations of the test sample.

(A)

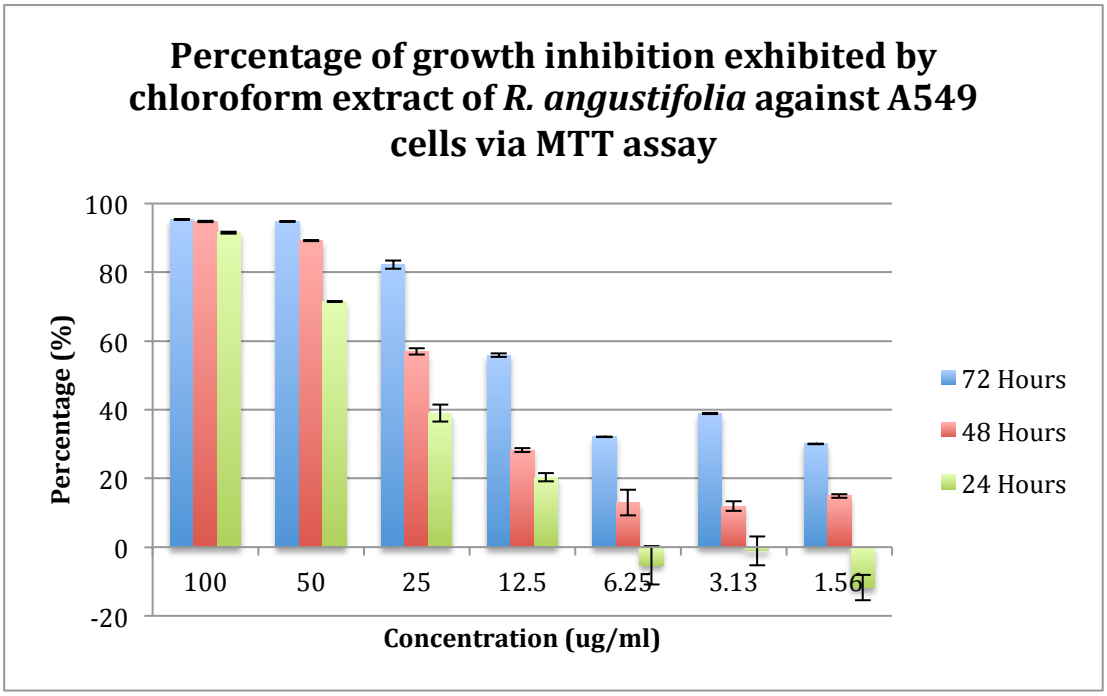

Figure 4.46(A): Graph showing the growth inhibition effect of chloroform extract of *R. angustifolia* at various incubation times. The data expressed as mean ± S.D. of three independent replicates (n=3).

(B)

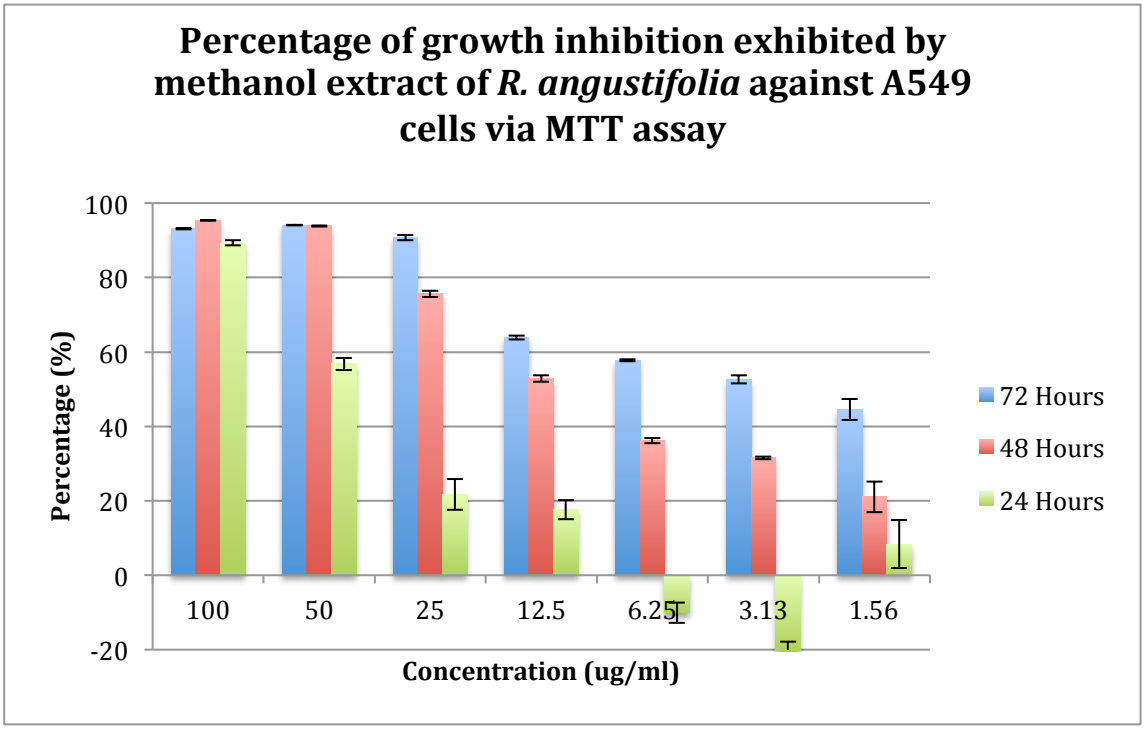

Figure 4.46(B): Graph showing the growth inhibition effect of methanol extract of *R. angustifolia* at various incubation times. The data expressed as mean ± S.D. of three independent replicates (n=3).

(C)

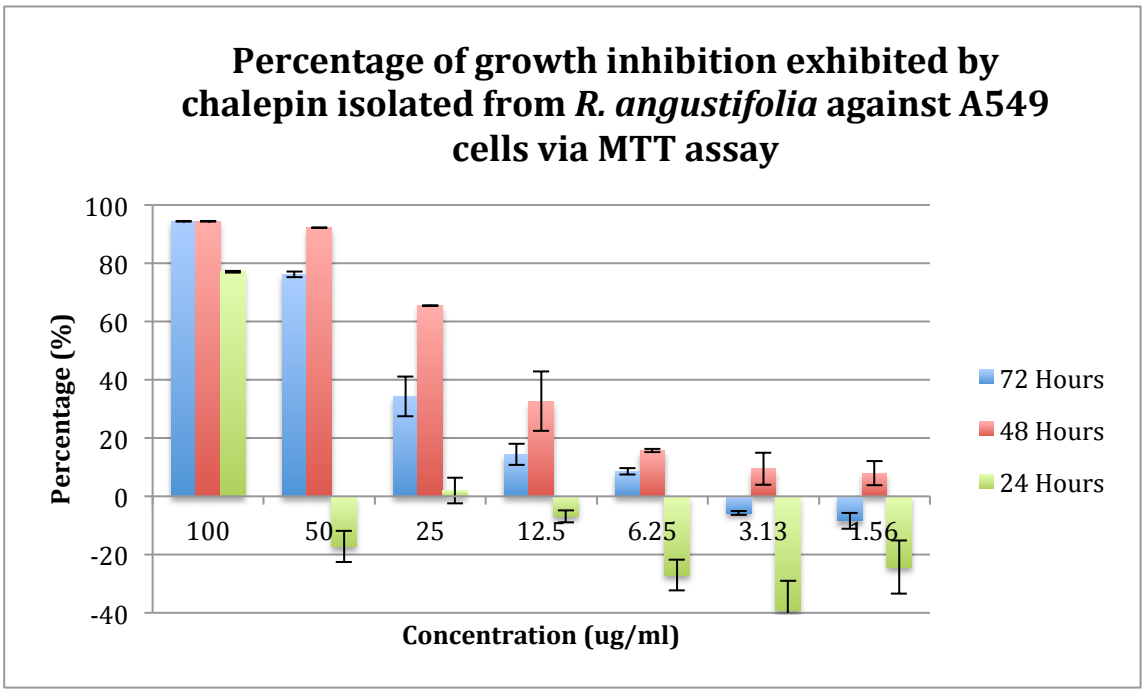

Figure 4.46(C): Graph showing the growth inhibition effect of chalepin isolated from *R. angustifolia* at various incubation times. The data expressed as mean ± S.D. of three independent replicates (n=3).

Table 4.7 : IC_{50} values of the selected extracts of *R. angustifolia* leaves and chalepin against A549 cell line at 24, 48 and 72 hours incubation

Test Sample	IC_{50} in µg/ml (A549)		
	24 hrs	**48 hrs**	**72 hrs**
Methanol Extract	14.3 ± 1.04	7.3 ± 0.17	2.5 ± 0.28
Chloroform Extract	11.9 ± 0.40	10.1 ± 0.06	9.1 ± 0.06
Chalepin	62.7 ± 0.31	49.3 ± 0.58	34.7 ± 1.27

It is noteworthy that the IC_{50} results obtained in SRB assay (Table 4.2) and MTT assay (Table 4.7) differs. This is due to the reason that both of these experiments have different mechanism of action and measures different parameters in a cell. SRB assay measures cell density in regards to protein content determination. However in MTT assay, the principle is based on the reduction of tetrazolium salt by metabolically active dehydrogenase enzyme in the cell. This justifies the difference in the IC_{50} value obtained in both of these experiments.

4.11.2 Anti-invasion Activity

The inhibitory activity on invasion was studied using the ECM 554 from Merck which consists of transwell chamber in 24 well plate. The transwell chamber was coated with basement membrane matrix of proteins derived from Engelbreth Holm-Swarm (EHS) mouse tumor which occludes the pore of the membrane. The purpose of this coating is to ensure that non-invasive cells are not migrated through the membrane while studying the effects of invasive cells to detach from surrounding cells and move through the membrane in response to the chemoattractant, FBS. The number of cells that are able to pass through the matrix and 8 µm sized pore signifies their invasive capacity. The invasion inhibitory capacity was measured using a fluorescence reader.

The cells were treated for 48 hours with various test samples. The results were shown in Figure 4.47 below.

Results shows that all the three test samples possessed significant anti-invasion property against A549 cells at various concentration. The highest anti-invasion activity was observed at methanol extract at a concentration 50 µg/ml with a percentage of inhibition of 91.10 ± 0.07 %. Chloroform extract showed almost equally high inhibitory percentage with 83.43 ± 0.16 %, 86.61 ± 0.17 % and 86.94 ± 0.19 % for 10, 20 and 50 µg/ml respectively. Chalepin showed relatively lower inhibitory effect as compared to methanol extract and chloroform extract. However, the anti-invasion activity of chalepin increased as the dose was increased. Chalepin showed and inhibition percentage of 27.08 ± 1.25 %, 28.15 ± 0.71 % and 35.40 ± 1.80 % for 10, 20 and 50 µg/ml treatment concentration, respectively.

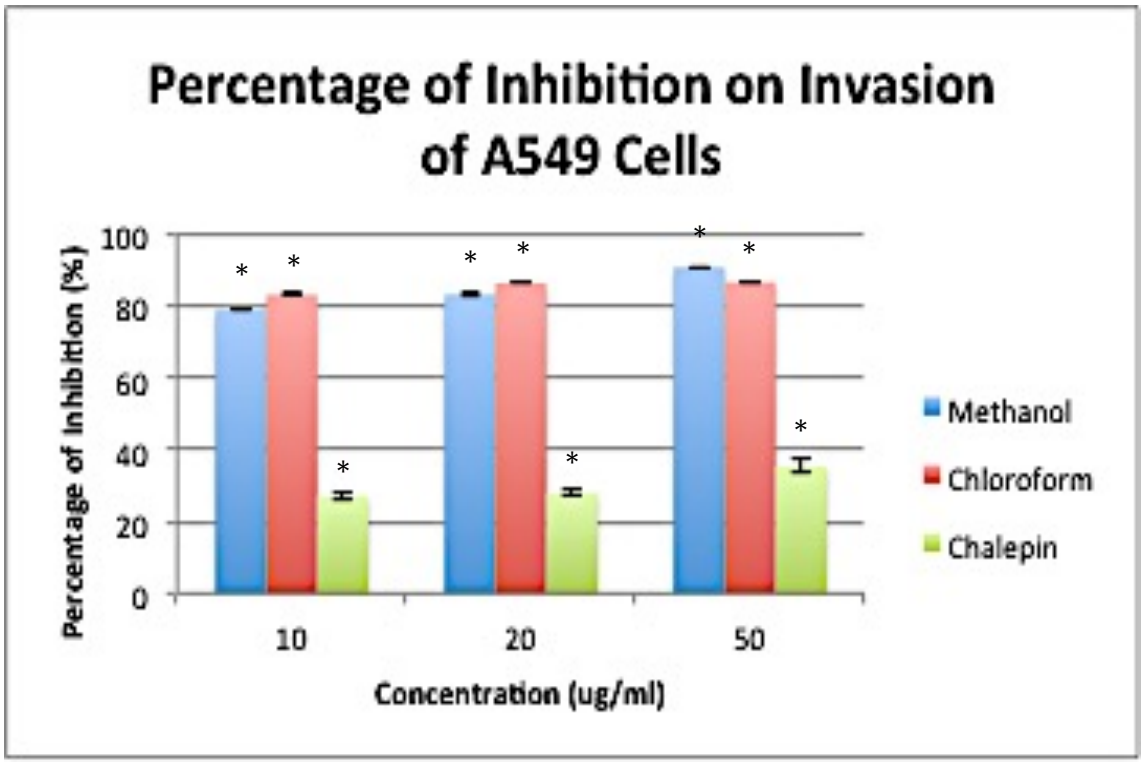

Figure 4.47: Graph showing the anti-invasion activity in percentage of inhibition, exhibited by test samples from *R. angustifolia* on A549 cells. The data expressed as mean ± S.D. of three independent replicates (n=3).

4.11.3 Inhibition on Cell Motility

Motility or more commoly known as the ability of the cell to move is studied using two experiments which is the anti-migration assay using transwell and wound closure assay. Cell motility and migration is an important step in organogenesis, inflammation and wound healing in normal development. Motility in cancer cells play a major role in metastasis.

4.11.3.1 Anti-migration assay

Anti-migration assay was conducted using the ECM 509 from Merck. This kit consists of 24 well plate with its transwell microporous membrane which has a pore size of 8 μm that studies the capacity of invasive cells to move through the pore in the direction of chemoattractant i.e. FBS which is present at the base of the well. This assay is based on the famous Boyden Chamber assay. The amount of the migrated cells were calculated between control and treated and the percentage of inhibition was deduced.

According to the results obtained, methanol and chloroform extracts of *R. angustifolia* showed almost 100% inhibition in the migratory effect of the A549 cells. Methanol extract showed 92.53 ± 0.11%, 95.43 ± 0.02% and 96.40 ± 0.06 % for 10, 20 and 50 μg/ml of extract respectively. Meanwhile, chlorofrom extract showed 94.08 ± 0.06%, 95.50 ± 0.01% and 95.90 ± 0.09 % for 10, 20 and 50 μg/ml of extract respectively. However, chalepin showed the lowest capacity to stop migration of cells with 10.41 ± 1.26 %, 19.26 ± 0.92 % and 34.00 ± 1.40 % for 10, 20 and 50 μg/ml of extract respectively.

The cells which has migrated to the bottom of the transwell through the microporous membrane was also photographed and shown in Figure 4.48(B). The migrated cells

were stained with cystal violet stain and then photographed with a light microscope at 10x magnification. The stained cells are visible in a purplish blue color when observed under the microscope. The observation tallies with the quantification results. In control, purplish blue cells were observed at the outer bottom part of the transwell. This shows that untreated cells could migrate through the membrane. The methanol and chloroform extracts showed almost no cells in the lower membrane at the focused field. However, chalepin showed decreasing number of cells present in the membrane as the concentration of chalepin increased.

(A)

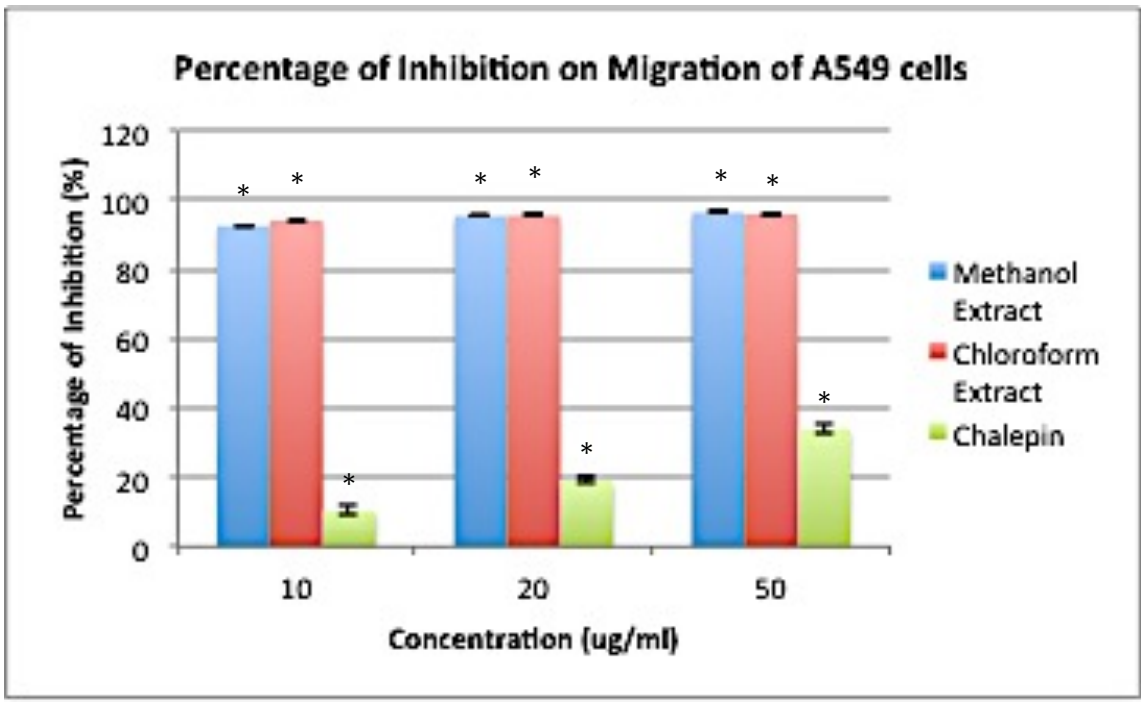

Figure 4.48(A): Graph showing the anti-migratory activity in percentage of inhibitionexhibited by test samples from *R. angustifolia* on A549 cells. The data expressed as mean ± S.D. of three independent replicates (n=3).

(B)

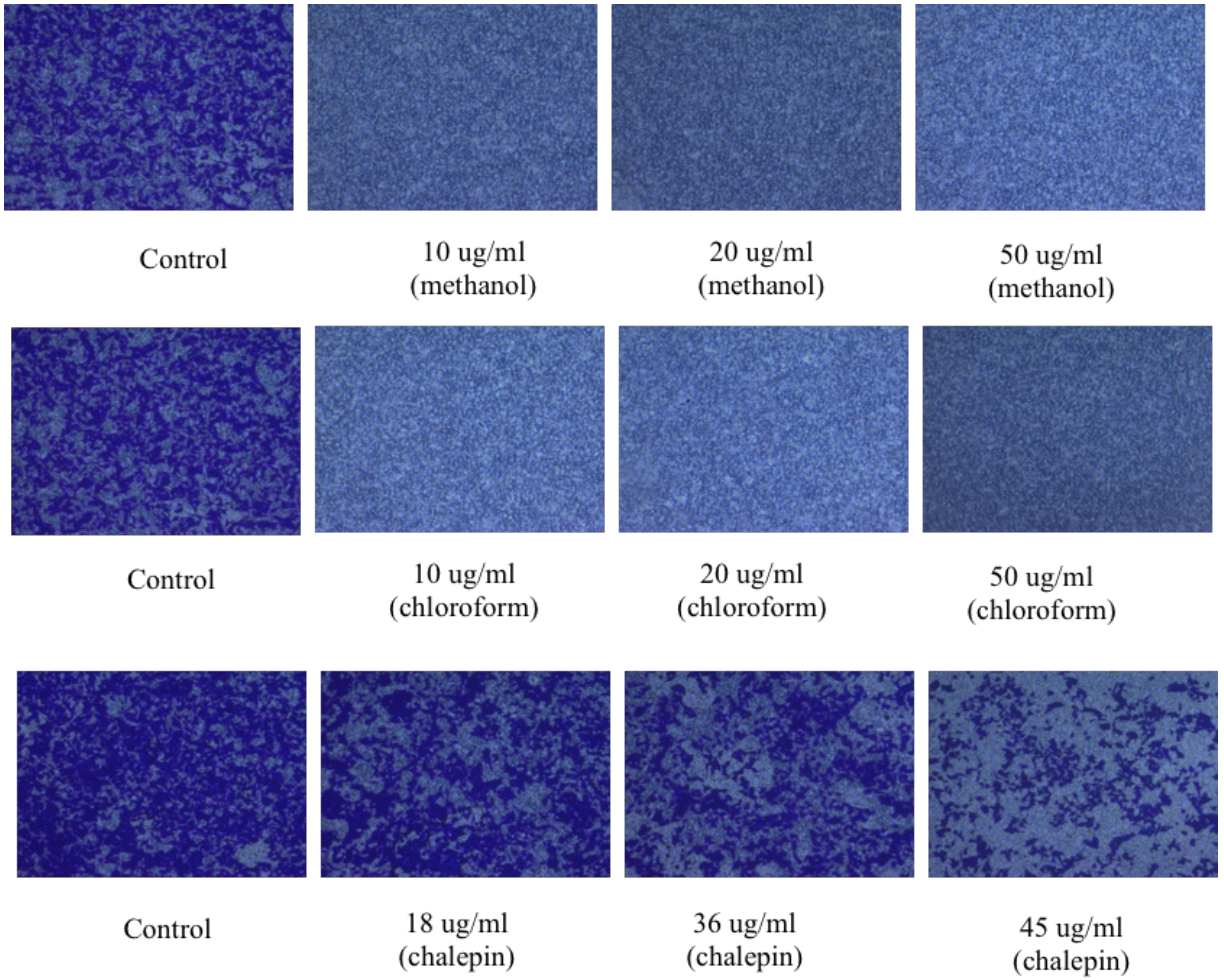

Figure 4.48(B): Images showing the migration inhibitory activity of methanol extract, chloroform extract and chalepin isolated from *R. angustifolia* on A549 cells.

4.11.3.2 Wound Closure Assay

Wound Closure activity in A549 Cells in response to methanol extract of *R. angustifolia*

Wound closure assay was done to measure the capacity of the cells to proliferate and move. It is a simple experiment where a scratch was created on the monolayer cells and the image of it was captured at the beginning and at certain intervals to observe the migration of cell. Observation on the wound closure activity of cells treated with methanol extracts revealed that the denuded zone did not close. The wound closure was inhibited. It was also observed that the denuded region gets wider as the incubation time increases. This is probably because the cells were killed by the extract. At higher concentration and incubation time, floating cells were observed (Figure 4.49(A)). This shows that methanol extract caused cell death which further prevented the motility.

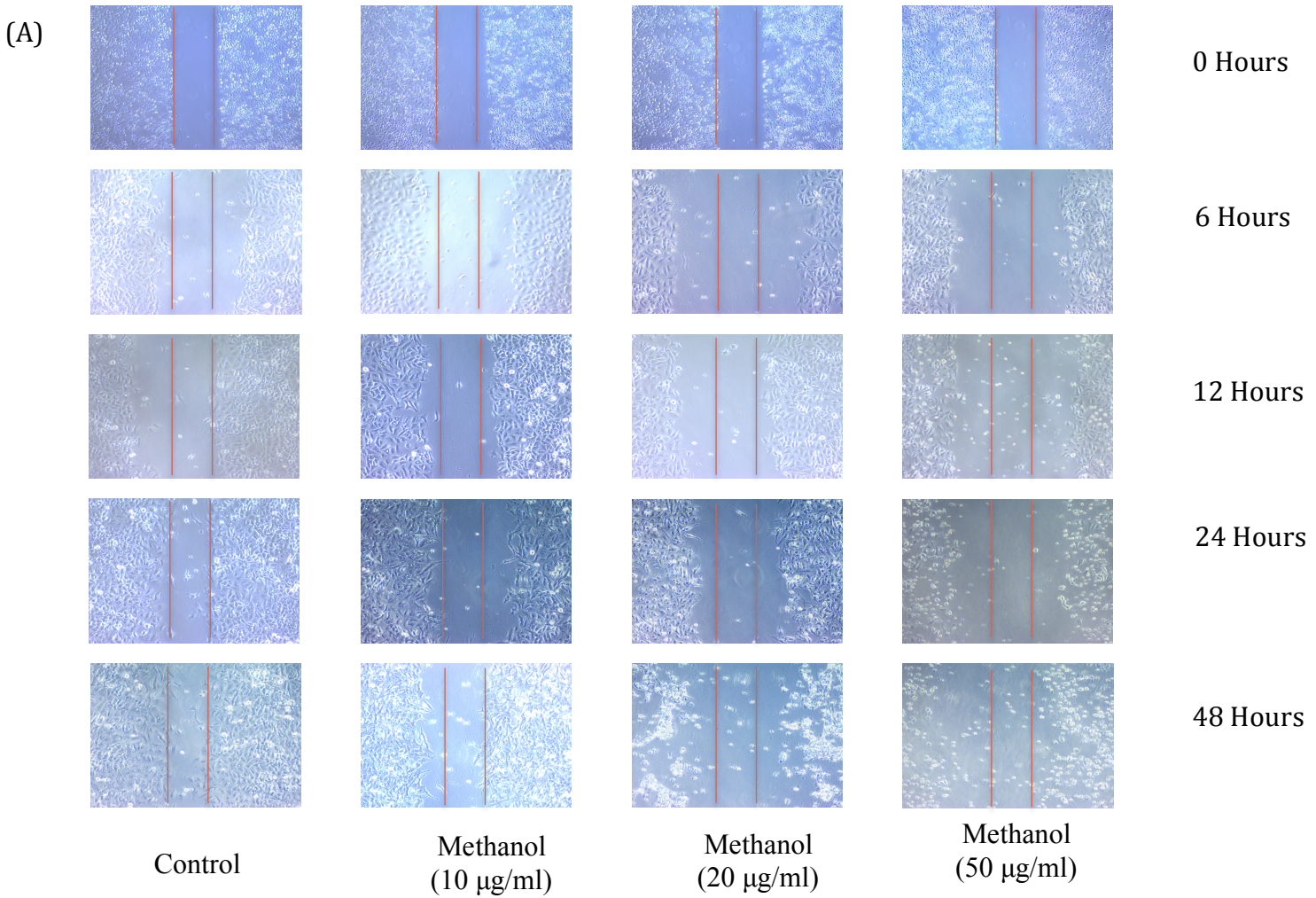

Figure 4.49(A): Images showing the effect of methanol extract of *R. angustifolia* on the wound closure activity on A549 cells at various concentration and time point at 10x magnification.

Wound Closure activity in A549 Cells in response to chloroform extract of *R. angustifolia*

Control cells showed almost complete closure in the scratched area at 48 hours incubation. This shows that A549 cells exhibits rapid motility and movement. However, treatment of chloroform extract inhibits the motility of the cells. At higher incubation time and concentration, the cells were floating showing the cells are dead (Figure 4.49(B)).

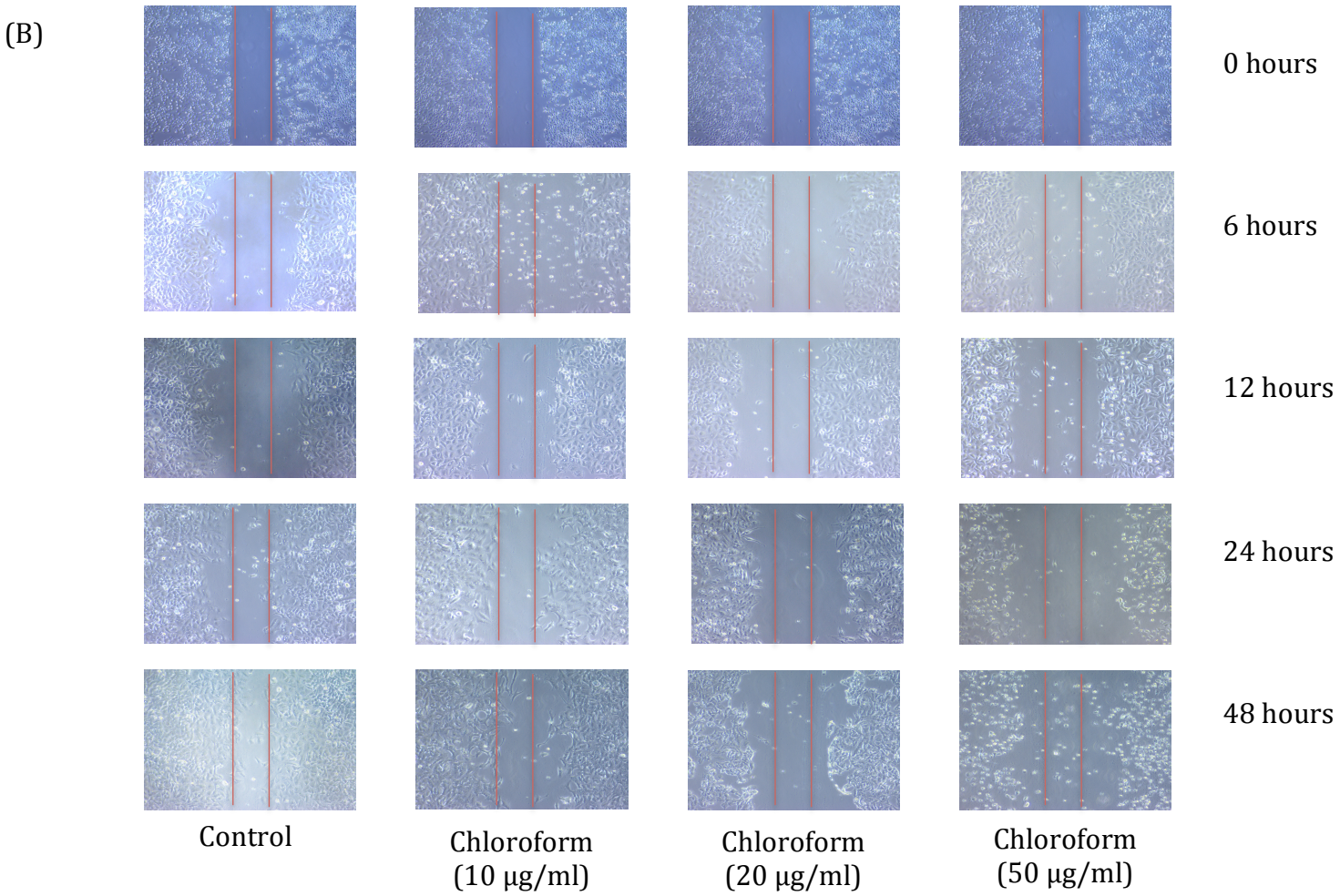

Figure 4.49(B): Images showing the effect of chloroform extract of *R. angustifolia* on the wound closure activity on A549 cells at various concentrations and timepoints at 10x magnifications.

Wound Closure activity in A549 Cells in response to chalepin of *R. angustifolia*

Chalepin exhibited almost similar pattern or characteristic in wound closure activity as compared to methanol and chloroform extract. The denuded zone remained not closed in the chalepin treated cells. However it was noticed that at higher incubation time, floating cells were observed as a result of cell death. As the incubation time increases, the denuded zone also gets wider which shows that the cells have lost their ability to be motile. This is shown in images in Figure 4.49(C).

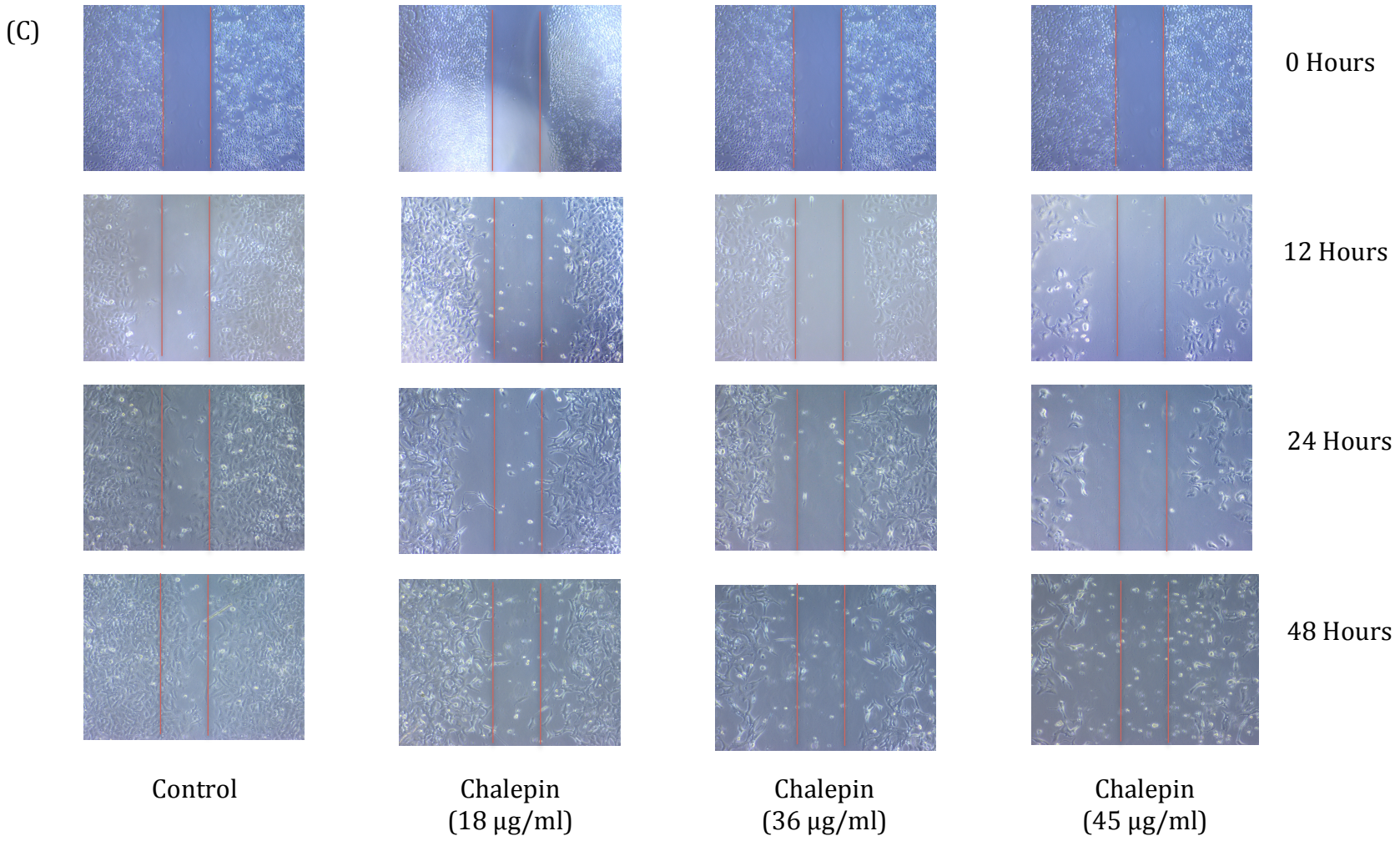

Figure 4.49(C): Images showing the effect of chalepin isolated from *R.angustifolia* on the wound closure activity on A549 cells at various concentrations and timepoints at 10x magnifications.

4.11.4 Cell Attachment Assay

For a cell to metastasize to different site, it has to first attach to the secondary site to proliferate. The effect of the methanol extract, chloroform extract and chalepin from *R.angustifolia* on the cell attachment of A549 cells were determined. The effect of these test samples on cell attachment was examined by detaching the treated cells from culture flasks and re-plating it onto a new tissue culture dish with the same number of treated cells. The treatment time was 24 hours. After re-plating, images were recorded at specific time intervals to determine the attachment onto the tissue culture dish.

Based on Figure 4.50(A) the A549 cells treated with methanol extract showed almost no attachment. This is showed by the high number of rounded cells. Rounded cells shows the cells are unattached. At highest concentration, the number of floating cells observed was lesser as compared to lower dose. The untreated control cells showed gradual attachment as the incubation time increases enabling the morphology of the cell to be observed and achieving almost 80% confluency at 24 hours incubation time.

Figure 4.50(B) shows the effect of chloroform extract on the cell attachment of A549 cells. Images taken at different intervals shows that at higher incubation time and treatment concentration, the higher is floating of the cells. At lower concentrations i.e. 10 µg/ml, there was some form of attachment occuring as the incubation time increases. At 24 hours incubation time, cell attachment was observed. However, at higher concentration of chalepin, almost all the cells were floating and appear rounded, which signifies that it is unattached.

(A)

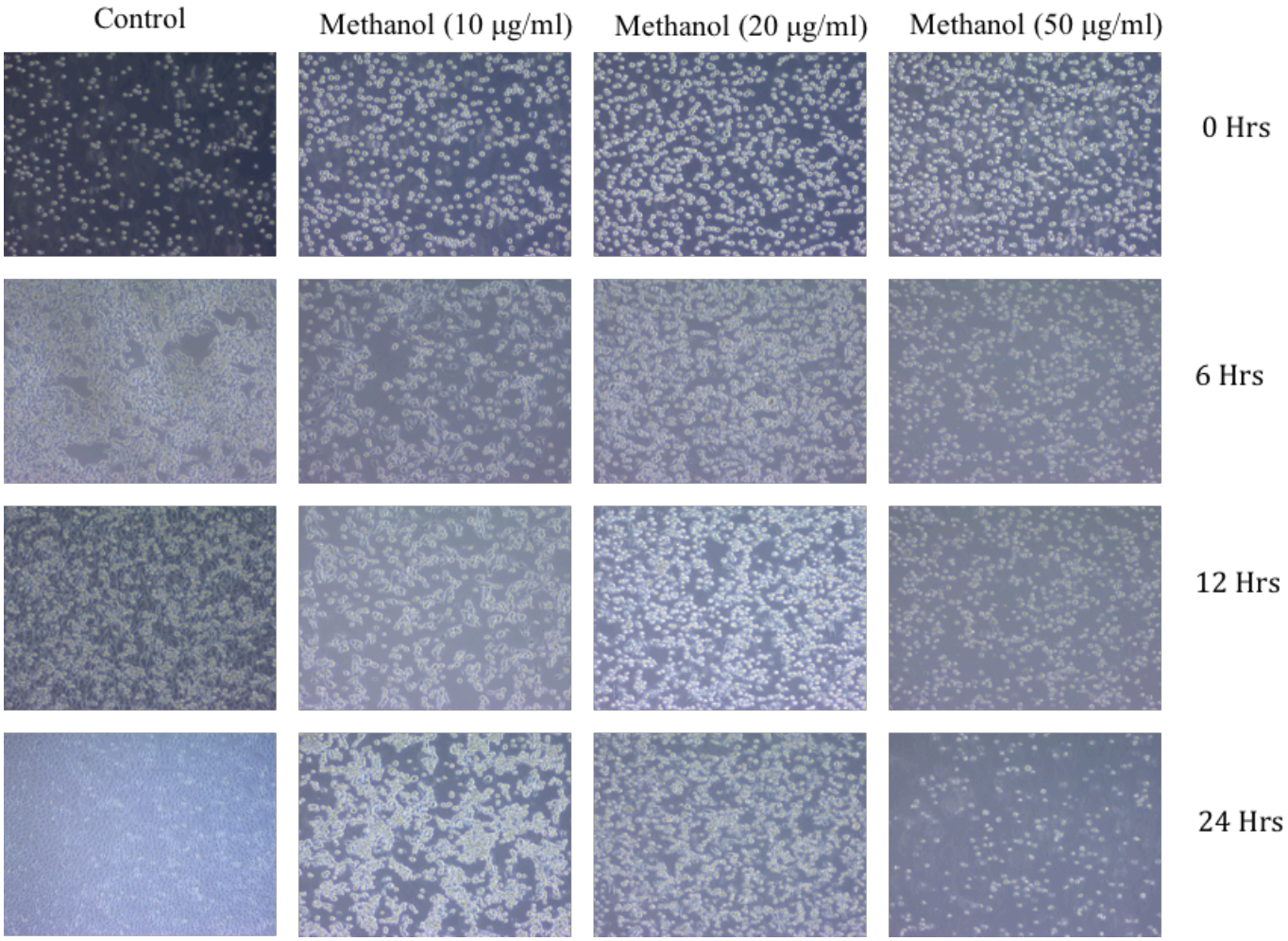

Figure 4.50(A): Images showing the effect of methanol extract of *R. angustifolia* on cell attachment of A549 cells at various concentrations and timepoints at 10x magnifications.

(B)

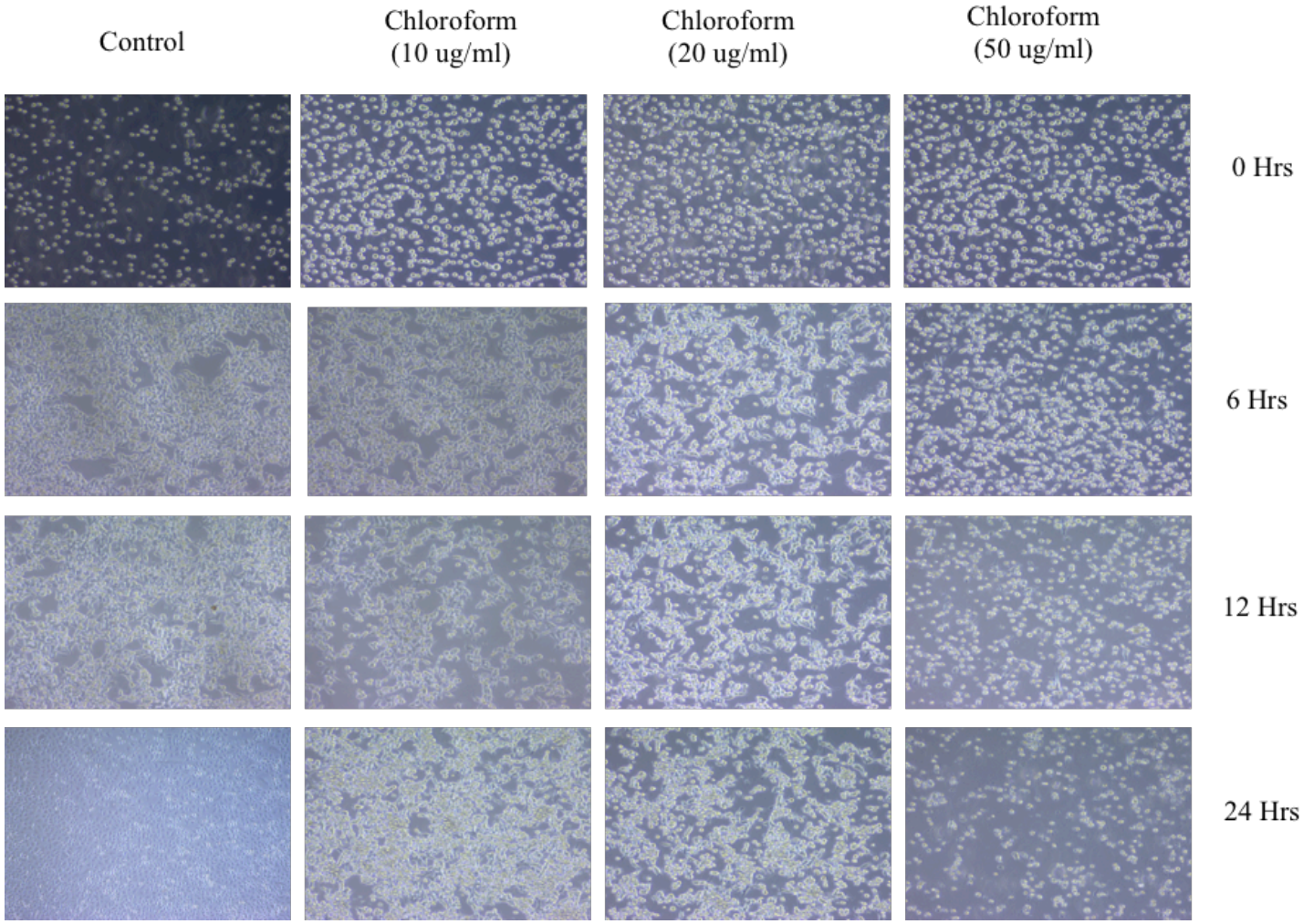

Figure 4.50(B): Images showing the effect of chloroform extract of *R.angustifolia* on cell attachment of A549 cells at various concentrations and timepoints at 10x magnifications.

(C)

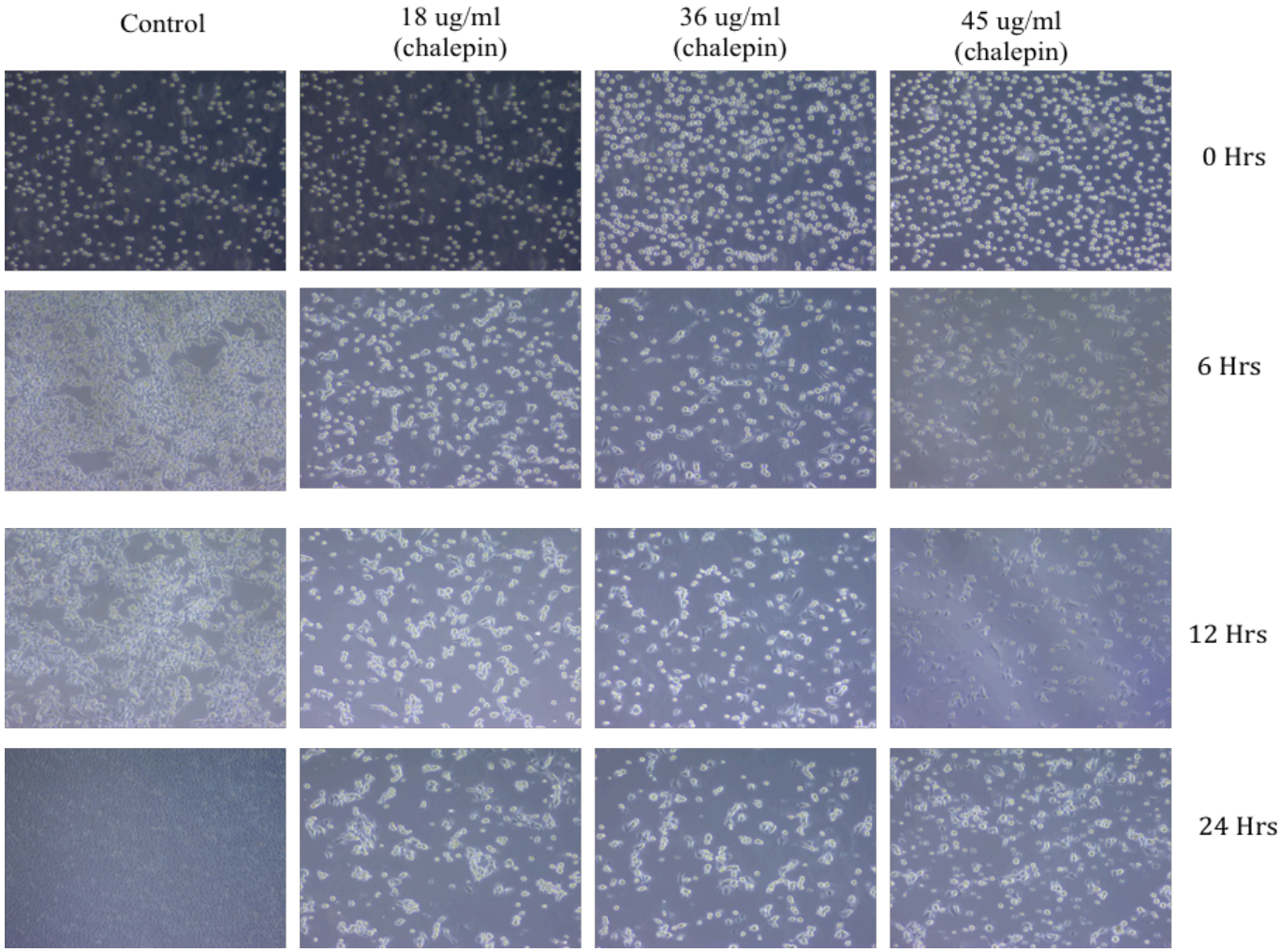

Figure 4.50(C): Images showing the effect of chalepin isolated from *R.angustifolia* on cell attachment of A549 cells at various concentrations and timepoints at 10x magnifications.

Figure 4.50(C) shows the ability of A549 cells treated with chalepin at various concentration to attach to the tissue culture flask. The images show that there are moderate cell attachment as compared to the control. The cell attachment although not as rapid as the control, it occurs and more cells are attached at a higher incubation time i.e. 24 hours. The number of rounded cells decreases as the incubation time increases and the cells with proper morphology appears. Chalepin shows that it is less efficient in inhibiting cell attachment as compared to methanol extract and chloroform extract which almost completely inhibits the cell attachment.

4.11.5 Cell adhesion assay

When cell invade and adhere to a secondary site, the cell adhere with the help of various extracellular matrix (ECM) proteins. Some of the important proteins for adhesion of cell are Collagen I, II, IV, Fibronectin, Laminin, Tenascin and Vitronectin. The effects of treatment of methanol extract, chloroform extract and chalepin from *R. angustifolia* in the adhesion proteins in the A549 cells were evaluated using the Merck ECM 554 Protein Array Adhesion Profile. This kit employs 96 well format with precoated adhesion molecules in different wells. The A549 cells were plated into the 96 well plates consisting of various adhesion molecules. Various concentration of test samples were added upon the cells and incubated for 48 hours before the ability of the test samples to inhibit adhesion were measured using the colorimetric method by taking absorbance was done. The absorbance value depicts the number of cells adhered. Control was the untreated cells. Based on Figure 4.51, Colagen I was highly inhibited by chloroform extract at 20 μg/ml concentration. Among the test samples, chloroform extract showed the highest inhibition for this adhesion molecule. As for Collagen II, chloroform extract at concentration of 50 μg/ml showed the highest inhibition. The absorbance that was observed was the lowest for this test sample. As for Collagen IV, lowest absorbance value was observed at 20 μg/ml chloroform extract. Chloroform extract observed to be the best in inhibiting the collagen I, II and IV. Fibronectin molecules was highly inhibited by chloroform

extract. Methanol extract equally showed high inhibition, however chalepin exhibited moderate inhibition. Inhibition in the laminin molecule showed similar trend as fibronectin. Chloroform extract was able to inhibit this molecule effectively. As for the adhesion molecule tenascin, chloroform extract showed overall best inhibition as compared to other test samples. Similar trend was observed for the inhibition on the adhesion molecule vitronectin. Chloroform extract was observed to be the most effective in inhibiting this molecule. However, the highest inhibition was observed with chalepin at a concentration of 45 μg/ml for both the molecules. BSA was used as the blank for this experiment to ensure that the adhesion of the cells are mainly due to the effect of the adhesion molecules. Hence, at the BSA coated wells, adherence of cells are at a very minimal level. Overall chloroform extract exhibited the best inhibition towards these adhesion molecules.

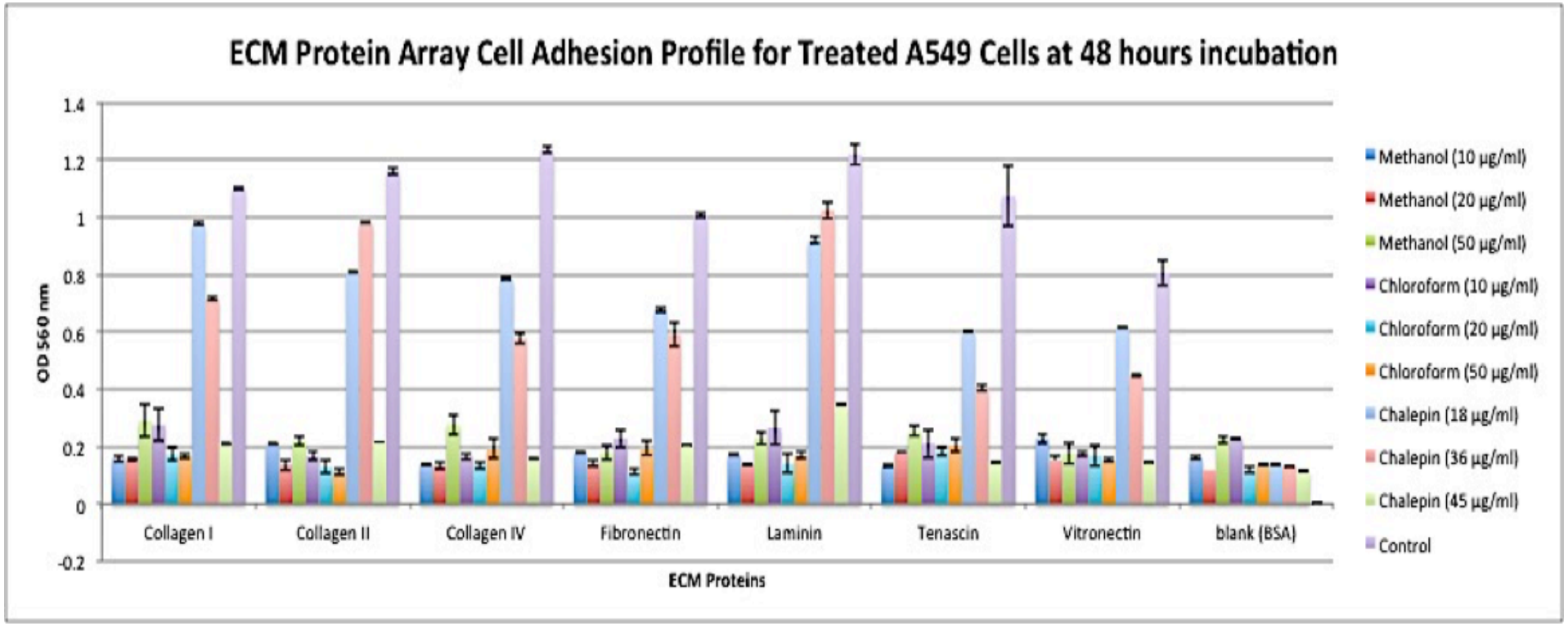

Figure 4.51: Bar chart showing the effect of methanol extract, chloroform extract and chalepin from *R. angustifolia* on the extracellular matrix proteins of A549 cells at 48 hours incubation. The data expressed as mean ± S.D. of three independent replicates (n=3).

4.11.6 Gelatin Zymography

Matrix metalloproteinases or more commonly known as MMPs has important function in the angiogenesis and cancer metastasis. It functions to degrade extracellular matrix proteins and this assists in cell invasion to the secondary site. Gelatin zymography is able to detect MMP2 and MMP9. In this study, only MMP2 was successfully detected and it is shown in Figure 4.52. In this experiment, the supernatant of the treated cells are collected and then loaded into gels which contains gelatin. MMP2 enzyme would cleave the gelatin present in the gel upon separation via electrophoresis. This reaction would leave an opaque band in the gel which is visible when the gel is stained with coomasie blue. MMP2 plays a significant role in cancer metastasis. Control showed a fairly thicker band as compared to the treated samples. This shows that in untreated cells, MMP2 is prevalent. In A549 cells treated with methanol, it was observed that as the treatment dosage is increased, the band is thinner. This shows that as the concentration of methanol extract increases, the amount of MMP2 present is lesser. Chloroform extract showed thinner bands as compared to other test samples. It showed similar trend as methanol extract in which as the treatment dosage of chloroform is increased, the MMP2 is inhibited more effectively. The inhibition of MMP2 in chalepin treated cells were observed to be almost similar in all the dosage. However as compared to control, the band represented by cells treated with chalepin were relatively thinner. This shows that chalepin inhibits the MMP2 up to a certain extend. Overall, the test samples were found to be able to inhibit the activity of MMP2 in the cell (Figure 4.52). This is an important characteristic in inhibition of metastasis. This is a preliminary screening and observation, to further prove this observation experiments need to be conducted extensively.

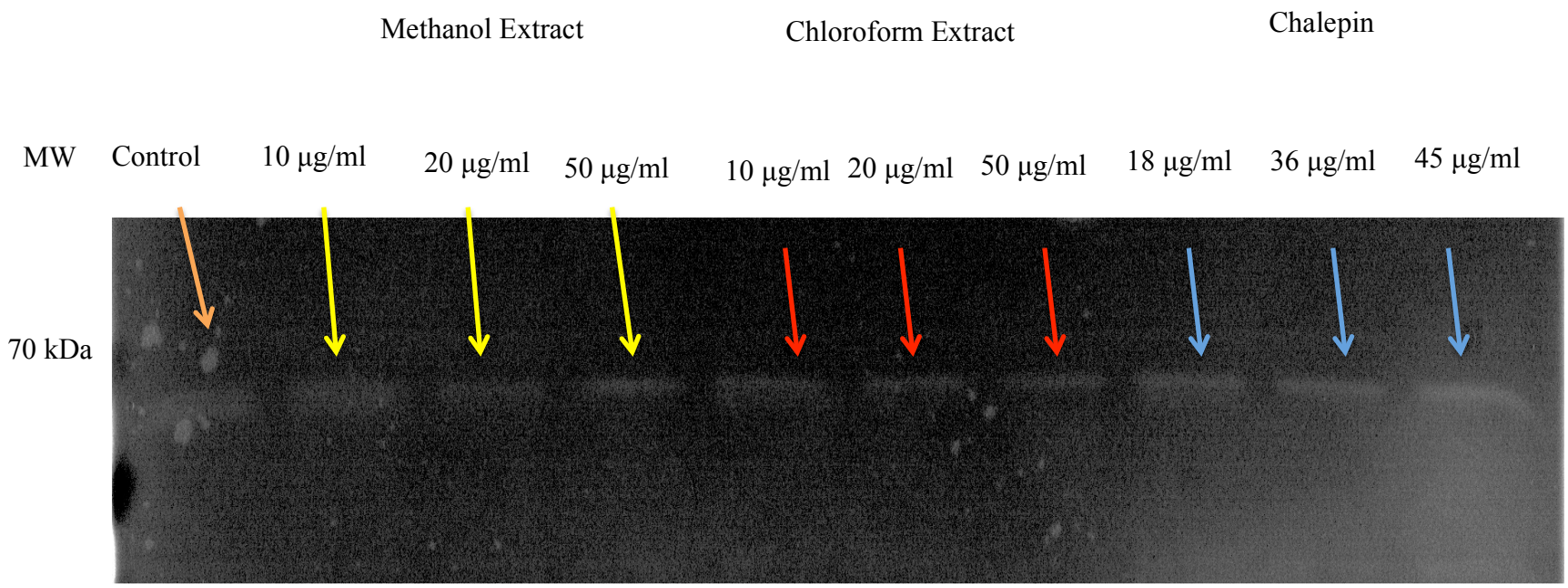

Figure 4.52: Image showing the bands representing MMP-2 in gelatin zymography of A549 cells treated with various concentrations of methanol extract, chloroform extract and chalepin from *R.angustifolia.*

CHAPTER 5: DISCUSSIONS

This is the first report on the cytotoxic potential of the methanol extract and the fractionated extracts of *R. angustifolia* on the human lung carcinoma (A549), human colon carcinoma (HCT-116) and human cervical carcinoma (CaSki) cells and also the human normal lung fibroblast (MRC5). A crude extract is considered to possess *in vitro* cytotoxicity if the IC_{50} value, at incubation time between 48 and 72 hours, is less than 20 μg/ml (Lee et al., 2005). Among all the extracts, the chloroform extract (without chlorophyll) exhibited the highest cytotoxic activity (IC_{50} value of 8.8 ± 0.32 μg/ml) and was thus selected for further investigation. The chloroform extract (without chlorophyll) exhibited better cytotoxicity than the total chloroform extract which could possibly be due to the removal of some inactive components by charcoal. Activated carbon was used as the absorbing material to remove the chlorophyll present in the extract, inevitably charcoal can also absorb other components besides chlorophyll.

The chloroform extract (without chlorophyll) was subjected to chemical isolation using the HPLC method. Twelve (12) components were successfully isolated and identified by NMR and GCMS analyses sufficient in quantity for further cytotoxicity screening. The compounds were graveoline, kokusaginine, bergapten, moskachan B, moskachan D, chalepensin, rutamarin, arborinine, chalepin and neophytadiene. Most of the compounds fall into the class of alkaloids, furanocoumarin and also dihydrofuranocoumarins. Arborinine, graveoline, moskachan B and moskachan D are alkaloids. Besides chalepin, moskachan D and arborinine showed good cytotoxic effect against A549 cell line at 72 hours incubation with IC_{50} values of 18.5 ± 0.65 μg/ml and 13.1 ± 0.06 μg/ml respectively. A previous report showed that arborinine isolated from *Ruta graveolens* showed IC_{50} values of 1.84 μg/ml, 11.74 μg/ml and 12.95 on cervical carcinoma (HeLa), breast adenocarcinoma (MCF-7) and skin epidermoid carcinoma

(A431) respectively (Réthy et al., 2007). Several alkaloids isolated from natural herbs exhibit antiproliferative and antimetastasis effects on various types of cancers both *in vitro* and *in vivo*. Alkaloids, such as camptothecin and vinblastine, have already been successfully developed into anticancer drug (Lu et al., 2012). Rutamarin and chalepin are furanocoumarins and it was reported that coumarins are the most abundant in Rutaceae and Umbelliferae family (Lacy et al., 2004). Bergapten, a furanocoumarin, exhibited mild cytotoxicity with an IC_{50} value of 43.53 ± 1.81 μg/ml against A549, human lung carcinoma cell line. Chalepin exhibited excellent cytotoxicity activity (IC_{50} value of 8.69 ± 2.43 μg/ml) whereas rutamarin exhibited mild cytotoxicity (IC_{50} value of 68.5 ± 3.06 μg/ml). Rutamarin is the acetylated form of chalepin. A previous report showed (Yang et al., 2007) that rutamarin had an IC_{50} value of 1.318 μg/ml against A549 cell line, this results were based on MTT assay. The reason for the lower activity of rutamarin in our hands, may be due to crystallisation in the media at higher concentration of rutamarin. Crystallization hinders the ability of the compound to effectively interact with the cancer cells to induce cell death. Based on all the collective results, chalepin was selected for further investigation.

Cells undergoing apoptosis show typical, well-defined morphological changes which includes plasma membrane blebbing, chromatin condensation with margination of chromatin to the nuclear membrane, karyorhexis (nuclear fragmentation), and formation of apoptotic bodies (Krysko et al., 2008). The morphological changes of A549 cells treated with various concentrations of chalepin were observed using a phase contrast microscope (Figure 4.21). Observation showed decrease in number of cells as the treatment concentration was increased. Formation of apoptotic bodies, vacuolisation, nuclear condensation, echinoid spikes were visible at higher magnification (400x). Longer incubation period shows bigger change in the morphology of the cells. In

contrast, the untreated control cells maintained a healthy structure and exponentially increased with time.

Early, late apoptosis or secondary necrosis, and necrosis were visualised using Hoechst 33342 and propidium iodide double staining assay. Hoechst 33342 dye can cross the nuclear membrane to tag the nucleus. Propidium iodide does not possess this capacity and could only cross compromised nuclear membrane to give a red staining. Nuclear membrane compromisation is a characteristic of late apoptosis or necrosis and this property could distinguish the cells undergoing early apoptosis or late apoptosis or necrosis. In primary necrosis, cytoplasmic swelling occurs and plasma membrane ruptures together with organelle breakdown but notably absence of nuclear fragmentation (Zhang et al., 2002). The low blue fluorescence represents viable cells, bright blue fluorescence represents cells undergoing early apoptosis, pink or red fluorescence with fragmented nuclear DNA represents cells at late apoptosis or secondary necrosis and red fluorescence with intact nucleus represents cells undergoing primary necrosis. The A549 cells treated with chalepin primarily showed bright blue fluorescence and the intensity of the fluorescence increased as treatment concentration of chalepin is increased. At higher concentraion and incubation time, pink or red fluorescence with fragmented DNA were observed (Figure 4.22). An apoptotic event *in vivo*, ends with phagocytosis by phagocytes to remove the apoptotic bodies. However, in *in vitro* conditions where the phagocytes are absent, the cells that initially were in early apoptotic phase would transform to late apoptotic or secondary necrotic phase which is visualized by pink or red fluorescence with fragmented nuclei and this was observed at chalepin treatment of 45 μg/ml at both 48 and 72 hours incubation. This could be an indication that at higher concentration of chalepin, the apoptosis cell death progresses faster. The primary necrotic cells are usually stained red but with uncompromised nucleus. The morphological studies gives a preliminary insight on the

morphological changes and the type of death the cell undergoes upon treament with chalepin.

Several biochemical criteria characterize apoptosis. These include phophatidylserine (PS) exposure on the outer leaflet of plasma membrane, changes in mitochondrial membrane permeability, release of intermembrane space mitochondrial proteins and caspase-dependent activation and nuclear translocation of a caspase activated DNAse resulting in DNA cleavage and fragmentation (Krysko et al., 2008). Expression of cell surface markers results in the early phagocytic recognition of apoptotic cells by adjacent cells, thus permitting quick phagocytosis with minimal compromise to the surrounding tissue. Flow cytometric Annexin V-FITC/PI double staining analysis can be used to determine early apoptosis and to distinguish between apoptotic and necrotic cells. In this study, we observed that the Annexin V positive cells which is the collective cells at the phase of early and late apoptosis increased with the increase of treatment concentration of chalepin and the treatment time. This clearly shows that chalepin has apoptosis inducing property. DNA fragmentation was observed in the TUNEL assay. Chalepin treated A549 cells also exhibited DNA fragmentation in a concentration and time dependent manner as shown in Figure 4.24. DNA fragmentation is a hallmark of apoptosis. The tightly controlled activation of the apoptosis-specific endonucleases provides an effective means to ensure the removal of unwanted DNA and the timely completion of apoptosis (Zhang et al., 2002). DNA which breaks exposes large amount of 3'-OH ends and this can serve as the starting point for terminal deoxynucleotidyl transferase (TdT) to add deoxyribonucleotides in a template independent manner. Addition of the deoxythymidine analog 5-bromo-2'-deoxyuridine 5'triphosphate (BrdUTP) to the TdT reaction acts to label the break sites. BrdU is then detected by an anti-BrdU antibody using immunohistochemical techniques.

Reactive oxygen species (ROS) are widely generated in biological systems. Due to this, humans have evolved antioxidant defence systems that limit their production. Intracellular production of reactive oxygen species such as •OH, O_2^- and H_2O_2 is associated with the arrest of cell proliferation. Similarly, generation of oxidative stress in response to various external stimuli has been implicated in the activation of transcription factors and to the triggering of apoptosis (Matés et al., 2000). It was described that ROS and the mitochondria plays a major role in apoptosis induction under both physiologic and pathologic conditions (Simon et al., 2000). Interestingly, mitochondria are both source and target of ROS. In our experiment, we have observed that there was an increase in the intracellular ROS level upon treatment with chalepin concentration and time dependent (Figure 4.26). The increase was significantly higher as compared to control for up to 6 hours of incubation with chalepin but a sharp drop was noticed after 8 hours. This could be due to the fact that after 8 hours the A549 cells started to die. Our experiment is designed such that ROS is only measured in viable cells as the dye used could only stain viable cells. A sharp decrease in the ROS content after 8 hours shows that cell death commences after 6 hours of incubation. The highest ROS fold increase was observed up to 62.24 fold at 45 μg/ml chalepin with 6 hours incubation. ROS promotes outer membrane permeabilization and mitochondria-to-cytosol translocation of cytochrome c, AIF or Smac/Diablo and triggers the caspase cascade. Thus, ROS stimulates apoptotic pathway (Circu et al., 2010). Irrespective of the morphological features of end-stage cell death (that may be apoptotic, necrotic, autophagic, or mitotic), mitochondrial membrane permeabilization (MMP) is frequently the decisive event that determines the survival and death of a cell (Kroemer et al., 2007). The treatment of chalepin on A549 cells at 48 hours incubation showed an increase in the reduction of mitochondrial membrane potential in a dose dependent manner (Figure 4.25). This shows that chalepin induces disruption in the mitochondrial

membrane potential. Depolarisation of the mitochondrial membrane often leads to the release of cytochrome c into the cytoplasm.

Caspases (cysteinyl aspartate-specific proteases) are synthesized as dormant proenzymes that, upon proteolytic activation, acquire the ability to cleave key intracellular substrates, resulting in the morphological and biochemical changes associated with apoptosis (Desagher et al., 2000). The caspase 9 activity was observed initially based on the analysis of cell population in a flow cytometer. The results showed that the caspase 9 activity was activated in A549 cells treated with chalepin in a concentration and time dependent manner. Caspase 9 is a member of the caspase family of cysteine proteases that have been implicated in apoptosis and cytokine processing. When cells receive apoptotic stimuli, the mitochondria releases cytochrome c which then binds to Apaf-1, together with dATP. The resultant complex recruits caspase 9 leading to its activation. Activated caspase 9 cleaves downstream caspases such as caspase-3, -6 and -7 initiating the caspase cascade (Kuida, 2000). Our results show that caspase 9 was activated which led to the downstream effector and the downstream effector caspase cascade. Caspase 3 or better known as the effector caspase is the caspase that executes the order received from caspase 9 to initiate apoptosis physically. In our preliminary analysis caspase 3 was activated in the A549 cells treated with chalepin in a concentration and also time dependent manner (Figure 4.28). Caspase 3 is a frequently activated death protease, catalyzing the specific cleavage of many key cellular proteins (Porter et al., 1999) which eventually will result in DNA fragmentation as illustrated by the results from the TUNEL assay.

The mitochondria play an important role in coordinating caspase activation through the release of cytochrome c (Desagher et al., 2000). The mitochondrial-mediated pathway is also known as BCL-2 regulated pathway, intrinsic pathway and stress-

induced pathway (Porter et al., 1999). Western blot technique was employed to study the regulation expression of apoptosis related proteins. The Bcl-2 family members determine the liberation of mitochondrial protein (Czabotar et al., 2014). Apoptotic threshold is set by interactions on the mitochondrial outer membrane between three functionally and structurally distinct subgroups of the Bcl-2 protein family: BH3 (the Bcl-2 homology 3) proteins (which convey signals to initiate apoptosis), the pro-survival cell guardians such as Bcl-2 itself, and the pro-apoptotic effector proteins Bax (Bcl-2-associated X protein) and Bak (Bcl-2 antagonist/killer). Thus, this family can be regarded as a tripartite apoptotic switch. When enough BH3-only proteins have been stimulated in response to various cytotoxic stresses to exceed the apoptotic threshold, Bax and/or Bak begin to oligomerize to a pore that permeabilize the mitochondrial outer membrane. This releases apoptogenic factors into the cytosol, particularly cytochrome c, which promotes the activation of procaspase 9 on APAF1; activated caspase 9 in turn processes and activates the effector caspases i.e. caspase 3 (Czabotar et al., 2014). In the western blot analysis, it was observed that the Bcl-2 protein and Bcl-XL, pro-survival cell proteins which also inhibit apoptosis, was downregulated in a time dependent manner (0, 2, 4, 8, 12, 24 hours). Bax and Bak was upregulated time dependently and this shows that the promoter of apoptosis is upregulated.

p53, is a critical tumor suppressor. It functions to induce apoptosis as a result of DNA damage, hypoxia and oncogenic activation. Various biological functions such as cell cycle arrest, angiogenesis, senescence, metastasis, metabolism, and autophagy is associated to p53 (Gu et al., 2008). In this study, upon treatment with chalepin, it was observed that there was an upregulation in the expression of p53 in Figure 4.33(A). Bax is directly activated by the p53 tumor suppressor proteins following stress induction or indirectly through the p53-activation of the Bcl-2 pro-apoptotic member Noxa and PUMA, or throughout the p53-independant mechanisms. The downregulation of Bcl-2

is necessary to prevent it from blocking Bax oligomerization. Formation of the Bax pore, as well as the loss of mitochondrial potential causes cytochrome c to leak out of the mitochondria to cytosol (Cai et al., 1998). We observed an increase in the level of cytochrome c in a time dependent manner. Cytochrome c would in turn activate the cleavage of procaspase 9 which is the initiator caspase, in which we observe in our study with a downregulation of the protein as time increases. Caspase 9 would inititate a signal cascade of caspases in which caspase 3; which is the effector caspase is activated. In this study it was observed that, procaspase 3 was downregulated which indicates the activation of procaspase 3 and an upregulation in the cleaved caspase. Inhibitor of apoptosis (IAP) proteins works in multiple ways in cell death regulation, ranging from inhibition of apoptosis and necrosis to the regulation of cell cycle and inflammation. Due to their ability to control cell death and elevated expression in a variety of cancer cell types, IAP proteins are attractive targets for the development of novel anti-cancer treatments (De Almagro et al., 2012). Some of the inhibitor of apoptosis such as survivin, XIAP, cFLIP, Bcl-2, Bcl-xl were found to be downregulated which allows apoptosis to proceed.

The effect of chalepin in the intrinsic apoptotic pathway is summarized in Figure 5.1.

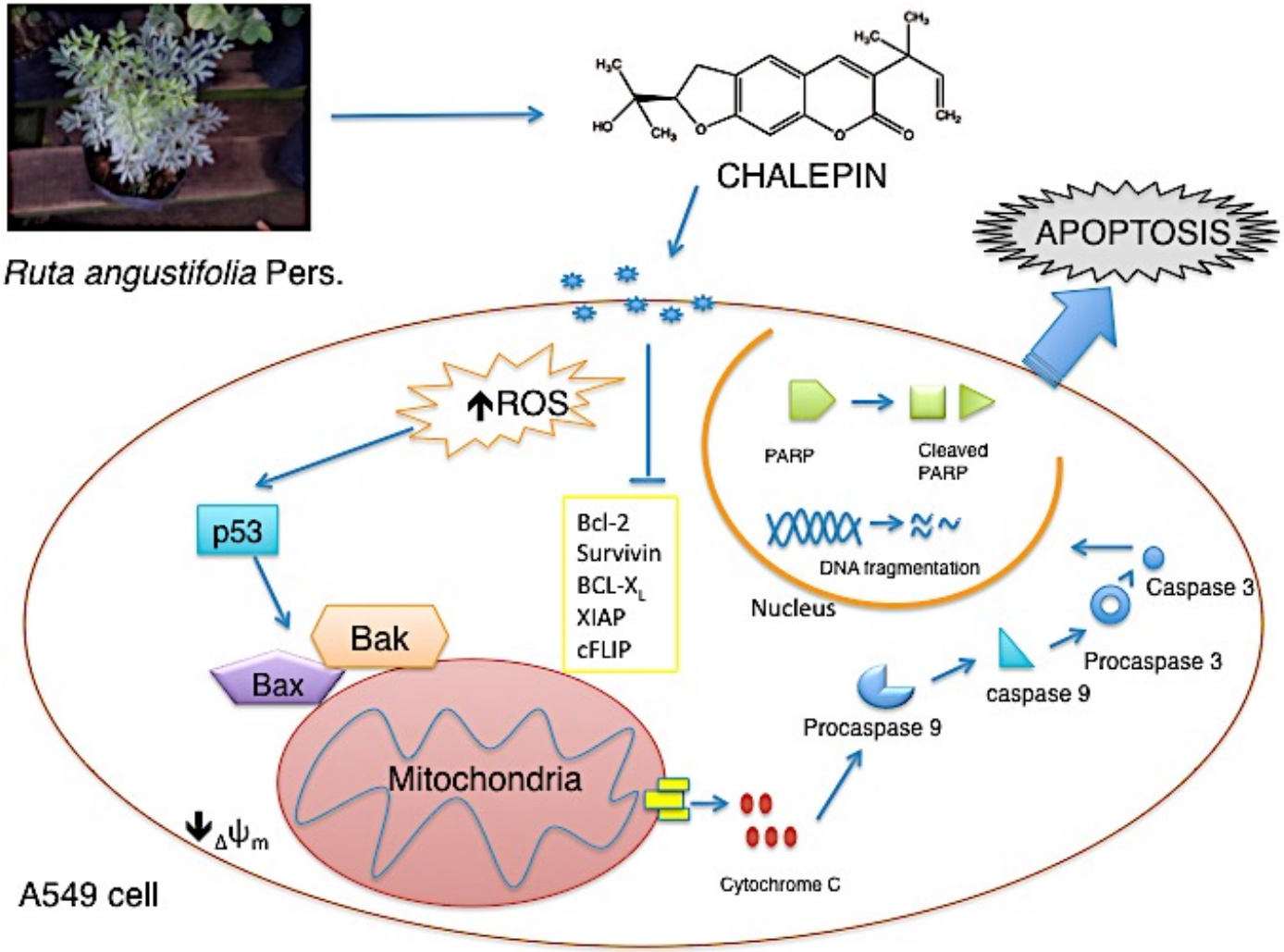

Figure 5.1: Graphical representation of the effect of chalepin in the intrinsic apoptotic pathway

This is also the first report which shows the capacity of chalepin to arrest cell cycle at S phase, to supress NF-κB pathway, to inhibit STAT3 phosphorylation and to induce extrinsic apoptotic pathway on the human lung carcinoma (A549) cells.

There is a strong correlation between cell cycle and cancer. Cell cycle is a machinery that controls cell proliferation and cancer is a disease, which is caused by inappropriate cell proliferation. There are several fiascos in the cell cycle's normal signal delivery which tells the cell to adhere, differentiate or die which causes the cancer cells to proliferate uncontrollably (Collins et al., 1997). The cell cycle comprises of a series of complex molecular and biochemical signalling pathways. It has four phases which includes G1 phase, S phase, G2 phase and M phase. G1 phase or also known as the first gap phase is a phase where the cell grows, accumulates energy and prepares to synthesize DNA. Synthesis of RNA and protein also occurs at this phase. The cells then proceed into the S phase which is also known as the synthesis phase. During this phase the cell synthesizes the DNA required for division. DNA replication takes place and the duplication of DNA results in duplication of chromosomes. The next phase after the S phase is the G2 phase. At the G2 phase, or also commonly known as the second gap phase, the cell continues to synthesize RNA and proteins such as macromolecules for spindle formation that are essential for the mitotic phase. The final stage in a cell cycle would be the mitotic phase or commonly known as M phase where cell division occurs. At this phase, two significant processes takes place i.e. karyokinesis which is the division of the nucleus which results in separation of the duplicated chromosomes into two equal group and cytokinesis which is the division of cytoplasm which results in two individual daughter cells. Following the M phase, a cell may proceed to G1 phase to further divide or enter G0 phase which is a resting phase. At this phase, there are no DNA replication or cell division, however the cells would still carry out their normal functions. There are several checkpoints which are important control points that

regulates the cell cycle to proceed further or to halt and undergo apoptosis. At the end of G1 phase, the cell goes through a checkpoint called G1/S phase. At the G1/S checkpoint, the cell checks for sufficiency in nutrient, cell growth factor, cell size and the occurance of any DNA damage. A decision is made at this point whether the DNA material is to be duplicated or the cell goes into rest phase i.e. the G0 phase. Cells with intact DNA continues to S phase for replication. Next checkpoint occurs at the G2 phase which is right after the S phase but before mitosis occurs. This checkpoint is known as G2/M phase. At this checkpoint, the replication that occurred at S phase is proof read and checked for any error. If mistakes were found, the cells tries to rectify them or self destructs (apoptosis). Finally at the M phase, a spindle assembly checkpoint happens where the chromosome attachment to spindle is checked upon.

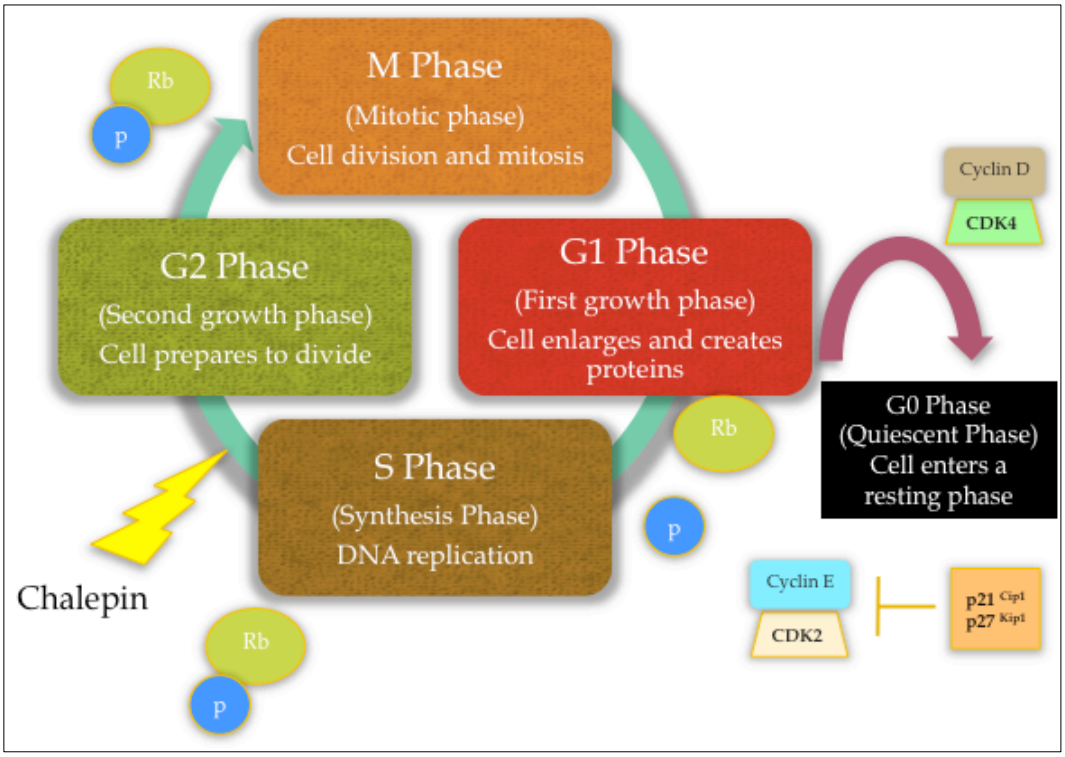

Figure 5.2: Graphical summarization of the effect of chalepin on cell cycle

Cells use a complex set of enzymes called kinases to control various steps in the cell cycle. Cyclin Dependent Kinases (CDKs), are a specific family of enzymes that uses signals to switch on cell cycle mechanisms. These kinases require association with a

second subunit, which is the regulatory proteins, known as cyclin. It is transiently expressed at the appropriate period of the cell cycle in order to be activated. Cyclin subunit complexes with its partner cyclin dependent kinase to create an active complex (Collins et al., 1997). When functioning properly, the cell cycle regulatory proteins (cyclins) act as tumor suppressors by controlling cell growth and inducing the death of damaged cells. Genetic mutations which can lead to absence of one or more of the regulatory proteins at the cell cycle checkpoints can result in the "molecular switch" being turned permanently on, permitting uncontrolled multiplication of the cell, leading to carcinogenesis, or tumor development. Throughout the G1 phase, retinoblastoma (Rb) is underphosphorylated. It is phosphorylated just before S phase and remains phosphorylated until late mitosis (Hunter et al., 1994). Cyclin E complexes with Cdk2 to regulate the G1/S phase transition whereas cyclin D complexes with Cdk4 to regulate the G1 phase (Vermeulen et al., 2003). Endogenous CDK inhibitors such as p21Cip and p27Kip or degradation of cyclin negatively regulate these CDK-cyclin complexes. Cdk4/cyclin D complex, which initiates the progression of cell cycle through the G1 phase, (Schwartz et al., 2009) is inhibited by $p21^{cip1}$, whilst Cdk2/cyclin E complex, which initiates the progression of cell cycle to the S phase (Schwartz et al., 2009), is inhibited by $p27^{Kip1}$. This inhibition would result in hypophosphorylation of Rb proteins that would result in inhibition of E2F transcription factor into nucleus that would subsequently activate the transcription of cell cycle related genes. $p21^{Cip1}$ arrested cells in both G1 and G2 cell cycle phases, $p27^{Kip1}$ blocks the G1/S-phase transition (Muñoz-Alonso et al., 2005).

Cell cycle analysis using the flow cytometry revealed that chalepin inhibited cell cycle at the S phase. Cell cycle analysis segregates cells based on its DNA content. The DNA is stained/labeled and measured to determine the phase in which the cell is located. Cells are found to be accumulated at the S phase i.e. the number of cells in this

population increased upon increasing treatment concentration of chalepin and also incubation time. As concentration of chalepin increases, the number of cells in S phase increased. This preliminary result was further studied by determining the expression of the cell cycle related proteins upon treatment of chalepin. The regulatory subunit i.e. cyclin D and E showed a downregulation upon treatment of chalepin at concentration 36 μg/ml (114.6 μM). Cdk2 and Cdk4 which complex with cyclin E and D respectively, showed a dramatic decrease in expression. This shows that the complex formation that is required for progression of cell cycle through G1 and S phase is inhibited. This could also be the reason why there was some accumulation of cells observed in the G1 phase in the flow cytometry cell cycle analysis. The inhibitors of Cdks (p21 and p27) showed slight downregulation however it was upregulated at higher incubation time. Total retinoblastoma protein showed downregulation and hypophosphorylation was observed. This is an indication that E2F gene is not activated and transcription of genes required for cell cycle progress is halted, as phosphorylation of retinoblastoma protein is essential for this downstream pathway. This result correlates with the S phase arrest. The effect of chalepin on the cell cycle is graphically expressed in Figure 5.2.

Inhibitor of apoptosis proteins (IAP) are commonly involved in the regulation of caspases and immune signaling. IAPs are highly conserved in viruses and mammals, and are also known as BIRCs (BIR domain containing proteins) that are a class of protein characterized by the presence of Baculovirus IAP Repeat (BIR) domain. IAPs are Zn^{2+} ion coordinating protein-protein interaction domain. IAPs are overexpressed in a number of tumors and are known to regulate carcinogenesis at various stages. c-IAP1 and c-IAP2 have been suggested as proto-oncogenes by various genetic studies (Oberoi-Khanuja et al., 2013). c-IAP1 and c-IAP2 are expressed in most human tissues. c-IAP1 expression is highest in the thymus, testis, and ovary, and c-IAP2 expression is highest in the spleen and thymus . c-IAP1 and c-IAP2 bind and inhibit caspase 3 and 7

(Schimmer, 2004). Rudimentaly cancer cells fails to respond to treatment because the malignant cells fail to respond to chemotherapy, radiation, or the immune surveillance by endogenous cytotoxic T cells and natural killer cells. The failure of cell death results from failure of the cells to undergo apoptosis and initiate caspase activation. IAPs, which is the antiapoptotic proteins plays a role in blocking cell death, by inhibiting the downstream caspase activation pathways (Schimmer, 2004). When c-IAP1 and c-IAP2 are absent in the death receptor complex, the binding of death ligands to their receptors leads to the formation of the death-inducing signalling complex (DISC) in which adaptor proteins (FADD and/or TRADD) bind with their death domain and induce the recruitment and activation of the initiator caspases, caspase-8 or -10. A new therapeutic approach is to develop small molecule drugs that mimic Smac (Second mitochondria derived activator of caspase), a pro-apoptotic mitochondrial protein that inhibits IAPs. IAPs represent the last line of defence for cancer cells against apoptosis and a key factor in cancer survival and progression. Smac mimetics also known as the IAP antagonists supresses IAPs to induce cancer cell death. The unique action of Smac mimetics could enhance therapeutic activity of many existing cancer therapies.

In our research, it is evident that treatment of chalepin on A549 cells inhibits the expression of c-IAP1 and c-IAP2 (Figure 4.35). Modulation of IAPs results in chalepin being similar to a Smac mimetic. The mode of action for commonly available drugs for the treatment of non-small cell lung carcinoma (NSCLC) such as doxorubicin, erlotinib, gemcitabine, paclitaxol, vinorelbine is through its ability to act as a Smac mimetic (Owens et al., 2013). Ability of chalepin to also act as a Smac mimetic is an interesting observation, which may promise a solution to the treatment of lung cancer.

The anti-apoptotic protein Mcl-1 functions as a key regulator of cancer cell survival and a known resistance factor for small-molecule Bcl-2 family inhibitors making it an

attractive therapeutic target (Leverson et al., 2015). Mcl-1 has been described as a very attractive drug target, and a small molecule that specifically inhibited Mcl-1 would have significant therapeutic potential in the many malignancies in which it is overexpressed (Brumatti et al., 2013). However to directly inhibit Mcl-1 requires the disruption of high-affinity protein–protein interactions, and therefore designing small molecules potent enough to inhibit Mcl-1 in cells has proven extremely challenging (Leverson et al., 2015). Mcl-1 has been proven to mediate multiple types of tumor. MCL-1 gene locus was found to be amplified in a variety of tumor types including the non-small cell lung cancer (NSCLC) (Leverson et al., 2015). A549 cells treated with chalepin showed downregulation in the expression of Mcl-1 protein (Figure 4.35). This result indicates that chalepin might be able to act as Mcl-1 specific BH3 mimetics. Members of the Bcl-2 family such as Bcl-2, Bcl-xL and Mcl-1 are antiapoptotic proteins which are overexpressed in many cancers. These proteins act to bind and sequester proapoptotic proteins such as Bax and Bak. Targetting the Bcl-2 family proteins promises good chemotherapeutic passage. Small molecules which has the capacity to mimic the BH3 domain of BH3 only Bcl-2 family members could serve as inhibitor. BH3 mimetics are generally short peptides or organic molecules. The latter are indeed antagonists of the prosurvival members (Besbes et al., 2015). Mcl-1 inhibition was found to cause tumor regression and cell death in various experiments. Mcl-1 inhibition could be executed via various approaches such as indirect cyclin-dependant kinase inhibitors, small molecules and BH3 peptides which could directly bind to Mcl-1 to antagonize its activity. However BH3 mimetics are considered to be the best type of Mcl-1 inhibitor. High binding affinity is difficult to achieve, which may be due to the nature of the protein/protein interaction and the conformational rigidity of the hydrophobic binding groove of Mcl-1 (Besbes et al., 2015). To determine the mode of action of chalepin in inhibition of Mcl-1, further studies need to be done.

Cyclooxygenase-2 (Cox-2) is formed by a cell in response to the presence of its substrate and not usually expressed in normal tissue. Cox-2 is overexpressed in neoplasms and premalignant lesions. Inhibitors of Cox-2 has been investigated as chemotherapeutic agents for chemoprevention. Preclinical data suggests inhibitors of Cox-2 may have the tendency to protect against colon, breast, lung, esophageal and oral tumors (Dang et al., 2002). Cox-2 overexpression is often associated with an increased production of prostaglandin E2 (PGE2) which is a major by product of Cox-2 that is involved in cell death, cell proliferation and tumor invasion in many types of cancer. PGE2 affects through membrane receptors such as EP1, EP2, EP3 and EP4 which activates different types of signalling pathways. NSCLC is associated with Ras mutation, which leads to upregulation of Cox-2 that results in increased PGE2 production. PGE2 increases cell proliferation in A549 cell line and this activation is associated with activation of Ras pathway through EP4 receptor. PGE2 acts by affecting the release of amphiregulin, which is the most abundant ligand in A549 cells. Several signaling pathways are associated with tumor progression, which is linked to PGE2, and this is why inhibition of Cox-2 is a good strategy in fighting cancer (Sobolewski et al., 2010). In our study, Cox-2 was downregulated upon treatment of chalepin towards A549 cells at 24 hours treatment time (Figure 4.36). This indicates that chalepin could inhibit the production of PGE2 and activation of Ras pathway thus inhibiting cell proliferation.

c-Myc is an oncogene which regulates cellular growth and metabolism. In cancer cells, metabolic changes need to take place to support the increased demand of nucleic acids, lipids and proteins that are necessary for rapid cellular proliferation. In these situations, c-myc is often overexpressed (Miller et al., 2012). The c-myc gene was found to be amplified in many human cancers, including breast cancer, lung cancer and colon cancer (Dang, 1999). According to a study by (Rapp et al., 2009), c-myc was

found to induce metastasis in non-small cell lung carcinoma. In our study, treatment of chalepin resulted in downregulation of c-myc at earlier time points such as 2 and 4 hours (Figure 4.36). This shows that this particular gene product which is responsible for cellular growth and metabolism is inhibited by chalepin. Chalepin could also be an agent which inhibit metastasis as c-myc was found to promote metastasis in A549 cells (Rapp et al., 2009).

One of the most studied transcription factor i.e. NF-κB, has been found to control multiple cellular processes in cancer including inflammation, transformation, proliferation, angiogenesis, invasion, metastasis, chemoresistance and radioresistance. NF-κB is activated in most tumor cells, and its suppression inhibits the growth of tumor cells, leading to the concept of 'NF-κB addiction' in cancer cells (Chaturvedi et al., 2011). Upon activation, NF-κB binds DNA as a heterodimeric complex composed of members of the Rel/ NF-κB family of polypeptides. Since it is involved in the defense against diseases, this transcription factor is an important target for therapeutic intervention (Singh et al., 1995). NF-κB is a ubiquitous transcription factor, which consists of p50, p65, and IκBα, that resides in the cytoplasm (Sethi et al., 2008). Activation would lead to the translocation of the transcription factors from the cytoplasm to the nucleus. In the cytoplasm complexes are held and prevented from activating transcription by a class of proteins referred to as inhibitors of NF-κB or IκB proteins (Sasaki et al., 2005). Upon activation in response to various inflammatory stimuli, environmental pollutants, prooxidants, carcinogens, stress, and growth factors, NF-κB translocate from the cytoplasm to the nucleus, bind DNA, and causes gene transcription. Numerous kinases have been linked with the activation of NF-κB, including IκBα kinase (IKK). Its activation has been shown to cause the expression of various gene products that regulate apoptosis, proliferation, chemoresistance, radioresistance, invasion, angiogenesis, metastasis, and inflammation (Sethi et al.,

2008). Upon stimulation, the IκB proteins are phosphorylated by one of a number of Iκβ kinases (IKK-α, -β, and -γ), ubiquitinylated, and degraded, which thereby allows the NF-κB complex to translocate into the nucleus (Sasaki et al., 2005).

Up till date, there has been no report on effects of chalepin on the NF-κB pathway activation. Chalepin was found to suppress the NF-κB activation, which are commonly induced by various carcinogens and inflammatory agents. In this study, chalepin was found to act through direct interaction with the p65 subunit of NF-κB pathway and also through its ability to inhibit phosphorylation of the inhibitor of NF-κB i.e. Iκβα thus causes the pathway to be in an inactive state. The pathway was inhibited through suppression of Iκβα phosphorylation and degradation. Our results showed that the Iκβα phosphorylation was downregulated upon treatment of chalepin (Figure 4.37). Degradation of Iκβα however showed an inconsistent result, with upregulation and slight downregulation in the protein expression. The inhibition was also through modulation of the p65 subunit of NF-κB where the phosphorylation of p65 and the translocation of the p65 subunit to nucleus are inhibited. Results obtained indicated an upregulation and then a downregulation at the 6 hours incubation time in the p65 subunit in the nuclear fraction. This shows that there is an inhibition in the translocation of p65 into the nucleus. Phosphorylation of p65 in the nucleus was inhibited, as there was a downregulation in the expression of the phosphorylated p65 upon treatment of chalepin. Serine phosphorylation at various sites of the p65 subunit has been shown to be important in initiating transcription (Sasaki et al., 2005).

Apoptosis can be initiated through two major interconnected pathways. The first one involves the activation of the TNF family of death receptors, also known as the extrinsic pathway. The second involves the release of cytochrome c from mitochondria, also known as the intrinsic apoptosis pathway. Caspase 8, exists in an inactive proenzyme

form and is converted to the active form upon recruitment to the cytoplasmic domain of death receptors. TNF-related apoptosis inducing ligand or commonly known as TRAIL, upon binding with DR4 or DR5 results in the recruitment of an adaptor protein FADD (Fas-Associated Death Domain). The activated caspase 8 initiates apoptosis via 2 different mechanisms: i) directly activates caspase 3 to stimulate apoptosis and ii) by cleaving BID i.e. the BH3 interacting Death Domain which acts as a precursor in activating the intrinsic apoptosis pathway (Rogalska et al., 2014). DR4 and DR5 showed an upregulation at 24 hours incubation time upon treatment with chalepin. Interestingly, there was an initial downregulation in the expression and then a significant upregulation at the 24 hours incubation time (Figure 4.39). Activation of caspase 8 which was observed through flow cytometry analysis (Figure 4.29) further confirms that the extrinsic pathway is activated upon treatment of chalepin. Caspase 8 could activate mitochondrial apoptosis pathway/intrinsic apoptosis pathway which is mediated by caspase 8 substrate Bid. Caspase 8 cleaves Bid to truncated Bid and it translocates to the mitochondria to interact with members of the Bcl2 family to promote cytochrome c release. Release of cytochrome c would then activate caspase 9 and then caspase 3 to initiate apoptosis (Gnesutta et al., 2003). Western blot analysis showed the downregulation of the protein BID (Figure 4.40). This indicated the cleavage of BID to truncated BID (tBID) which would initiate mitochondria to release cytochrome c and activate apoptosis through the mitochondrial pathway. A recent report by Richardson et al. (2016) showed that chalepin activated caspase 9 and caspase 3 which confirmed the occurance of the downstream intrinsic apoptosis pathway.

The effect of chalepin on NF-κB pathway, extrinsic apoptotic pathway and cell cycle has been summarized in Figure 5.3.

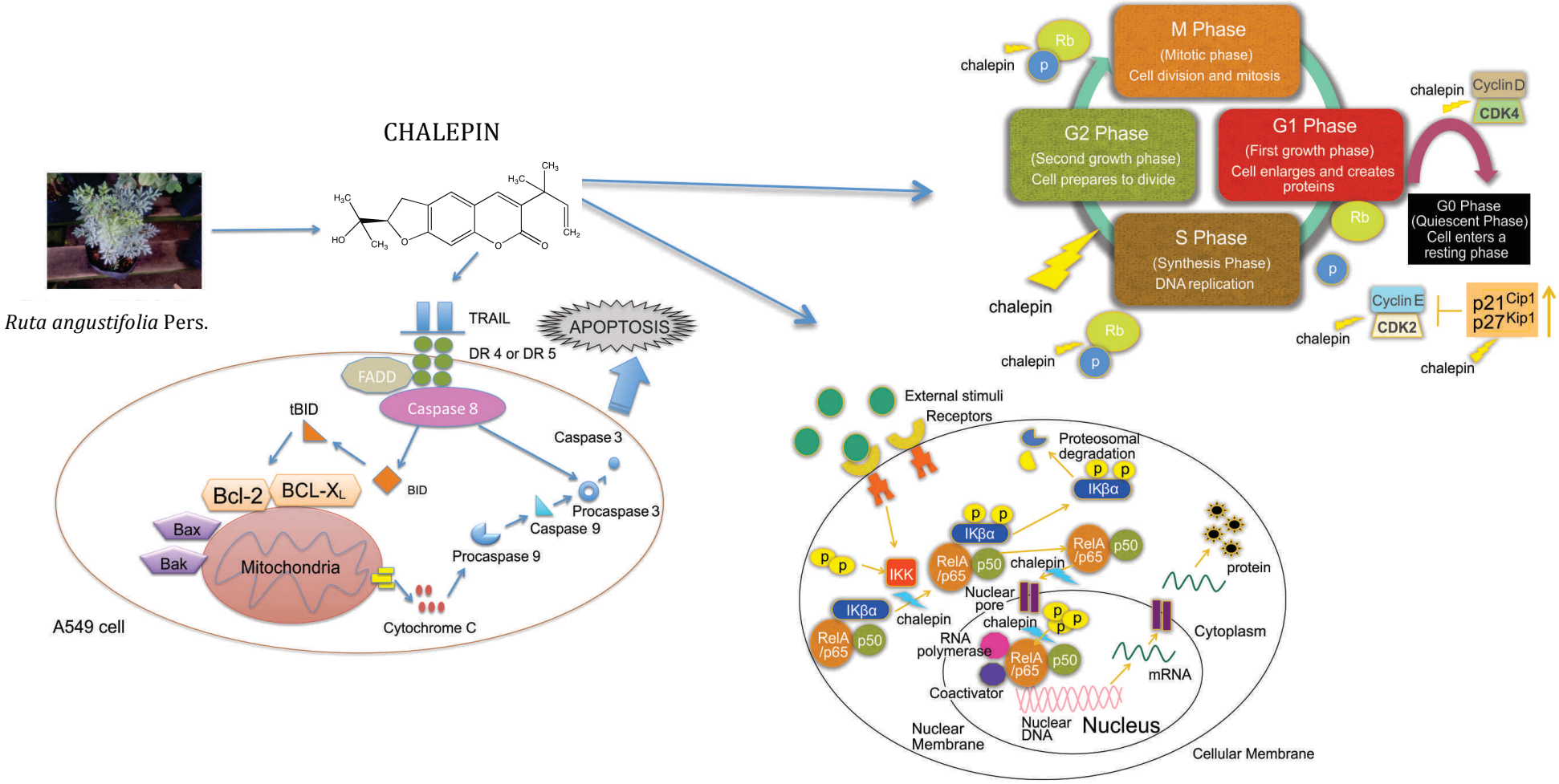

Figure 5.3: Graphical summary of the effect of chalepin on the NF-κB pathway, extrinsic apoptotic pathway and cell cycle

Signal transducer and activator of transcription 3 or STAT3 is overexpressed in many human tumors. The STAT3 family of transcription factor controls various physiological processes such as immunity, metabolism, development, and differentiation. STAT3 is often abnormally expressed in cancer (Siveen et al., 2014). STAT3 have been a promising target for the development of novel cancer drugs. Several studies have shown that modulation of constitutive STAT3 has a critical role in the tumor progression (Yue et al., 2009). Phosphorylation of STAT3 contributes to an important role in cell proliferation and survival of tumor cells in various types of cancer including head and neck cancer, multiple myeloma, lymphomas and leukemia (Sethi et al., 2014). In our study, treatment of chalepin suppressed the phosphorylation of STAT3 thus indicating an inactivation of the transcription factor (Figure 4.38). Chalepin therefore could inhibit the progression of A549 cells. Chalepin is good candidate for the modulation of STAT3. However, further research need to be conducted. Chalepin was found to be able to suppress expression of several STAT3 regulated gene products such as cyclin D1 which is responsible for cell proliferation, several anti apoptotic gene products such as Mcl-1 and c-Myc, immune suppression and inflammation related gene products e.g. Cox-2 and p21 which is associated with cell survival and metastasis.

Intracellular adhesion molecule-1 (ICAM-1), which is also known as CD54, has a significant role in adhesion involved in the immune response. The strength of adhesion was found to be determined by the changes in the ICAM-1 gene expression (Roy et al., 2001). It is a transmembrane glycoprotein in the immunoglobulin superfamily which is present at basal levels in a many types of cells (Usami et al., 2013). This molecule was found to play a significant role in various malignancies. Increase in expression of ICAM-1 in breast, gastric and colorectal cancers were found to enhance immune surveillance. However, in lung, melanoma and other cancers, there were reports of increase in expression of ICAM-1 causing cancer invasion and metastasis (Usami et al.,

2013). Our results showed that ICAM-1 was drastically downregulated upon exposure to chalepin. This could help inhibit A549 cells' ability to invade and metastasize. Studies have shown that ICAM-1 molecule is a highly NF-κB-dependent gene in A549 pulmonary epithelial cells and is therefore a useful endogenous reporter of NF-κB-dependent transcription (Holden et al., 2004). Our results also showed that chalepin inhibits NF-κB pathway and this correlates to the results of ICAM-1 downregulated expression upon treatment of chalepin.

Vascular endothelial growth factor (VEGF) which is also known as vascular permeability factor (VPF) is a potent angiogenic factor. It was first defined as an essential growth factor for vascular endothelial cells. Studies have shown that VEGF is upregulated in many tumors and this contributes to tumor angiogenesis. VEGF also has functions on normal physiological purpose such as bone formation, development, wound healing and hematopoiesis. In cancer treatment, various anti-VEGF methods have been employed. This is to inhibit the pro-angiogenic role of VEGF and thus inhibit neovascularization (Duffy et al., 2004). Chalepin has shown to downregulate the expression of VEGF in A549 cells based on the western blot analysis. Chalepin has the potency to inhibit the pro-angiogenic agent, which results in the termination of metastasis. This is because the angiogenesis, which helps in formation of blood vessels to provide nutrition for the growth of cancer cells, could be halted. Conventional treatment of cancer i.e. chemotherapy and radiotherapy have been shown to increase VEGF within the tumor. In this situation, VEGF might protect the cells from this apoptosis and increase their resistance to these treatment methods. It has been suggested that combination therapy, which consists of anti-VEGF therapy and conventional chemotherapy and radiotherapy, could be a more ideal way of treatment of cancer. This is because VEGF blockage would enable block of pro-angiogenic activity and anti-apoptotic function of VEGF (Duffy et al., 2004). Chalepin could be a good candidate to

be considered for the anti-VEGF therapy due to its ability to downregulate the expression of this protein. The ability of chalepin to inhibit ICAM-1 and VEGF shows that chalepin has anti-metastatic property and is able to block the metastasis of A549 cells.

Epidermal growth factor receptor (EGFR) signaling pathway is an important pathway that regulates proliferation, differentiation, growth and survival in mammalian cells (Oda et al., 2005). EGFR is classified under the ErbB family of receptor tyrosine kinases (RTK). It is a transmembrane protein, which is activated following binding with peptide growth factors. Researches have shown that the EGFR is involved in different carcinomas. Overexpression of EGFR is commonly found in various human cancers such as lung, head and neck, colon, pancreas, breast ovary, kidney and gliomas. More than 60% of NSCLC shows EGFR overexpression however no overexpression is detected in small cell lung cancer (Zhang et al., 2010). In cancer patients, amplification of EGFR gene and mutations in EGFR tyrosine kinase domain has been found to occur (Normanno et al., 2006). Autophosphorylation by intrinsic tyrosine/kinase activity often occurs when EGFR binds to its ligand. This results in more aggressive tumor phenotypes. Mutations in EGFR have been discovered in some lung cancers. These mutations have significant responses to tyrosine kinase inhibitors (Bethune et al., 2011). EGFR overexpression has been reported in many human malignancies, which includes NSCLC. EGFR overexpression has been shown to cause reduced survival, poor chemosensitivity and lymph node metastasis (Bethune et al., 2011). Gefitinib and Erlotinib are oral anti-cancer drugs that inhibit EGFR and are currently used in treatment of NSCLC. In our study, chalepin was found to reduce the expression and activation via phosphorylation of EGFR. Upon treatment of chalepin, both EGFR and pEGFR was found to be downregulated over a time period of 24 hours and has a potential use as a drug for EGFR inhibition.

Jak1, which is also known as Janus Kinase 1, is a gene that encodes a membrane protein. It is a member of a class of protein-tyrosine kinases (PTK). It functions to phosphorylate STAT proteins that are signal transducers and activators of transcription. The STAT family of transcription factors is potential targets for the treatment and prevention of cancers in NSCLC. Cytokine receptors and tyrosine kinases can phosphorylate and activate STAT proteins. Previous studies have shown that inhibition of JAK1 with small molecules or RNA interference results in loss of STAT3 tyrosine phosphorylation and thus inhibiting cell growth (Song et al., 2011). Our results show that the pSTAT3 was downregulated upon treatment of chalepin. JAK1 which also downregulated upon treatment of chalepin which correlates to this could be possibly act as a small molecule inhibitor of JAK1. Chalepin functions as a potent inhibitor of A549 lung cancer cell growth by targeting JAK1/STAT3 signaling pathways.

Extracellular signal-regulated kinase (ERK) signaling pathway plays an important role in the control of various cellular functions such as proliferation, survival, motility and differentiation. In human tumors, this pathway is often upregulated and thus it is an important target for the development of anticancer drugs. Since this pathway plays a significant role in various physiological processes, inhibiting this pathway would result in not only an anti-proliferative effect but also in anti-metastatic and anti-angiogenic effect in tumor cells (Kohno et al., 2006). AKT and ERK are both important signaling molecules that promote survival in different types of cancer (Cho et al., 2009). The fiasco in AKT and ERK signaling cascade results in malignancy. Continuous activation through phosphorylation causes these deregulated signals to cause uncontrolled cellular proliferation, tumor invasion, and prolonged cancer cell survival. Previous reports on NSCLC studies showed the presence of phosphorylated AKT in 33-79% of tumors and are found to cause aggressive tumor. ERK isoform 1 and 2 are the key modulators of cell proliferation and the phosphorylation of ERK causes activation of this protein,

which leads to uncontrolled cell proliferation. Phosphorylated ERKs were found in up to one third of NSCLCs (Crosbie et al., 2016). AKT, which is also known as protein kinase B, is an important target for cancer intervention. Activation of AKT is downstream of phosphoinositide 3-kinase (PI3K) through phosphorylation on Thr-308 and ser-473 site. Activation of AKT is important for cell proliferation and survival. Activated AKT was found to be present in many types of human tumors such as breast cancer, lung cancer, myeloma and leukemia (Cho et al., 2009). ERK 1/2 is an important molecule in cell proliferation and formation of cancer. It is activated via phosphorylation at Thr-202 and Tyr-204 residues. Various human cancer tissues such as NSCLC, colon, kidney, breast and head and neck have exhibited activated ERK1/2. Phosphorylated ERK causes cell survival by inhibiting apoptosis in various pathological conditions (Cho et al., 2009). In our study, we observed that the ERK, phosphorylated ERK (pERK), AKT and phosphorylated AKT (pAKT) protein was downregulated upon treatment of chalepin up to 12 hours of incubation period and showed slight upregulation at the 24 hours incubation time. Chalepin could be a potent agent to inhibit of ERK, AKT and phosphorylation of ERK and AKT. The data presented shows that chalepin selectively inhibits the proliferation of lung cancer cells by inhibiting the activation and it facilitates apoptosis by ERK inhibition. Since AKT activity could alter the sensitivity of non-small cell lung cancer to chemotherapeutic agents and irradiations (Cho et al., 2009), lung cancer treatment with chalepin has possibility to enhance the efficiency of these conventional cancer treatments and increase the apoptotic potential in lung cancer cells.

There are a total of 3 known mammalian Raf isoforms, which are the A, B and C-Raf, which is also known as Raf-1 or c-Raf. Majority of research is on c-Raf as it is the most commonly expressed isoform (Leicht et al., 2007). c-Raf is overexpressed in many human cancers especially human lung cancers. It was found to play evident role in

cancer such as by acting as a primary target downstream of Ras. Ras is found mutated in up to 30% of all human cancers. c-Raf also plays a role in modulating growth factors, which leads to stimulation of cancer proliferation. This is significant especially in the ovarian cancer. It was also found to function as to increase tumor invasiveness when it is upregulated or when in the decreased presence of the inhibitor of this molecule (Leicht et al., 2007). c-Raf is activated through phosphorylation. Chalepin was found to inhibit the phosphorylation of c-Raf and this is shown through the downregulation in the expression on p-c-Raf.

mTOR also known as proteins regulating the mammalian target of rapamycin is a serine/threonine kinase and a downstream mediator in phosphatidylinositol 3-kinase/AKT signaling pathway. It plays an important role in cellular growth and proliferation (Gridelli et al., 2008). mTOR are overexpressed or mutated in cancer cells (Easton et al., 2006). This has led to the notion that the mTOR inhibitors might be useful in oncology. mTOR was found to regulate cell growth by controlling mRNA translation, ribosome biogenesis, autophagy and metabolism (Guertin et al., 2007). In our study, chalepin resulted in the downregulation of the expression of phosphorylated mTOR and however the total mTOR remained constant. Chalepin was found to be an inhibitor of phosphorylation. A study reported that a combination of EGFR tyrosine kinase inhibitor and mTOR inhibitor could be an excellent therapy to treat NSCLC (Gridelli et al., 2008). Chalepin that possess the ability to inhibit mTOR activation and acts as an EGFR receptor inhibitor opens possibility of having the potential to be an excellent agent to treat NSCLC.

MEK1 and MEK2, also known as MAPK or Erk kinases, are dual-specificity protein kinases that function in a mitogen activated protein kinase cascade controlling cell growth and differentiation. Activation of MEK1 and MEK2 occurs through

phosphorylation of two serine residues at positions 217 and 221, located in the activation loop of subdomain VIII, by Raf-like molecules (Alessi et al., 1994). MEK1/2 is activated by various growth factors and cytokines and also by membrane depolarization and calcium influx. MEK activates p44 and p42 MAP kinase by phosphorylating both threonine and tyrosine residues at sites located within the activation loop of kinase subdomain VIII. One of the most common mutations in NSCLC is the *KRAS* mutation. This mutation is associated with adenocarcinoma histology and history of tobacco use, however there is not much targeted therapy that is available for these patient populations. Targets of the *KRAS* pathway could be either directly targeting the RAS protein or by inhibition of the downstream proteins in the MEK-ERK pathway. MEK inhibition has been one of the most promising treatments for patients with advanced *KRAS* mutations in NSCLC (Stinchcombe et al., 2014). In our analysis, MEK showed fluctuations in expression over a 24 hours incubation time with chalepin. Phosphorylated MEK (pMEK) i.e. the activated MEK, showed downregulation upon treatment with chalepin. This indicates that chalepin acts as a MEK inhibitor in NSCLC cells. Previous research has also shown results of MEK inhibitors exhibiting synergistic effects when combined with chemotherapy (Stinchcombe et al., 2014).

Ras protein controls signaling pathways that are important regulators of normal cell growth and malignant transformation. In human tumors they are deregulated due to activating mutations in the RAS genes. Therapies that target the RAS pathways may inhibit tumor growth, survival and spread (Downward, 2003). Ras is a small protein, which is found in our cells. It sits on the inner surface of the cell's membrane, to be activated by external signals. Under normal situations, Ras starts to transmit signals under tightly controlled mechanisms. In cancer, however, it loses the need to receive stimulations from outside and is constantly activated. A drug that could switch off the

Ras proteins in cancer cells could be a potent and promising drug in various types of cancer. Chalepin was found to downregulate the expression of Ras protein in NSCLC. Chalepin could be a potential drug, which could switch the notorious Ras protein off to inhibit malignancy in cells.

JNK was thought to mediate cell apoptosis in response to variety of signals induced by stress. However researches have proven that JNK plays significant role in cell growth and survival in tumor cells. JNK was found to be upregulated in colorectal cancer. Activated JNK increases cell proliferation. Lung cancer especially NSCLC has evidences of JNKs are phosphorylated at Thr183/Tyr185. This promotes cell proliferation and motility (Song et al., 2014). Activation of SAPK/JNK signaling pathway was reported to regulate the expression of numerous genes that are associated with apoptosis, invasion, metastasis and survival (Li et al., 2016). Our study revealed that chalepin could inhibit the phosphorylation of JNK in NSCLC. There was a drastic downregulation in the expression of pJNK upon treatment of chalepin. In another literature, it was reported that SAPK/JNK activation is important for EGF mediated cell proliferation (Bost et al., 1997). In our study, the inhibition of pSAPK/JNK and also the inhibition of the pEGFR further strengthen this idea.

Activation of p38 MAPKs has shown to contribute to the epithelial-mesenchymal transition (EMT) of cells in primary tumor. It contributes to the acquisition of invasion, migrating and extravasation of tumor cells. Decreasing the activity of p38 plays an important role in cancer as continuous cell proliferation requires the activity of p38 in most cancer cells (Koul et al., 2013). An interesting observation of our study is that chalepin is able to downregulate the expression of p38 and phosphorylated p38. It shows downregulation at earlier time points which is up to 4 hours and shows fluctuations in expressions henceforth. In NSCLC, p38 was found to be continuously

activated (Greenberg et al., 2002). Chalepin which is able to downregulate p38 expression and activation provides a promising therapeutic target.

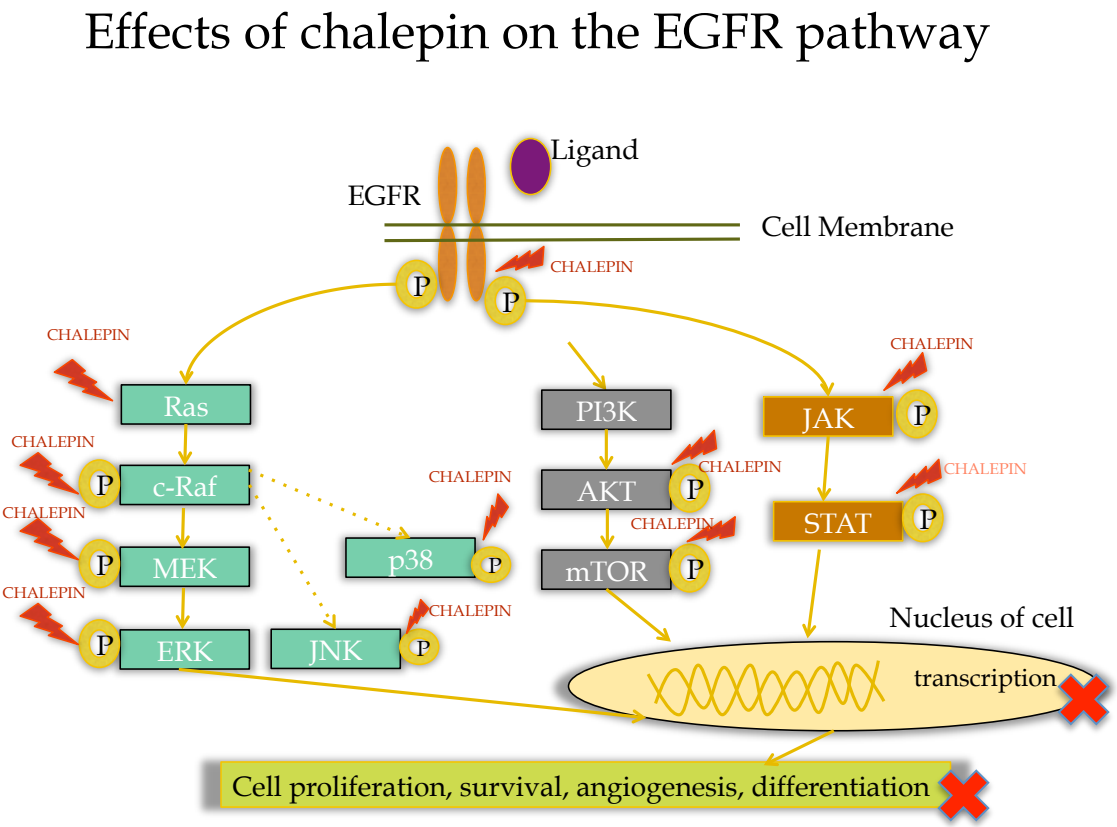

Figure 5.4: Summary of the effects of chalepin on the EGFR pathway and its related proteins.

Bioavailability refers to the extent and rate to which an active ingredient of a drug is absorbed or becomes available at the site of action (Chow, 2014). Drugs which are administered orally must pass through intestinal wall and then the hepatic portal and then to the circulatory system. Drugs may be metabolized before reaching optimal plasma concentrations. Low bioavailability is the most common predicament in oral dosages. Some studies have shown that the furanocoumarins such as bergamottin, and 6',7'-dihydroxybergamottin in grapefruit belonging to the family Rutaceae could inhibit

and alter the activity of Cytochrome P450 intestinal enzyme. This is specifically via inhibiting the isozyme CYP3A4 which is responsible for oxidization of various drugs and xenobiotics. This results in increment of bioavailability of certain drugs in presence of grapefruit juice (Cingi et al., 2013). The isolated compounds in our research consists of various furanocoumarins such as bergapten, chalepin and rutamarin which might have this effect of increasing bioavailability of a certain drug. However in our study, we did not test the isolated compounds on its bioavailability or its ability to increase bioavailability of other drugs. This could be a promising topic of research for future research.

Growth inhibition study was carried out on methanol extract, chloroform extract and chalepin from *R. angustifolia* via MTT assay. This is to determine the best time point for the study of anti-metastatic activity. To study the anti-metastatic acitivity, the treated cells should not be completedly inhibited and it should be viable. Hence the time point of 24 hours incubation was selected as the best time point for further research on the anti-metastatic studies. Metastasis is one of the most complex process and remains a major fiasco in management of cancer. The situation of which a cancer patient might develop metastasis years or even decades after diagnosis of primary tumor makes it even more of a complex problem (Hunter et al., 2008). To successfully colonize a secondary site, a cancer cell must must complete a sequence of steps before it becomes a clinically detectable lesion (Hunter et al., 2008). These series of steps includes separation of cells from primary tumor site, invasion through surrounding tissues and basement membranes, influx of cells into the circulation or lymphatics and arrest into distant organ. This would be most frequently followed by extravasation into the surrounding tissue and survival in the new microenvironment followed by proliferation, angiogenesis and evasion of apoptotic cell death and immunological responses (Hunter et al., 2008). Motility or ability of the cells to move is an essential characteristics of live

cells. Cell migration is one of the most important characteristic of cancer metastasis. The wound closure assay and transwell migration assay are the assays that are widely used by the scientific community to study the motility of the cancer cells (Justus et al., 2014). Migration is generally defined as the direct movement of cells on a 2D surface without any obstructive fiber networks. This includes substrate such as basal membranes, ECM fibers or plastic plates (Kramer et al., 2013). The transwell migration assay that was performed in our study showed that the methanol extract and chloroform extract of *R. angustifolia* showed almost complete inhibition for cell motility in the A549 cells. This shows that the extracts of this plant could be an excellent compound to inhibit cell motility and stop metastasis. These results were further confirmed with the observation of the cells via phase contrast microscope after crystal violet staining. The total inhibition in the A549 cells treated with extracts of *R. angustifolia* was shown in the Figure 4.48(B). Almost no visible cells are present in the lower part of the transwell membrane. Only the mesh of the membrane was seen. However, the pure compound, chalepin which was isolated from the chloroform extract of *R. angustifolia* showed a moderate capacity to stop the motility of the cells. The ability to inhibit cell migration was observed to be increasing with the increasing dose of the treament concentration. The cell culture wound closure assay is an assay in which a scratch is generated on a confluent cell monolayer and the speed of the wound closure and cell migration could be observed by taking snapshot pictures at regular time intervals using an inverted microscope (Justus et al., 2014). There are various advantages of conducting this assay. This assay to a certain extent mimics the *in vivo* migration of cells. It enables to study the extent of cell-cell interaction and cell-extracellular matrix (ECM) interactions as the cells are in attached form. This is also a fairly simple assay which could be conducted using commonly available laboratory supplies in a cell culture lab (Liang et al., 2007). The wound closure activity was inhibited almost completely in cells treated with

methanol and chloroform extracts of *R. angustifolia* and chalepin. To further add, the denuded zone became even larger upon treatment of these test samples and floating cells were observed at higher incubation period. This shows that the cell motility which is an important aspect in the metastasis cascade, is inhibited. The wound of untreated A549 cells movement was almost completely closed 24 hours after wounding while the treated cells stayed wide apart which displays inhibition of cell motility in a dose-dependent manner.

Penetration of tissue barriers such as passing the basement membrane and intrusion into the interstitial tissues by malignant tumor cells is defined as invasion. Invasion in experimental cell biology could be defined as a cell movement through a 3D matrix. This is often accompanied by restructuring of the 3D environment. To be able to move through the matrix, the cell must be able to modify its shape and interact with the ECM. ECM would provide the cell attachment substrate and also be a barrier towards the moving cell. Hence invasion is a process which requires adhesion, proteolysis of ECM components and migration (Kramer et al., 2013). The ECM used in this assay was Engelbreth–Holm–Swarm (EHS) mouse sarcomas. It occludes the membrane pores thus blocking non-invasive cells from migrating through. However, invasive cells can degrade this matrix and move through the ECM layer and adhere to the bottom of the filter (Kramer et al., 2013). In our study it was observed that the methanol and chloroform extract of *R. angustifolia* exhibited excellent anti-invasiveness, which is about 80% inhibition (Figure 4.47). Chalepin, however, exhibited moderate anti-invasive property. The ability of chalepin to inhibit the invasive property of A549 cells increased with increasing treatment concentration. This results show that methanol and chloroform extract has the ability to halt the A549 cell's invasive capacity.

The effect of the methanol extract, chloroform extract and chalepin from *R. angustifolia* was examined by detaching the treated cells from the cultured flasks and plating them onto a new culture plate with the same number of viable treated cells in each group. Round cells shows that the cells remain unattached. Therefore the higher the number of cells that remain unattached at a certain time point shows a defect or delay in their attachment. Figure 4.50 shows the different attachment ability of the A549 cells treated with different concentrations of test samples at various time points. Based on the figure, the control cells have started attachment at 6 hours and formed monolayer after 24 hours incubation. The cells treated with methanol and chloroform extracts of *R. angustifolia* remained unattached and exhibited a rounding morphology and it moved when the plate was gently tapped, even at the lowest treatment concentration. Chalepin treated cells showed approximately 40% cell attachment at the highest incubation time (24 hours). Almost all the treated plates exhibited cells which has defect in attachment. However at higher concentrations and incubation time, almost all the cells remained in the suspension. This shows that the ability of attachment in the A549 cells treated with extracts and chalepin were defected. In cells which are treated with lower concentrations of the respective test samples, some amount of adhesion was observed and the adhesion increased as the incubation time increases.

One of the important starting point in metastasis is the adhesion of cancer cells to ECM or vascular endothelium. Therapeutic methods to prevent or stop cancer adhesion and metastasis can significantly improve the survival of cancer patients (Xiang et al., 2015).

ICAM-1 which is a biomarker for metastasis was found to be downregulated upon treatment of chalepin in our studies (Figure 4.41). ICAM-1 which is an endothelial adhesion cell playes a critical role in cancer metastasis (Xiang et al., 2015), thus

inhibition of this molecule could significantly inhibit the ability of the A549 cells to metastasize. Vascular endothelial growth factor (VEGF) and VEGF receptors plays an important role in tumor angiogenesis. High expression of VEGF in the tumor microenvironment which leads to activation of its signalling pathway would result in stimulated growth and migration of blood and lymphatic endotelial cells. This would provide large vascular areas for tumor extravasation. VEGF can also assist in tumor intravasation via increasing vascular permeability (Moserle et al., 2013). In our research, chalepin was found to downregulate the expression of VEGF (Figure 4.41) and thus is capable of repressing the angiogenesis in tumor microenvironment which would assist in metastasis.

During multi steps of tumor metastasis, various adhesion molecules on tumor cells and host cells or components of the ECM plays a role in the cell-cell and cell-ECM adhesions. Carcinoma cells may discover suitable adhesion structures and attach, then invade and grow. Many different adhesion molecules and receptos are directly and indirectly involved in the malignancy of tumor. Interference in the adhesive interactions might block or suppress metastasis (Saiki, 1997). Adhesion is feasible by connecting intracellular cytoskeleton between cells or connecting cytoskeleton with ECM components such as collagen, fibronectin, laminin through a group of cell adhesion molecules (CAMs). CAMs are surface glycoproteins. Examples of CAMs includes integrins, cadherins and selectins. Different CAM molecules functions to adhere different types of cells. Integrins are responsible for cell–ECM adhesion. They are members of a glycoprotein family that form heterodimeric receptors for ECM molecules such as fibronectin (FN), laminin (LN), collagen (Col), fibrinogen, and vitronectin (VN) (Guan, 2015).

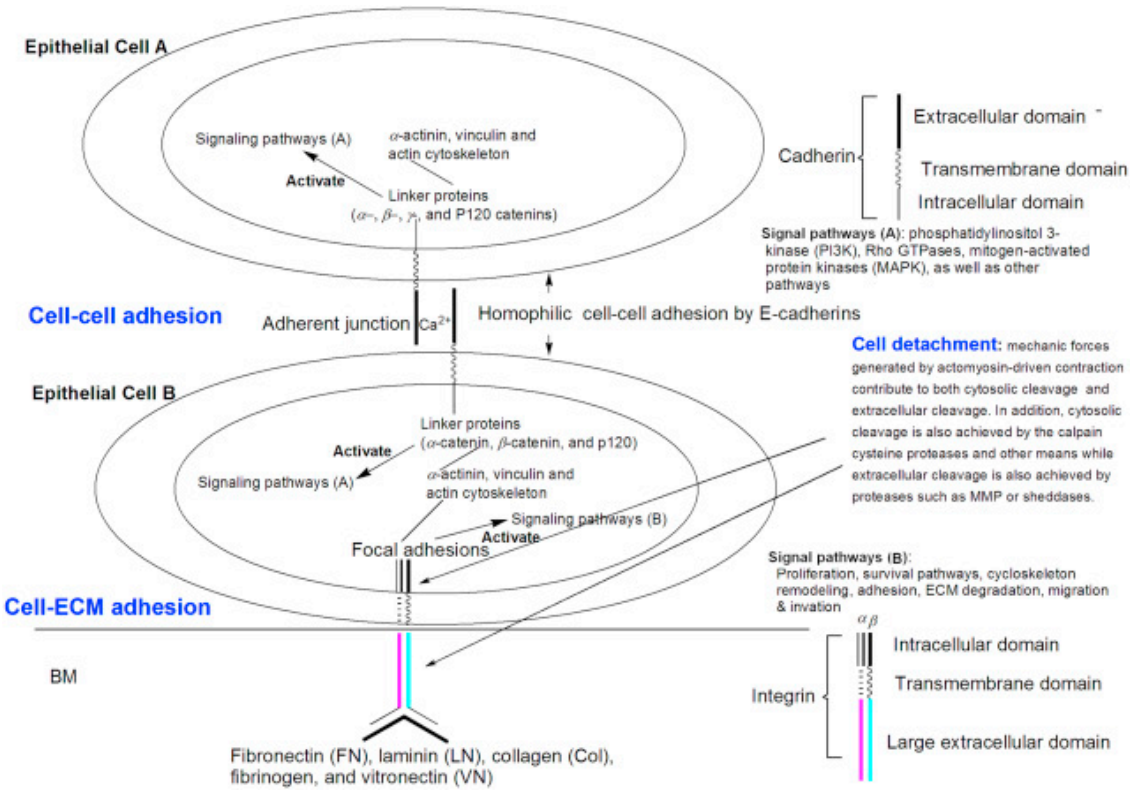

Figure 5.5: Graphic representing the involvement of various adhesion molecules in cell detachment, cell–cell adhesion and cell–matrix adhesion of epithelial cells by E-cadherins and integrins. Image excerpted from Guan (2015).

In our study, A549 cells treated with test samples from *R. angustifolia* showed remarkable inhibition in the adhesion with the ECM proteins, as compared to the untreated cells. Well with untreated cells showed higher absorbance value which correlates to the amount of cells adhered to the adhesion molecules and thus present in the well. Treatment of the cells with methanol extract, chloroform extract and chalepin repressed the ability of the cells to interact with the ECM proteins. Among the test samples, methanol and chloroform extracts showed remarkable anti-adhesive activity with relatively small amount of cells adhered as compared to the untreated control cells.The absorbance value was almost comparable to blank wells which was coated with BSA. Chalepin showed moderate activity and the least ability to inhibit interaction with these molecules as compared to other test samples. It can be deduced that the methanol and chloroform extracts have high potential in defecting the adhesion

molecule's function. These test samples from *R. angustifolia* could possibly be behaving as inhibitors of integrin to a certain degree.

Research have shown that increased expression of matrix metalloproteinases (MMPs) is often involved in tumor invasion and metastasis in various cancer types. Over 20 human MMPs have been identified and among them, MMP-2 and MMP-9 are the most important enzymes in the tumor invasion. This is due to its ability to degrade the ECM and type IV collagen rich basement membranes. MMP-2 is constitutively expressed highly in metastatic tumors. MMP-9, on the other hand, could be induced by cytokines, growth factors, and xenobiotics (Liu et al., 2013). Data obtained from our study suggests that A549 cells treated with test samples from *R. angustifolia* exhibits greater hinderance in production of MMP, especially MMP-2. The band exhibited by control cells are broader as compared to treated cells. This would limit the invasive and metastatic capacity of the tumor cells. However, further clarficiation and studies are needed to further strengthen and support this preliminary results.

CHAPTER 6: CONCLUSION

Based on this study, it was found that the cytotoxic effect of chalepin isolated from chloroform extract of *R.angustifolia* against A549 cell line is via the induction of apoptosis. Apoptosis was mediated by the mitochondria through Bax and Bak upregulation and the downregulation of inhibitor of apoptosis such as Bcl-2, survivin, Bcl-xL and cFLIP, release of cytochrome c and activation of caspases 9 and caspase 3. Chalepin was also found to exert DNA fragmentation and PS externalisation in A549 cells treated with it. This compound could be an excellent candidate to be considered as a chemotherapeutic agent. Chalepin exhibited cytotoxicity against A549 cell line on the mechanistic pathway of cell death and modulation in the cell cycle of A549 cells. Cell cycle arrest was found to occur at the S phase with downregulation in cyclin D, cyclin E, CDK2 and CDK4 and also with slight upregulation in the inhibitors of CDKs i.e. p21 and p27. A downregulation was observed in the pRb protein. Chalepin showed suppression of the NF-κB pathway with downregulation in the pIκβα and Iκβα degradation and inhibition in the phosphorylation and translocation of the p65 protein subunit. Besides that, extrinsic apoptosis pathway was triggered upon chalepin treatment towards the A549 cells. Activation of caspase 8, which is a key initiator kinase in the extrinsic apoptosis pathway, was activated upon treatment of chalepin. Besides that, DR4 and DR5 death receptors were upregulated and Bid cleavage further strengthen the results of the activation of extrinsic apoptosis pathway by chalepin. Phosphorylation of STAT3 was inhibited upon introduction of chalepin. Chalepin was found to inhibit several STAT3 regulated genes such as c-myc, Cox-2, Mcl-1, proteins. STAT3 and pSTAT3 were also downregulated. c-IAP1 and c-IAP2, which are anti-apoptotic proteins, were found to be downregulated after treatment of chalepin. It can therefore be concluded that chalepin induces death receptor mediated apoptosis, suppresses STAT3 phosphorylation, the NF-κB pathway and the extrinsic apoptosis

pathway through Bid cleavage. Besides that, chalepin was also found to attenuate EGFR pathway by downregulate the expression of protein related to this pathway. Upon treatment with chalepin, phosphorylation of EGFR and the receptor itself was found to be downregulated. There was a decrease in the expression of Jak1, and phosphorylation of ERK was inhibited by chalepin. Chalepin also showed inhibition in phosphorylation of Akt up till 12 hours. SAPK/JNK pathway, MAPK pathway and MEK pathway that plays a critical role in advancement of cancer was inhibited by chalepin. Besides that, anti-metastatic activity against A549 cells which was studied using methanol extract, chloroform extract and chalepin showed that the methanol extract showed the best activity among the test samples. The extracts exhibited better anti-metastatic property as compared to the isolated compound, chalepin. *R. angustifolia* was found to possess anti-invasion property, able to stop motility of cancer cells by inhibiting the migration and stopping the wound closure, able to stop the attachment of the cells, anti-adhesion property and able to inhibit matrix metalloproteinase. It was also shown that metastasis related proteins such as VEGF and ICAM-1 was downregulated upon exposure to chalepin.

Mechanism based therapies may be the most successful treatment of cancer. A therapeutic agent that focuses on these pathways instead of an individual phenotype or hallmark can be a promising mode of treatment. Chalepin, which is able to inhibit various cancers related pathways, could be a potential therapeutic agent in the treatment of cancer. However, further *in vivo* studies and clinical trials need to be conducted to enhance these results further.

REFERENCES

Adamska-Szewczyk, A., Glowniak, K., & Baj, T. (2016). Furochinoline alkaloids in plants from Rutaceae family – a review. *Current Issues in Pharmacy and Medical Sciences, 29*(1), 33-38.

Adnan, M.M. MBBS Medicine (Humanity First). *Programmed cell death* (no date). Retrieved on 19th December 2016 from: http://medicinembbs.blogspot.my/2011/03/programmed-cell-death-apoptosis.html

Aherne, G. W., Hardcastle, A., Valenti, M., Bryant, A., Rogers, P., Pettit, G. R., . . . Kelland, L. R. (1996). Antitumour evaluation of dolastatins 10 and 15 and their measurement in plasma by radioimmunoassay. *Cancer Chemotherapy and Pharmacology, 38*(3), 225-232.

Akalin, E., & Ertug, F. (2003). An anatomical and ethnobotanical study on Ruta species in Turkey. *Journal of Faculty Pharmacy of Istanbul University, 35*, 121-132.

Alberts, B., Johnson, A., Lewis, J., Raff, M., Roberts, K. & Walter, P. (2002). *Molecular biology of the cell* (4th ed.). New York: Garland Science.

Alessi, D. R., Saito, Y., Campbell, D., Cohen, P., Sithanandam, G., Rapp, U., . . . Cowley, S. (1994). Identification of the sites in MAP kinase kinase-1 phosphorylated by p74raf-1. *The EMBO Journal, 13*(7), 1610.

Amar, Z., Abdelwahab, B., Abdelhakim, B., & Noureddine, G. (2012). Environmental impact on the chemical composition and yield of essential oils of Algerian *Ruta Montana* (Clus.) L and their antioxidant and antibacterial activities. *Advances in Environmental Biology*, *6*(10), 2684-2689.

American Cancer Society (16 May 2016). *What is non-small cell lung cancer?* Retrieved on 4th December 2016 from: https://www.cancer.org/cancer/non-small-cell-lung-cancer/about/what-is-non-small-cell-lung-cancer.html

Annie's remedy. Rue, *Ruta graveolens* L. (no date). Retrieved on 14th May 2018 from: https://www.anniesremedy.com/ruta-graveolens-rue.php

Arias-Santiago, S. A., Fernández-Pugnaire, M. A., Almazán-Fernández, F. M., Serrano-Falcón, C., & Serrano-Ortega, S. (2009). Phytophotodermatitis due to *Ruta graveolens* prescribed for fibromyalgia. *Rheumatology (Oxford), 48*(11), 1401-1401.

Bachmeier, B., Killian, P., Pfeffer, U., & Nerlich, A. (2009). Novel aspects for the application of Curcumin in chemoprevention of various cancers. *Frontiers in Bioscience (Scholar edition), 2*, 697-717.

Benazir, J., Suganthi, R., Renjini Devi, M., Suganya, K., Monisha, K., Nizar Ahamed, K., & Santhi, R. (2011). Phytochemical profiling, antimicrobial and cytotoxicity studies of methanolic extracts from *Ruta graveolens*. *Journal of Pharmacy Research, 4*(5), 1407-1409.

Besbes, S., & Billard, C. (2015). First MCL-1-selective BH3 mimetics as potential therapeutics for targeted treatment of cancer. *Cell Death & Disease, 6*(7), e1810.

Bethune, G., Bethune, D., Ridgway, N., & Xu, Z. (2011). Epidermal growth factor receptor (EGFR) in lung cancer: An overview and update. *Journal of Thoracic Disease, 2*(1), 48-51.

Bio-Rad Life Science Research. *Introduction to protein electrophoresis* (no date). Retrieved on 4th December 2016 from: http://www.bio-rad.com/en-sg/applications-technologies/introduction-protein-electrophoresis

Bio-Rad Life Science Research. *Introduction to western blotting* (2017). Retrieved on 10th December 2017 from: http://www.bio-rad.com/en-sg/applications-technologies/introduction-western-blotting

Bost, F., McKay, R., Dean, N., & Mercola, D. (1997). The JUN kinase/stress-activated protein kinase pathway is required for epidermal growth factor stimulation of growth of human A549 lung carcinoma cells. *Journal of Biological Chemistry, 272*(52), 33422-33429.

Brower, V. (2008). Back to nature: Extinction of medicinal plants threatens drug discovery. *Journal of the Natural Cancer Institute*, *100*, 838-839.

Brumatti, G., & Ekert, P. (2013). Seeking a MCL-1 inhibitor. *Cell Death and Differentiation, 20*(11), 1440-1441.

Cai, J., Yang, J., & Jones, D. (1998). Mitochondrial control of apoptosis: The role of cytochrome c. *Biochimica et Biophysica Acta (BBA)-Bioenergetics, 1366*(1), 139-149.

Caputi, L. John Innes Centre. *Vinblastine and vincristine: life-saving drugs from a periwinkle* (28 March 2018). Retrieved on 4th April 2018 from: https://www.jic.ac.uk/news-and-events/blog-copy/2018/03/vinblastine-and-vincristine-life-saving-drugs-peri/

Carmeliet, P. (2005). VEGF as a key mediator of angiogenesis in cancer. *Oncology, 69*(Suppl. 3), 4-10.

Cell senescence and apoptosis (no date). Retrieved on 4th November 2016 from: http://cc.scu.edu.cn/G2S/Template/View.aspx?courseType=1&courseId=17&topMenuId=113308&menuType=1&action=view&type=&name=&linkpageID=113786

Chalah, A., & Khosravi-Far, R. (2008). The mitochondrial death pathway. *In Programmed cell death in cancer progression and therapy*. *Advances in Experimental Medicine and Biology, 615*, 25-45.

Chang, L., Graham, P., Hao, J., Ni, J., Bucci, J., Cozzi, P., . . . Li, Y. (2014). PI3K/Akt/mTOR pathway inhibitors enhance radiosensitivity in radioresistant prostate cancer cells through inducing apoptosis, reducing autophagy, suppressing NHEJ and HR repair pathways. *Cell Death & Disease, 5*(10), e1437.

Chaturvedi, M., Sung, B., Yadav, V., Kannappan, R., & Aggarwal, B. (2011). NF-κB addiction and its role in cancer: 'One size does not fit all'. *Oncogene, 30*(14), 1615-1630.

Chen, H., Tang, X., Zhou, B., Xu, N., & Wang, Y. (2016). Mechanism of Deca-BDE-induced apoptosis in Neuro-2a cells: Role of death-receptor pathway and reactive oxygen species-mediated mitochondrial pathway. *Journal of Environmental Sciences, 46, 241-251.*

Chen, H.C. (2005). Boyden chamber assay. *Cell Migration: Developmental Methods and Protocols*, *294*, 15-22.

Chiang, G. G., & Abraham, R. T. (2005). Phosphorylation of mammalian target of rapamycin (mTOR) at Ser-2448 is mediated by p70S6 kinase. *Journal of Biological Chemistry, 280*(27), 25485-25490.

Cho, H. S., Chang, S. H., Chung, Y. S., Shin, J. Y., Park, S. J., Lee, E. S., . . . Woo, M. (2009). Synergistic effect of ERK inhibition on tetrandrine-induced apoptosis in A549 human lung carcinoma cells. *Journal of Veterinary Science, 10*(1), 23-28.

Chow, A. (2010). Cell cycle control by oncogenes and tumor suppressors: Driving the transformation of normal cells into cancerous cells. *Nature Education, 3*(9), 7.

Chow, S. C. (2014). Bioavailability and bioequivalence in drug development. *Wiley Interdisciplinary Reviews: Computational Statistics, 6*(4), 304-312.

Cingi, C., Toros, S. Z., Gürbüz, M. K., Ince, I., Cakli, H., Erdogmus, N., . . . Kaya, E. (2013). Effect of grapefruit juice on bioavailability of montelukast. *The Laryngoscope, 123*(4), 816-819.

Circu, M. L., & Aw, T. Y. (2010). Reactive oxygen species, cellular redox systems, and apoptosis. *Free Radical Biology and Medicine, 48*(6), 749-762.

Collins, K., Jacks, T., & Pavletich, N. P. (1997). The cell cycle and cancer. *Proceedings of the National Academy of Sciences, 94*(7), 2776-2778.

Cossarizza, A., & Salvioli, S. (1998). Analysis of mitochondrial membrane potential with the sensitive fluorescent probe JC-1. *Purdue Cytometry CD-ROM Series, 4*.

Cragg, G. M., & Pezzuto, J. M. (2016). Natural products as a vital source for the discovery of cancer chemotherapeutic and chemopreventive agents. *Medical Principles and Practice, 25*(Suppl. 2), 41-59.

Crosbie, P. A., Crosbie, E. J., Aspinall-O'Dea, M., Walker, M., Harrison, R., Pernemalm, M., . . . Pierce, A. (2016). ERK and AKT phosphorylation status in lung cancer and emphysema using nanocapillary isoelectric focusing. *BMJ Open Respiratory Research, 3*(1), e000114.

Crowley, L. C., Scott, A. P., Marfell, B. J., Boughaba, J. A., Chojnowski, G., & Waterhouse, N. J. (2016). Measuring cell death by propidium iodide uptake and flow cytometry. *Cold Spring Harbor Protocols, 2016*(7), pdb. prot087163.

Cui, Y., Lu, P., Song, G., Liu, Q., Zhu, D., & Liu, X. (2016). Involvement of PI3K/Akt, ERK and p38 signaling pathways in emodin-mediated extrinsic and intrinsic human hepatoblastoma cell apoptosis. *Food and Chemical Toxicology, 92*, 26-37.

Czabotar, P. E., Lessene, G., Strasser, A., & Adams, J. M. (2014). Control of apoptosis by the BCL-2 protein family: Implications for physiology and therapy. *Nature Reviews Molecular Cell Biology, 15*(1), 49-63.

da Cunha Santos, G., Shepherd, F. A., & Tsao, M. S. (2011). EGFR mutations and lung cancer. *Annual Review of Pathology: Mechanisms of Disease, 6*, 49-69.

Dang, C.T., Shapiro, C. L., & Hudis, C. A. (2002). Potential role of selective COX-2 inhibitors in cancer management. *Oncology (Williston Park, NY), 16*(5 Suppl 4), 30-36.

Dang, C.V. (1999). c-Myc target genes involved in cell growth, apoptosis, and metabolism. *Molecular and Cellular Biology, 19*(1), 1-11.

Darzynkiewicz, Z., Galkowski, D., & Zhao, H. (2008). Analysis of apoptosis by cytometry using TUNEL assay. *Methods, 44*(3), 250-254.

de Almagro, M., & Vucic, D. (2012). The inhibitors of apoptosis (IAP) proteins are critical regulators of signaling pathways and targets for anti-cancer therapy. *Experimental Oncology, 34*(3), 200-211.

Del Castillo, J. B., Luis, F. R., & Secundino, M. (1984). Angustifolin, a coumarin from *Ruta angustifolia*. *Phytochemistry, 23*(9), 2095-2096.

Del Castillo, J.B., Secundino, M., & Luis, F. R. (1986). Four aromatic derivatives from *Ruta angustifolia*. *Phytochemistry, 25*(9), 2209-2210.

Desagher, S., & Martinou, J.C. (2000). Mitochondria as the central control point of apoptosis. *Trends in Cell Biology, 10*(9), 369-377.

Desai, A. G., Qazi, G. N., Ganju, R. K., El-Tamer, M., Singh, J., Saxena, A. K., . . . Bhat, H. K. (2008). Medicinal plants and cancer chemoprevention. *Current Drug Metabolism, 9*(7), 581-591.

Downward, J. (2003). Targeting RAS signalling pathways in cancer therapy. *Nature Reviews Cancer, 3*(1), 11-22.

Duffy, A. M., Bouchier-Hayes, D. J., & Harmey, J. H. (2004). Vascular endothelial growth factor (VEGF) and its role in non-endothelial cells: Autocrine signalling by VEGF. In J.H. Harmey (Ed), *VEGF and cancer* (pp. 134-144). Austin (TX): Landes Bioscience.

Easton, J., & Houghton, P. (2006). mTOR and cancer therapy. *Oncogene, 25*(48), 6436-6446.

eBioscience.com – For apoptosis reagents. *Multicolor annexin v* (2012). Retrieved on 5th December 2016 from: http://www.level.com.tw/html/front/bin/ptdetail.phtml?Part=2012-09-03_

Elmore, S. (2007). Apoptosis: A review of programmed cell death. *Toxicologic Pathology, 35*(4), 495-516.

Emerole, G., Thabrew, M. I., Anosa, V., & Okorie, D. A. (1981). Structure-activity relationship in the toxicity of some naturally occurring coumarins-chalepin, imperatorin and oxypeucedanine. *Toxicology, 20*(1), 71-80.

Eskelinen, E.-L., & Saftig, P. (2009). Autophagy: A lysosomal degradation pathway with a central role in health and disease. *Biochimica et Biophysica Acta (BBA)-Molecular Cell Research, 1793*(4), 664-673.

Fadlalla, K., Watson, A., Yehualaeshet, T., Turner, T., & Samuel, T. (2011). *Ruta graveolens* extract induces DNA damage pathways and blocks Akt activation to inhibit cancer cell proliferation and survival. *Anticancer Research, 31*(1), 233-241.

Flow cytometry – application. *Flow cytometry apoptosis* (no date). Retrieved on 4th December 2016 from: http://www.flow-cytometry.us/index.php?page=apoptosis

Flow cytometric analysis of cell cycle with propidium iodide DNA staining. *Flow cytometry cell cycle analysis using propidium iodide DNA staining* (no date). Retrieved on: 4th December 2016 from: http://www.abcam.com/protocols/flow-cytometric-analysis-of-cell-cycle-with-propidium-iodide-dna-staining

Flow cytometry (FCM)/FACS Application Apoptosis. *Changes of plasma membrane* (no date). Retrieved on 5th December 2016 from: http://www.sinobiological.com/flow-cytometry-fcm-facs-application-apoptosis.html

Frankowski, H., Gu, Y.-H., Heo, J. H., Milner, R., & del Zoppo, G. J. (2012). Use of gel zymography to examine matrix metalloproteinase (gelatinase) expression in brain tissue or in primary glial cultures. *Astrocytes: Methods and Protocols, 814*, 221-233.

Ganapathy, V., Moghe, P. V., & Roth, C. M. (2015). Targeting tumor metastases: Drug delivery mechanisms and technologies. *Journal of Controlled Release, 219*, 215-223.

Geiger, T. R., & Peeper, D. S. (2009). Metastasis mechanisms. *Biochimica et Biophysica Acta (BBA)-Reviews on Cancer, 1796*(2), 293-308.

Gentile, M. T., Ciniglia, C., Reccia, M. G., Volpicelli, F., Gatti, M., Thellung, S., . . . Colucci-D'Amato, L. (2015). *Ruta graveolens* L. induces death of glioblastoma cells and neural progenitors, but not of neurons, via ERK 1/2 and AKT activation. *PLoS ONE, 10*(3), e0118864.

Ghatage, D. D., Gosavi, S. R., Ganvir, S. M., & Hazarey, V. K. (2012). Apoptosis: Molecular mechanism. *Journal of Orofacial Sciences, 4*(2), 103.

Ghosh, S., Sikdar, S., Mukherjee, A., & Khuda-Bukhsh, A. R. (2015). Evaluation of chemopreventive potentials of ethanolic extract of *Ruta graveolens* against A375 skin melanoma cells *in vitro* and induced skin cancer in mice *in vivo*. *Journal of Integrative Medicine, 13*(1), 34-44.

Glick, D., Barth, S., & Macleod, K. F. (2010). Autophagy: Cellular and molecular mechanisms. *The Journal of Pathology, 221*(1), 3-12.

Gnesutta, N., & Minden, A. (2003). Death receptor-induced activation of initiator caspase 8 is antagonized by serine/threonine kinase PAK4. *Molecular and Cellular Biology, 23*(21), 7838-7848.

Gomes, A., Fernandes, E., & Lima, J. L. (2005). Fluorescence probes used for detection of reactive oxygen species. *Journal of Biochemical and Biophysical Methods, 65*(2), 45-80.

Greenberg, A. K., Basu, S., Hu, J., Yie, T.-a., Tchou-Wong, K. M., Rom, W. N., & Lee, T. C. (2002). Selective p38 activation in human non–small cell lung cancer. *American Journal of Respiratory Cell and Molecular Biology, 26*(5), 558-564.

Gridelli, C., Maione, P., & Rossi, A. (2008). The potential role of mTOR inhibitors in non-small cell lung cancer. *The Oncologist, 13*(2), 139-147.

Gu, H., Wang, X., Rao, S., Wang, J., Zhao, J., Ren, F. L., . . . Liu, W. (2008). Gambogic acid mediates apoptosis as a p53 inducer through down-regulation of mdm2 in wild-type p53-expressing cancer cells. *Molecular Cancer Therapeutics, 7*(10), 3298-3305.

Guan, X. (2015). Cancer metastases: Challenges and opportunities. *Acta Pharmaceutica Sinica B, 5*(5), 402-418.

Guertin, D. A., & Sabatini, D. M. (2007). Defining the role of mTOR in cancer. *Cancer Cell, 12*(1), 9-22.

Hanahan, D., & Weinberg, R. A. (2000). The hallmarks of cancer. *Cell, 100*(1), 57-70.

Hanahan, D., & Weinberg, R. A. (2011). Hallmarks of cancer: The next generation. *Cell, 144*(5), 646-674.

Harvey, A. L. (2008). Natural products in drug discovery. *Drug Discovery Today, 13*(19), 894-901.

Hassan, M., Watari, H., AbuAlmaaty, A., Ohba, Y., & Sakuragi, N. (2014). Apoptosis and molecular targeting therapy in cancer. *BioMed Research International, 150845*, 1-23.

Herbal medicine. *Herbal medicine use of Ruta angustifolia*. (no date). Retrieved on 14th May 2018 from: https://www.herbs-medicine.com/2016/04/herbal-medicine.html#

Ho, Y. F., Karsani, S. A., Yong, W. K., & Abd Malek, S. N. (2013). Induction of apoptosis and cell cycle blockade by helichrysetin in A549 human lung adenocarcinoma cells. *Evidence-Based Complementary and Alternative Medicine, 2013*, 857257.

Hoesel, B., & Schmid, J. A. (2013). The complexity of NF-κB signaling in inflammation and cancer. *Molecular Cancer, 12*(1), 86.

Holden, N. S., Catley, M. C., Cambridge, L. M., Barnes, P. J., & Newton, R. (2004). ICAM‐1 expression is highly NF‐κB‐dependent in A549 cells. *European Journal of Biochemistry, 271*(4), 785-791.

Horvitz, H. R. (1999). Genetic control of programmed cell death in the nematode *Caenorhabditis elegans*. *Cancer Research, 59*(7 Supplement), 1701s-1706s.

Houghton, P., Fang, R., Techatanawat, I., Steventon, G., Hylands, P. J., & Lee, C. (2007). The sulphorhodamine (SRB) assay and other approaches to testing plant extracts and derived compounds for activities related to reputed anticancer activity. *Methods, 42*(4), 377-387.

Humphries, M. J. (2009). Cell adhesion assays. In Walker & John M. (Eds.) *Extracellular matrix protocols* (2nd ed.)*, (*pp. 203-210). New York, NY: Humana Press.

Hunter, K. W., Crawford, N. P., & Alsarraj, J. (2008). Mechanisms of metastasis. *Breast Cancer Research, 10*(Suppl 1), S2.

Hunter, T., & Pines, J. (1994). Cyclins and cancer II: Cyclin D and CDK inhibitors come of age. *Cell, 79*(4), 573-582.

Indran, I. R., Tufo, G., Pervaiz, S., & Brenner, C. (2011). Recent advances in apoptosis, mitochondria and drug resistance in cancer cells. *Biochimica et Biophysica Acta (BBA)-Bioenergetics, 1807*(6), 735-745.

Inggu, the magical plant efficacious (no date). Retrieved on 14th May 2018 from: http://natudays.blogspot.my/2012/02/rue.html

Intracellular ROS assay (no date). Retrieved on 7th July 2016 from: http://www.cellbiolabs.com/sites/default/files/STA-342%20Fig%201.jpg

Israël, A. (2010). The IKK complex, a central regulator of NF-κB activation. *Cold Spring Harbor Perspectives in Biology, 2*(3), a000158.

Justus, C. R., Leffler, N., Ruiz-Echevarria, M., & Yang, L. V. (2014). *In vitro* cell migration and invasion assays. *JoVE (Journal of Visualized Experiments),* (*88*), e51046-e51046.

Kan, C., & Chan, K. (2016). A Review of lung cancer research in Malaysia. *The Medical Journal of Malaysia, 71*(Suppl 1), 70.

Karin, M. (1999). How NF-κB is activated: The role of the IκB kinase (IKK) complex. *Oncogene, 18*(49), 6867-6874.

Kasibhatla, S., & Tseng, B. (2003). Why target apoptosis in cancer treatment? *Molecular Cancer Therapeutics, 2*(6), 573-580.

Kaushal, V., Herzog, C., Haun, R. S., & Kaushal, G. P. (2014). Caspase protocols in mice. In V. Bozhkov, Peter, Salvensen, Guy (Eds.) *Caspases, paracaspases, and metacaspases: methods and protocols* (pp. 141-154). New York, NY: Humana Press.

Keglevich, P., Hazai, L., Kalaus, G., & Szántay, C. (2012). Modifications on the basic skeletons of vinblastine and vincristine. *Molecules, 17*(5), 5893-5914.

Kohno, M., & Pouyssegur, J. (2006). Targeting the ERK signaling pathway in cancer therapy. *Annals of Medicine, 38*(3), 200-211.

Koul, H. K., Pal, M., & Koul, S. (2013). Role of p38 MAP kinase signal transduction in solid tumors. *Genes & Cancer, 4*(9-10), 342-359.

Kramer, N., Walzl, A., Unger, C., Rosner, M., Krupitza, G., Hengstschläger, M., & Dolznig, H. (2013). *In vitro* cell migration and invasion assays. *Mutation Research/Reviews in Mutation Research, 752*(1), 10-24.

Krasinskas, A. M. (2011). EGFR signaling in colorectal carcinoma. *Pathology Research International, 2011*, 932932.

Kroemer, G., Galluzzi, L., & Brenner, C. (2007). Mitochondrial membrane permeabilization in cell death. *Physiological Reviews, 87*(1), 99-163.

Kroemer, G., Galluzzi, L., Vandenabeele, P., Abrams, J., Alnemri, E., Baehrecke, E., . . .Green, D. (2009). Classification of cell death: Recommendations of the Nomenclature Committee on Cell Death 2009. *Cell Death & Differentiation, 16*(1), 3-11.

Kruidering, M., & Evan, G. I. (2000). Caspase‐8 in Apoptosis: The Beginning of "The End"? *IUBMB Life, 50*(2), 85-90.

Krysko, D. V., Berghe, T. V., D'Herde, K., & Vandenabeele, P. (2008). Apoptosis and necrosis: Detection, discrimination and phagocytosis. *Methods, 44*(3), 205-221.

Kuida, K. (2000). Caspase-9. *The International Journal of Biochemistry & Cell Biology, 32*(2), 121-124.

Lacy, A., & O'kennedy, R. (2004). Studies on coumarins and coumarin-related compounds to determine their therapeutic role in the treatment of cancer. *Current Pharmaceutical Design, 10*(30), 3797-3811.

Lee, C., & Houghton, P. (2005). Cytotoxicity of plants from Malaysia and Thailand used traditionally to treat cancer. *Journal of Ethnopharmacology, 100*(3), 237-243.

Leicht, D. T., Balan, V., Kaplun, A., Singh-Gupta, V., Kaplun, L., Dobson, M., & Tzivion, G. (2007). Raf kinases: Function, regulation and role in human cancer. *Biochimica et Biophysica Acta (BBA)-Molecular Cell Research, 1773*(8), 1196-1212.

Leverson, J., Zhang, H., Chen, J., Tahir, S., Phillips, D., Xue, J., . . . Xiao, Y. (2015). Potent and selective small-molecule MCL-1 inhibitors demonstrate on-target cancer cell killing activity as single agents and in combination with ABT-263 (navitoclax). *Cell Death & Disease, 6*(1), e1590.

Li, H., Zhu, H., Xu, C.-J., & Yuan, J. (1998). Cleavage of BID by caspase 8 mediates the mitochondrial damage in the Fas pathway of apoptosis. *Cell, 94*(4), 491-501.

Li, L., Wu, J., Zheng, F., Tang, Q., Wu, W., & Hann, S. S. (2016). Inhibition of EZH2 via activation of SAPK/JNK and reduction of p65 and DNMT1 as a novel mechanism in inhibition of human lung cancer cells by polyphyllin I. *Journal of Experimental & Clinical Cancer Research, 35*(1), 112.

Liam, C. K., Andarini, S., Lee, P., Ho, J. C. M., Chau, N. Q., & Tscheikuna, J. (2015). Lung cancer staging now and in the future. *Respirology, 20*(4), 526-534.

Liang, C. C., Park, A. Y., & Guan, J. L. (2007). *In vitro* scratch assay: A convenient and inexpensive method for analysis of cell migration *in vitro*. *Nature Protocols, 2*(2), 329-333.

Lim, G. C. C. (2002). Overview of cancer in Malaysia. *Japanese Journal of Clinical Oncology, 32*(suppl 1), S37-S42.

Lim, S., & Kaldis, P. (2013). Cdks, cyclins and CKIs: Roles beyond cell cycle regulation. *Development, 140*(15), 3079-3093.

Ling, L., Tan, K., Lin, H., & Chiu, G. (2011). The role of reactive oxygen species and autophagy in safingol-induced cell death. *Cell Death & Disease, 2*(3), e129.

Liu, Y., Cao, W., Zhang, B., Liu, Y. Q., Wang, Z. Y., Wu, Y. P., . . . Zhou, G. B. (2013). The natural compound magnolol inhibits invasion and exhibits potential in human breast cancer therapy. *Scientific Reports, 3*, 3098.

Loo, D. T. (2011). *In situ* detection of apoptosis by the TUNEL assay: An overview of techniques. In Didenko (Ed.), *DNA damage detection in situ, ex vivo, and in vivo: methods and protocols*, (pp. 3-13). New York, NY: Humana Press.

Lowe, S. W., & Lin, A. W. (2000). Apoptosis in cancer. *Carcinogenesis, 21*(3), 485-495.

Lu, J. J., Bao, J. L., Chen, X. P., Huang, M., & Wang, Y. T. (2012). Alkaloids isolated from natural herbs as the anticancer agents. *Evidence-Based Complementary and Alternative Medicine, 2012*, Article ID 485042.

Lung cancer (no date). Retrieved on 17th December 2016 from: http://www.cancer.org/cancer/lungcancer/

Mahmood, T., & Yang, P. C. (2012). Western blot: Technique, theory, and troubleshooting. *North American Journal of Medical Sciences, 4*(9), 429.

Manual, I. *Mini Trans-Blot® electrophoretic transfer cell instruction manual*. Retrieved on 16th December 2016 from: http://www.biorad.com/webroot/web/pdf/lsr/literature/M1703930.pdf

Martinkova, J., Gadher, S. J., Hajduch, M., & Kovarova, H. (2009). Challenges in cancer research and multifaceted approaches for cancer biomarker quest. *FEBS Letters, 583*(11), 1772-1784.

Matés, J. M., & Sánchez-Jiménez, F. M. (2000). Role of reactive oxygen species in apoptosis: Implications for cancer therapy. *The International Journal of Biochemistry & Cell Biology, 32*(2), 157-170.

McChesney, J. D., Venkataraman, S. K., & Henri, J. T. (2007). Plant natural products: Back to the future or into extinction? *Phytochemistry, 68*(14), 2015-2022.

McIlwain, D. R., Berger, T., & Mak, T. W. (2013). Caspase functions in cell death and disease. *Cold Spring Harbor Perspectives in Biology, 5*(4), a008656.

Miguel, E. S. (2003). Rue (*Ruta* L., Rutaceae) in traditional Spain: Frequency and distribution of its medicinal and symbolic applications. *Economic Botany, 57*(2), 231-244.

Miller, D. M., Thomas, S. D., Islam, A., Muench, D., & Sedoris, K. (2012). c-Myc and cancer metabolism. *Clinical Cancer Research, 18*(20), 5546-5553.

Mishra, B. B., & Tiwari, V. K. (2011). Natural products: An evolving role in future drug discovery. *European Journal of Medicinal Chemistry, 46*(10), 4769-4807.

Mizushima, N. (2007). Autophagy: Process and function. *Genes & Development, 21*(22), 2861-2873.

Mohanty, S., & Xu, L. (2010). Experimental metastasis assay. *JoVE (Journal of Visualized Experiments), 42*, e1942-e1942.

Molina, J. R., Yang, P., Cassivi, S. D., Schild, S. E., & Adjei, A. A. (2008). Non-small cell lung cancer: Epidemiology, risk factors, treatment, and survivorship. *Mayo Clinic Proceedings. Mayo Clinic, 83*(5), 584-594.

Moserle, L., & Casanovas, O. (2013). Anti‐angiogenesis and metastasis: A tumour and stromal cell alliance. *Journal of Internal Medicine, 273*(2), 128-137.

Mukhopadhyay, S., Frias, M. A., Chatterjee, A., Yellen, P., & Foster, D. A. (2016). The enigma of rapamycin dosage. *Molecular Cancer Therapeutics*, *15*(3), 347-353.

Muñoz-Alonso, M. J., Acosta, J. C., Richard, C., Delgado, M. D., Sedivy, J., & León, J. (2005). p21Cip1 and p27Kip1 induce distinct cell cycle effects and differentiation programs in myeloid leukemia cells. *Journal of Biological Chemistry, 280*(18), 18120-18129.

MyBiosource.Com. *MTT cell proliferation assay*, (2014). Retrieved on 16th May 2016 from: https://www.mybiosource.com/prods/Assay-Kit/CytoSelect-MTT-Cell-Proliferation-Assay/datasheet.php?products_id=168154

Nascimento, F. R., Cruz, G. V., Pereira, P. V. S., Maciel, M. C., Silva, L. A., Azevedo, A. P. S., . . . Guerra, R. N. (2006). Ascitic and solid Ehrlich tumor inhibition by *Chenopodium ambrosioides* L. treatment. *Life Sciences, 78*(22), 2650-2653.

Neuzillet, C., Tijeras-Raballand, A., de Mestier, L., Cros, J., Faivre, S., & Raymond, E. (2014). MEK in cancer and cancer therapy. *Pharmacology & Therapeutics, 141*(2), 160-171.

Newman, D. J., & Cragg, G. M. (2016). Natural products as sources of new drugs from 1981 to 2014. *Journal of Natural Products, 79*(3), 629-661.

NF-κB. *Mechanism of NF-κB action*. (3 October 2007). Retrieved on 12th August 2016 from: https://en.wikipedia.org/wiki/NFκB#/media/File:NFKB_mechanism_of_action.png

Normanno, N., De Luca, A., Bianco, C., Strizzi, L., Mancino, M., Maiello, M. R., . . . Salomon, D. S. (2006). Epidermal growth factor receptor (EGFR) signaling in cancer. *Gene, 366*(1), 2-16.

Oberoi-Khanuja, T. K., Murali, A., & Rajalingam, K. (2013). IAPs on the move: Role of inhibitors of apoptosis proteins in cell migration. *Cell Death & Disease, 4*(9), e784.

Oda, K., Matsuoka, Y., Funahashi, A., & Kitano, H. (2005). A comprehensive pathway map of epidermal growth factor receptor signaling. *Molecular Systems Biology, 1(*2005.0010), E1-E17.

Olorunsogo, O. O., Emerole, G. O., Malomo, S. O., & Thabrew, M. I. (1983). Inhibition of mitochondrial respiration by chalepin, a naturally occurring furocoumarin. *Toxicology Letters, 15*(4), 323-327.

Orlanda, J. F., & Nascimento, A. (2015). Chemical composition and antibacterial activity of *Ruta graveolens* L. (Rutaceae) volatile oils, from São Luis, Maranhão, Brazil. *South African Journal of Botany, 99*, 103-106.

Orlita, A., Sidwa‐Gorycka, M., Kumirska, J., Maliński, E., Siedlecka, E. M., Gajdus, J., . . . Stepnowski, P. (2008). Identification of *Ruta graveolens* L. metabolites accumulated in the presence of abiotic elicitors. *Biotechnology Progress, 24*(1), 128-133.

Orlita, A., Sidwa‐Gorycka, M., Paszkiewicz, M., Malinski, E., Kumirska, J., Siedlecka, E. M., . . . Stepnowski, P. (2008). Application of chitin and chitosan as elicitors of coumarins and furoquinolone alkaloids in *Ruta graveolens* L. (common rue). *Biotechnology Applied Biochemistry, 51*(2), 91-96.

Owens, T. W., Gilmore, A. P., Streuli, C. H., & Foster, F. M. (2013). Inhibitor of apoptosis proteins: Promising targets for cancer therapy. *Journal of Carcinogenesis & Mutagenesis*. *Suppl 14*, S14-004.

Park, M. H., & Hong, J. T. (2016). Roles of NF-κB in cancer and inflammatory diseases and their therapeutic approaches. *Cells, 5*(2), E15.

Pathak, S., Multani, A. S., Banerji, P., & Banerji, P. (2003). Ruta 6 selectively induces cell death in brain cancer cells but proliferation in normal peripheral blood lymphocytes: A novel treatment for human brain cancer. *International Journal of Oncology, 23*(4), 975-982.

Pavão, F., Castilho, M., Pupo, M., Dias, R., Correa, A., Fernandes, J., . . . Oliva, G. (2002). Structure of *Trypanosoma cruzi* glycosomal glyceraldehyde‑3‑phosphate dehydrogenase complexed with chalepin, a natural product inhibitor, at 1.95 Å resolution. *FEBS Letters, 520*(1-3), 13-17.

Perciavalle, R. M., Stewart, D. P., Koss, B., Lynch, J., Milasta, S., Bathina, M., . . . Schuetz, J. D. (2012). Anti-apoptotic MCL-1 localizes to the mitochondrial matrix and couples mitochondrial fusion to respiration. *Nature Cell Biology, 14*(6), 575-583.

Perelman, A., Wachtel, C., Cohen, M., Haupt, S., Shapiro, H., & Tzur, A. (2012). JC-1: Alternative excitation wavelengths facilitate mitochondrial membrane potential cytometry. *Cell Death & Disease, 3*(11), e430.

Pezzuto, J. M. (1997). Plant-derived anticancer agents. *Biochemical Pharmacology, 53*(2), 121-133.

Phoenix flow systems. *APO-BrdU TUNEL assay*. (no date). Retrieved on 15th May 2016 from: http://www.phnxflow.com/apobrdu.html

Plants for a future. *Ruta graveolens* (no date). Retrieved on 11th December 2016 from: http://www.pfaf.org/User/Plant.aspx?LatinName=Ruta+graveolens

Pollio, A., De Natale, A., Appetiti, E., Aliotta, G., & Touwaide, A. (2008). Continuity and change in the Mediterranean medical tradition: *Ruta spp*. (*Rutaceae*) in Hippocratic medicine and present practices. *Journal of Ethnopharmacology, 116*(3), 469-482.

Pópulo, H., Lopes, J. M., & Soares, P. (2012). The mTOR signalling pathway in human cancer. *International Journal of Molecular Sciences, 13*(2), 1886-1918.

Porter, A. G., & Jänicke, R. U. (1999). Emerging roles of caspase-3 in apoptosis. *Cell Death and Differentiation, 6*(2), 99-104.

Pouliot, N., Pearson, H. B., & Burrows, A. (2012). Investigating metastasis using *in vitro* platforms. In *Madame Curie bioscience database*, (p.24). Austin (TX): Landes Bioscience.

Preethi, K., Kuttan, G., & Kuttan, R. (2006). Anti-tumour activity of *Ruta graveolens* extract. *Asian Pacific Journal of Cancer Prevention, 7*(3), 439-443.

QCM™ 24-well cell invasion assay manual (2003). Retrieved on 4th January 2017 from: http://www.merckmillipore.com/MY/en/product/QCM-ECMatrix-Cell-Invasion-Assay.html

QCM™ 24-well fluorimetric cell migration assay (2009). Retrieved on 4th May 2016 from: https://www.merckmillipore.com/MY/en/product/QCM-Chemotaxis-Cell-Migration-Assay.html

Rabinovitch, P. (no date). *Introduction to cell cycle analysis*. Retrieved on 12 June 2014 from: http://www.phoenixflow.com/cellcyclemath.pdf

Raghav, S., Gupta, B., Agrawal, C., Goswami, K., & Das, H. (2006). Anti-inflammatory effect of *Ruta graveolens* L. in murine macrophage cells. *Journal of Ethnopharmacology, 104*(1), 234-239.

Rajesh, E., Sankari, L. S., Malathi, L., & Krupaa, J. R. (2015). Naturally occurring products in cancer therapy. *Journal of Pharmacy & Bioallied Sciences, 7*(Suppl 1), S181.

Rapp, U. R., Korn, C., Ceteci, F., Karreman, C., Luetkenhaus, K., Serafin, V., . . . Potapenko, T. (2009). MYC is a metastasis gene for non-small-cell lung cancer. *PLoS ONE, 4*(6), e6029.

Rayan, A., Raiyn, J., & Falah, M. (2017). Nature is the best source of anticancer drugs: Indexing natural products for their anticancer bioactivity. *PLoS ONE, 12*(11), e0187925.

Reddy, L., Odhav, B., & Bhoola, K. (2003). Natural products for cancer prevention: A global perspective. *Pharmacology & Therapeutics, 99*(1), 1-13.

Reinert, T., Baldotto, C. S. d. R., Nunes, F. A. P., & Scheliga, A. A. d. S. (2013). Bleomycin-induced lung injury. *Journal of Cancer Research, 2013* (2013), 1-9.

Renehan, A. G., Booth, C., & Potten, C. S. (2001). What is apoptosis, and why is it important? *British Medical Journal, 322*(7301), 1536.

Réthy, B., Zupkó, I., Minorics, R., Hohmann, J., Ocsovszki, I., & Falkay, G. (2007). Investigation of cytotoxic activity on human cancer cell lines of arborinine and furanoacridones isolated from *Ruta graveolens*. *Planta Medica, 73*(01), 41-48.

Riss, T. L., Moravec, R. A., Niles, A. L., Benink, H. A., Worzella, T. J., & Minor, L. (2013). *Cell viability assays*. Retrieved on 5th January 2016 from: https://www.ncbi.nlm.nih.gov/books/NBK144065/

Rochem (28 February 2012). *Manfaat Inggu (Ruta angustifolia)*. Retrieved on 4th January 2017 from: https://rochem.wordpress.com/2012/02/28/manfaat-inggu-ruta-angustifolia/

Rogalska, A., Gajek, A., & Marczak, A. (2014). Epothilone B induces extrinsic pathway of apoptosis in human SKOV-3 ovarian cancer cells. *Toxicology in Vitro, 28*(4), 675-683.

Rosette, C., Roth, R. B., Oeth, P., Braun, A., Kammerer, S., Ekblom, J., & Denissenko, M. F. (2005). Role of ICAM1 in invasion of human breast cancer cells. *Carcinogenesis, 26*(5), 943-950.

Roy, J., Audette, M., & Tremblay, M. J. (2001). Intercellular adhesion molecule-1 (ICAM-1) gene expression in human T cells is regulated by phosphotyrosyl phosphatase activity involvement of NF-κB, ets, and palindromic interferon-γ-responsive element-binding sites. *Journal of Biological Chemistry, 276*(18), 14553-14561.

Russo, P., Frustaci, A., Del Bufalo, A., Fini, M., & Cesario, A. (2013). From traditional European medicine to discovery of new drug candidates for the treatment of dementia and Alzheimer's disease: Acetylcholinesterase inhibitors. *Current Medicinal Chemistry, 20*(8), 976-983.

Ruta angustifolia Pers (no date). Retrieved on 11th December 2016 from: http://www.globinmed.com/index.php?option=com_content&view=article&id=62899:ruta-angustifolia-pers&Itemid=113

Sachithanandan, A., & Badmanaban, B. (2012). Screening for lung cancer in Malaysia: Are we there yet? *Medical Journal of Malaysia, 67*(1), 3-6.

Saiki, I. (1997). Cell adhesion molecules and cancer metastasis. *The Japanese Journal of Pharmacology, 75*(3), 215-242.

Sasaki, C. Y., Barberi, T. J., Ghosh, P., & Longo, D. L. (2005). Phosphorylation of RelA/p65 on serine 536 defines an IκBα-independent NF-κB pathway. *Journal of Biological Chemistry, 280*(41), 34538-34547.

Sato, M., Sagawa, M., Nakazato, T., Ikeda, Y., & Kizaki, M. (2007). A natural peptide, dolastatin 15, induces G2/M cell cycle arrest and apoptosis of human multiple myeloma cells. *International Journal of Oncology, 30*(6), 1453-1459.

Scaltriti, M., & Baselga, J. (2006). The epidermal growth factor receptor pathway: A model for targeted therapy. *Clinical Cancer Research, 12*(18), 5268-5272.

Schimmer, A. D. (2004). Inhibitor of apoptosis proteins: Translating basic knowledge into clinical practice. *Cancer Research, 64*(20), 7183-7190.

Schwartz, G. K., & Dickson, M. (2009). Development of cell cycle inhibitors for cancer therapy. *Current Oncology, 16*(2), 36-43.

Sethi, G., Ahn, K. S., & Aggarwal, B. B. (2008). Targeting nuclear factor-κB activation pathway by thymoquinone: Role in suppression of antiapoptotic gene products and enhancement of apoptosis. *Molecular Cancer Research, 6*(6), 1059-1070.

Sethi, G., Chatterjee, S., Rajendran, P., Li, F., Shanmugam, M. K., Wong, K. F., . . . Hui, K. M. (2014). Inhibition of STAT3 dimerization and acetylation by garcinol suppresses the growth of human hepatocellular carcinoma *in vitro* and *in vivo*. *Molecular Cancer, 13*(66), 1-14.

Seyfried, T. N., & Shelton, L. M. (2010). Cancer as a metabolic disease. *Nutrition & Metabolism, 7*(7), 1-22.

Shackelford, R. E., Kaufmann, W. K., & Paules, R. S. (1999). Cell cycle control, checkpoint mechanisms, and genotoxic stress. *Environmental Health Perspectives, 107*(Suppl 1), 5-24.

Sherr, C. J. (1996). Cancer cell cycles. *Science, 274*(5293), 1672-1677.

Sigismund, S., Avanzato, D., & Lanzetti, L. (2018). Emerging functions of the EGFR in cancer. *Molecular Oncology, 12*(1), 3-20.

Simon, H.-U., Haj-Yehia, A., & Levi-Schaffer, F. (2000). Role of reactive oxygen species (ROS) in apoptosis induction. *Apoptosis, 5*(5), 415-418.

Singh, S., & Aggarwal, B. B. (1995). Activation of transcription factor NF-κB is suppressed by curcumin (diferuloylmethane). *Journal of Biological Chemistry, 270*(42), 24995-25000.

Siveen, K. S., Sikka, S., Surana, R., Dai, X., Zhang, J., Kumar, A. P., . . . Bishayee, A. (2014). Targeting the STAT3 signaling pathway in cancer: Role of synthetic and natural inhibitors. *Biochimica et Biophysica Acta (BBA)-Reviews on Cancer, 1845*(2), 136-154.

Sobolewski, C., Cerella, C., Dicato, M., Ghibelli, L., & Diederich, M. (2010). The role of cyclooxygenase-2 in cell proliferation and cell death in human malignancies. *International Journal of Cell Biology, 2010,* 215158.

Song, L., Rawal, B., Nemeth, J. A., & Haura, E. B. (2011). JAK1 activates STAT3 activity in non-small–cell lung cancer cells and IL-6 neutralizing antibodies can suppress JAK1-STAT3 signaling. *Molecular Cancer Therapeutics, 10*(3), 481-494.

Song, W., Ma, Y., Wang, J., Brantley-Sieders, D., & Chen, J. (2014). JNK signaling mediates EPHA2-dependent tumor cell proliferation, motility, and cancer stem cell–like properties in non–small cell lung cancer. *Cancer Research, 74*(9), 2444-2454.

Stinchcombe, T. E., & Johnson, G. L. (2014). MEK inhibition in non-small cell lung cancer. *Lung Cancer, 86*(2), 121-125.

Suen, D.-F., Norris, K. L., & Youle, R. J. (2008). Mitochondrial dynamics and apoptosis. *Genes & Development, 22*(12), 1577-1590.

Suhaimi, S., Hong, S., & Abdul Malek, S. (2017). Rutamarin, an active constituent from *Ruta angustifolia* Pers., induced apoptotic cell death in the HT29 colon adenocarcinoma cell line. *Pharmacognosy Magazine, 13*(50), 179-188.

Stansbury, J. (1st May 2011). Naturopathic Doctor News and Review – Anti-Aging, Dermatology, Oncology . *Photosensitizing herbs: skin diseases and cancers.* Retrieved on 15th May 2018 from: http://ndnr.com/oncology/photosensitizing-coumarins-for-skin-diseases-and-cancers/

Stern, R. S., Liebman, E. J., & Väkevä, L. (1998). Oral psoralen and ultraviolet-A light (PUVA) treatment of psoriasis and persistent risk of nonmelanoma skin cancer. *Journal of the National Cancer Institute, 90*(17), 1278-1284.

Tabll, A., & Ismail, H. (2011). The Use of Flow Cytometric DNA Ploidy Analysis of Liver Biopsies in Liver Cirrhosis and Hepatocellular Carcinoma. In Takahashi, H. (Ed), *Liver biopsy*. Retrieved on 6th July 2014 from: https://www.intechopen.com/books/liver-biopsy/the-use-of-flow-cytometric-dna-ploidy-analysis-of-liver-biopsies-in-liver-cirrhosis-and-hepatocellul

Tang, Y.-Q., Jaganath, I. B., & Sekaran, S. D. (2010). *Phyllanthus spp*. induces selective growth inhibition of PC-3 and MeWo human cancer cells through modulation of cell cycle and induction of apoptosis. *PLoS ONE, 5*(9), e12644.

Tarique, M., Siddiqui, H. H., Khushtar, M., & Rahman, M. A. (2016). Protective effect of hydro-alcoholic extract of *Ruta graveolens* Linn. leaves on indomethacin and pylorus ligation-induced gastric ulcer in rats. *Journal of Ayurveda and Integrative Medicine*, *7*(1), 38-43.

Taylor, S. C., & Posch, A. (2014). The design of a quantitative western blot experiment. *BioMed Research International, 2014*, 361590.

The cell cycle, mitosis and meiosis. *The cell cycle* (no date). Retrieved on 14th December 2016 from: http://www2.le.ac.uk/departments/genetics/vgec/schoolscolleges/topics/cellcycle-mitosis-meiosis

Toth, M., Sohail, A., & Fridman, R. (2012). Assessment of gelatinases (MMP-2 and MMP-9) by gelatin zymography. *Methods in Molecular Biology*, *878*, 121-135.

Tulp, M., & Bohlin, L. (2004). Unconventional natural sources for future drug discovery. *Drug Discovery Today, 9*(10), 450-458.

Usami, Y., Ishida, K., Sato, S., Kishino, M., Kiryu, M., Ogawa, Y., . . . Toyosawa, S. (2013). Intercellular adhesion molecule‐1 (ICAM‐1) expression correlates with oral cancer progression and induces macrophage/cancer cell adhesion. *International Journal of Cancer, 133*(3), 568-578.

Valastyan, S., & Weinberg, R. A. (2011). Tumor metastasis: Molecular insights and evolving paradigms. *Cell, 147*(2), 275-292.

van Zijl, F., Krupitza, G., & Mikulits, W. (2011). Initial steps of metastasis: Cell invasion and endothelial transmigration. *Mutation Research/Reviews in Mutation Research, 728*(1), 23-34.

Vanlangenakker, N., Berghe, T. V., Krysko, D. V., Festjens, N., & Vandenabeele, P. (2008). Molecular mechanisms and pathophysiology of necrotic cell death. *Current Molecular Medicine, 8*(3), 207-220.

Venditto, V. J., & Simanek, E. E. (2010). Cancer therapies utilizing the camptothecins: A review of the *in vivo* literature. *Molecular Pharmaceutics, 7*(2), 307-349.

Venkateshwaran, R. (14 June 2016). Wild Turmeric. *5 Top medicinal uses of Ruta graveolens*. Retrieved on 14th May 2018 from: https://www.wildturmeric.net/ruta-graveolens-rue-ruda-medicinal-uses-side-effects/

Vermeulen, K., Van Bockstaele, D. R., & Berneman, Z. N. (2003). The cell cycle: A review of regulation, deregulation and therapeutic targets in cancer. *Cell Proliferation, 36*(3), 131-149.

Voigt, W. (2005) Sulforhodamine B assay and chemosensitivity. *Methods Molecular Medicine, 110*, 39–48.

Wahyuni, T. S., Widyawaruyanti, A., Lusida, M. I., Fuad, A., Soetjipto, Fuchino, H., . . Hotta, H. (2014). Inhibition of hepatitis C virus replication by chalepin and pseudane IX isolated from *Ruta angustifolia* leaves. *Fitoterapia, 99*, 276-283.

Wee, P., & Wang, Z. (2017). Epidermal growth factor receptor cell proliferation signaling pathways. *Cancers, 9*(5), 52.

Williams, G. H., & Stoeber, K. (2012). The cell cycle and cancer. *The Journal of Pathology, 226*(2), 352-364.

Wong, R. S. (2011). Apoptosis in cancer: From pathogenesis to treatment. *Journal of Experimental & Clinical Cancer Research, 30*(1), 87.

Wu, T. S., Shi, L. S., Wang, J. J., Iou, S. C., Chang, H. C., Chen, Y. P., . . . Tenge, C. M. (2003). Cytotoxic and antiplatelet aggregation principles of *Ruta graveolens*. *Journal of the Chinese Chemical Society, 50*(1), 171-178.

Xia, Y., Shen, S., & Verma, I. M. (2014). NF-κB, an active player in human cancers. *Cancer Immunology Research, 2*(9), 823-830.

Xiang, L., Chi, T., Tang, Q., Yang, X., Ou, M., Chen, X., . . . Shao, J. (2015). A pentacyclic triterpene natural product, ursolic acid and its prodrug US597 inhibit targets within cell adhesion pathway and prevent cancer metastasis. *Oncotarget, 6*(11), 9295-9312.

Yang, Q.-Y., Tian, X.-Y., & Fang, W.-S. (2007). Bioactive coumarins from *Boenninghausenia sessilicarpa*. *Journal of Asian Natural Products Research, 9*(1), 59-65.

Yang, Y., & Ma, H. (2009). Western blotting and ELISA techniques. *Researcher, 1*(2), 67-86.

Yue, P., & Turkson, J. (2009). Targeting STAT3 in cancer: How successful are we? *Expert Opinion on Investigational Drugs, 18*(1), 45-56.

Zayas-Pinedo, P., Gabilondo-Zubizarreta, F., & Torrero-López, V. (2014). Fototoxicidad tras exposición a *Ruta graveolens*. *Cirugía Plástica Ibero-Latinoamericana, 40*(4), 455-458.

Zhang, D., Lin, J., & Han, J. (2010). Receptor-interacting protein (RIP) kinase family. *Cellular & Molecular Immunology, 7*(4), 243-249.

Zhang, J., & Xu, M. (2002). Apoptotic DNA fragmentation and tissue homeostasis. *Trends in Cell Biology, 12*(2), 84-89.

Zhang, Q., Lenardo, M. J., & Baltimore, D. (2017). 30 years of NF-κB: A blossoming of relevance to human pathobiology. *Cell, 168*(1-2), 37-57.

Zhang, Z., Stiegler, A. L., Boggon, T. J., Kobayashi, S., & Halmos, B. (2010). EGFR-mutated lung cancer: A paradigm of molecular oncology. *Oncotarget, 1*(7), 497-514.

Zhou, W., & Christiani, D. C. (2011). East meets West: Ethnic differences in epidemiology and clinical behaviors of lung cancer between East Asians and Caucasians. *Chinese Journal of Cancer*, *30*(5), 287-292.

Ziegler, U., & Groscurth, P. (2004). Morphological features of cell death. *Physiology, 19*(3), 124-128.

Zymography: Enzymes in action (no date). Retrieved on 12th December 2016 from: http://docsdrive.com/images/scienceinternational/sciintl/2013/fig1-2k13-70

LIST OF PUBLICATIONS AND PAPERS PRESENTED

List of Publications

1. Richardson, J. S. M., Sethi, G., Lee, G. S., & Malek, S. N. A. (2016). Chalepin: Isolated from *Ruta angustifolia* L. *Pers* induces mitochondrial mediated apoptosis in lung carcinoma cells. *BMC Complementary and Alternative Medicine, 16*(1), 389.

2. Richardson, J. S. M., Aminudin, N. H., & Malek, S. N. A. (2017). Chalepin: A Compound from *Ruta angustifolia* L. *Pers* Exhibits Cell Cycle Arrest at S phase, Suppresses NF-κB Pathway, STAT3 Phosphorylation and Extrinsic Apoptotic Pathway in Non-small Cell Lung Cancer Carcinoma (A549). *Pharmacognosy Magazine*, *13*(51), 489-498.

List of Papers Presented

1. Oral presentation entitled "Chalepin: Isolated from *Ruta angustifolia* L. *Pers* induces mitochondrial mediated apoptosis in lung carcinoma cells" on 10 December 2015 at 20th Biological Sciences Graduate Congress (BSGC), Chulalongkorn University, Bangkok, Thailand.

2. Poster presentation entitled "Chalepin: Isolated from *Ruta angustifolia* L. *Pers* induces mitochondrial mediated apoptosis in lung carcinoma cells (A549)" on November 2015 at Frontiers of Cancer Science, National University of Singapore, Singapore.